

LONDON
SCHOOL of
HYGIENE
& TROPICAL
MEDICINE



LSHTM Research Online

Wijnant, GJ; (2018) New pharmacokinetic and PK/PD drug development methodologies for cutaneous leishmaniasis. PhD (research paper style) thesis, London School of Hygiene & Tropical Medicine. DOI: <https://doi.org/10.17037/PUBS.04651224>

Downloaded from: <https://researchonline.lshtm.ac.uk/id/eprint/4651224/>

DOI: <https://doi.org/10.17037/PUBS.04651224>

Usage Guidelines:

Please refer to usage guidelines at <https://researchonline.lshtm.ac.uk/policies.html> or alternatively contact researchonline@lshtm.ac.uk.

Available under license. To note, 3rd party material is not necessarily covered under this license: <http://creativecommons.org/licenses/by-nc-nd/3.0/>

<https://researchonline.lshtm.ac.uk>

LONDON
SCHOOL *of*
HYGIENE
& TROPICAL
MEDICINE



New pharmacokinetic and PK/PD drug development methodologies for cutaneous leishmaniasis

A thesis submitted by

Gert-Jan Wijnant

in

July 2018

In accordance with the requirements for the degree of
Doctor of Philosophy of the University of London

Professor Dr Simon L. Croft

Dr Sudaxshina Murdan

Department of Immunology and Infection
Faculty of Infectious and Tropical Diseases
London School of Hygiene and Tropical Medicine

DECLARATION

I, Gert-Jan Wijnant, confirm that the work presented in this thesis is my own. Where information has been derived from other sources, I confirm that this has been indicated in the thesis.

Gert-Jan Wijnant

July 2018



ABSTRACT

Cutaneous leishmaniasis (CL) is a vector-borne neglected tropical disease caused by over 15 species of the intracellular *Leishmania* parasite. This skin infection is the most common and widely distributed form of leishmaniasis, with an estimated 0.7-1.2 million new cases annually, mainly in the Middle East and Latin America. CL is rarely fatal, but the ulcerative skin lesions often leave lifelong scars, disfigurement, and social stigma. Current treatment of CL is far from optimal. The pentavalent antimonials remain the standard of care since their discovery in the 1940s, but typically require three weeks of painful, toxic injections into the lesions. An alternative therapeutic option is liposomal amphotericin B, but cure rates are variable, access is problematic and invasive drug administration is required. Basic research tools that could accelerate the successful discovery and development of much needed new drugs are currently limited. This thesis aims to provide a coherent set of R&D methodologies to evaluate (i) the penetration of drugs into the infected skin lesions (pharmacokinetics, PK), (ii) the ability to kill the causative *Leishmania* parasites (pharmacodynamics, PD) and (iii) the interaction between PK and PD (PK/PD) parameters.

- In chapter 3.1, the limitations of the current *in vitro* models to predict *in vivo* drug activity were confirmed. Additionally, combination therapy of standard antileishmanial drugs with chloroquine was found unlikely to be a successful new treatment strategy for CL.
- In chapter 3.2, we demonstrated a clear relationship between PK and PD parameters for the standard liposomal amphotericin B formulation AmBisome in a mouse model of CL, providing a PK/PD basis for the rational design of better clinical dose regimens.
- In chapter 3.3, we compared the *in vivo* effects of AmBisome with Fungisome, an alternative liposomal amphotericin B formulation on the market in India. Fungisome was less efficacious than AmBisome due to lower drug accumulation in skin lesions and had a narrower therapeutic index in the treatment of murine CL.
- In chapter 3.4, we showed that the CL infection and associated local skin inflammation has a profound effect on the PK of AmBisome and can contribute to its variable therapeutic efficacy against Old and New World *Leishmania* species. The increased vascular permeability of the dermal capillaries might be exploited for enhanced delivery of small (< 500 Da) oral drugs to the infected skin.
- Finally, in chapter 3.5, we evaluated a new drug candidate from the Drugs for Neglected Diseases Initiative (DNDI) for visceral leishmaniasis. Our PK and PD data, based on innovative skin microdialysis and qPCR techniques, support the further preclinical development of the nitroimidazole DNDI-0690 as a promising new oral treatment for CL.

Overall, the strategies, lessons and research tools provided in this PhD thesis could contribute to the development of safe, effective, affordable and patient-friendly new drugs for the treatment of CL.

ACKNOWLEDGEMENTS

I had the great privilege to start my doctoral project in July 2015 under the excellent mentoring of my promotors Professor Simon Croft (Faculty of Infectious and Tropical Diseases, LSHTM) and Dr Sudax Murdan (Department of Pharmaceutics, School of Pharmacy). Thank you both for all the guidance, advice and support throughout my entire Ph.D., especially to occasionally take a step back and see the wood from the trees. I learnt to focus my time and energy on ambitious yet realistic goals and that, in the words of the great Rick Sanchez, sometimes science is more art than science. Simon, your passion, insights and no-nonsense approach have been an inspiration for me to continue pursuing a career in antimicrobial drug research. No doubt, your many wise lessons, ranging from “a model is only a model” to “if you can’t have a glass of wine with them, do not collaborate”, will help me along the way.

I strongly doubt that this PhD project would have been half as good or as productive without the exceptional training and continuous help at every single step of my Flemish colleague Katrien Van Bocxlaer. Kat, een ongelofelijk dikke merci voor alles, van de vlotte samenwerking tot de vele leuke die we samen hebben gehad! Many thanks to Vanessa Yardley for all-round organizational support and awesomeness. And thanks to the rest of the Croft group and associated leishmaniacs for all the good times in and out of the lab: Alec O’Keeffe, Alaa Riezk, Markella Koniordou and John Hamp.

I want to acknowledge Andrew Voak and Karin Seifert for early guidance and technical support during for pharmacokinetic experiments. Thanks to everyone at Pharmidex Pharmaceutical Services who assisted in the set-up, analysis or discussion of such studies: Andy Harris, Amit Giram, Desmond O’Connor, Raul De la Flor, Janette Robertson and Mo Alavijeh. The animal work would not have been possible without the advice and assistance from the staff of the biological services faculty at LSHTM and Arturo Fernandez. Thanks to Angela Richard-Londt and others at UCL Institute of Neurology for performing the histopathology work and Amanda Fortes Francisco at LSHTM for the analysis. Another thank you to everyone at the Institute of Hygiene Tropical Medicine in Lisbon: Isabel Mauricio, Sandra Antunes, Catarina Rosa and Rita Silva-Pedrosa, who helped to turn my time in Portugal into an incredible experience.

My project was part of a European Innovative Training Network together with 14 other PhD students working on leishmaniasis, many of which have become great friends. Thanks in particular to David Mateus, who started his PhD in London together with me, for many afternoons of coffee and nights of good fun. Professor Michael Miles, the Euroleish project coordinator for LSHTM, was always there for help and feedback. The network and my project have received funding from the European Union’s Horizon 2020 research and innovation programme under the Marie Skłodowska-Curie grant agreement N° 642609.

Finally, thanks to all of my friends and family who have supported me throughout the process. In particular, to my mum, dad and sister, without whom I would have never got here in the first place, and Raluca, whose support and confidence has helped to keep me sane during these last couple of months of writing throughout experiments.

I would like to dedicate this PhD thesis to my late grandfather Willy Haegeman, who taught me the value of hard work and stimulated my eagerness to learn more about the world from an early age. Opa, ik hoop dat ge trots op mij zou zijn geweest.

ABBREVIATIONS

ADME	Absorption - Distribution - Metabolism – Elimination
AmB	Amphotericin B
ANOVA	Analysis of Variance
Anti-Iba-1	Anti-ionized calcium-binding adapter molecule 1 antibody stain
AUC	Area Under Curve
(aq)	Aqueous
CI	Confidence interval
CL	Cutaneous leishmaniasis
<i>Cl</i>	Clearance
C_{max}	Maximum concentration
DAmB	Deoxycholate amphotericin B
DCL	Diffuse cutaneous leishmaniasis
DMEM	Dulbecco's Modified Eagle's Medium
DMSO	Dimethyl sulfoxide
DNA	Deoxyribonucleic acid
DNDI	Drugs for Neglected Diseases Initiative
ED ₅₀	50% effective dose
ED ₉₀	90 % effective dose
EMA	European Medicines Agency
FDA	Federal Drug Agency
HiFCS	Heat-inactivated fetal calf serum
HTS	High Throughput Screening
H&E	Hematoxylin-eosin stain
IC ₅₀	50% effective concentration
IC ₉₀	90 % effective concentration
IM	Intramuscular
IP	Intraperitoneal
IV	Intravenous
LAmB	Liposomal Amphotericin B
LCL	Local cutaneous leishmaniasis
LC-MS/MS	Liquid Chromatography tandem-mass spectrometry
LD ₅₀	50% lethal dose
LD ₉₀	90% lethal dose
LSHTM	London School of Hygiene and Tropical Medicine
MCL	Mucocutaneous leishmaniasis
MD	Microdialysis
MF	Miltefosine
NTD	Neglected Tropical Disease
PBS	Phosphate buffered saline
PD	Pharmacodynamics
PEG400	Polyethylene glycol 400
PEM	Peritoneal exudate macrophage
PG	Propylene glycol
PK	Pharmacokinetics
PK/PD	Pharmacokinetic/pharmacodynamic

PKDL	Post Kala Azar Dermal leishmaniasis
PM	Paromomycin
p.o.	Per os (oral)
qPCR	quantitative Polymerase Chain Reaction
R&D	Research and development
RNA	Ribonucleic acid
RR	Relative Recovery
RT-qPCR	Reverse Transcriptase Polymerase Chain Reaction
SbIII	Trivalent antimony
SbV	Pentavalent antimony
SD	Standard Deviation
SEM	Standard Error of the Mean
SMD	Skin microdialysis
SSG	Sodium stibogluconate
$T_{1/2}$	Half-life
T_{max}	Time-point corresponding with maximum concentration
UCL	University College London
UK	United Kingdom
USA	United States of America
Vd	Volume of distribution
VL	Visceral leishmaniasis
WHO	World Health Organization
2D	Two Dimensional
3D	Three Dimensional

CONTENTS

ABBREVIATIONS	V
LIST OF FIGURES	IX
LIST OF TABLES	XI
1. General introduction.....	1
1.1. <i>Leishmania</i> species and leishmaniasis	1
1.1.1. Parasite life cycle.....	2
1.1.2. Vectors and transmission.....	3
1.2. Cutaneous leishmaniasis (CL).....	4
1.2.1. Clinical manifestations	4
1.2.2. Immunopathology.....	5
1.2.3. Species-specific differences	7
1.3. Current treatment of CL.....	8
1.3.1. Systemic chemotherapeutics	9
1.3.1.1. Pentavalent antimonials	9
1.3.1.2. Miltefosine	11
1.3.1.3. Amphotericin B	12
1.3.1.4. Pentamidine	13
1.3.1.5. Azoles	14
1.3.2. Local chemotherapeutics	15
1.3.2.1. Paromomycin	15
1.3.3. Physical treatments.....	16
1.3.4. Immunotherapy	16
1.4. Treatment challenges in CL.....	17
1.5. Drug development for CL.....	19
1.5.1. Drug discovery and development	19
1.5.2. R&D pipeline for CL.....	21
1.5.3. Profile of an ideal CL drug	23
1.5.4. Introduction to the pharmacology of CL drugs	24
1.5.5. Current drug development tools for CL	29
1.5.6. PK and PK/PD in CL drug development	33
2. Aims and objectives	35
3. Experimental results	36
3. 1: Combination therapies with chloroquine for CL treatment	39

3.2: AmBisome treatment of CL - relation between skin PK and efficacy	53
3.3: AmBisome treatment of CL – comparison with Fungisome	67
3.4: Local skin inflammation in CL as a source of variable PK and efficacy of AmBisome®	79
3.5: PK and PK/PD-based efficacy evaluation of the drug candidate DNDI-0690 for the treatment of CL.....	100
3.5.1. Introduction	100
3.5.2. Physicochemical properties of DNDI-0690	101
3.5.3. <i>In vitro</i> antileishmanial activity of DNDI-0690	102
3.5.4. Dose-response of DNDI-0690 in the <i>L. major</i> -BALB/c model of CL	102
3.5.4.1. Aim	102
3.5.4.2. Materials and methods	102
3.5.4.3. Results and discussion	104
3.5.5. Skin microdialysis of DNDI-0690	107
3.5.5.1. An introduction to skin microdialysis.....	107
3.5.5.2. Skin microdialysis: development of the system.....	108
3.5.5.3. Lesion, control skin and tail vein microdialysis after oral dosing of DNDI-0690.	116
3.5.6. Discussion.....	119
4. Summary of key findings.....	121
5. General discussion: recapitulation and future perspectives	122
5.1. Scientific challenges and problems in current R&D for CL	122
5.2. New PK and PK/PD drug development methodologies for CL.....	124
5.3. New drug candidates tested for the treatment of CL.....	127
5.4. Directions for future R&D for CL.....	130
6. References in the thesis text.....	134
7. Appendix	151
7.1. Networks, partners and institutes	151
7.1.1. Euroleish.....	151
7.1.2. Pharmidex Pharmaceutical Services Ltd.	152
7.1.3. Institute of Hygiene and Tropical Medicine, Lisbon	152
7.1.4. Drugs for Neglected Diseases <i>initiative</i>	153
7.2. Supplementary material	154
7.2.1. DNA- and RNA- based qPCR results	154

LIST OF FIGURES

Figure 1: Geographical distribution of <i>Leishmania</i> in the Old (A) and New (B) World. Adapted from (3).	2
Figure 2: <i>Leishmania</i> life cycle in humans (5)	3
Figure 3: Taxonomy of <i>Leishmania</i> in relation to clinical manifestations (10).	4
Figure 4: Disease stages in CL and involvement of the different layers of the skin (15)	5
Figure 5: Histology (H&E stain) of a single CL nodule on the arm of a patient (upper left). The x 40 magnification shows a dense inflammatory infiltrate within the dermal layer of the skin (right). Higher magnification (x 1250) reveals the intracellular <i>Leishmania</i> amastigotes (red arrows) within the phagolysosome of macrophages (green arrows point at host cell nuclei) located in the upper layers of the dermis (derived from (20)).	6
Figure 6: Clinical polymorphism of CL caused by different <i>Leishmania</i> species (14, 24-30).	7
Figure 7: Treatment strategies for the different forms of CL and their limitations (39). Syst=systemic. Tx= treatment. ACL=asymptomatic CL.....	9
Figure 8: Chemical structure of sodium stibogluconate (Pentostam™, left) and meglumine antimoniate (Glucantime™, right). Pentavalent antimonials typically require three weeks of painful injections into the lesions (photos).	10
Figure 9: Miltefosine - chemical structure and capsules	11
Figure 10: Amphotericin B – chemical structure and the different formulations AmBisome® (unilamellar liposome of AmB), Fungisome® (multilamellar liposome of AmB) and Fungizone® (deoxycholate salt of AmB) for intravenous infusion.	13
Figure 11: Pentamidine – chemical structure	14
Figure 12: Fluconazole (left) and ketoconazole (right) – chemical structure	14
Figure 13: Paromomycin – chemical structure and ointment	16
Figure 14: The classic drug discovery and development pathway (116)	19
Figure 15: Attrition rate and current R&D pipeline for (neglected) tropical diseases. HAT = Human African Trypanosomiasis (sleeping sickness). TB = tuberculosis. Adapted from (123).....	20
Figure 16: R&D pipeline for leishmaniasis (June 2018, DNDI, 132)	22
Figure 17: Actors and relationships in the anti-parasitic activity of a CL drug	25
Figure 18: <i>In vitro</i> and <i>in vivo</i> models of CL – <i>Leishmania</i> -infected macrophages (nuclei: N, intracellular amastigotes, A and arrows) and BALB/c mice with skin lesions on the rump (L)	29
Figure 19: an oral drug discovery scheme for CL. MTA = material transfer agreement. T.I = therapeutic index. HepG2 = human liver cell line (preclinical toxicity assay).	32
l.p. = intraperitoneal. MLS = mouse leishmaniasis suppression. ID = identification. MLL = mouse leishmaniasis lesion. P.o. = <i>per os</i> (oral). PK = pharmacokinetics. IVMN = <i>in vitro</i> micronucleus assay (preclinical genotoxicity assay). hERG = human ether-a-go-go-related gene (preclinical cardiotoxicity assay). Ames testing (preclinical carcinogenicity assay). DDI = drug-drug interaction. SAR = structure activity relationship.....	32
Figure 20: Overview of the basic concepts of PK/PD modelling (171)	33
Figure 21: Chemical structure of the nitroimidazole compound DNDI-0690	100
Figure 22: Predicted 3D structure of DNDI-0690 (Chem3D 16.0)	101
Figure 23: Dose-response effect of oral DNDI-0690 (left) and positive control drug intraperitoneal paromomycin (right) in the <i>L. major</i> –BALB/c model of CL. ** = p<0.01, *** = p<0.005, **** p <0.001 in comparison to untreated control.....	104

Figure 24: DNDI-0690 levels in the skin lesion (ng/g, 24 hours after 10 doses once daily) in relation to (i) dose level (left) and (ii) relative reduction in parasite load and lesion size compared to the untreated control (right).....	105
Figure 25: Principles of skin microdialysis.....	108
Figure 26: <i>In vitro</i> skin microdialysis set-up.....	110
Figure 27: <i>In vitro</i> recovery of DNDI-0690.	111
Figure 28: Lomir Biomedical rodent jackets on BALB/c mice	112
Figure 29: Clinical monitoring of temperature (left graph) and breathing patterns (right graph) of BALB/c mice under the anaesthetic effects of urethane.....	114
Figure 30: insertion of the microdialysis probe in the tail vein and the lesion skin. Top row (left to right): microdialysis probe, probe inserted in tail vein, probe inserted in tail vein secured by tape. Bottom row (left to right): probe inserted in lesion skin secured by glue, detail confirming intradermal insertion of the probe in the inflammatory mass of the lesion, probe after removal from lesion tissue.	115
Figure 31: Essential set-up of the <i>in vivo</i> skin microdialysis test experiment	116
Figure 32: Set-up of lesion, control skin and microdialysis after administration of oral DNDI-0690 in the <i>L. major</i> -BALB/c model of CL. A: microdialysis probe (6 kDa cut-off). B: Microdialysis set-up (9 channels) – pumps (left), mice on a hot plate (middle) and automated fraction collectors (right). C: Mice after insertion of probes. D: Detail of one mouse after insertion of microdialysis probes in the lateral tail vein (red arrow), dermal layer of the lesion skin (orange arrow) and dermal layer of healthy control skin (green arrow).	117
Figure 33: Unbound dermal tissue and plasma concentration-over-time profile of DNDI-0690 after oral administration of a single 50 mg/kg dose to <i>L. major</i> -infected BALB/c mice (n=3). Photo: PK sampling sites (microdialysis): plasma (red arrow), healthy control skin (orange arrow) and lesion (yellow arrow).	119
Figure 34: Example of a screening cascade for CL drug development and where the new methodologies (red circles) could be implemented. qPCR PL: quantitate PCR to measure parasite load. #mΦ: image analysis to estimate the number of macrophages in skin tissue. SMD: skin microdialysis.	127
Figure 35: Opportunities (green) and challenges (red) along the pharmacokinetic path of oral (blue) and topical (yellow) drugs against CL.	132
Figure 36: Outcomes of the DNA- and RNA-based qPCR methods to quantify parasite load (see chapter 5.3)	154

LIST OF TABLES

Table 1: Target product profile for CL (DNDI)	24
Table 2: Overview of fundamental PK parameters.....	26
Table 3: Physicochemical properties of DNDI-0690	101
Table 4: <i>in vitro</i> antileishmanial activity of DNDI-0690 (ND: not determined).....	102
Table 5: Comparative 50 % and 90 % effective doses (lesion size, parasite load) for oral DNDI-0690 and the positive control drug intraperitoneal PM (means).....	105
Table 6: Comparison between skin homogenate and skin microdialysis to measure drug concentrations in animal models of CL.....	107
Table 7: Overview of the phases of the <i>in vitro</i> recovery experiment	110

1. GENERAL INTRODUCTION

1.1. *Leishmania* species and leishmaniasis

The leishmaniases are a group of vector-borne neglected tropical diseases, caused by over 20 species of the protozoan *Leishmania* parasite that are transmitted to humans via sand flies. The disease mainly affects vulnerable, marginalized populations in Asia, Africa and Latin America and is associated with poverty, malnutrition, conflict, mass migration, poor housing and immunosuppression. Around 10 million present cases occur in over one hundred countries, the worldwide incidence is estimated at 1.5 million new cases per year and 350 million people are at risk (1).

A large fraction of infected individuals remain asymptomatic, but others develop one of the three main forms of the disease: visceral leishmaniasis (VL), cutaneous leishmaniasis (CL) or mucocutaneous leishmaniasis (MCL).

- VL, also known as kala-azar, is a potentially fatal infection of the liver, spleen and bone marrow caused by *Leishmania donovani* and *Leishmania infantum*. 200,000-400,000 new cases occur annually, mainly in Brazil, Ethiopia, India, Bangladesh, Somalia, South Sudan and Sudan. Among the 20,000 to 30,000 deaths resulting from VL per year, many are children under five.
- CL is characterized by disfiguring and disabling skin lesions and has the highest incidence (700,000-1,200,000) in the Middle East (Iran, Afghanistan, Syria, and Saudi Arabia, caused by the so-called 'Old world' *Leishmania* species) and South America (mainly Brazil, Colombia and Peru, caused by the so-called 'New World' *Leishmania* species).
- In MCL, the lesions can lead to the partial or complete destruction of the mucous membranes of face, mouth and throat cavities. MCL is typically caused by *Leishmania Viannia* subgenus parasite species and over 90 % of cases occur in Bolivia, Brazil and Peru (2).

Figure 1 shows an overview of the endemicity of pathogenic *Leishmania* species worldwide (3).

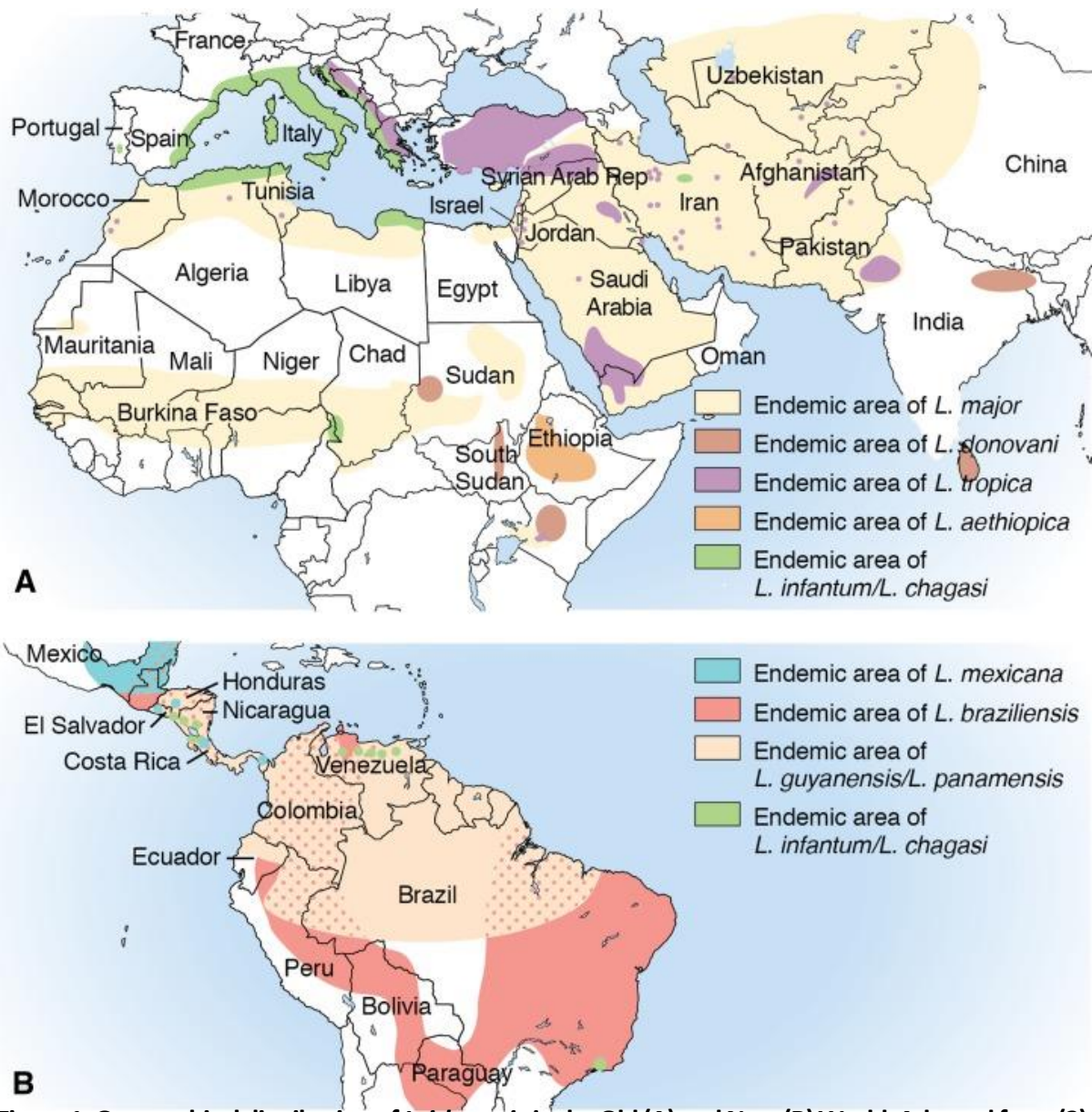


Figure 1: Geographical distribution of *Leishmania* in the Old (A) and New (B) World. Adapted from (3).

1.1.1. Parasite life cycle

Figure 2 summarizes the life cycle of *Leishmania*. Flagellated, extracellular *Leishmania* promastigotes are transmitted to humans via the proboscis (feeding apparatus) of infected female sandflies as they take a blood meal. After ingestion of the pathogen by macrophages (and to a lesser degree, other immune cells), the parasite transforms into its immobile, intracellular amastigote life stage within the phagolysosome. Parasite proliferation leads to host cell lysis and uptake by other phagocytes, causing and maintaining re-infection. When a naive insect bites an infected individual and takes a blood meal, the amastigotes transform to again promastigotes in the sand fly gut (4, 5).

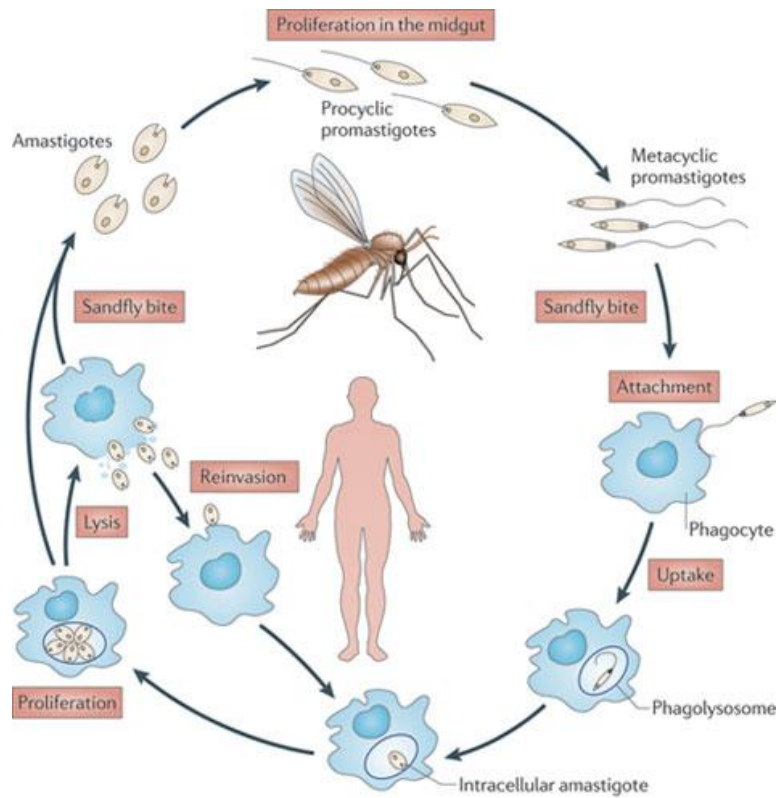


Figure 2: *Leishmania* life cycle in humans (5)

1.1.2. Vectors and transmission

The vectors of transmission are tiny (2-3 mm), blood-feeding (female) insects called sand flies, of the genus *Phlebotomus* (in Asia, Africa and the Mediterranean Basin, 'Old World') and *Lutzomyia* (in the Americas, 'New World'). The epidemiology of leishmaniasis is diverse and complex, with variations in types of sand fly vectors (6), transmission cycles (zoonotic and anthroponotic) (7), animal reservoirs (including dogs, mice and possums) (8), causative *Leishmania* species and environments (rural and urban) (9).

1.2. Cutaneous leishmaniasis (CL)

1.2.1. Clinical manifestations

Clinical features of CL vary in severity and outcomes, depending on factors relating to the host, the sand fly vector and the parasite. An overview of the taxonomy of *Leishmania* in relation to clinical manifestations is shown in figure 3 (10).

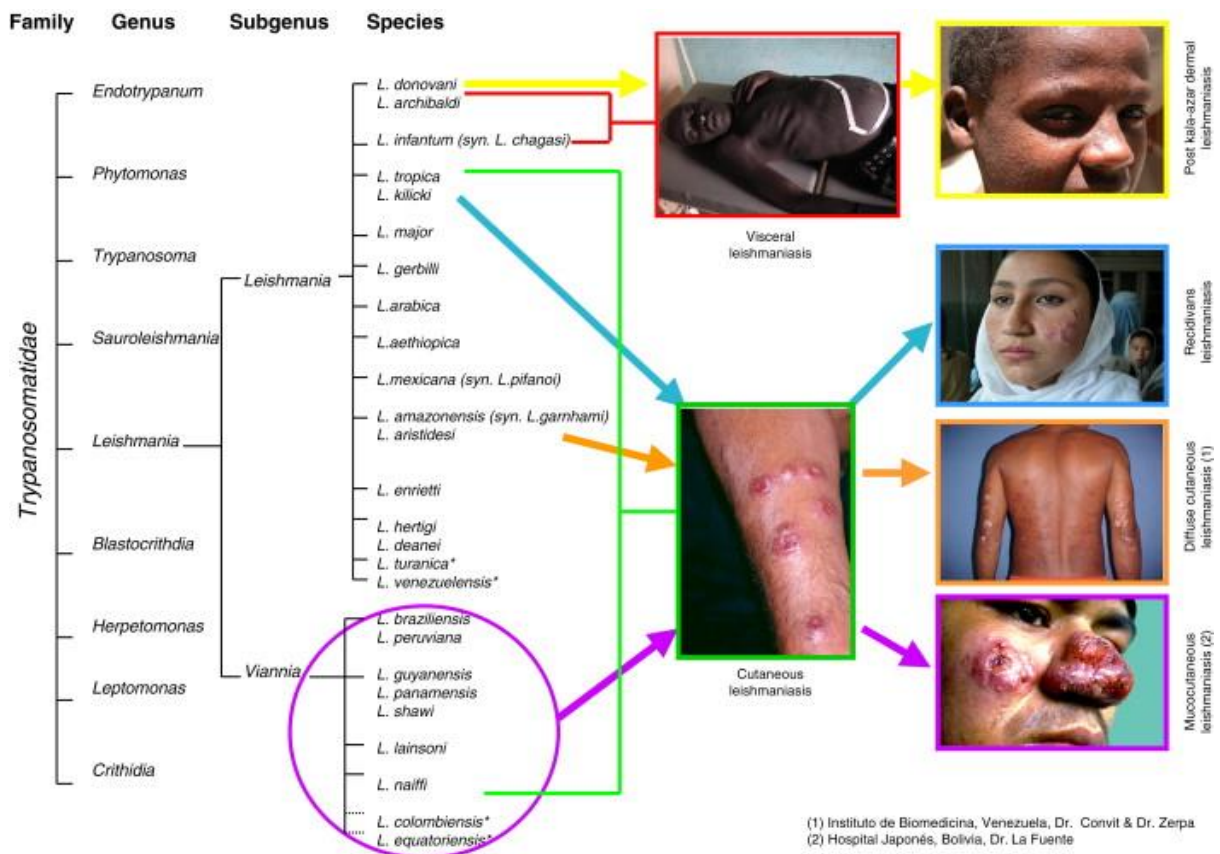


Figure 3: Taxonomy of *Leishmania* in relation to clinical manifestations (10).

Simple, uncomplicated CL (green in figure 3) is the most common form. It is characterized by disfiguring skin lesions on exposed body parts (face, arms, legs) which often self-heal within months to years. While rarely fatal, the resulting ulcers leave permanent scars, disability and stigma (11). Lesions and scars are associated with psychological and psychiatric conditions (depression, anxiety and low self-image), social exclusion (education, work and marriage) and an overall significantly lower quality of life (12, 13). The most common Old World (Middle East, Africa, Europe) species include *L. major*, *L. tropica*, *L. aethiopica*, while New World (the Americas) species include *L. mexicana*, *L. amazonensis*, *L. panamensis* and *L. braziliensis*.

The prevalence of complex CL is lower, but the related morbidity and mortality are far more severe. In leishmaniasis recidivans (LR, blue in figure 3), chronic ‘satellite lesions’ with a plaque-like appearance surround initially healing lesions. In diffuse CL (orange in figure 3), parasites disseminate through the skin and cause numerous non-ulcerated nodules. If the pathogen spreads to the mucosa of the nasal-oral cavity and/or laryngopharynx, a tissue-destructive form called mucocutaneous leishmaniasis (MCL, purple in figure 3) can develop.

An outsider in this array of skin pathologies is post-kala-azar dermal leishmaniasis (PKDL, yellow in figure 3), a cutaneous sequel after curing of VL (red in figure 3) (14).

1.2.2. Immunopathology

We will focus on the disease progression of a single CL lesion because it is the most common clinical presentation and the human disease phenotype that is mimicked in the animal models of infection. Figure 4 gives an overview of the developmental stages of local CL (15). Single (or a limited number of) lesions form at the bite site of the parasite-infected female sand fly. A small papule forms, which develops into a nodule that forms a crusted ulcer. Eventually, after shedding of the crust and removal of the epidermis, an open wound with raised borders and crater-like appearance appears. Alternatively, non-ulcerative, erythematous nodules or crust-like plaques can occur.

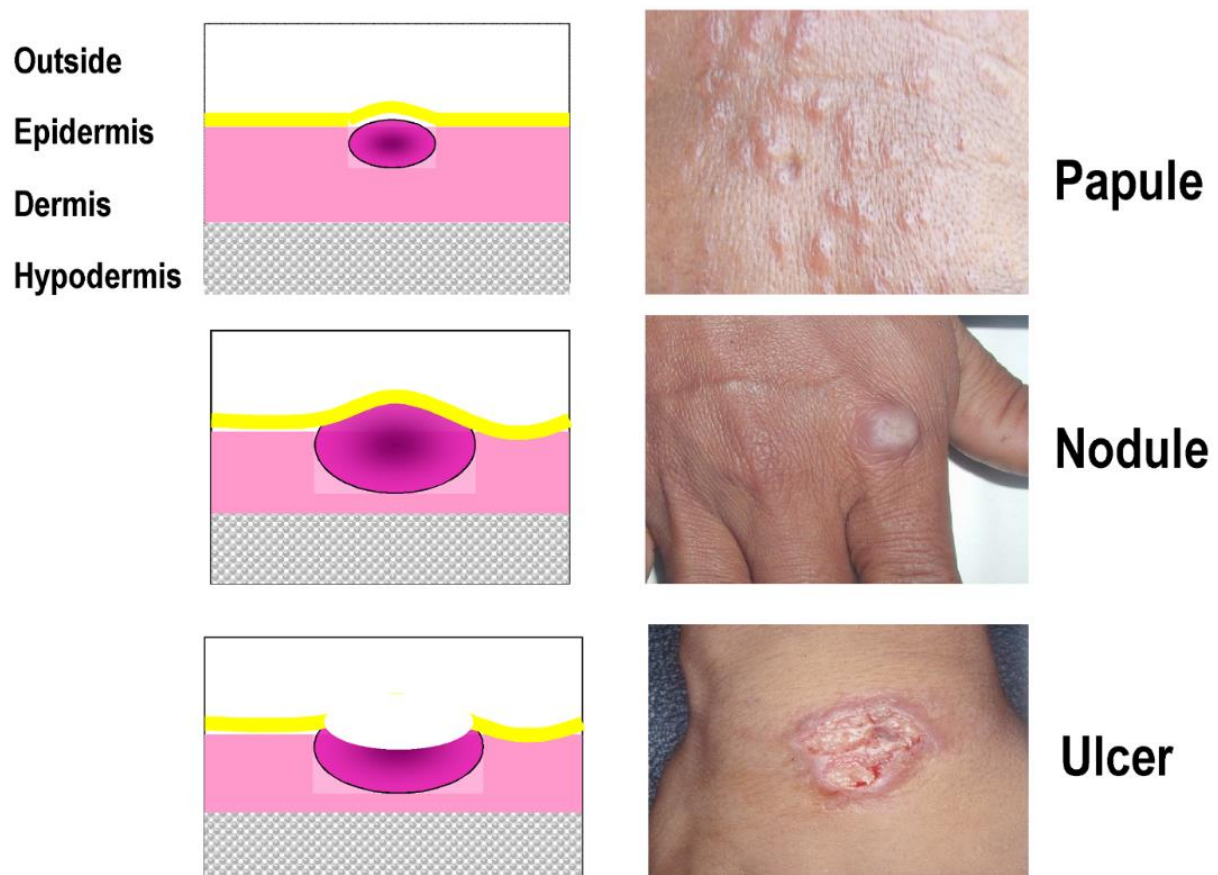


Figure 4: Disease stages in CL and involvement of the different layers of the skin (15)

Tissue damage and disease in CL are primarily caused by an excessive host immune response against the intracellular infection of macrophages by *Leishmania* (16). Figure 5 shows a hematoxylin-eosin (H&E) stain of a local CL skin lesion in the nodular stage of development. The intracellular amastigotes can be predominantly found within macrophages in the upper dermal layers of the lesion (figure 5, bottom left).

As the dermis fills with a dense and diffuse mixed inflammatory cell infiltrate (including macrophages, lymphocytes, neutrophils, mast cells and plasma cells), the associated oedema drives swelling of the tissue (17, 18). Epidermal changes (hyperkeratosis, acanthosis and degeneration of the basal layer) and damage to the connective tissue damage (collagen matrix disruption) occur (19, 20). Healing of the lesion is associated with the generation of the appropriate immunological TH1-response and the related cytokines such as IFN- γ , TNF- α and IL-12 (21, 22): recruitment of leukocytes and activation of macrophages results in necrosis and the formation of generally non-caseating granuloma (23).

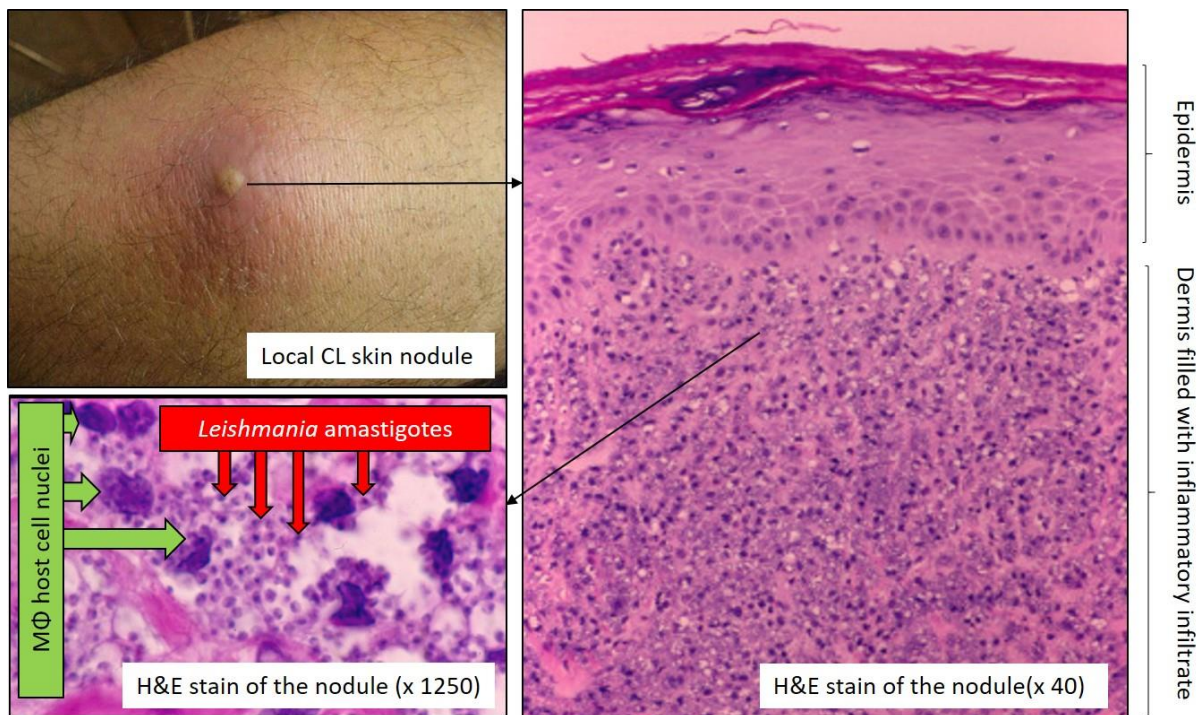


Figure 5: Histology (H&E stain) of a single CL nodule on the arm of a patient (upper left). The x 40 magnification shows a dense inflammatory infiltrate within the dermal layer of the skin (right). Higher magnification (x 1250) reveals the intracellular *Leishmania* amastigotes (red arrows) within the phagolysosome of macrophages (green arrows point at host cell nuclei) located in the upper layers of the dermis (derived from (20)).

1.2.3. Species-specific differences

Figure 6 illustrates the clinical polymorphism of CL. The immunopathology of local CL shows both similarities (chronic, often ulcerative dermatosis) and differences (clinical presentation, incubation and resolution time) among different causative *Leishmania* species. For example, the anthroponotic Old World species *L. tropica* occurs in urban settings and is typically responsible for 'dry' (crusty, plaque-like) lesions, which slowly appears and cures over the course of 10-14 months (24). Zoonotic *L. major* is mostly found in rural villages and associated with larger, 'wet' (stronger inflammation and exudation) lesions that heal over 3-4 months (25, 26). Many New World form round lesions sometimes described as "weeping" or "pizza-like", such as *L. braziliensis* (27, 28). *L. mexicana* often causes chronic "Chiclero's ulcers" on the face or ear, which resolve over months, up to years (29, 30). In this work, we have used two mouse models of CL: Old World *L. major*-BALB/c and New World *L. mexicana*-BALB/c.

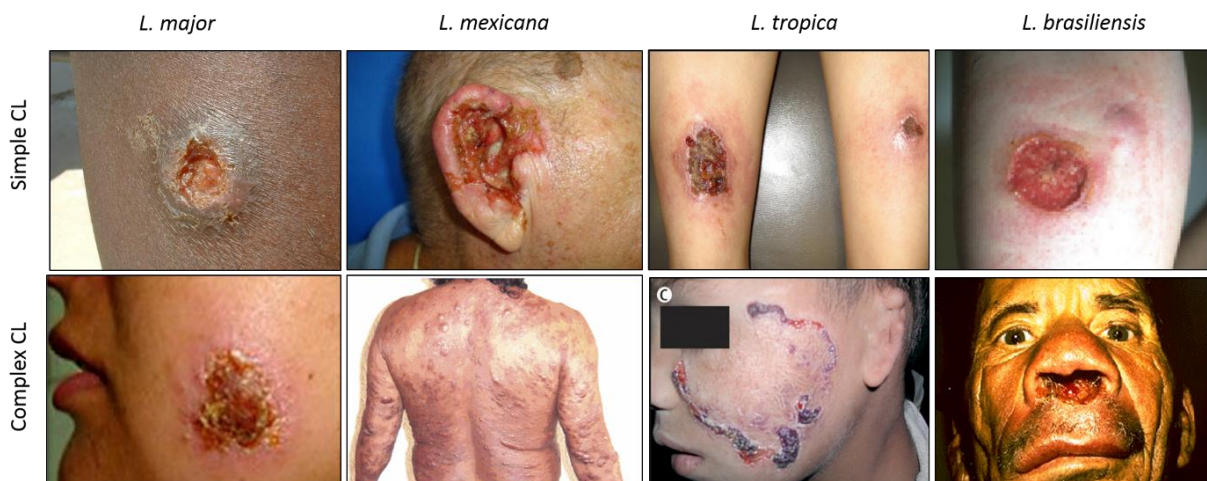


Figure 6: Clinical polymorphism of CL caused by different *Leishmania* species (14, 24-30).

1.3. Current treatment of CL

In contrast to VL, CL is rarely a fatal disease. However, the skin lesions and resulting scars cause considerable morbidity due to social stigma and psychological burden. In addition, the economic impact on individuals and communities in endemic areas is significant (11-14). The primary goal of treatment is to eliminate the causative parasites to accelerate wound healing and reduce the risk of scarring, while also preventing relapses, parasite dissemination and secondary infections. From an epidemiological and public health point of view, treatment of the patient reservoir is important to limit further transmission of the disease (31).

There is no universally applicable therapy for CL: the drug, dose and duration depend on factors such as the parasite, the host and the clinical presentation. The World Health Organization (WHO) has specific recommended clinical regimens based on the diagnosed parasite species (32-35) and different treatment guidelines for CL in the New (36) and the Old (37) World. Treatment can consist of (i) chemotherapy (direct killing of the parasite with antileishmanial drugs), (ii) local physical treatments (exposure of the thermosensitive pathogens in the skin to cryo- or thermotherapy) or (iii) immunotherapy (modulators that induce a host effector immune response against *Leishmania*) (38).

Figure 7 shows the current treatment strategies for the different forms of CL and their limitations. The available chemotherapeutics can be divided into systemic (transport of the drug to the infected skin via the blood) or local (direct application of a topical formulation to the lesion) treatments. Local treatment is attractive for the management of mild disease and has the potential advantages of reduced systemic toxicity, outpatient care, ease of use and high drug exposure at the site of action (the infected dermis underneath the skin lesions). Systemic treatments (injections or oral formulations such as tablets) come at a higher risk of adverse effects and are typically reserved for patients with more severe disease (3), including:

- Large (> 5 cm), multiple (>4) or disseminated lesions
- Disabling and immobilizing lesions (joints, feet)
- Disfiguring and mutilating lesions on cosmetically sensitive areas where the application of local treatments is challenging (face, lips, ears, eyes)
- Lesions that do not respond to local treatment
- Lesions caused by parasites associated with the risk of mucosal (many *Leishmania Viannia* species), chronic (*L. tropica*) or diffuse (*L. aethiopica*) syndromes.
- Immunosuppressed patients

In some cases, treatment is not required. Many simple CL cases with small (< 1 cm), uncomplicated, single lesions self-heal over a couple of months. Therefore, there can be a negative risk-benefit ratio to expose patients to the currently available drugs, many of which, as the following sections will show, have major limitations: variable efficacy, considerable toxicity, invasiveness or high cost (39).

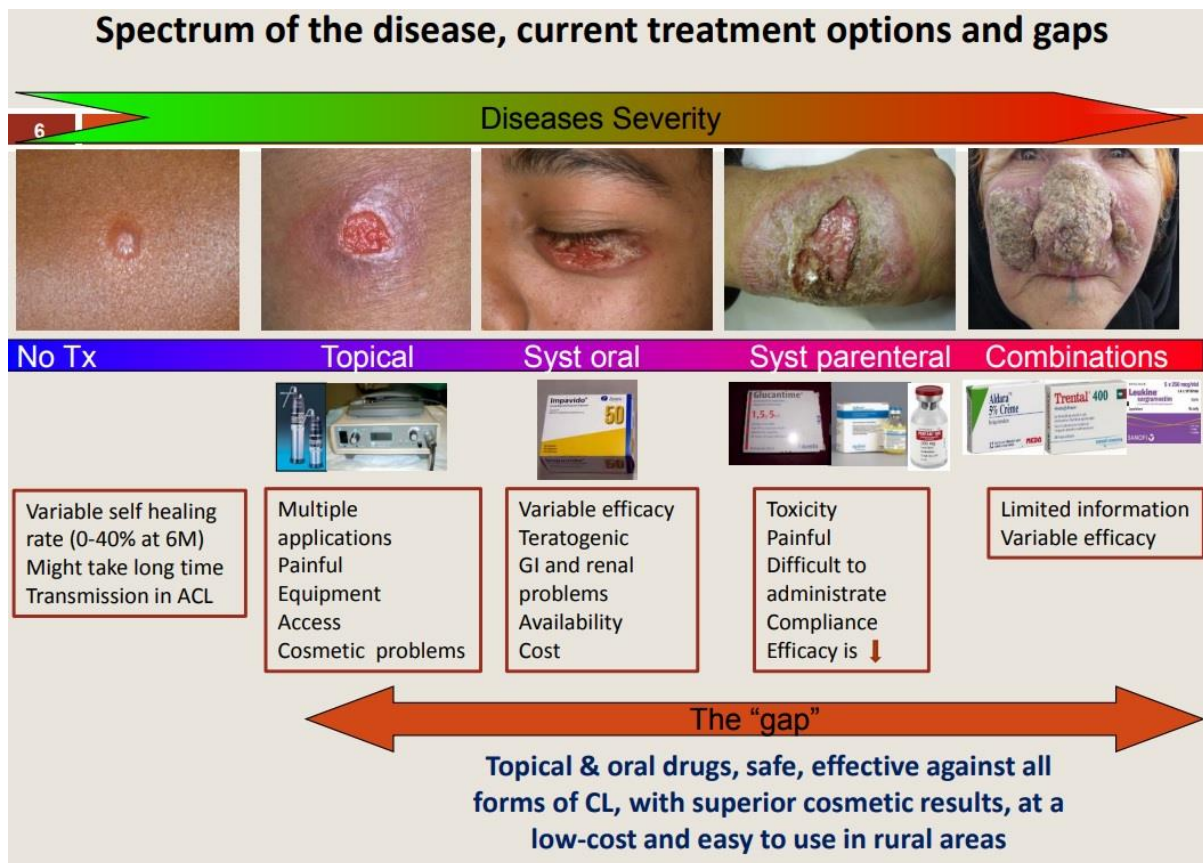


Figure 7: Treatment strategies for the different forms of CL and their limitations (39). Syst=systemic. Tx= treatment. ACL=asymptomatic CL.

1.3.1. Systemic chemotherapeutics

1.3.1.1. Pentavalent antimonials

Pentavalent antimonials (Sb^V) have been the standard of care for CL since their development in the 1940s (40). Sodium stibogluconate (Pentostam[®], GSK and generics) contains 100 mg/ml Sb^V , whereas meglumine antimoniate (Glucantime[®], Sanofi) contains 85 mg/ml (figure 8) (41). The drugs are typically administered via injections into the edges of the skin lesions (~ 1-1.5 ml, every 2-3 days for up to 2-3 weeks), with or without supplementary thermo- or cryotherapy. These Sb^V injections are associated with local inflammation, burning sensations and malaise and many patients struggle to complete treatment (32). In complex CL, antimonials can also be administered systemically (intramuscularly or intravenously at 20 mg/kg daily for 10-20 days), but close clinical monitoring is required due to the risk of hepatic- and cardiotoxicity (10). While there is some evidence for the efficacy of pentavalent antimonials in CL, large, high quality and placebo-controlled randomized clinical trials are lacking (36, 37). In addition, therapeutic outcomes vary in the different endemic regions of CL. *In vitro* studies confirmed variable *in vitro* susceptibility of *Leishmania* species to Sb^V (42,

43). In addition, in a clinical trial in Guatemala, the cure rates after treatment with Pentostam® were higher for *L. braziliensis* compared to *L. mexicana* CL (44).

Despite being used against leishmaniasis for over seven decades, the molecular and cellular mechanism(s) of action of the antimonials remain poorly understood. Three models have been proposed. The prodrug model states that Sb^V is reduced by macrophages or amastigotes to a much more toxic/active metabolite, the trivalent form (Sb^{III}). This interferes with the redox homeostasis by inhibition of the trypanothione reductase system and leaves the parasites vulnerable to oxidative stress (45, 46). Alternatively, DNA fragmentation could lead to apoptosis of the pathogen (47). According to another model, Sb^V exerts intrinsic antileishmanial activity by inhibition of type I DNA topoisomerase, leading to a depletion of intracellular ATP and reduced biosynthesis of macromolecules. A final model postulates that antimonials clear intracellular *Leishmania* via activation of the host immune system (48).

The pharmacokinetics of sodium stibogluconate in CL after intramuscular administration to patients are characterized by relatively rapid and complete drug uptake into the skin lesions, albeit slower and lower than in blood. Comparing affected and healthy skin, the CL infection does not seem to have a major influence on Sb^V accumulation at the target site (49). The PK profile of Sb^V could be described by a one-compartmental model with a volume of distribution (Vd) of 45.7 l, a plasma half-life ($T_{1/2}$) of 9.5 h and a renal clearance of 12.7 l/h. Analysis of distribution patterns of area-under-curve (AUC) among patients suggested the existence of rapid and slow drug eliminators, partly explaining the variability in therapeutic response after antimonial treatment of CL (50).

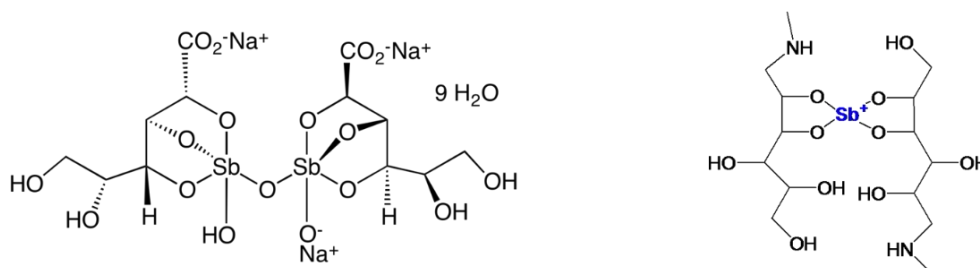


Figure 8: Chemical structure of sodium stibogluconate (Pentostam™, left) and meglumine antimoniate (Glucantime™, right). Pentavalent antimonials typically require three weeks of painful injections into the lesions (photos).

1.3.1.2. Miltefosine

Miltefosine (MF, figure 9), is an alkylphosphocholine and the only oral drug available for the treatment of leishmaniasis. It is used in VL and complex cases of CL (2.5mg/kg/day for 28 days) (51)). Phospholipids such as MF were originally developed as anti-cancer chemotherapeutics, but their antileishmanial activity was discovered in the 1980s (52). The efficacy of MF varies among CL-causing parasite species, explaining variability in clinical settings. Cure rates in randomized clinical trials in Colombia were 91 % against *L. panamensis* (38% in placebo group), while those in similar studies in Guatemala were only 53 % against *L. mexicana* and *L. braziliensis* (32 % in placebo group) (53). In Iran, the efficacy of MF against *L. major* was similar to that of intramuscular meglumine antimoniate (81%) (54). *In vitro* laboratory studies confirm intrinsic differences in drug susceptibility among *Leishmania* species (55).

The mode of action of MF against *Leishmania* is currently unclear. Direct interaction with the parasite membrane (56), inhibition of phospholipids synthesis (57), mitochondrial dysfunction (58) and induction of apoptosis-like cell death (59) have been proposed.

While the registration of MF in India as the first oral antileishmanial in 2002 was considered a breakthrough in the treatment of VL, access today in various regions of endemic for CL remains problematic. Shortages due to faulty supply chains, substandard generic formulations and variable prices (\$ 50-200 in many developing countries, up to \$ 10000-50000 in the EU and the USA) cause issues related to availability and affordability (60).

In terms of pharmacokinetics (PK), MF is the most-studied drug in CL pharmacotherapy. A PK clinical trial in Colombia revealed that overall MF exposure (AUC) in children was significantly lower than in adults, while *in vitro* susceptibility of the parasites (predominantly *L. panamensis*) was similar in both groups. Thus, optimized treatment regimens for CL in pediatric populations might be required (61, 62). The PK of MF is characterized by high protein binding properties (>95%), its exclusive metabolism by phospholipase D and very slow removal from the body ($T_{1/2}$ = 7 days, total elimination after 31 days). This last property causes concern for its general therapeutic use in elimination programs, due to the teratogenicity and the risk of the emergence of resistance. Moreover, while this oral drug is generally relatively well-tolerated, gastrointestinal side effects such as vomiting and diarrhoea are common (63).

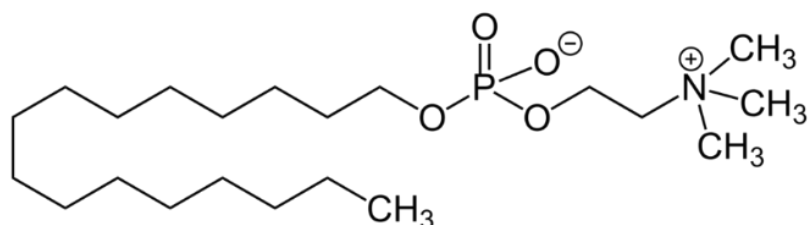


Figure 9: Miltefosine - chemical structure and capsules

1.3.1.3. Amphotericin B

Amphotericin B (AmB, figure 10) is a polyene antibiotic used in the treatment of leishmaniasis. AmB is mainly reserved for complex cases of CL (such as MCL) and is administered via slow intravenous infusion of deoxycholate (0.7 mg/kg/day for 25-30 days) or liposomal formulations (2-3 mg/kg/day for a total dose of 20-40 mg/kg) (32).

AmB was discovered in the 1950s as a macrolide derived from *Streptomyces* cultures with potent antifungal activity. It was licensed and introduced on the market in 1959 as a sodium deoxycholate solution (DAmB, for intravenous use) that forms a micellar suspension when reconstructed in saline. DAmB remained the gold standard for invasive fungal infections for decades. However, this formulation suffers from dose-limiting nephrotoxicity and fever, anaemia, malaise and abdominal pain side effects (64).

To overcome such issues, different new formulations based on lipid carrier systems with reduced toxicity have been developed since the 1990s. These include lipid complexes (Abelcet) colloidal dispersions (Amphocil) and liposomes (AmBisome, Fungisome) (65). AmBisome (LAmB), a unilamellar liposome marketed by the pharmaceutical company Gilead Sciences (US), has a superior efficacy and safety profile than conventional AmB and has been commercially the most successful (66). However, the cost (up to \$ 250 per vial) and challenging logistics (cold chain) severely hamper access to LAmB in many primary health care settings (67). In 2016, a partnership between Gilead and WHO resulted in a \$ 20 million drug donation over 5 years for the treatment of VL (68).

As is the case in fungi, the mode of action against *Leishmania* is related to complexation of the drug's hydrophobic polyene region with ergosterol in the plasma membrane of the pathogen. After binding, pores are formed that cause a collapse of ion gradient and consequent death of the parasite (69, 70). Recent research has suggested an alternative mechanism: large, extramembranous aggregates of AmB extract ergosterol out of the lipid bilayers, rather than forming channels within them (71). Interestingly, AmB also exerts immunomodulatory effects. After binding to Toll-like receptors, it induces oxidative stress in immune cells (including macrophages, neutrophils, natural killer cells, B-cells and T-cells) and alters expression of several cytokines and chemokines leading to (predominantly) pro-inflammatory responses (64, 72, 73).

The activity of the different lipid formulations of AmB has already been compared in the *L. major*-BALB/c mouse model of CL: the efficacy of AmBisome was superior to that of Abelcet and Amphocil. However, *in vitro* activity was higher for Amphocil than for AmBisome and Abelcet (74, 75). The pharmacokinetics of DAmB and LAmB differ greatly, as shown by studies in both rodents (76, 77) and humans (78, 79). After IV administration, DAmB reaches the peripheral tissues more rapidly than LAmB, but its systemic circulation is shorter for the non-liposomal form. In contrast to DAmB, with its narrow therapeutic margin, LAmB can achieve high yet safe plasma and tissue levels (80). Elimination patterns from the body are similar for both formulations, with a tri-phasic kinetics and a primary plasma half-life of around 6 hours.

The underlying pharmacological and physiological mechanisms that could explain the variable therapeutic outcomes of different pharmaceutical formulations of AmB in CL were investigated in chapters 3.2, 3.3 and 3.4. Please note the similar and possibly confusing trade names of AmB deoxycholate (Fungizone) and the multilamellar AmB liposome (Fungisome).

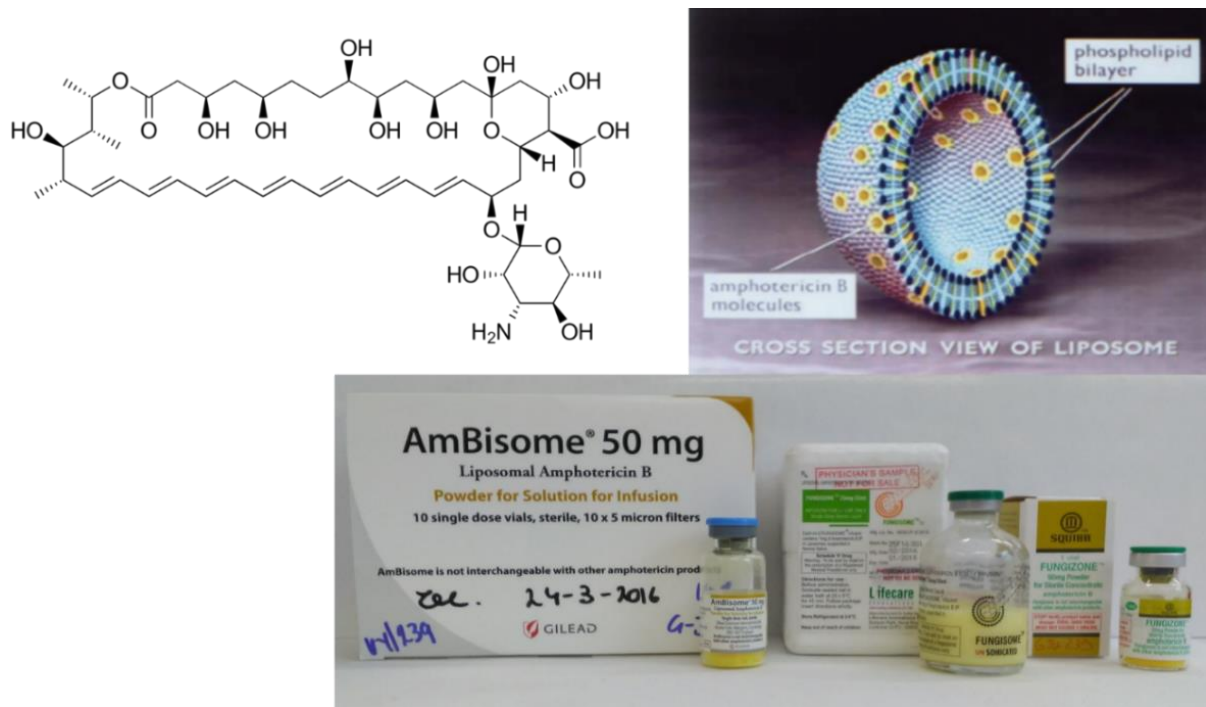


Figure 10: Amphotericin B – chemical structure and the different formulations AmBisome® (unilamellar liposome of AmB), Fungisome® (multilamellar liposome of AmB) and Fungizone® (deoxycholate salt of AmB) for intravenous infusion.

1.3.1.4. Pentamidine

Pentamidine (figure 11), a synthetic derivate of amidine, is a systemic second-line drug for New World CL, specifically for *L. guyanensis* and *L. panamensis* (32). It has also been used to treat *Pneumocystis carinii* infections in AIDS patients and sleeping sickness. The drug is administered as an isethionate salt via the intramuscular or intravenous route at 4 mg/kg (salt) every other day for 3 doses (81, 82). The mechanism of action is poorly understood, but interference with *Leishmania* DNA synthesis and the mitochondrial membrane have been suggested. The pharmacokinetics of the drug are best described by a 2- or 3-compartmental model, with rapid and extensive tissue distribution, predominant hepatic metabolism and biliary clearance. No data is available on drug accumulation in the skin. Pentamidine has been progressively abandoned in the treatment of leishmaniasis due to severe adverse effects including shock, hypoglycemia, diabetes mellitus, myocarditis and nephrotoxicity (62).

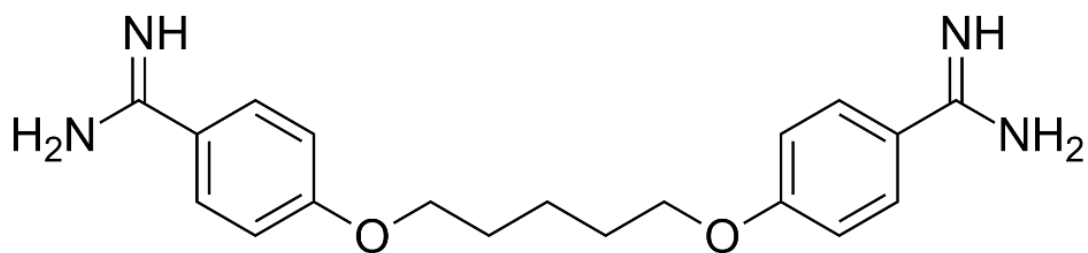


Figure 11: Pentamidine – chemical structure

1.3.1.5. Azoles

Fluconazole and ketoconazole (figure 12) are oral imidazole antifungals that are also used in the 2nd-line treatment of CL. There is some evidence to recommend fluconazole for *L. major* therapy (200 mg oral, daily for 6 weeks) and ketoconazole for *L. mexicana* and *L. panamensis* (600 mg oral, daily for 28 days) (32). However, overall clinical experience with these drugs in CL remains limited: a recent systematic review concluded there is insufficient evidence to support the use of azole therapy as a single agent for leishmaniasis treatment (83). The mechanism of action against *Leishmania* is identical as for fungi: inhibition of ergosterol synthesis, leading to cell membrane instability and death. Adverse effects of azoles include gastrointestinal symptoms and hepatic toxicity (62). Interestingly for the treatment of CL, fluconazole concentrations in plasma and dermis after oral dosing are similar and exposure in the skin is prolonged due to a high binding affinity for the stratum corneum (84, 85).

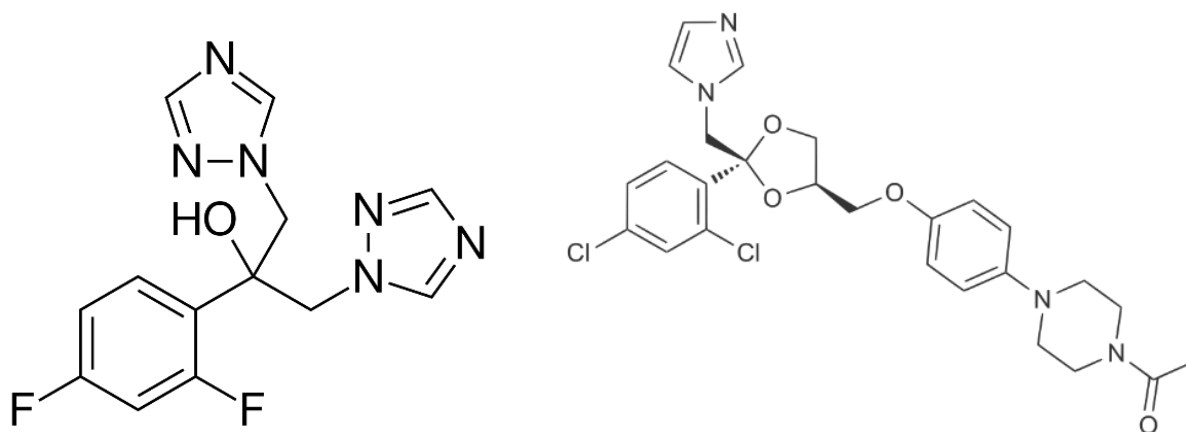


Figure 12: Fluconazole (left) and ketoconazole (right) – chemical structure

1.3.2. Local chemotherapeutics

1.3.2.1. Paromomycin

Paromomycin (PM, figure 13), also known as monomycin or aminosidine, is a broad spectrum aminoglycoside antibiotic. PM is used as a sulfate salt in the treatment of both VL (11 mg/kg for 21 days, IM) and local, simple CL (15% PM + 12 % methylbenzethonium chloride (MBCL) ointment twice daily for 20 days, topical) (32). The majority of CL patients are treated with Leishcutan® (Teva, Israel), the only commercially available ointment of topical PM (86). WE279,396 is an experimental, more hydrophilic cream containing 0.5% gentamycin in addition to 15 PM % (87). The antileishmanial activity of PM was discovered in the 1960s (88). In the 1980s, El-On and colleagues demonstrated the excellent efficacy of PM against *L. major* after intraperitoneal (50 mg/kg daily for 10 days) and topical (2x daily for 10 days) drug administration in mice (89), followed by promising results in humans (90). Topical 15% PM + 12% MBCL was also active in mice infected with New World species such as *L. mexicana*, but inactive against *L. panamensis* and *L. amazonensis* (89). A meta-analysis of 14 randomized trials concluded that topical PM+MBCL could be a therapeutic alternative to antimonials in uncomplicated Old World CL, while no existing data support use in New World CL (91). Clinical trials for WE279,396, with or without gentamycin, failed to show an increased cure rate compared to placebo.

The exact antileishmanial mode of action for PM is poorly understood. Research has suggested inhibition of protein synthesis (92), energy metabolism (93) and vesicle-mediated cellular trafficking (94).

Penetration of topically applied PM into the skin lesion is challenging: the large (molecular weight = 714 g/mol), hydrophilic compound requires quaternary ammonium compounds such as MBCL to enhance permeation across the epidermis. Unfortunately, MBCL is also the responsible agent for local irritation and side effects. Some clinical trials (87) give a misleading representation of the skin pharmacokinetics of topical PM, for example by manual removal of the crust or wound debris from the lesion, exposing the infected dermis directly. In patients with CL treated once daily for 20 days with topical PM creams with or without gentamycin, the estimated dose absorbed was 10-12 % and systemic exposure is limited ($C_{max} = 0.6-1 \mu\text{g/ml}$) (95). Little is known about the differences in skin penetration of PM formulations in early closed nodules with intact skin, crusted lesions with early skin damage or open ulcerative wounds, or how to best use topical treatments for the different disease forms of CL in general.

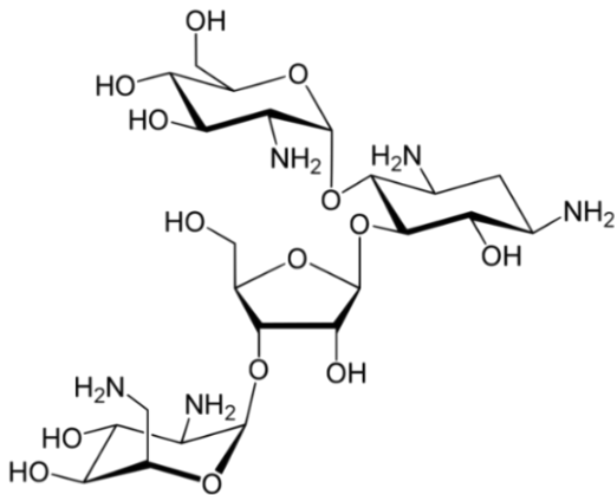


Figure 13: Paromomycin – chemical structure and ointment

1.3.3. Physical treatments

Thermo- and cryotherapy are physical therapies with the aim to eliminate the CL-causing parasites by temperature rather than by chemotherapy. This could overcome many of the limitations of antileishmanial drugs, which are related to adherence, cost, contraindications and side effects (32). In thermotherapy, heat is induced in the superficial skin layers by ultrasound, radiofrequency or infrared radiation. Typical treatment involves 30 seconds of exposure at 50 °C once per week for one month (96, 97). During cryotherapy, a cotton swab dipped in liquid nitrogen is applied to the lesion for 10-25 seconds for several weeks (98). A recent meta-analysis of 8 randomized trials showed that thermotherapy is not inferior to intralesional antimonials and the two could be used in combination for the treatment of CL (99). Issues related to these treatments include the need for expensive equipment, trained staff and electricity, which could be an issue in the remote CL-endemic regions.

1.3.4. Immunotherapy

Immunotherapy could be a useful adjunct to chemotherapy to stimulate the host immune response to clear the parasite from the system (100). Imiquimod is an imidazoquinoline immunomodulator that is on the market for the treatment of genital warts as a topical cream called Aldara (Meda Pharma, UK). During a phase II trial for CL in Peru, it was found to be safe, enhance the efficacy of pentavalent antimony and reduce scarring (101). Cytokine granulocyte-macrophage colony stimulating factor (GM-CSF) is another topical immunomodulator that supports wound healing. In Brazilian CL patients, GM-CSF in combination with antimonials reduced the healing time of lesion compared to antimonials alone (102).

1.4. Treatment challenges in CL

CL is one of most neglected of the neglected tropical diseases (NTD), an umbrella term for a diverse group of infectious diseases that affect around 2.7 billion people living on less than \$ 2 per day (103, 104). This causes a number of major issues for treatment, which, as the previous section has shown, currently relies on drugs that are considerably toxic, poorly tolerated, variably effective in different endemic settings or invasive in terms of administration route. These challenges include:

- **The economic reality of pharmaceutical research into NTDs.** Overall, the main challenge for finding new CL treatments is to ensure that the disease is actually on the drug research and development (R&D) agenda and that the necessary leadership, strategy and expertise are provided. Development of a new drug is typically a long (10-15 years) and expensive process: the actual costs is a controversial topic and estimates range widely from \$ 92 to \$ 888.6 million (105-107). Medicines for NTDs are not attractive targets for the profit-driven pharmaceutical industry, as the ability-to-pay of both patients and the healthcare systems is low (60). Unfortunately, without investment, there is no research and thus no new drugs. To make matters more complex, CL is not a single disease (LCL, MCL, DCL, LR) and is not caused by a single parasite (over 15 different *Leishmania* species, with known variability in drug susceptibility). Identifying one drug active against all types of CL is not a simple mission, but if the lucrative market size is smaller, the chance of capturing the interest of major pharmaceutical companies becomes even more limited. Repurposing and reformulation of existing drugs are common strategies to overcome the high costs of *de novo* drug discovery for NTDs (108), including CL. Indeed, the 2nd-line drugs MF, PM and AmB were originally developed as agents against cancer and bacterial and fungal infections, respectively.
- **Access to treatment.** Even if government-funded programs provide CL treatment for free or at a reduced cost, many of the affected people delay their visit to the clinic because health facilities are far from their communities and travel is difficult or expensive (11). This could cause patients to only present in the hospital after local, home-made, or herbal remedies have failed and when lesions are far-advanced and often harder to treat. Additionally, the long duration of therapy, such as the three weeks required for antimonial treatment, keeps them away from work and their ability to provide for their family. In the health care centre, the direct costs of diagnosis, treatment, hospitalization and drug administration add to overall expenditure, contributing to the perpetuation of a vicious cycle of poverty (109).
- **The hidden true burden of CL.** Because the disease often occurs in marginalized populations living in remote areas, the current epidemiological numbers are likely underestimates of the actual prevalence and incidence. According to WHO, CL is only a reportable disease in 40 out of 88 countries where it is considered endemic (2). Moreover, much of the burden of CL is mainly socio-psychological in nature, making

direct quantification of its impact more challenging (11). As a result, overall efforts from authorities for the control of CL, such as stimulating the search for better treatments, are limited.

- **Logistics.** Access to diagnostics and medicines in remote health care centres can be problematic, as can be the thermal stability of drugs and pharmaceutical formulations in tropical climates (110).
- **The standardization and quality of clinical trials.** Many studies are poorly designed and conducted on a small number of participants that are variably diagnosed in terms of *Leishmania* species (while there are known differences in drug susceptibility) and unclear in defining treatment outcomes (which is extremely problematic for an often self-healing disease). Systematic reviews on CL treatments pointed out these issues: Olliaro and colleagues formulated methodological guidelines for a clinical trial for CL (111, 112). Such standardized, randomized and controlled clinical studies are required to evaluate what therapeutic interventions work and are safe for patients. But first, we will need new drug candidates to actually be tested in such studies.

1.5. Drug development for CL

1.5.1. Drug discovery and development

Drug discovery and development is a slow, costly and challenging process. As explained before, for every 100000 compounds screened, only one might make it out of the research and development (R&D) pipeline as a marketed drug, after at least 10 years and an expenditure as high as \$ 2.6 billion (113). Figure 14 gives an overview of the classic drug discovery and development process. During the ‘hit-to-lead’ drug discovery phase, an extensive list of ‘hits’ against a specific target is identified within a library, from which ‘leads’ with the most suitable profile are selected. Leads are tested in terms of activity, safety, metabolism and PK and can be optimized by chemical modification. When a drug candidate is finally selected, the compound is characterized in depth during preclinical development studies. After clinical research in humans (phase I, II and III) and regulatory agency approval, the new medicine reaches the market and its safety in the wider population is surveilled (phase IV) (114). However, attrition rates of new compounds in drug development are high: more than half of the drug candidates fail during clinical trials due to a lack of efficacy, another third due to safety issues and narrow therapeutic index (115). Our poor ability to translate our advances in the biological understanding of human disease into effective new therapeutics and the many failures along the R&D process has been coined as the notorious “valley of death” of drug development (116).

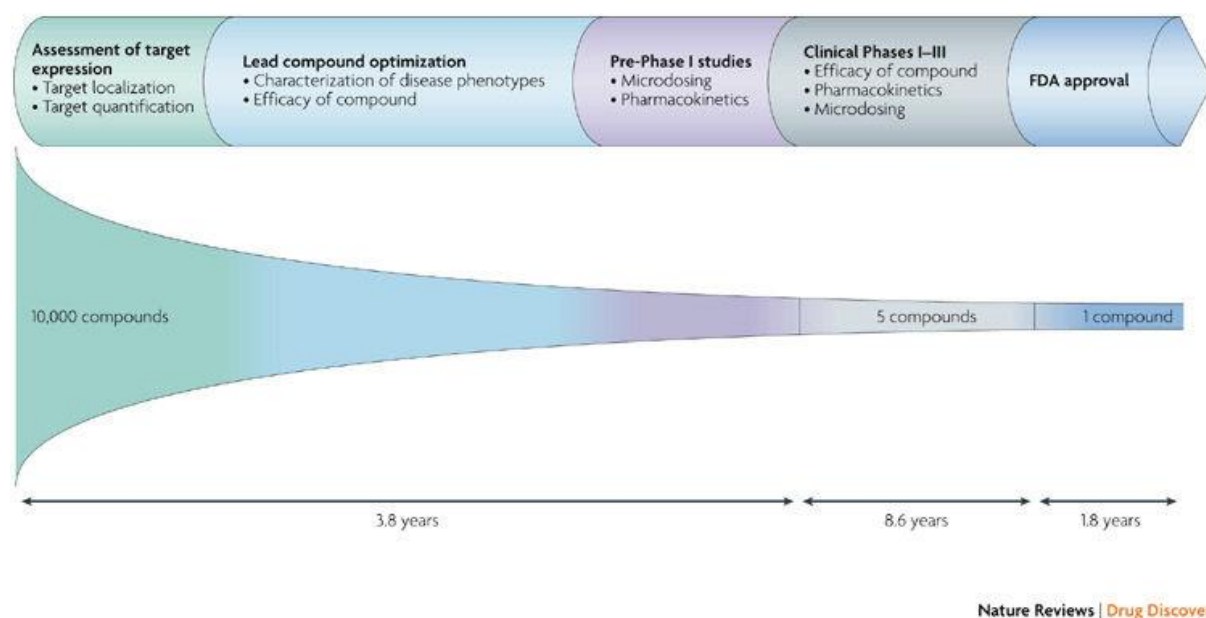


Figure 14: The classic drug discovery and development pathway (116)

Improving the likelihood of clinical success requires the availability of validated predictive models, assays and methodologies during discovery and preclinical development phases. These are tools for screening and evaluation of hits, leads and drug candidates based on specific criteria (117, 118). Setting clear and well-considered go/no-go criteria are crucial to focus time and resources on new chemical entity (NCE) series that stand a reasonable chance of delivering a potential new medicine (119).

This is especially important for drug development for infectious diseases that disproportionately affect populations in the developing world, where financial incentives are limited. Today, two contrasting trends are present in the global infectious disease market: on the one hand, there is an unprecedented growth for the antiviral (hepatitis C, HIV) and vaccine areas. On the other, the antibiotic market has been in decline for decades (120). Annual revenues for antibacterial agents dropped from \$ 15 to \$ 8 billion between 2010 and 2017, due to generic competition and limited innovation in the pipeline (121). Indeed, anti-infectious drug R&D is a therapeutic problem area, due to scientific challenges, regulatory hurdles and low return on investment: a worrying trend in an era of rising antimicrobial resistance. In recent years, many pharmaceutical companies have been gradually reducing their commitment to this field; some, such as Astra Zeneca, even pulled out entirely (122).

Among the infectious diseases, NTDs are a particularly commercially unattractive area for R&D. The overall pipelines for NTDs remain weak and chances that many new drugs for the treatments leishmaniasis, Chagas disease, sleeping sickness or helminthiasis will soon flood the market are minimal (123). Figure 15 shows the number of projects at each stage of discovery and development in 2009.

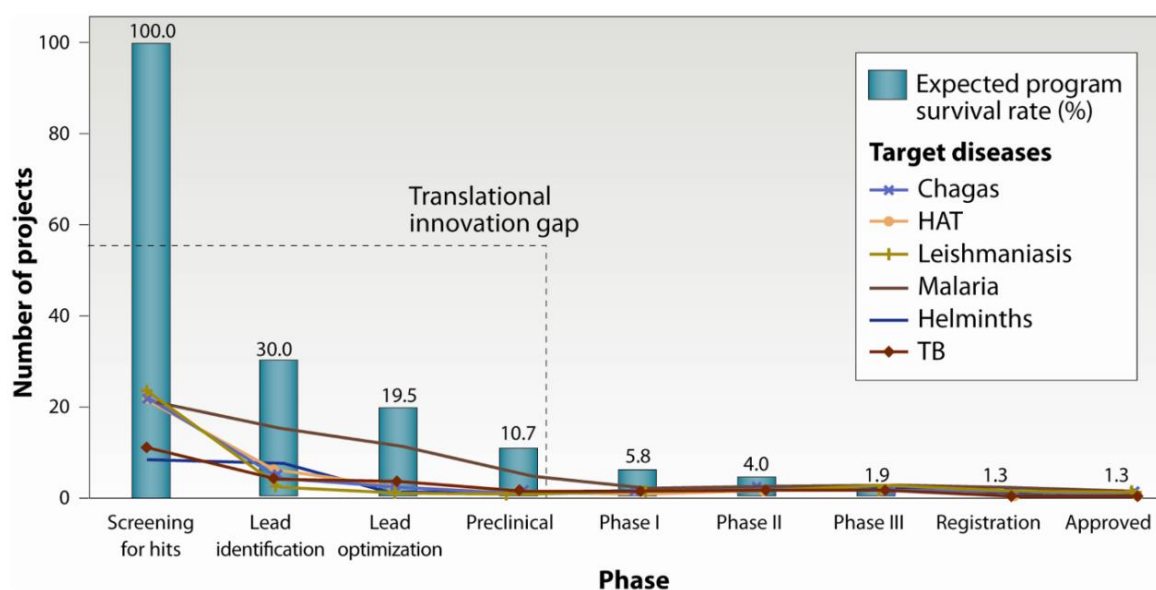


Figure 15: Attrition rate and current R&D pipeline for (neglected) tropical diseases. HAT = Human African Trypanosomiasis (sleeping sickness). TB = tuberculosis. Adapted from (123).

However, events in recent years have given us reasons for cautious optimism.

Around the beginning of the new millennium, public-private partnerships (PPP) such as Medicines for Malaria Venture, Institute for One World Health, Global Health Innovative Technology Fund, TB Alliance and Drugs for Neglected Diseases Initiative (DNDI) emerged (124). These small-to-medium-sized organizations bring together partners from academia, the pharmaceutical industry and the public sector and provide the flexibility and efficiency to quickly move new medicines through the R&D pipeline (125). Since 2003, DNDI has developed seven new treatments and formulations for malaria, pediatric HIV, sleeping sickness, Chagas disease and VL (126). However, a lack of sustainable funding and direct impact evaluations threaten the long-term viability of PPP as a business model to develop new drugs, vaccines and diagnostics for NTDs (127).

Two important events occurred in 2012. The WHO's roadmap "accelerating work to overcome the global impact of NTDs" produced a shared commitment with global pharmaceutical companies to contribute to the control of these diseases of poverty (128). Building on this momentum, the "London Declaration on NTDs" was signed later that year by officials of 13 leading multinational pharma companies, the World Bank, WHO, the Bill & Melinda Gates Foundation and governments from endemic and non-endemic countries. Partners committed to advancing R&D for NTDs by 2020, in addition to expanding and sustaining drug access and donation programs (129).

Finally, 2015 saw the birth of the "Neglected Tropical Diseases Drug Discovery Booster", a consortium with the aim to accelerate, expand and reduce the costs of early-stage drug development for Chagas disease and leishmaniasis. This global collaboration brought together DNDI and six pharmaceutical companies ((Eisai Co Ltd, Shionogi & Co Ltd, Takeda Pharmaceutical Company Limited, AstraZeneca plc., Celgene Global Health and Merck KGaA) to identify new potential anti-parasitic agents in one other's compound libraries (130).

1.5.2. R&D pipeline for CL

In recent years, academic researchers from around the world have identified a plethora of compounds with antileishmanial activity. Some are repurposed (tamoxifen, nelfinavir, imipramine, delamanid, fexinidazole), others are derived from natural products (quinones, pyrimidines, diamidines) and there are novel scaffolds from phenotypic screens (131). The public-private partnership DNDI has a number of new drug candidates in its pipeline for CL (132, figure 16). These novel candidate treatments include:

- **Immunotherapy.** **CPG-D35** oligonucleotides are synthetic, single-stranded DNA molecules that activate immune cells in the skin that could be used alone or in combination treatment for CL. Currently in the preclinical phase.
- **New combinations of current CL therapeutics.** Three weeks of oral miltefosine is currently being tested with or without a single application of thermotherapy (30

seconds at 50 °C) on patients in Peru and Columbia. This could improve efficacy, reduce side effects and shorten the duration of treatment.

- **Three chemotherapeutic lead series** with oral bioavailability and excellent activity in cellular and animal models of leishmaniasis have been identified:
 1. **Aminopyrazoles**, originally explored by Pfizer for the treatment of cancer. Compounds of this class, such as DNDI-5561, are currently in preclinical phases.
 2. **Oxaboroles** (cyclic, boron-containing drugs), initially identified for their antifungal potential by Anacor Pharmaceuticals and developed by DNDI for the human African trypanosomiasis (HAT) and extended to Chagas Disease and leishmaniasis. SCYX-7158 is in clinical phase II/III for HAT, while DNDI-5421 and DNDI-5610 are in the lead (optimization) phases for leishmaniasis. DNDI-6148 has recently entered clinical phases.
 3. **Bicyclic nitroimidazoles** DNDI-8219 and DNDI-0690 (clinical candidate), from a tuberculosis library, show excellent *in vitro* activity and *in vivo* efficacy against VL and CL. Results for another compound, DNDI-VL-2098, were initially promising, but development was discontinued due to observed testicular toxicity.

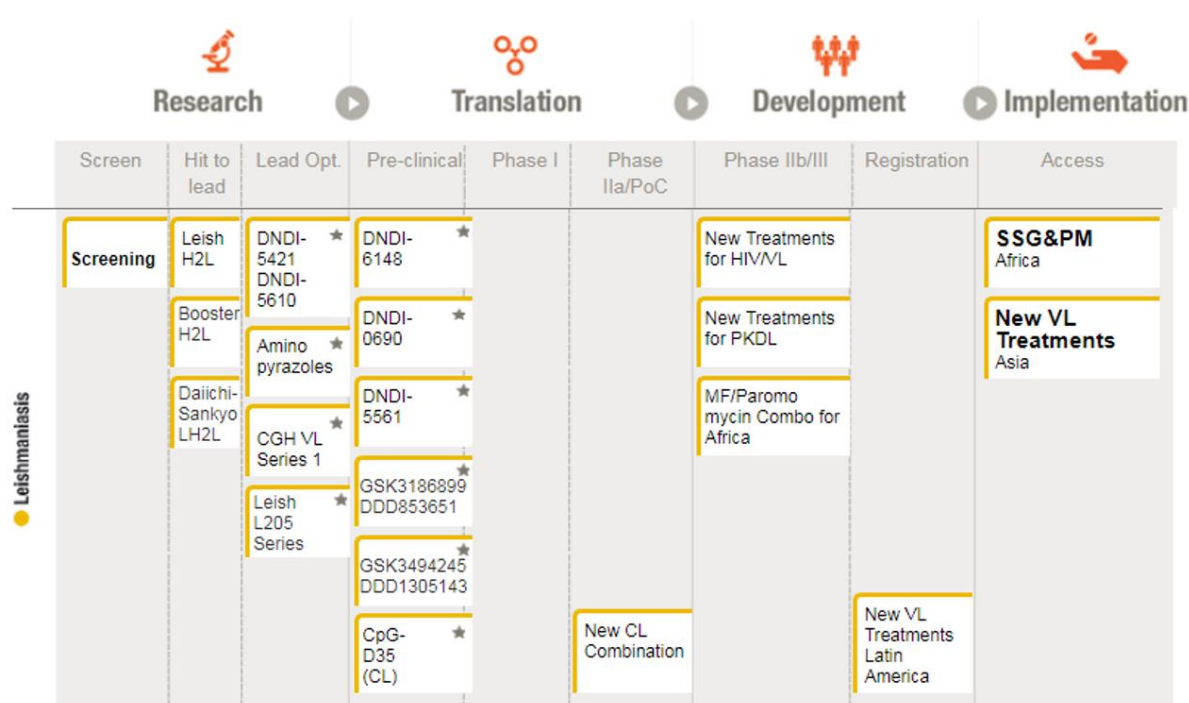


Figure 16: R&D pipeline for leishmaniasis (June 2018, DNDI, 132)

The British pharmaceutical company GlaxoSmithKline, in partnership with the Drug Discovery Unit of the University of Dundee, is collaborating with DNDI on two new chemotherapeutic compounds (**GSK3186899/DDD853651** and **GSK3494245/DDD1305143**) that are currently in preclinical phases of drug development for VL. Finally, apart from DNDI and GSK, the Swiss multinational pharmaceutical company Novartis also has a leishmaniasis portfolio. **GNF6702**, a selective kinetoplastid proteasome inhibitor, is a promising drug candidate for leishmaniasis. In mouse models of VL, the compound demonstrates excellent *in vivo* activity, does not inhibit the mammalian proteasome and is well tolerated at therapeutic doses. Even more exciting is the fact that the molecular proteasome target is conserved among kinetoplastid parasites and GNF6702 is also active against *Trypanosoma cruzi* and *Trypanosoma brucei*. This gives rise to the possibility of a single class of drugs to treat not only leishmaniasis but also Chagas disease and sleeping sickness (133).

While the current R&D pipeline is promising and gives genuine hope for delivering new therapeutics for CL, it is important to remember the sobering attrition rates during the early phases of clinical trials. Therefore, continuous drug discovery efforts and the availability of suitable backup candidates is critical to maximizing the chance of bringing new, safe and effective treatment to patients in the near future (134).

1.5.3. Profile of an ideal CL drug

An ideal new treatment for CL would be safe in all populations, efficacious against all *Leishmania* species, affordable, feasible for use in the field, be of a short time course and be available in an easy-to-use formulation, such as a tablet or a local topical (cream, ointment, spray). Optimal pharmacotherapy may well be a combination of two or more agents (chemotherapy with or without complementary immunomodulators) to maximize efficacy or safety and to minimize treatment duration or the risk of the emergence of antileishmanial drug resistance. Target product profiles play a central role in the entire drug development process to provide focus and facilitate decision-making. An example of a target product profile for CL used by DNDI is shown in table 1 (135).

Table 1: Target product profile for CL (DNDI)

Attribute	Ideal	Acceptable
Target Species		
Species dependent treatment response	One treatment for all species of <i>Leishmania</i>	<i>L. tropica</i> or <i>L. braziliensis</i>
Safety		
Safety monitoring requirement	None	Primary Health Care (minimal contact). No major safety concerns.
Tolerability Common Terminology Criteria for AE ²	Well tolerated All AR's < grade 1	Well tolerated in >95% of patients treated. Systemic AR > grade 2 in <5%. Local AR = grade 2 in <30%. No treatment induced mortality.
Contraindications	None	Can be assessed at PHC level.
Pregnancy	Safe in pregnancy and lactation	Category B ²
Efficacy		
Complete clinical cure at 3 months from treatment onset	>95% patients	60% for <i>L. tropica</i> 70% for <i>L. braziliensis</i>
100% epithelialization / flattening (primary outcome)		
Improved scar formation	Minimal scar	No worse than natural healing
Prevention of relapse and recidivans	No relapse or recidivans/ML	<5% rate of relapse or recidivans/ML at 1 year
Parasitological endpoint requirement	None	None
Drug / Treatment schedule		
Route of administration	Topical / oral	Non-parenteral or few doses if parenteral
Topical	14 days	28 days
Oral	< 7 days	Oral: bid for 28 days
Parenteral	No	3 injections
Target Population		
Age	No restrictions	> 9 months of age

1.5.4. Introduction to the pharmacology of CL drugs

Antileishmanial drug activity in CL is the result of a complex interaction between three pharmacological actors, namely the active drug in the pharmaceutical drug formulation, the *Leishmania* parasite and the host cells and tissues. Figure 17 gives an overview of these relationships.

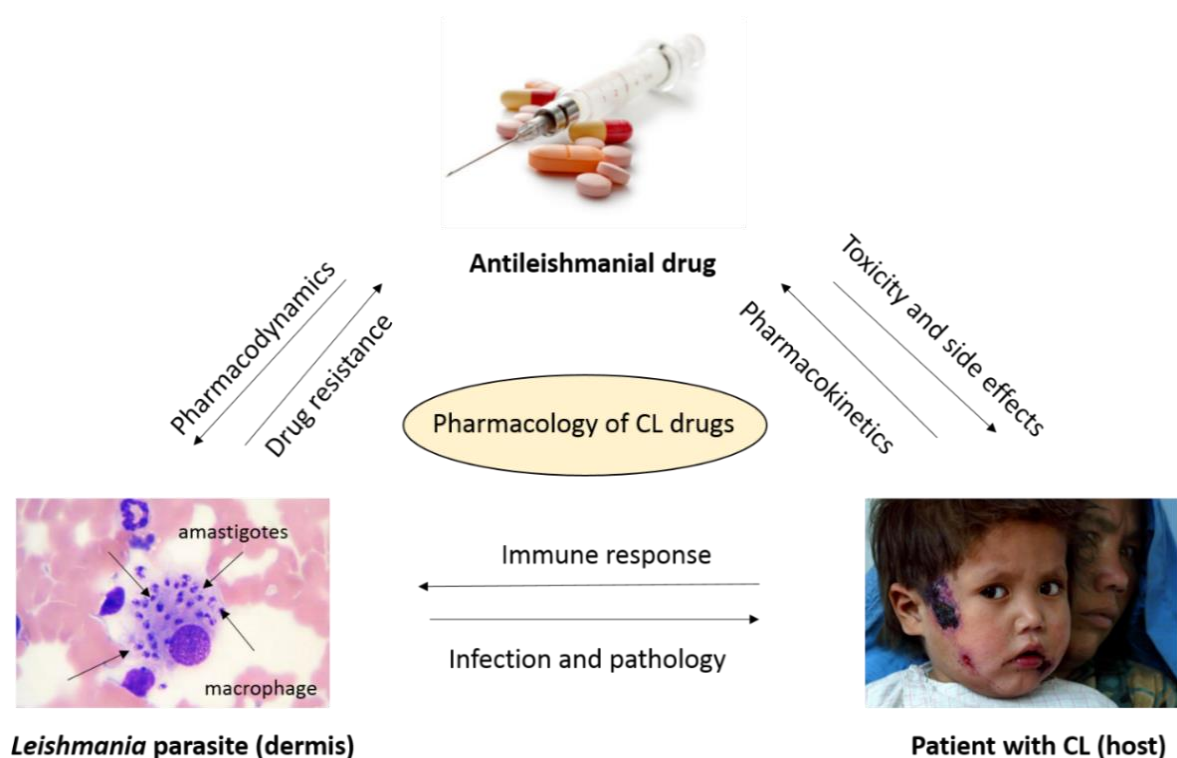


Figure 17: Actors and relationships in the anti-parasitic activity of a CL drug

- Infection and pathology kinetics describe how the presence of the parasite within the phagolysosome of the dermal macrophages affects the host, resulting in skin lesions. In CL, pathology and disease is mainly the consequence of an excessive host immune response against the pathogen: a severe local inflammation and associated oedema cause swelling and damage to the tissue at the site of infection.
- Pharmacokinetics (PK), “what the body does to the drug”, describes the fate of a drug as the host handles it through the mechanisms of absorption, distribution, metabolism and elimination (ADME). Based on the route of administration, this will result in specific drug concentration over time in the bloodstream (systemic exposure), the dermal interstitial fluid of the infected skin (the target site) and other parts of the body (off-target). Mathematical models can describe the behaviour of the drug in the blood (the central compartment) and the tissues (the peripheral compartment). Adequate drug exposure at the site of infection in terms of both concentration and time course are essential for an antimicrobial to exert its activity (136). Achieving the right therapeutic drug exposure is a delicate balance: sub-therapeutic exposure could lead to a lack of efficacy or the emergence of resistant parasite populations, supra-therapeutic drug levels can lead to toxicity and off-target effects. Table 2 lists the most important PK parameters.

Table 2: Overview of fundamental PK parameters

Parameter	Symbol	Description	Unit (example)	Formula
Dose	D	the dose of drug administered	Mg	Design parameter
Dose interval	τ	once per day (QD) twice per day (BD) trice per day (TID)	Per hour, per day	Design parameter
C_{max}	C _{max}	the maximal concentration in a specific matrix (usually in plasma, but can be in any part of the body) after drug administration	µg/ml	Direct measurement
T_{max}	T _{max}	the time corresponding to C _{max}	Hours	Direct measurement
Volume of distribution	V _d	the apparent volume in which a drug is distributed. Relates drug concentration to the amount of drug in the body and can give information about tissue distribution	Litre	=D/C ₀
Elimination rate constant	K _e	the rate at which a drug is removed from the system	Per hour	= Cl/V _D = ln(2)/T _{1/2}
Clearance	Cl	the volume of body fluid cleared per time unit quantifies drug elimination from the system by kidney, liver and other organs	litre/hour	= V _d .K _e =D/AUC
Half-life	T _{1/2}	the time needed for the concentration to fall to half of its previous value	Hours	= ln(2)/K _e
AUC	AUC	the area under the curve, an expression of total exposure	mg/liter.hour	= $[\int_0^{\infty} C. dt]$
Bioavailability	F	oral bioavailability, the fraction of the administered dose that reaches the systemic circulation.	N/A (fraction)	=AUC _(po) / AUC _(iv) × Dose _(iv) /Dose _(po)

Some important concepts for the PK of CL drugs include:

- The **target site** for drug action is the dermis underneath the skin lesion, where parasites survive and multiply as intracellular amastigotes in the phagolysosomes of (predominantly) macrophages. Hence, plasma and even extracellular dermal fluid might not be a good surrogate for the intracellular concentrations to which the pathogen is exposed, based on the ability of a systemic drug to extravasate at the infection site or the tendency of the drug to predominantly distribute extra-

or intracellularly (136). The acidic environment of the phagolysosome (pH=4-5) and several biological membranes could form biological barriers for a drug on its cellular route towards its molecular target (137). The effect of manipulation of the low pH of the phagolysosome with alkaline lysosomotropic drugs such as chloroquine (CQ) on parasite survival has not yet been explored. Therefore, we studied the *in vitro* and *in vivo* antileishmanial effects of standard drugs alone or in combination with CQ in chapter 3.1.

- Not only the physicochemical properties but also the **route of administration** influences the PK route of a drug. For example, an oral compound requires sufficient uptake through the intestinal epithelia to reach the bloodstream (bioavailability), limited first-pass metabolism (unless it is a prodrug) and distribution from the systemic circulation to the skin. A successful topical drug, on the other hand, needs the ability to permeate through the stratum corneum of the epidermis and to be retained in the dermis (139). Local, disease-inflicted tissue damage and pathophysiological alterations might affect local drug accumulation, but this has not been studied for most antileishmanial drugs. Local acidosis of the extracellular fluid due to inflammation, low oxygen tension and altered local blood flow, capillary density, capillary permeability and lymphatic clearance could all affect the fate of a drug within CL skin lesions (136). However, the significance of these phenomena for the pharmacology of CL drugs is poorly understood.
- Once **drug penetration** into the skin has occurred, **drug disposition** within the infected tissue is unlikely to be a uniform, rapid or complete process. Little is known about drug penetration in the non-caseating granuloma in which infected macrophages are organized (140), drug uptake by off-target cells, or binding of drugs to extracellular biological material in the skin.
- Only the **unbound drug concentration**, free of protein binding, surrounding the therapeutic target is pharmacologically active and can lead to *in vivo* efficacy by binding to and acting on its molecular target. At the same time, compounds with low protein binding are cleared from the system to a greater extent and can have a shorter plasma half-life (141).
- A drug can be both inactivated and activated by the **metabolism** of the parasite or the host (in macrophages, skin and liver). *Leishmania*-specific enzymes, such as type I nitroreductases, could be exploited for the activation of prodrugs within the parasite (142).
- Different types of CL require variable PK profiles for drug efficacy, for example, local accumulation within a single simple CL lesion *versus* high systemic exposure and distribution to all skin sites for DCL and PKDL. Moreover, drug exposure could vary in specific populations such as children or immunosuppressed patients.

- Pharmacodynamics (PD), “what the drug does to the body”, describe how the drug affects the parasite that causes infection and pathology to the host. Drug concentrations at specific sites of the body can result in the desired antileishmanial (target) as well as undesired toxic (off-target) effects. Indeed, selective drug distribution and toxicity to target the pathogen rather than the host is the basis of the “magic bullet” concept coined by Paul Ehrlich, the father of anti-infective chemotherapy (143). Binding of protein-free drug to its molecular target for a specific duration of time is the pharmacological basis for antileishmanial activity. PD can be described in terms of activity (inhibitory concentrations, such as EC₅₀, EC₉₀), potency (maximal effect) and rate of kill (time-dependence of the effect) (144). Some important PD concepts for CL drugs include:
 - ***Leishmania* species** show a significant **variation in their sensitivity** to standard (Sb^V, PM, MF) and experimental drugs, as observed *in vitro*, *in vivo* and during clinical trials (145, 146).
 - Recent research has shown that *Leishmania* can have metabolically semi-dormant and actively replicating states *in vivo*. Latency is a well-characterized phenomenon for other pathogens such as *Mycobacterium tuberculosis*. Hence, drug activity against **parasite subpopulations with different growth rates** might be variable, leading to persisting parasites and the risk of treatment failure and relapse (147-149).
 - Therapeutic efficacy of a drug against CL is a combination of its leishmanicidal activity and the protective **role of the immune system**. Particularly important to therapy are **macrophages**, the *Leishmania* host cells. These are heterogeneous cell populations, with variable phenotypes based on their resident tissue microenvironment (150), activation status (5) and host-pathogen interaction (16). Therefore, it is important to understand the role of drug accumulation (uptake and efflux transporters, metabolism) within infected macrophages, as well as their own independent antileishmanial activity upon activation (138). *In vitro* activity of standard antileishmanial drugs has already been shown to be dependent on the type of the macrophage host cell (150).

1.5.5. Current drug development tools for CL

The current predictive models and tools to evaluate antileishmanial activity can be classified into *in vitro* and *in vivo* tests. Figure 18 shows the most important models in CL drug research.

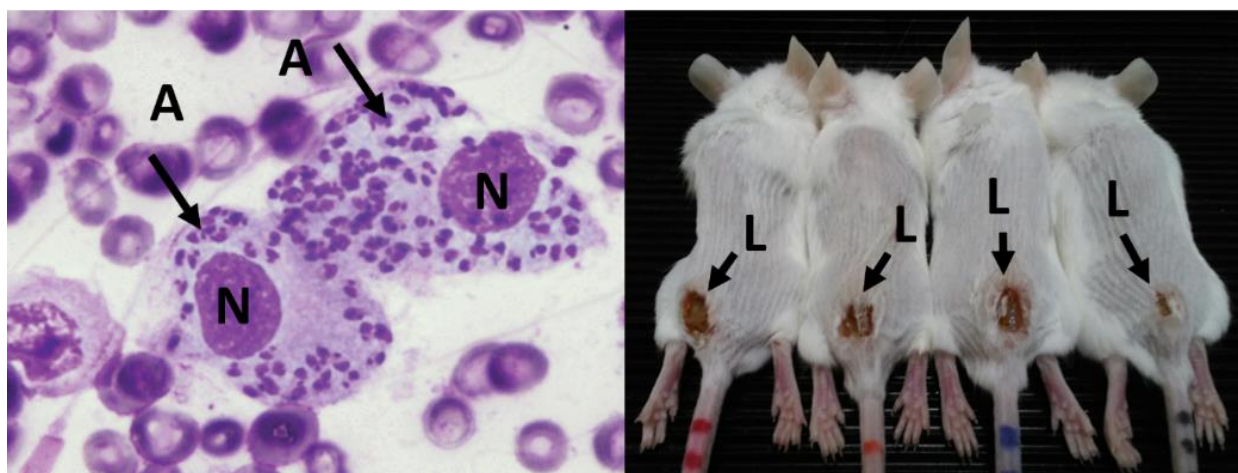


Figure 18: *In vitro* and *in vivo* models of CL – *Leishmania*-infected macrophages (nuclei: N, intracellular amastigotes, A and arrows) and BALB/c mice with skin lesions on the rump (L)

- ***In vitro*** phenotypic screening assays evaluate activity and potency of the drug against *Leishmania*. These can be categorized as promastigote, axenic (extracellular) amastigote and intracellular amastigote assays. Extracellular models (promastigote and axenic amastigote) allow for higher-throughput, cheaper, quicker and more straightforward screening. However, they do not reflect the biological complexity of CL in humans (parasites reside within the macrophages of the dermal skin layer) and can thus lead to false positives and negatives. The intracellular amastigote model (infected macrophages) is the gold standard. Macrophages can be derived from mouse peritoneum (PEMs) or bone-marrow (BMM), or chemically differentiated from human cancer cell lines (THP-1). Infected macrophages are exposed to specific drug concentrations for a standardised period (such as 2, 3 or 5 days), after which cells are fixed with methanol and stained with Giemsa dye before microscopic counting of the number of amastigotes per host cell (parasite burden) or the percentage of host cells containing at least one amastigote (% infection). Back-transformation assays, in which viable amastigotes return to their promastigote life-stage in culture, can be used to confirm findings. Alternatively, *Leishmania*-specific enzymatic, colourimetric or fluorometric reactions allow higher throughput, automated and more rapid screening. New compounds can be selected based on the 50 % and 90 % effective concentrations (EC_{50} , EC_{90}) after comparison with an untreated control and a control drug. Macrophage viability (Alamar Blue, Lactate Dehydrogenase) and general cytotoxicity assays (HEPG2 assays) should accompany activity screening assays to ensure selective toxicity towards the parasites rather than the mammalian host cells (151, 152). The use of different macrophage cell lines (which can affect antileishmanial activity (150))

and the broad range of exposure times make a comparison of available scientific data challenging. Harmonisation of *Leishmania* drug research procedures is urgently required.

A major issue with these *in vitro* models is their lack of biological relevance, as they are static and two-dimensional culture systems: drug activity is evaluated at a single time point after exposure of cells adhered to a surface of a culture well slide to a single drug concentration. Yet, *in vivo*, efficacy is a dynamic process of rate and magnitude of parasite kill as a result of fluctuating drug levels surrounding infected dermal macrophages, with or without the assistance of the host immune response. The oversimplification can cause a poor *in vitro* – *in vivo* correlation. 3D cell culture and flow systems help to bridge the gap between *in vitro* models and live tissue during drug discovery (153, 154).

In this simple *in vitro* model, the only biological barriers in terms of PK a drug needs to pass in order to exert its antileishmanial activity are cellular (macrophage, phagolysosome, parasite). *In silico* modelling based on physicochemical drug properties and physiological determinants are used to predict the PK profile of new compounds (155). General *in vitro* ADME assays (MDCKII-hMDR1 cell permeability, CYP450 interactions, metabolic stability in liver and skin) can provide a more robust evaluation and improve the likelihood of success for lead candidates (156).

- ***In vivo*** models of CL for the evaluation drug efficacy are mainly mouse-based. A standardized inoculum of virulent *Leishmania* promastigotes is injected intradermally or subcutaneously in the footpad, rump or ear of a mouse. *L. major*-BALB/c is the most common and best-studied animal model of CL. The major advantages are its high reproducibility, robustness and relatively rapid development of skin lesions (typically within 2-4 weeks). Because the susceptible BALB/c mouse is immunologically incapable of self-curing *L. major* infection, the model forms a rigorous drug evaluation test as only potent compounds show efficacy. Because humans do often self-cure CL, this lack of clinical relevance is also the main limitation of the model. Alternative rodent models of CL, such as C57/bl6 mice or golden hamsters do show self-cure profiles, but disease onset is typically much slower, resulting in lower throughput and higher maintenance costs. *In vivo* drug efficacy in animal models of CL is determined in terms of reduction of lesion size compared to an untreated control. However, because inflammation is an important factor in lesion size and thus a potential confounding factor for drug activity, quantification of *Leishmania* parasite load should be considered as another indicator of therapeutic effect. This can be done via limiting dilution assays, quantitative polymerase chain reaction (qPCR), microscopy, ELISA, or *in vivo* imaging of bioluminescent parasites. Based on dose-response studies, the 50% and 90 % effective dose (ED₅₀ and ED₉₀) can be calculated. The therapeutic index describes the window between the desired therapeutic and undesired toxic/lethal effects of the drug (ED₅₀/LD₅₀). *In vivo* toxicity measures can be death, weight loss or behavioural abnormalities in animals (157, 158).

Alongside activity and toxicity data, PK information should also be collected, as the ability of the drug to permeate biological barriers and reach the infected dermal macrophages is crucial for therapeutic efficacy. However, skin PK research in animal models of CL is a poorly explored area (159-161), while some work has been done in recent years for VL (162-166). An issue for skin PK studies is the cost related to the required number of animals. While tail vein sampling in mice makes plasma drug levels easy to obtain, these are poor surrogate markers for drug exposure at the actual infection site in the skin. Tissue homogenates from skin necropsies or skin biopsies are straightforward to perform and give a crude PK measure of drug distribution in lesions. However, grinding up tissues results in combined drug levels from various skin compartments that can be difficult to interpret. For intracellularly accumulating drugs, such as quinolones and macrolides (AmB), this can lead to a relative dilution and underestimation of the exposure within the amastigote-containing macrophages. Alternatively, this approach might overestimate intracellular levels of drugs with a preferential distribution in the extracellular compartments, such as β -lactams and aminoglycosides (PM) (137, 167). The strengths and limitations of skin homogenates are discussed further in chapters 3.1, 3.2, 3.3 and 3.4. A more appropriate method for the study of the penetration of anti-infective drugs in tissues is microdialysis (MD). This minimally invasive technique allows real-time sampling of unbound drug concentrations but requires technical skill and a more complex, expensive experimental set-up (168, 169). This method is described in detail in chapter 3.5.

Combining *in vitro* and *in vivo* assays, figure 19 shows an example of an algorithm for selecting new oral drug candidates for CL. The cascade follows specific tests to evaluate the drug's antileishmanial efficacy, toxicity, metabolism and PK (in order of increasing biological relevance, but also costs, time and workload) and provides go/no-go criteria for the selection of the most promising compounds along the way (170).

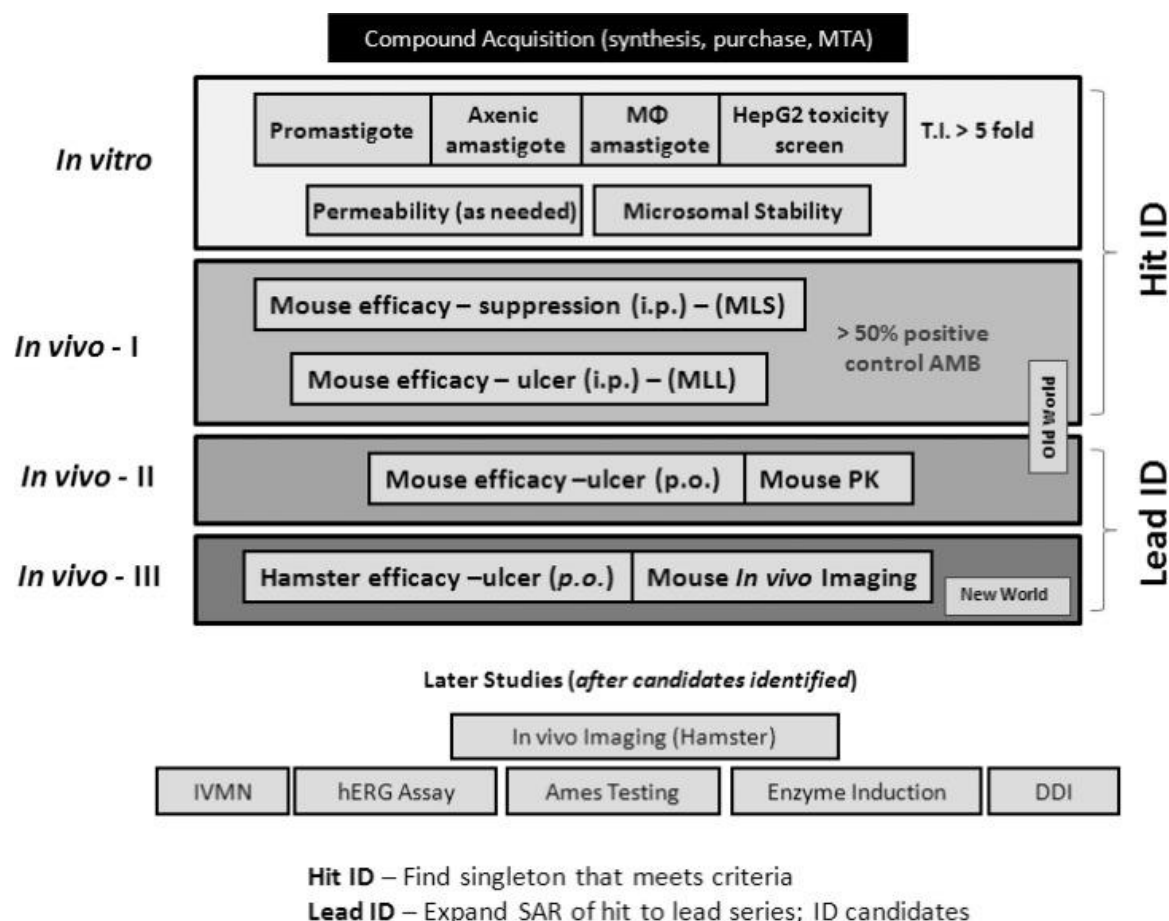


Figure 19: an oral drug discovery scheme for CL. MTA = material transfer agreement. T.I = therapeutic index. HepG2 = human liver cell line (preclinical toxicity assay).

I.p. = intraperitoneal. MLS = mouse leishmaniasis suppression. ID = identification. MLL = mouse leishmaniasis lesion. P.o. = *per os* (oral). PK = pharmacokinetics. IVMN = *in vitro* micronucleus assay (preclinical genotoxicity assay). hERG = human ether-a-go-go-related gene (preclinical cardiotoxicity assay). Ames testing (preclinical carcinogenicity assay). DDI = drug-drug interaction. SAR = structure activity relationship.

However, high failure rates in the clinic remind us to be cautious when interpreting activity, safety or ADME results from preclinical models of disease. Our predictive models for CL R&D might not represent the pathogenicity, virulence, diversity and susceptibility of the parasites or the behaviour of the drug in clinical situations. This may lead to decisions to advance the wrong compounds through drug discovery programmes, ending up with an enormous loss of time and resources rather than a new treatment. So how can we translate data from preclinical to clinical trials? How do we bridge the gaps between cellular/animal models of infection and human disease? An important strategy to overcome such issues is a better understanding of PK/PD relationships.

1.5.6. PK and PK/PD in CL drug development

Antimicrobial activity of an antibiotic is classically defined in terms of inhibitory concentrations, such as minimally inhibitory concentration (MIC) and 90 % effective concentration (EC_{90}). These values, however, do not give information about the time-dependency of the antimicrobial effect. By incorporating PD potency measures with PK data, it is possible to identify the most important parameters for antimicrobial effect by understanding the relationship between PK and PD (PK/PD). Based on the PK/PD profile, drugs can be classified in roughly three groups: concentration-dependent, time-dependent or dependent on both time and concentration. For example, for aminoglycosides such as PM, the maximum plasma concentration (C_{max}/MIC) is most important for its antibacterial effect (concentration-dependence). For antibiotic classes such as β -lactams, the period that plasma concentrations are above the MIC ($T > MIC$) is the crucial determinant of activity (time-dependence) (171, 172). Figure 20 gives an overview of these basic concepts and parameters in PK/PD. By integrating PK and PD information derived from preclinical *in vitro* and *in vivo* studies, translational drug research and PK/PD modelling can predict human dose regimens with clinical efficacy. Various mechanism-based and empirical PK/PD mathematical modelling approaches exist to describe the exposure-response relationship (173 - 175), but details are beyond the scope of this thesis.

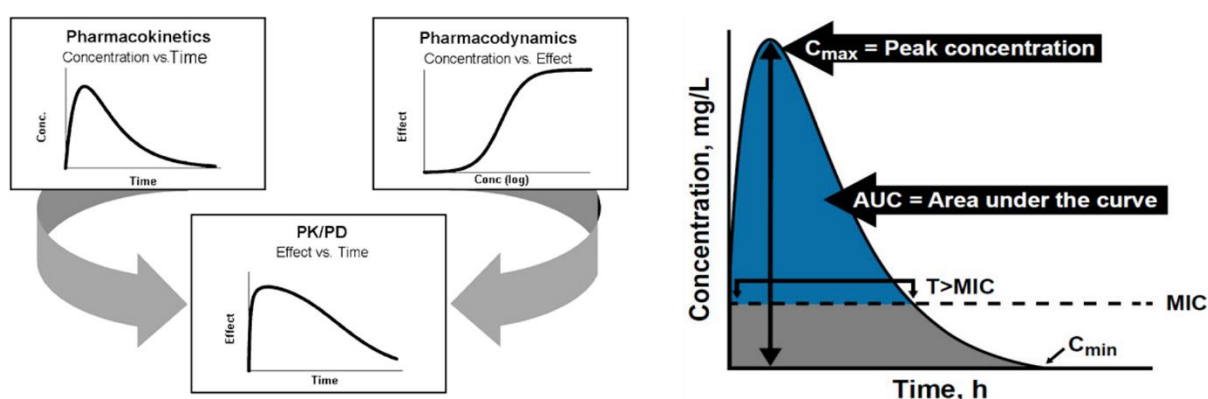


Figure 20: Overview of the basic concepts of PK/PD modelling (171)

In recent years, analysis of PK/PD relationships has become central to drug development. A team from Pfizer analysed the role of fundamental PK/PD in the survival rate of compounds in clinical trials (176). The majority of failures were caused by a lack of efficacy during Phase II. They defined the “three pillars of survival” for a new drug candidate as (i) exposure at the target site of action over a desired period of time (ii) binding to the pharmacological target as expected for its mode of action and (iii) expression of pharmacological activity as expected for the demonstrated target exposure and target binding. These are concepts directly related to fundamental pharmacology and PK/PD. The Food and Drug Administration (FDA) and European Medicines Agency (EMA) have not only endorsed PK/PD as a valuable approach to

optimize and streamline drug development, today it is a critical requirement for licensing a new medicine (177, 178).

Translational PK/PD modelling can minimize the risk of failure and shorten the time and cost of drug development for new antimicrobial drugs (179-181). Indeed, an analysis of 19 antibacterial drug approval decisions from 1996 to 2011 showed that as the probability of PK/PD target attainment for a given dosing regimen increased, so did the chance of regulatory approval (182). PK/PD plays a critical role in establishing safe and effective combination therapies for major tropical diseases such as malaria (183) and tuberculosis (184).

For leishmaniasis, researchers have only very recently begun to investigate the PK, PD and PK/PD of standard antileishmanial drugs (AmB, MF) in preclinical models of VL, to serve as a model for the evaluation of new drug candidates (166, 185). In addition, the PK and PD properties of current drugs in leishmaniasis pharmacotherapy are poorly understood. As a result, treatment regimens are empirical and based on the maximum tolerated doses, rather than rationally designed and optimized. This leaves patients at risk of drug-related adverse and toxic effects, therapeutic failure and relapse after initial cure (62).

Thus, the PK/PD concept holds untapped potential to support in the delivery of new and better treatments for CL. Drug development for CL is scientifically challenging, due to (i) the dermal site of infection, (ii) the intracellular location of the causative parasite within macrophages and (iii) the variability in drug sensitivity among *Leishmania* species. At the same time, there is a lack of rational approaches to accelerate successful drug R&D for this disfiguring disease. By combining aspects of infection site PK and *Leishmania* kill kinetics, PK/PD analysis is able to quantitatively describe and simulate the complex interaction between antileishmanial drug, parasite and patient. However, before the role of PK/PD can be explored in CL treatment, improved tools are needed to evaluate the PK and PD properties of established and new antileishmanial drugs.

2. AIMS AND OBJECTIVES

The aim of this thesis is to develop new tools to support the preclinical development of much needed novel drugs for cutaneous leishmaniasis (CL). Such tools include predictive models, methodologies and strategies to evaluate the therapeutic efficacy of new compounds based on assessing favorability of their skin pharmacokinetics (PK), antileishmanial pharmacodynamics (PD) and pharmacokinetic/pharmacodynamic (PK/PD) relationships. These were established and validated using standard antileishmanial drugs such as amphotericin B, miltefosine and paromomycin (chapter 3.1, 3.2, 3.3 and 3.4) and then applied to a new clinical drug candidate for leishmaniasis (chapter 3.5), as detailed below.

- In chapter 3.1, we investigated the potential of combination therapy of standard antileishmanial drugs with the 4-aminoquinoline as a new treatment strategy for CL. The chapter discusses the challenges of *in vitro-in vivo* translation and species-specific drug sensitivity in CL drug discovery.
- In chapters 3.2 and 3.3, we compared PK and efficacy of different formulations of the 2nd-line drug AmB (Fungizone® (deoxycholate), AmBisome® (unilamellar liposome) and Fungisome® (multilamellar liposome)) in a mouse model of *L. major* CL. The aim was to learn lessons for liposomal drug delivery to the CL target site and to provide a basis for rational design of clinical drug dose regimens.
- In chapter 3.4, we studied the influence of local skin inflammation in *L. major* and *L. mexicana* CL of the PK and PK/PD of AmBisome®. The aim was to identify whether the influence of pathophysiology on PK could be a contributing factor in variable treatment outcomes in Old and New World CL.
- In chapter 3.5, we evaluated the PK and efficacy of DNDI-0690, an oral nitroimidazole and clinical candidate for VL, in preclinical models of CL. The aim was to characterize drug distribution in the infected skin (using an innovative microdialysis method) and study the dose-response effect in the *L. major* BALB/c model of CL.

3. EXPERIMENTAL RESULTS

The results of this project will be shown in the following pages as four chapters in the form of research papers (chapters 3.1, 3.2, 3.3 and 3.4) and one book style chapter (chapter 3.5).

The four publications arising from this PhD project are:

- 3.1. Wijnant G-J, Van Boclaer K, Yardley V, Murdan S, Croft SL. 2017. Efficacy of Paromomycin-Chloroquine Combination Therapy in Experimental Cutaneous Leishmaniasis. *Antimicrob Agents Chemother* 61.
- 3.2. Wijnant G-J, Van Boclaer K, Yardley V, Harris A, Murdan S, Croft SL. 2018. Relation between Skin Pharmacokinetics and Efficacy in AmBisome Treatment of Murine Cutaneous Leishmaniasis. *Antimicrob Agents Chemother* 62.
- 3.3. Wijnant, G.-J., Van Boclaer, K., Yardley, V., Harris, A., Alavijeh, M., Silva-Pedrosa, R., Antunes, S., Mauricio, I., Murdan, S., and Croft, S.L. 2018. Comparative efficacy, toxicity and biodistribution of the liposomal amphotericin B formulations Fungisome® and AmBisome® in murine cutaneous leishmaniasis. *International Journal for Parasitology: Drugs and Drug Resistance*.
- 3.4. Wijnant, G.-J., Van Boclaer, K., Francisco, A.F., Yardley, V., Harris, A., Alavijeh, M., I., Murdan, S., and Croft, S.L. 2018. Local skin inflammation in cutaneous leishmaniasis as a source of variable pharmacokinetics and therapeutic efficacy of liposomal amphotericin B. Manuscript under review for publication by *Antimicrobial Agents and Chemotherapy* – minor corrections.

Chapter 3.1:

Combination therapies of chloroquine with standard antileishmanial drugs for CL treatment



3. 1: Combination therapies with chloroquine for CL treatment

ANNEX 1: WIJNANT G-J, VAN BOCXLAER K, YARDLEY V, MURDAN S, CROFT SL. 2017. EFFICACY OF PAROMOMYCIN-CHLOROQUINE COMBINATION THERAPY IN EXPERIMENTAL CUTANEOUS LEISHMANIASIS. ANTIMICROB AGENTS CHEMOTHER 61.

Key points, novel results and implications

- This work was started in July 2015 to allow basic training for *in vitro* (cell culture, molecular biology) and *in vivo* (animal handling, infection, drugging) methods for the rest of the project (chapter 3.2, 3.3, 3.4 and 3.5).
- The 4-aminoquinoline chloroquine (CQ) is a safe, oral antimalarial medication. In addition, the drug is also clinically used in combination with doxycycline to cure chronic Q fever, as it enhances the activity of the antibiotic against the causative bacterium *Coxiella burnetii*. The mechanism for therapeutic synergy between doxycycline and CQ is related to CQ-mediated manipulation of the pH of the macrophage phagolysosomes where *C. burnetii* multiplies. As *Leishmania* parasites occupy a similar intracellular site within the host, it was hypothesized that a similar drug combination approach might be the basis for a new, improved treatment for CL.
- Of the three standard drugs (miltefosine, amphotericin B, paromomycin) evaluated *in vitro* in combination with CQ in 72-hour intracellular drug assays, we identified significant increases in antileishmanial activity for paromomycin (PM).
- The PM-CQ drug combination was then tested in murine models of *L. major* and *L. mexicana* CL. Daily co-administration of 50 mg/kg PM and 25 mg/kg CQ (IP) for 10 days resulted in a significant reduction in lesion size but not in parasite load compared to those found for controls which received PM alone.
- Overall, our data indicate that **a drug combination of PM and CQ is unlikely** to be a potential **candidate for further preclinical development for CL**. The paper discusses the current preclinical drug development scenario for CL and its limitations, with special attention for the challenging translation from *in vitro* to *in vivo*.
- In the frame of the thesis, this chapter identified (i) *in vitro* activities for standard drugs against the two main *Leishmania* strains used in this work (Old World *L. major* JISH118 and New World *L. mexicana* M379) and confirmed species-specific differences in antileishmanial drug sensitivity. Furthermore, the paromomycin dose regimen (10 x 50 mg/kg, IP) served as a strong positive control for *in vivo* activity against *L. major* in later studies (chapter 3.3 and chapter 3.4).

Candidate's contribution

The candidate generated and analysed all the data described in the paper. Moreover, he prepared the first draft of the manuscript, which was accepted for publication by Antimicrobial Agents and Chemotherapy in May 2017 after academic peer review.

Research paper cover sheet

London School of Hygiene & Tropical Medicine
Keppel Street, London WC1E 7HT
www.lshtm.ac.uk



Registry
T: +44(0)20 7299 4646
F: +44(0)20 7299 4656
E: registry@lshtm.ac.uk

RESEARCH PAPER COVER SHEET

PLEASE NOTE THAT A COVER SHEET MUST BE COMPLETED FOR EACH RESEARCH PAPER INCLUDED IN A THESIS.

SECTION A – Student Details

Student	GERT-JAN WIJNANT
Principal Supervisor	SIMON CROFT
Thesis Title	NEW ORAL AND DRUG DEVELOPMENT METHODOLOGIES FOR CUTANEOUS LEISHMANIASIS

If the Research Paper has previously been published please complete Section B. If not please move to Section C

SECTION B – Paper already published

Where was the work published?	AAC	
When was the work published?	MAY 2017	
If the work was published prior to registration for your research degree, give a brief rationale for its inclusion	N/A	
Have you retained the copyright for the work?*		Was the work subject to academic peer review? YES

*If yes, please attach evidence of retention. If no, or if the work is being included in its published format, please attach evidence of permission from the copyright holder (publisher or other author) to include this work.

SECTION C – Prepared for publication, but not yet published

Where is the work intended to be published?	/
Please list the paper's authors in the intended authorship order:	
Stage of publication	

SECTION D – Multi-authored work

For multi-authored work, give full details of your role in the research included in the paper and in the preparation of the paper. (Attach a further sheet if necessary)	ALL WORK + MANUSCRIPT
--	-----------------------

Student Signature: _____ Date: 17/4/2018

Supervisor Signature: _____ Date: 18.04.2018

Improving health worldwide

www.lshtm.ac.uk

Copyright proof

Re: Copyright for AAC papers: confirmation



Drought, Heather <hdrought@asmusa.org>
Today, 16:00
Gert Wijnant ✕

Reply all | v

Inbox

Label: Staff mailbox default delete after 7 years (7 years) Expires: 25/07/2025 16:00

Greetings,

Thank you for your email. When you choose open access publishing, you/the author retains copyright: <https://creativecommons.org/licenses/by/4.0/>
Regardless of OA status, all ASM authors retain certain rights, including use of their article in their thesis or dissertation: http://journals.asm.org/site/misc/ASM_Author_Statement.xhtml

It is fine to use the manuscript in your thesis/dissertation, but you will need to add to the manuscript once accepted that it was used in the thesis (I see you currently note: "Gert-Jan Wijnant's doctoral project is part of the EuroLeish.Net Training Network (www.euroleish.net).") Please check with production staff after final acceptance/at proof stage to see whether this is sufficient). I will make a note of this on the manuscript for the production staff.

I hope this helps, but please let me know if there are any additional questions.

Very best,
Heather

Heather Drought
Editorial Coordinator
American Society for Microbiology
1752 N Street, N.W., Washington, D.C. 20036-2904
Phone: 202-942-9363 | Fax: 202-942-9355



Efficacy of Paromomycin-Chloroquine Combination Therapy in Experimental Cutaneous Leishmaniasis

Gert-Jan Wijnant,^{a,b} Katrien Van Boecklaer,^a Vanessa Yardley,^a
Sudaxshina Murdan,^b Simon L. Croft^a

Department of Immunology and Infection, Faculty of Infectious and Tropical Diseases, London School of Hygiene and Tropical Medicine, London, United Kingdom^a; Department of Pharmaceutics, UCL School of Pharmacy, London, United Kingdom^b

ABSTRACT The 4-aminoquinoline chloroquine (CQ) is clinically used in combination with doxycycline to cure chronic Q fever, as it enhances the activity of the antibiotic against the causative bacterium *Coxiella burnetii* residing within macrophage phagolysosomes. As there is a similar cellular host-pathogen biology for *Leishmania* parasites, this study aimed to determine whether such an approach could also be the basis for a new, improved treatment for cutaneous leishmaniasis (CL). We have evaluated the *in vitro* and *in vivo* activities of combinations of CQ with the standard drugs paromomycin (PM), miltefosine, and amphotericin B against *Leishmania major* and *Leishmania mexicana*. In 72-h intracellular antileishmanial assays, outcomes were variable for different drugs. Significantly, the addition of 10 μ M CQ to PM reduced 50% effective concentrations (EC_{50} s) by over 5-fold against *L. major* and against normally insensitive *L. mexicana* parasites. In murine models of *L. major* and *L. mexicana* CL, daily coadministration of 50 mg/kg of body weight PM and 25 mg/kg CQ for 10 days resulted in a significant reduction in lesion size but not in parasite load compared to those for mice given the same doses of PM alone. Overall, our data indicate that PM-CQ combination therapy is unlikely to be a potential candidate for further preclinical development.

KEYWORDS cutaneous leishmaniasis, *Leishmania major*, *Leishmania mexicana*, combination therapy, paromomycin, chloroquine

Cutaneous leishmaniasis (CL) is a group of skin infections caused by obligate intracellular protozoa belonging to the genus *Leishmania*, which are transmitted via the bite of female sandflies. Over 15 different parasite species are responsible for CL in humans, with a diverse clinical spectrum ranging from self-limiting but scarring skin lesions (localized CL) to rarer and more complex forms of CL. These forms can be diffuse (diffuse cutaneous leishmaniasis), chronic (*leishmaniasis recidivans*), and destructive to the mucosal tissue (mucocutaneous leishmaniasis) (1). The estimated global prevalence is 12 million cases per year in more than 98 countries (the majority of which occurs in Latin America and the Middle East), and more than 350 million people are at risk (2). Despite its increasing incidence (3) and high burden (due to physical disfigurement and related social stigmatization), vaccines and satisfactory treatment options are currently lacking for this poverty-related and neglected tropical disease. A painful and lengthy series of injections of toxic pentavalent antimonials, associated with severe side effects and reduced sensitivity in some species, still remains the first-line therapy after more than 7 decades of clinical use (4). More recent second-line drugs, such as the aminoglycoside antibiotic paromomycin (PM), the phospholipid miltefosine (MF), and the polyene antifungal amphotericin B (AmB) (available in deoxycholate salts or lipid nanoparticle formulations), also suffer from similar limitations related to toxicity, efficacy, cost,

Received 17 February 2017 Returned for modification 27 March 2017 Accepted 13 May 2017

Accepted manuscript posted online 12 June 2017

Citation Wijnant G-J, Van Boecklaer K, Yardley V, Murdan S, Croft SL. 2017. Efficacy of paromomycin-chloroquine combination therapy in experimental cutaneous leishmaniasis. *Antimicrob Agents Chemother* 61:e00358-17. <https://doi.org/10.1128/AAC.00358-17>.

Copyright © 2017 Wijnant et al. This is an open-access article distributed under the terms of the Creative Commons Attribution 4.0 International license.

Address correspondence to Simon L. Croft, simon.croft@ehim.ac.uk.

(Double-click to open attached file)



Efficacy of Paromomycin-Chloroquine Combination Therapy in Experimental Cutaneous Leishmaniasis

Gert-Jan Wijnant,^{a,b} Katrien Van Bocxlaer,^a Vanessa Yardley,^a
Sudaxshina Murdan,^b Simon L. Croft^a

Department of Immunology and Infection, Faculty of Infectious and Tropical Diseases, London School of Hygiene and Tropical Medicine, London, United Kingdom^a; Department of Pharmaceutics, UCL School of Pharmacy, London, United Kingdom^b

ABSTRACT The 4-aminoquinoline chloroquine (CQ) is clinically used in combination with doxycycline to cure chronic Q fever, as it enhances the activity of the antibiotic against the causative bacterium *Coxiella burnetii* residing within macrophage phagolysosomes. As there is a similar cellular host-pathogen biology for *Leishmania* parasites, this study aimed to determine whether such an approach could also be the basis for a new, improved treatment for cutaneous leishmaniasis (CL). We have evaluated the *in vitro* and *in vivo* activities of combinations of CQ with the standard drugs paromomycin (PM), miltefosine, and amphotericin B against *Leishmania major* and *Leishmania mexicana*. In 72-h intracellular antileishmanial assays, outcomes were variable for different drugs. Significantly, the addition of 10 μ M CQ to PM reduced 50% effective concentrations (EC₅₀s) by over 5-fold against *L. major* and against normally insensitive *L. mexicana* parasites. In murine models of *L. major* and *L. mexicana* CL, daily coadministration of 50 mg/kg of body weight PM and 25 mg/kg CQ for 10 days resulted in a significant reduction in lesion size but not in parasite load compared to those for mice given the same doses of PM alone. Overall, our data indicate that PM-CQ combination therapy is unlikely to be a potential candidate for further preclinical development.

KEYWORDS cutaneous leishmaniasis, *Leishmania major*, *Leishmania mexicana*, combination therapy, paromomycin, chloroquine

Cutaneous leishmaniasis (CL) is a group of skin infections caused by obligate intracellular protozoa belonging to the genus *Leishmania*, which are transmitted via the bite of female sandflies. Over 15 different parasite species are responsible for CL in humans, with a diverse clinical spectrum ranging from self-limiting but scarring skin lesions (localized CL) to rarer and more complex forms of CL. These forms can be diffuse (diffuse cutaneous leishmaniasis), chronic (*leishmaniasis recidivans*), and destructive to the mucosal tissue (mucocutaneous leishmaniasis) (1). The estimated global prevalence is 12 million cases per year in more than 98 countries (the majority of which occurs in Latin America and the Middle East), and more than 350 million people are at risk (2). Despite its increasing incidence (3) and high burden (due to physical disfigurement and related social stigmatization), vaccines and satisfactory treatment options are currently lacking for this poverty-related and neglected tropical disease. A painful and lengthy series of injections of toxic pentavalent antimonials, associated with severe side effects and reduced sensitivity in some species, still remains the first-line therapy after more than 7 decades of clinical use (4). More recent second-line drugs, such the aminoglycoside antibiotic paromomycin (PM), the phospholipid miltefosine (MF), and the polyene antifungal amphotericin B (AmB) (available in deoxycholate salts or lipid nanoparticle formulations), also suffer from similar limitations related to toxicity, efficacy, cost,

Received 17 February 2017 Returned for
modification 27 March 2017 Accepted 13
May 2017

Accepted manuscript posted online 12
June 2017

Citation Wijnant G-J, Van Bocxlaer K, Yardley V,
Murdan S, Croft SL. 2017. Efficacy of
paromomycin-chloroquine combination
therapy in experimental cutaneous
leishmaniasis. Antimicrob Agents Chemother
61:e00358-17. <https://doi.org/10.1128/AAC.00358-17>.

Copyright © 2017 Wijnant et al. This is an
open-access article distributed under the terms
of the [Creative Commons Attribution 4.0
International license](https://creativecommons.org/licenses/by/4.0/).

Address correspondence to Simon L. Croft,
simon.croft@lshtm.ac.uk.

TABLE 1 *In vitro* activities of miltefosine, amphotericin B, and paromomycin in monotherapy (alone) and in combination therapy with 10 μ M CQ (plus CQ) against intracellular *L. major* and *L. mexicana* in PEMs after 72 h^a

Organism	EC ₅₀ (μ M)					% infection PEMs (72 h)	
	Miltefosine		Amphotericin B alone	Paromomycin		Untreated	Treated with 10 μ M CQ
	Alone	Plus CQ		Alone	Plus CQ		
<i>L. major</i>	33.9 \pm 5.9	10.7 \pm 1.8*	9.9 \times 10 ⁻² \pm 0.6 \times 10 ⁻²	58.1 \pm 6.1	11.6 \pm 2.4*	98	97.5
<i>L. mexicana</i>	15.7 \pm 1.0	10.0 \pm 1.6	9.9 \times 10 ⁻² \pm 0.5 \times 10 ⁻²	>360	86.6 \pm 17.4	98.5	96.8

^aData are expressed as means \pm 95% CI. *, statistically significant difference in EC₅₀s for drugs as monotherapy and CQ combination therapy ($P < 0.05$ by an extra-sum-of-squares F test). With amphotericin B plus CQ, there was microscopically visible cytotoxicity toward PEMs. After 72 hours, viability of PEMs treated with 10 μ M CQ alone was 85.8% \pm 15.6% (alamarBlue assay) and 100% \pm 0% (LDH assay).

or an invasive administration route. There is an urgent requirement for new treatments that can eliminate the parasite and safely accelerate lesion healing with minimal scarring and are feasible for use in low-resource health care systems (5, 6). In recent years, combination therapy of commercially available drugs has received more attention as an alternative strategy to develop more effective, lower-dose, and shorter treatments for many infectious diseases, including CL (7–11). With the goal of identifying such an improved therapeutic option for *Leishmania major* and *Leishmania mexicana* CL, we investigated the potential of the cheap, safe, and orally bioavailable 4-aminoquinoline chloroquine (CQ) to increase the activities of three standard antileishmanial drugs. The rationale for this approach was based upon evidence that the addition of CQ to treatment regimens for chronic stages of Q fever shortens the duration of therapy and prevents relapses (12, 13). CQ enhances the antimicrobial activity of doxycycline against the causative obligate intracellular bacterium *Coxiella burnetii*, which resides and multiplies within the phagolysosomes of its macrophage host cells (14). Likewise, CQ improves the effects of specific antibiotics against other intracellular pathogens such as *Tropheryma whipplei* (Whipple's disease) and persistent *Staphylococcus aureus* populations in chronic systemic infections (15, 16). Despite the similar macrophage tropism of *Leishmania* species causing CL, the effect of CQ on the activity of standard antileishmanial drugs has not yet been evaluated. Thus, in this study, our aim was to determine whether combination therapies of PM, MF, and AmB deoxycholate with CQ could be a new approach for the treatment for CL. Promising associations identified during *in vitro* screenings were then assessed *in vivo* by using murine models of *L. major* and *L. mexicana* CL. These Old and New World species were compared due to their known differences in drug sensitivities (17) and morphological characteristics of the parasitophorous vacuoles (18).

RESULTS AND DISCUSSION

We investigated the possible enhancing effect of CQ on the *in vitro* activities of three standard antileishmanial drugs against intracellular *L. major* and *L. mexicana*. A specific CQ concentration of 10 μ M was selected because of (i) the lack of host cell cytotoxicity (the viabilities of peritoneal exudate macrophages [PEMs] were determined to be 85.8% \pm 15.6% and 100% \pm 0% in alamarBlue and lactate dehydrogenase [LDH] assays, respectively), (ii) the absence of independent antileishmanial effects (the percent inhibition against *L. major* and *L. mexicana* amastigotes was <5% compared to untreated controls), and (iii) the reported enhanced activity of different antibiotics against other intramacrophage pathogens at similar CQ concentrations (14–16). We observed various effects of coincubation with 10 μ M CQ for different drugs in standard 72-h drug assays (Table 1). A small but significant ($P < 0.0001$) increase in antileishmanial activity was found for MF against *L. major* (50% effective concentrations [EC₅₀s] decreased from 33.9 \pm 5.9 to 10.7 \pm 1.8 μ M) but not for *L. mexicana* (from 15.7 \pm 1.0 to 10.0 \pm 1.6 μ M). In the case of AmB, combination with CQ was highly toxic to host cells, and EC₅₀s were incalculable. For PM, coincubation with CQ resulted in a significant ($P < 0.0001$) 5-fold decrease in EC₅₀s against *L. major* (from 58.1 \pm 6.1 to 11.6 \pm 2.4 μ M) and reduced EC₅₀s against *L. mexicana*, from >360 μ M (i.e., too high to accurately estimate because the

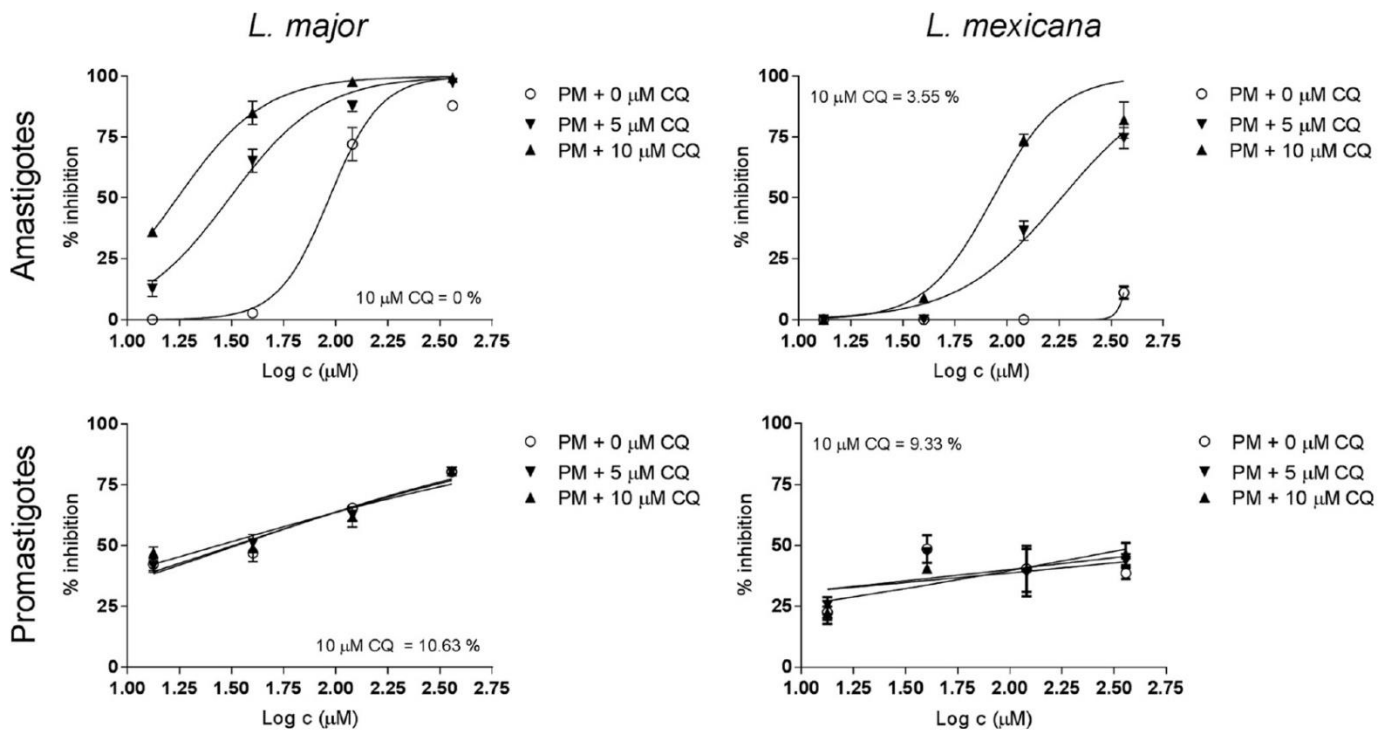


FIG 1 Effect of CQ on the *in vitro* antileishmanial activity of PM against intracellular and extracellular *L. major* (left) and *L. mexicana* (right) parasites. For the amastigote drug assays (top row), PEMs were infected with stationary-phase promastigotes and exposed to fixed PM concentrations (13.3, 40, 120, and 360 μM) combined with 0 to 5 to 10 μM CQ for 72 h, followed by microscopic counting of the number of infected macrophages. For the promastigote drug assays (bottom row), exponential-growth-phase parasites were treated identically, and inhibition was evaluated by using the alamarBlue assay. Values are expressed relative to untreated controls (percent inhibition). 10 μM CQ = indicates the percent inhibition at 10 μM CQ.

concentration was above the maximum drug level tested) to $86.6 \pm 17.4 \mu\text{M}$ (no *P* value was calculable). The improved activity of PM by the addition of CQ was notable because of the known relative insensitivity of *L. mexicana* to this aminoglycoside antibiotic (19–21). Thus, of the three standard antileishmanial drugs tested, PM in combination with CQ was evaluated further.

Next, the concentration dependency of the enhancing effect of CQ on the antileishmanial activity of PM was determined. Fixed concentrations of PM with multiple CQ doses (all $\leq 10 \mu\text{M}$, due to macrophage cytotoxicity at higher concentrations, with the 50% lethal concentration [LC_{50}] being $18.1 \pm 2.9 \mu\text{M}$) were tested against promastigotes and amastigotes of *L. major* and *L. mexicana*. Figure 1 shows the corresponding dose-response curves. Increasing CQ concentrations from 0 to 5 to 10 μM did not alter the antileishmanial activity of PM against extracellular promastigotes, with respective EC_{50} s of 33.3 ± 8.4 , 32.2 ± 8.3 , and $27.3 \pm 12.3 \mu\text{M}$ for *L. major* and $>360 \mu\text{M}$ for all three concentrations for *L. mexicana*. In contrast, we observed a gradual decrease in EC_{50} s against intracellular amastigotes as CQ levels similarly increased (from 91.7 ± 11.2 to 31.0 ± 4.0 to $16.9 \pm 1.6 \mu\text{M}$ against *L. major* and from $>360 \mu\text{M}$ to 182.1 ± 25.7 to $86.7 \pm 22.3 \mu\text{M}$ against *L. mexicana*). The mechanism of *in vitro* synergy between CQ and PM to eliminate the intracellular parasites within the parasitophorous vacuoles of the PEMs remains unclear. For the Q fever agent *C. burnetii*, the mode of action for CQ to enhance the antimicrobial activity of doxycycline, a pH-sensitive antibiotic, is related to its ability to accumulate within the normally acidic macrophage phagolysosomes and alkalinize this pathogen-harboring organelle (14). A similar host-pathogen interaction could be taking place in this setting, as indicated by (i) the presence of lysosomotropic properties of CQ at 10 μM (14–16), (ii) the absence of host cell toxicity and antileishmanial activity of CQ at the chosen concentration, (iii) the specificity of the association synergy for intracellular over extracellular parasites, (iv) the acidophilic nature of *Leishmania* (22), and (v) the reduced activity of aminoglycoside antibiotics such as PM at acidic pH (23). However, this hypothesis was not confirmed as we did not

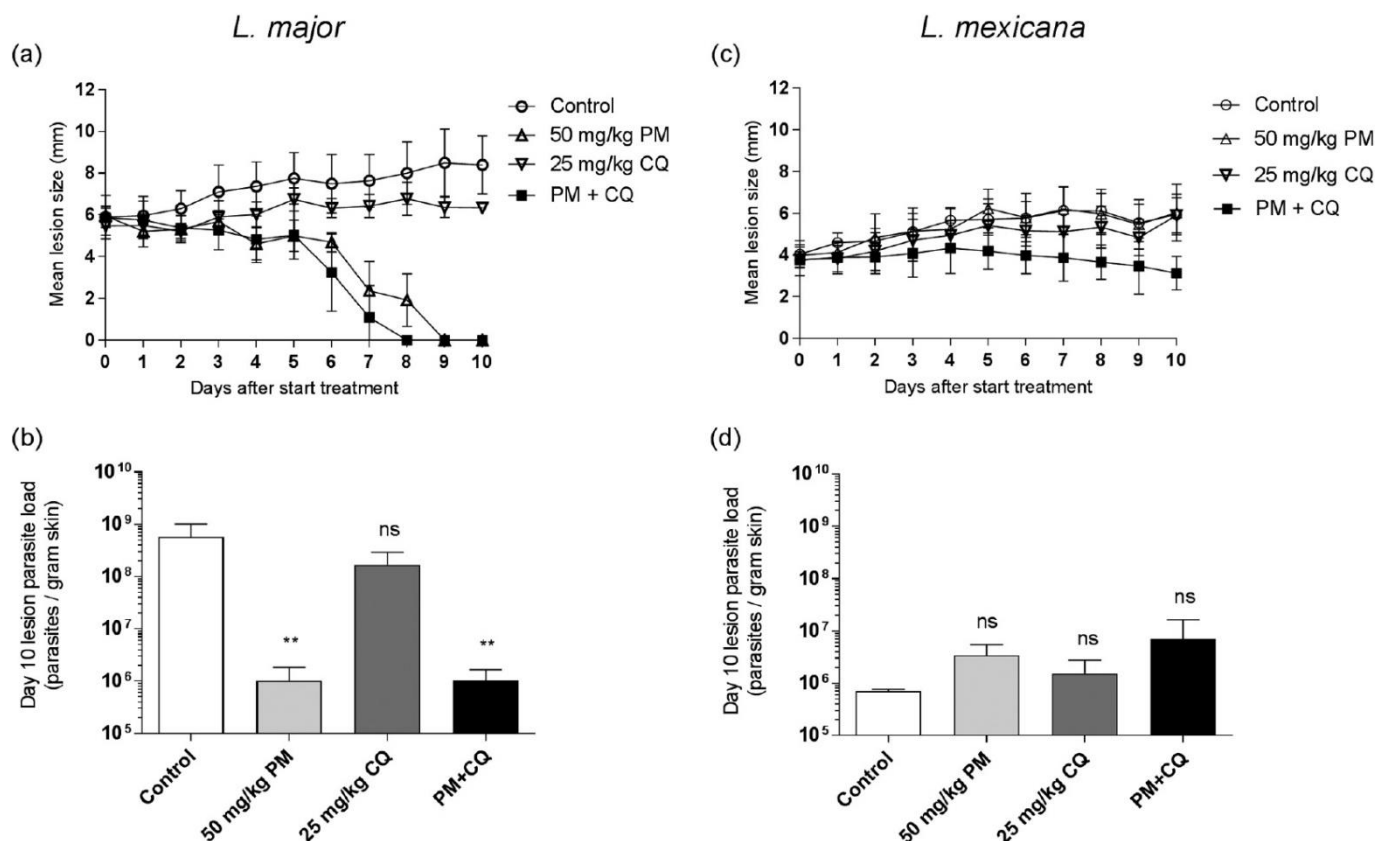


FIG 2 Evaluation of the *in vivo* efficacy of the combination of PM and CQ in murine models of *L. major* (left) and *L. mexicana* (right) CL. Female BALB/c mice were infected with stationary-phase promastigotes in the rump above the tail ($n = 3$ to 5 per group). At 12 days (*L. major*) and 6 weeks (*L. mexicana*) postinoculation, animals presenting with CL nodules were dosed daily via the i.p. route for 10 consecutive days with PBS (control), 50 mg/kg PM, 25 mg/kg CQ, or a combination of 50 mg/kg PM and 25 mg/kg CQ (PM+CQ). One day after the administration of the last dose (day 10), animals were sacrificed, lesions were harvested, and parasite burden was quantified by DNA-based qPCR. Lesion size evolution (a and c) and lesion parasite load at the end of treatment (b and d) are shown as means and SD. ANOVA (1 way for parasite load and repeated measures for lesion size) followed by Turkey's multiple-comparison tests was used to compare outcomes among the groups. The difference between untreated controls and individual PM-, CQ-, and PM-CQ-treated groups was considered statistically significant if the P value was <0.05 (**, $P < 0.001$) or insignificant if not (ns).

test whether increased phagolysosomal pH is linked to improved antileishmanial activity.

Finally, the efficacy of the PM-CQ combination was assessed in murine models of CL caused by the selected *Leishmania* species. For *L. major*- and *L. mexicana*-infected rodents, differences in lesion sizes and day 10 parasite loads among the groups were analyzed (Fig. 2). There was a good correlation between lesion size (Fig. 2a) and parasite load (Fig. 2b) in the *L. major* BALB/c model. Compared to the untreated controls (phosphate-buffered saline [PBS]), lesion sizes in *L. major*-infected animals receiving only 25 mg/kg of body weight CQ were slightly smaller (but the difference between the groups was insignificant; $P = 0.072$) but were significantly reduced in the groups receiving 50 mg/kg PM and 50 mg/kg PM plus 25 mg/kg CQ (PM-CQ) ($P < 0.0001$ for both). When mice treated with PM alone were compared to those treated with PM-CQ, lesions in the combination group were smaller and fully resolved (0 ± 0 mm) 1 day earlier (by day 8 versus day 9), but the difference was not statistically significant ($P = 0.823$). The parasite load was not significantly reduced in the CQ group compared to the untreated group ($P = 0.062$) but was significantly lower for PM alone and the PM-CQ groups ($P = 0.006$ for both). No additional reduction in parasite load was found between the PM and PM-CQ groups ($1.0 \times 10^6 \pm 0.8 \times 10^6$ amastigotes per g skin tissue for both), and the difference was insignificant ($P > 0.999$). For the *in vivo* experiment with *L. mexicana*, lesion sizes (Fig. 2c) again correlated fairly well with parasite loads (Fig. 2d). *L. mexicana* lesion sizes in rodents treated with PM, CQ, and PM-CQ were not significantly reduced compared to those in the placebo group ($P >$

0.999, $P = 0.890$, and $P = 0.216$, respectively). However, in specific comparisons of the PM and PM-CQ groups at the end of treatment (day 10), the lesion sizes were smaller for the combination group (3.1 ± 0.8 versus 6.0 ± 1.4 mm), and the difference at this time point was significant ($P = 0.0014$). Parasite burdens were similar in the placebo, PM, CQ, and PM-CQ groups ($P > 0.05$ for all differences). No significant difference ($P = 0.824$) between parasite loads in the PM-CQ group ($7.0 \times 10^6 \pm 9.3 \times 10^6$) and the PM-alone group ($3.4 \times 10^6 \pm 2.2 \times 10^6$) was found. Over the course of treatment of *L. major*- and *L. mexicana*-infected mice, no events of severe weight loss or adverse drug effects occurred (data not shown).

We conclude that while combination therapy of 50 mg/kg PM combined with 25 mg/kg CQ did not show increased toxicity, there was not significant additional activity compared to those of the component drugs. Against both tested *Leishmania* species, the association resulted in a small decrease in lesion size toward the end of treatment (which is remarkable for *L. mexicana* CL due to the known and hereby confirmed unresponsiveness of this species to PM treatment), but the corresponding parasite loads were not significantly reduced. The independent anti-inflammatory properties of CQ rather than a synergistic mechanism with PM might explain this phenomenon, as we also observed a small but not significant suppressive effect on lesion size in controls treated with CQ alone. While the inhibition of proinflammatory cytokine production and release could hinder classic macrophage activation and the consequent elimination of intracellular parasites, this may reduce skin tissue damage and prevent further inflammation-driven lesion proliferation (24–26). Furthermore, antileishmanial activity of CQ in the *L. amazonensis* CBA mouse ear model has been reported, although this was observed after higher-dose oral treatment (50 mg/kg) over longer periods (5 weeks) (27).

The poor *in vitro-in vivo* translation of the PM-CQ combination might be explained by several factors. First, skin pharmacokinetics could play a role. The daily 50-mg/kg PM regimen over a 10-day period showed efficacy, in agreement with data from previous work with the *L. major*-BALB/c mouse model (28), indicating that the drug must be bioavailable at the dermal infection site to exert its antileishmanial activity. Based on the extrapolation of data on CQ accumulation in rat skin after intraperitoneal (i.p.) administration (29, 30), the daily 25-mg/kg dose regimen over 10 days should have resulted in the desired dermal micromolar concentrations within the chosen time frame. The ability of CQ to sequester in skin has been extensively reported, as it is used in the treatment of cutaneous lupus and is thought to be a factor in adverse reactions such as pruritus and itching (31). Moreover, Leimer and colleagues (16) showed the additional efficacy of flucloxacillin-CQ compared to the antibiotic as monotherapy against *S. aureus* in a murine systemic infection model after only 2 i.p. doses of 10 mg/kg CQ over a period of 3 days. Hence, while exposure levels of CQ and PM at the target site were likely sufficient to allow theoretical synergy between the drugs, this could not be confirmed experimentally. Second, in the dermis, CQ might not be able to penetrate infected macrophages to interact with PM for the elimination of intracellular parasites. Ionization of CQ in the acidified extracellular fluid present in many tumors is known to limit its passive passage through the membranes of the targeted cancer cells (32). The well-known phenomenon of local acidosis in inflamed tissues (33), such as *Leishmania*-infected skin (34), could have led to a similar limitation of uptake at this site. Third, there may be *in vivo* antagonistic effects between PM and CQ. This is unlikely because the drugs have not been reported to affect each other's absorption, distribution, metabolism, or excretion (30). Finally, although the *in vitro* intracellular amastigote drug assay using murine macrophages has proven to be a suitable model to predict *in vivo* activity in mice, the lack of biological relevance (macrophage behavior and the presence of many other types of cells and compounds under physiological conditions) might confound this assumption. There is still a need for more complex *in vitro* antileishmanial drug assays to bridge this gap in preclinical CL drug research. Taken together, the variable susceptibilities of *L. major* and *L. mexicana* to the tested drugs also highlight the vast challenge in the identification of

a single new (combination) treatment active against the plethora of *Leishmania* species causing CL.

In summary, our data suggest that the high-dose combination of PM and CQ provides only limited enhanced efficacy (mild effect on the evolution of lesion sizes without an additional reduction in parasite burdens) in *L. major*- and *L. mexicana*-infected mice compared to PM monotherapy. These findings indicate that further research, such as optimization of the drug dose ratio, into this combination as a novel treatment for CL is not justified.

MATERIALS AND METHODS

Drugs. For the *in vitro* drug assays, stocks of paromomycin sulfate (20 mM [aq]; Sigma, UK), MF (20 mM [aq]; Paladin Inc., UK), amphotericin B deoxycholate (5.2 mM [aq]) (Fungizone; Gibco, UK), and chloroquine diphosphate (10 mM [aq]; Sigma, UK) were prepared, aliquoted, and kept at -20°C until use. From the same original drug batches, solutions in PBS (0.9% NaOH [pH 7.4]; Sigma, UK) were made for the rodent experiments (mean weight per animal of 20 g) at concentrations of 50 mg/kg PM (5.797 mg/ml), 25 mg/kg CQ (4.032 mg/ml), and 50 mg/kg PM plus 25 mg/g kg CQ (coadministration of the same doses).

Macrophages. Peritoneal mouse macrophages (PEMs) were obtained from female 8- to 12-week-old CD1 mice. A 2% (wt/vol) starch (VWR, USA) solution in PBS was injected *i.p.*, and PEMs were harvested 24 h later by peritoneal lavage with RPMI medium containing 1% penicillin-streptomycin (PenStrep; Sigma, UK). After centrifugation at 1,500 rpm at 4°C for 15 min, the supernatant was removed, and the pellet was resuspended in minimal essential medium Eagle (MEME; Sigma, UK) with 10% heat-inactivated fetal calf serum (HiFCS; Gibco, UK). The number of cells was estimated by counting with a Neubauer hemocytometer using light microscopy ($\times 40$ magnification).

Parasites. *L. major* MHOM/SA85/JISH118 and *L. mexicana* MNYC/BZ/62/M379 parasites were cultured in Schneider's insect medium (Sigma, UK) supplemented with 10% HiFCS. These parasites were passaged each week at a 1:10 ratio of the existing culture to fresh medium in 25-ml culture flasks without a filter and incubated at 26°C . For infection of macrophages (*in vitro*) and mice (*in vivo*), stationary-phase parasites (as confirmed by light microscopy) were centrifuged for 10 min at 2,100 rpm at 4°C . The supernatant was removed, and the pellet was resuspended in MEME containing 10% HiFCS. The number of cells was estimated by microscopic counting with a Neubauer hemocytometer.

Cytotoxicity assays. Macrophages in a $200\text{-}\mu\text{l}$ suspension (4×10^5 macrophages per ml) were allowed to adhere to the bottom of 96-well plates for 48 h and then exposed to specific drug concentrations over 72 h. Cytotoxicity was evaluated by using the alamarBlue assay (Serotec, UK) and a lactate dehydrogenase assay (LDH kit; Promega, UK) to assess metabolism (cell viability) and enzyme leakage through damaged cell membranes (cell death), respectively. After the addition of alamarBlue (10%) to $150\text{-}\mu\text{l}$ of the treated PEM culture, the latter was incubated at 37°C in 5% CO_2 , and viability was measured over a period of 1 to 24 h by fluorescence (SpectraMax M3 plate reader; Molecular Devices) at a wavelength of 530 nm, with a 580-nm emission wavelength and a 550-nm cutoff. Results were expressed as percent viability compared to the untreated controls after correction for the blank signal. In separate wells, an LDH substrate mix was added to $50\text{-}\mu\text{l}$ of the treated PEM culture at a 1:1 ratio. The plates were incubated at room temperature for 30 min on a mechanical shaker with slow rotation. Stop solution ($50\text{-}\mu\text{l}$) was then added, and the absorbance at 490 nm was determined. Results were expressed as percent cell death compared to the positive controls (PEMs treated with $80\text{-}\mu\text{M}$ podophyllotoxin; Sigma, UK) after correction for the blank. An alamarBlue assay (with the same experimental settings as the ones described above for macrophages) was also used to assess the viability of exponential-phase promastigotes during drug assays. Results were expressed as percent inhibition = $100\% - x\%$ viability (means \pm 95% confidence intervals [CI]).

Seventy-two-hour intracellular antileishmanial drug activity assay. One hundred microliters of the PEM culture (4×10^5 macrophages per ml) was added to each well of 16-well LabTek culture slides (Thermo Fisher, UK) and incubated for 24 h at 37°C in 5% CO_2 . Host cells were then infected at a 1:3 ratio (*L. major* or *L. mexicana*) using $100\text{-}\mu\text{l}$ stationary-phase low-passage-number parasites and further incubated for 24 h at 34°C in 5% CO_2 . On the day of treatment, drug stocks were thawed and diluted to the appropriate concentrations. After confirmation that macrophage infection levels were above 80% (light microscopy), extracellular parasites were removed by washing, and $100\text{-}\mu\text{l}$ of a drug dilution in MEME with 10% HiFCS, alone or supplemented with $10\text{-}\mu\text{M}$ CQ, was added to the infected PEMs. The final drug concentrations were $360\text{-}\mu\text{M}$ for PM, $30\text{-}\mu\text{M}$ for MF, and $0.5\text{-}\mu\text{M}$ for AmB, which were 1:3 serially diluted, resulting in quadruplicates of 4 different concentrations. After incubation for 72 h at 34°C , the medium was removed, and the slides were fixed with 100% methanol for 2 min and stained with 10% Giemsa for 10 min. The number of infected cells was then measured under each treatment condition by microscopically counting 100 macrophages. The percentage of infected cells after treatment was determined and expressed relative to the untreated control (percent inhibition). Dose-response curves and EC_{50} s were calculated by using GraphPad Prism version 7.02 software. Results represent means \pm 95% CI.

***In vivo L. major* and *L. mexicana* models of CL.** Female BALB/c mice around 6 to 8 weeks old were purchased from Charles River Ltd. (Margate, UK). These mice were kept in humidity- and temperature-controlled rooms (55 to 65% and 25 to 26°C , respectively) and fed water and rodent food *ad libitum*. After acclimatization for 1 week, mice were randomized and subcutaneously (*s.c.*) infected in the shaven rump

above the tail with 200 μ l of a parasite suspension containing 4×10^7 low-passage-number ($P < 5$), stationary-phase *L. major* or *L. mexicana* promastigotes in RPMI medium. Lesion size was measured daily, and treatment was not started until the development of a 3- to 4-mm nodule. Animals were allocated to 4 groups ($n = 3$ for *L. mexicana* and $n = 5$ for *L. major* *in vivo* assays) to ensure comparable lesion sizes under each condition. Mice were treated every 24 h with 25 mg/kg CQ, 50 mg/kg PM, or a combination of these drugs at the same doses for 10 days (in PBS, by the i.p. route). The control group received a similar volume (200 μ l) of PBS (i.p.). Drug efficacy was evaluated by daily measurements of lesion size and quantification of parasite loads in the infected skin at the end of treatment. Digital calipers were used to determine the mean size of the nodule in 2 dimensions (length and width). Body weight was recorded daily to monitor clinical deterioration due to pathology or systemic drug toxicity.

Ethics statement. All animal experiments were conducted under license X20014A54 according to UK Home Office regulations under the Animals (Scientific Procedures) Act 1986 and EC Directive 2010/63/E.

Parasite DNA extraction from lesions and parasite loads. The harvested lesion was cut into 1- to 2-mm-long pieces and placed into SureLock microcentrifuge tubes (StarLab, UK) together with 1 ml PBS and 100 mg of 2-mm zirconium oxide beads (NextAdvance, UK). The tissue was ground by using a BulletBlender Storm 24 instrument (NextAdvance, UK) set at maximum speed (setting 12) for 15 min. DNA from a 200- μ l volume of the homogenate was extracted by using the Qiagen DNeasy kit for blood and tissue. Twenty microliters of proteinase K and 200 μ l tissue lysis buffer were added, mixed, and left to incubate for 1 h in a water bath at 56°C. According to the manufacturer's protocols, DNA was precipitated by using ethanol and transferred to a DNeasy minicolumn, which retained DNA during multiple washing steps until 50 μ l was eluted with the appropriate buffer. For the calibration curve standards, this DNA extract from 10^9 *L. major* or *L. mexicana* promastigotes was added to 450 μ l water, and consequent serial dilutions ranging from 10^8 to 10^1 were made. A previously established quantitative PCR (qPCR) methodology based on the amplification of the 170-bp region in the *Leishmania* 18S gene (35) was used to quantify the parasite burden in the lesion. Two-microliter DNA extract samples (diluted 1/100) were amplified in 10- μ l reaction mixtures in the presence of 5 μ l SensiFAST SYBR No-ROX master mix, 0.25 μ M probe, and 0.4 μ M each primer. Each run included a negative or no-template control where master mix or DNA was replaced by purified water, respectively. Triplicates of standards (10^8 to 10^1) and duplicates of unknown samples were included. The tubes were placed into a 72-sample rotor of the RotorGene 3000 instrument, set at 40 cycles at a denaturation setting of 95°C for 5 min followed by a 2-step amplification cycle of 95°C for 10 s and 60°C for 30 s.

Statistical analysis. For the outcomes of *in vitro* assays (Fig. 1), the percentage of inhibition was expressed relative to the untreated 72-h control, and the corresponding sigmoidal dose-response curves were established by using a nonlinear fit with variable slope models. Related EC_{50} s were compared by using extra-sum-of-squares *F* tests. For *in vivo* experiments (Fig. 2), the differences in lesion sizes and parasite loads among the groups were assessed by using repeated-measures 2-way analysis of variance (ANOVA) and 1-way ANOVA, both of which were followed by Tukey's multiple-comparison test. *In vitro* data are presented as means \pm 95% CI, and *in vivo* data are presented as means \pm standard deviations (SD). *P* values of <0.05 were considered statistically significant. All analyses were performed by using GraphPad Prism version 7.02.

ACKNOWLEDGMENTS

Gert-Jan Wijnant's doctoral project is part of the EuroLeish.Net Training Network (www.euroleish.net) and has received funding from the European Horizon's 2020 Research and Innovation Programme under Marie Skłodowska-Curie grant agreement number 642609.

We are grateful to Karin Seifert for many fruitful discussions and to the staff of the Biological Service Facilities for assistance during animal studies.

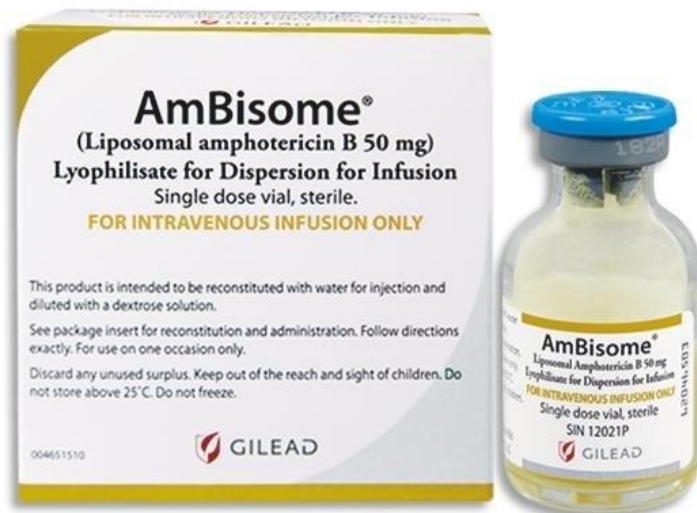
REFERENCES

- Reithinger R, Dujardin J-C, Louzir H, Pirmez C, Alexander B, Brooker S. 2007. Cutaneous leishmaniasis. *Lancet Infect Dis* 7:581–596. [https://doi.org/10.1016/S1473-3099\(07\)70209-8](https://doi.org/10.1016/S1473-3099(07)70209-8).
- Alvar J, Vélez ID, Bern C, Herrero M, Desjeux P, Cano J, Jannin J, den Boer M. 2012. Leishmaniasis worldwide and global estimates of its incidence. *PLoS One* 7:e35671. <https://doi.org/10.1371/journal.pone.0035671>.
- Eiras DP, Kirkman LA, Murray HW. 2015. Cutaneous leishmaniasis: current treatment practices in the USA for returning travelers. *Curr Treat Options Infect Dis* 7:52–62. <https://doi.org/10.1007/s40506-015-0038-4>.
- World Health Organization. 2010. Control of the leishmaniasis. World Health Organization technical report series. World Health Organization, Geneva, Switzerland.
- Croft SL, Olliaro P. 2011. Leishmaniasis chemotherapy—challenges and opportunities. *Clin Microbiol Infect* 17:1478–1483. <https://doi.org/10.1111/j.1469-0691.2011.03630.x>.
- Uliana SRB, Trincon CT, Coelho AC. Chemotherapy of leishmaniasis: present challenges. *Parasitology*, in press.
- Amer EI, Eissa MM, Mossallam SF. 2016. Oral azithromycin versus its combination with miltefosine for the treatment of experimental Old World cutaneous leishmaniasis. *J Parasit Dis* 40:475–484. <https://doi.org/10.1007/s12639-014-0529-0>.
- Trincon CT, Reimão JQ, Yokoyama-Yasunaka JKU, Miguel DC, Uliana SRB. 2014. Combination therapy with tamoxifen and amphotericin B in experimental cutaneous leishmaniasis. *Antimicrob Agents Chemother* 58:2608–2613. <https://doi.org/10.1128/AAC.01315-13>.
- Santarem AAA, Greggianin GF, Debastiani RG, Ribeiro JBP, Polli DA, Sampaio RNR. 2014. Effectiveness of miltefosine-pentoxifylline compared to miltefosine in the treatment of cutaneous leishmaniasis in C57Bl/6 mice. *Rev Soc Bras Med Trop* 47:517–520. <https://doi.org/10.1590/0037-8682-0202-2013>.
- Aguiar MG, Silva DL, Nunan FA, Nunan EA, Fernandes AP, Ferreira LAM. 2009. Combined topical paromomycin and oral miltefosine treatment of mice experimentally infected with *Leishmania (Leishmania) major* leads to reduction in both lesion size and systemic parasite burdens. *J Antimicrob Chemother* 64:1234–1240. <https://doi.org/10.1093/jac/dkp365>.
- de Moraes-Teixeira E, Aguiar MG, Soares de Souza Lima B, Ferreira LAM,

- Rabello A. 2015. Combined suboptimal schedules of topical paromomycin, meglumine antimoniate and miltefosine to treat experimental infection caused by *Leishmania* (Viannia) *braziliensis*. *J Antimicrob Chemother* 70:3283–3290. <https://doi.org/10.1093/jac/dkv254>.
12. Calza L, Attard L, Manfredi R, Chiodo F. 2002. Doxycycline and chloroquine as treatment for chronic Q fever endocarditis. *J Infect* 45:127–129. <https://doi.org/10.1053/jinf.2002.0984>.
 13. Kersh GJ. 2013. Antimicrobial therapies for Q fever. *Expert Rev Anti Infect Ther* 11:1207–1214. <https://doi.org/10.1586/14787210.2013.840534>.
 14. Maurin M, Benoliel AM, Bongrand P, Raoult D. 1992. Phagolysosomal alkalization and the bactericidal effect of antibiotics: the *Coxiella burnetii* paradigm. *J Infect Dis* 166:1097–1102. <https://doi.org/10.1093/infdis/166.5.1097>.
 15. Ghigo E, Capo C, Aurouze M, Tung C-H, Gorvel J-P, Raoult D, Mege J-L. 2002. Survival of *Tropheryma whipplei*, the agent of Whipple's disease, requires phagosome acidification. *Infect Immun* 70:1501–1506. <https://doi.org/10.1128/IAI.70.3.1501-1506.2002>.
 16. Leimer N, Rachmühl C, Palheiros Marques M, Bahlmann AS, Furrer A, Eichenseher F, Seidl K, Matt U, Loessner MJ, Schuepbach RA, Zinkernagel AS. 2016. Nonstable *Staphylococcus aureus* small-colony variants are induced by low pH and sensitized to antimicrobial therapy by phagolysosomal alkalization. *J Infect Dis* 213:305–313. <https://doi.org/10.1093/infdis/jiv388>.
 17. Croft SL, Sundar S, Fairlamb AH. 2006. Drug resistance in leishmaniasis. *Clin Microbiol Rev* 19:111–126. <https://doi.org/10.1128/CMR.19.1.111-126.2006>.
 18. Real F, Mortara RA. 2012. The diverse and dynamic nature of *Leishmania* parasitophorous vacuoles studied by multidimensional imaging. *PLoS Negl Trop Dis* 6:e1518. <https://doi.org/10.1371/journal.pntd.0001518>.
 19. el-On J, Hamburger AD. 1987. Topical treatment of New and Old World cutaneous leishmaniasis in experimental animals. *Trans R Soc Trop Med Hyg* 81:734–737. [https://doi.org/10.1016/0035-9203\(87\)90011-3](https://doi.org/10.1016/0035-9203(87)90011-3).
 20. Neal RA, Murphy AG, Olliaro P, Croft SL. 1994. Aminosidine ointments for the treatment of experimental cutaneous leishmaniasis. *Trans R Soc Trop Med Hyg* 88:223–225. [https://doi.org/10.1016/0035-9203\(94\)90307-7](https://doi.org/10.1016/0035-9203(94)90307-7).
 21. Neal RA, Allen S, McCoy N, Olliaro P, Croft SL. 1995. The sensitivity of *Leishmania* species to aminosidine. *J Antimicrob Chemother* 35:577–584. <https://doi.org/10.1093/jac/35.5.577>.
 22. Glaser TA, Baatz JE, Kreishman GP, Mukkada AJ. 1988. pH homeostasis in *Leishmania donovani* amastigotes and promastigotes. *Proc Natl Acad Sci U S A* 85:7602–7606. <https://doi.org/10.1073/pnas.85.20.7602>.
 23. Levison ME, Levison JH. 2009. Pharmacokinetics and pharmacodynamics of antibacterial agents. *Infect Dis Clin North Am* 23:791–815. <https://doi.org/10.1016/j.idc.2009.06.008>.
 24. Jang C-H, Choi J-H, Byun M-S, Jue D-M. 2006. Chloroquine inhibits production of TNF-alpha, IL-1beta and IL-6 from lipopolysaccharide-stimulated human monocytes/macrophages by different modes. *Rheumatology* (Oxford) 45:703–710. <https://doi.org/10.1093/rheumatology/kei282>.
 25. de Oliveira Cardoso F, da Silva Freitas de Souza C, Gonçalves Mendes V, Abreu-Silva AL, Costa D, Gonçalves SC, da Silva Calabrese K. 2010. Immunopathological studies of *Leishmania amazonensis* infection in resistant and in susceptible mice. *J Infect Dis* 201:1933–1940. <https://doi.org/10.1086/652870>.
 26. Faria DR, Gollob KJ, Barbosa J, Schriefer A, Machado PRL, Lessa H, Carvalho LP, Romano-Silva MA, de Jesus AR, Carvalho EM, Dutra WO. 2005. Decreased in situ expression of interleukin-10 receptor is correlated with the exacerbated inflammatory and cytotoxic responses observed in mucosal leishmaniasis. *Infect Immun* 73:7853–7859. <https://doi.org/10.1128/IAI.73.12.7853-7859.2005>.
 27. Rocha VPC, Nonato FR, Guimarães ET, Rodrigues de Freitas LA, Soares MBP. 2013. Activity of antimalarial drugs in vitro and in a murine model of cutaneous leishmaniasis. *J Med Microbiol* 62:1001–1010. <https://doi.org/10.1099/jmm.0.058115-0>.
 28. El-On J, Lang E, Kuperman O, Avinoach I. 1989. *Leishmania major*: histopathological responses before and after topical treatment in experimental animals. *Exp Parasitol* 68:144–154. [https://doi.org/10.1016/0014-4894\(89\)90091-X](https://doi.org/10.1016/0014-4894(89)90091-X).
 29. Adelusi SA, Salako LA. 1982. Tissue and blood concentrations of chloroquine following chronic administration in the rat. *J Pharm Pharmacol* 34:733–735. <https://doi.org/10.1111/j.2042-7158.1982.tb06211.x>.
 30. Adelusi SA, Salako LA. 1982. The effect of protein-energy malnutrition on the absorption, distribution and elimination of chloroquine in the rat. *Gen Pharmacol* 13:505–509. [https://doi.org/10.1016/0306-3623\(82\)90025-8](https://doi.org/10.1016/0306-3623(82)90025-8).
 31. Grayson ML, Crowe SM, McCarthy JS, Mills J, Mouton JW, Norrby SR, Paterson DL, Pfaller MA. 2010. Kucers' the use of antibiotics: a clinical review of antibacterial, antifungal and antiviral drugs, 6th ed. CRC Press, Boca Raton, FL.
 32. Pellegrini P, Strambi A, Zipoli C, Hägg-Olofsson M, Buoncervello M, Linder S, De Milito A. 2014. Acidic extracellular pH neutralizes the autophagy-inhibiting activity of chloroquine: implications for cancer therapies. *Autophagy* 10:562–571. <https://doi.org/10.4161/auto.27901>.
 33. Ueno T, Tsuchiya H, Mizogami M, Takakura K. 2008. Local anesthetic failure associated with inflammation: verification of the acidosis mechanism and the hypothetical participation of inflammatory peroxynitrite. *J Inflamm Res* 1:41–48.
 34. Scott P, Novais FO. 2016. Cutaneous leishmaniasis: immune responses in protection and pathogenesis. *Nat Rev Immunol* 16:581–592. <https://doi.org/10.1038/nri.2016.72>.
 35. van der Meide W, Guerra J, Schoone G, Farenhorst M, Coelho L, Faber W, Peekel I, Schallig H. 2008. Comparison between quantitative nucleic acid sequence-based amplification, real-time reverse transcriptase PCR, and real-time PCR for quantification of *Leishmania* parasites. *J Clin Microbiol* 46:73–78. <https://doi.org/10.1128/JCM.01416-07>.

Chapter 3.2:

AmBisome treatment of CL -
relation between skin
pharmacokinetics and efficacy



3.2: AmBisome treatment of CL - relation between skin PK and efficacy

ANNEX 2: WIJNANT G-J, VAN BOCXLAER K, YARDLEY V, HARRIS A, MURDAN S, CROFT SL. 2018. RELATION BETWEEN SKIN PHARMACOKINETICS AND EFFICACY IN AMBISOME TREATMENT OF MURINE CUTANEOUS LEISHMANIASIS. ANTIMICROB AGENTS CHEMOTHER 62.

Key points, novel results and implications

- One of the main aims of this thesis was to develop methodologies to investigate the PK, PD and PK/PD properties of new drug candidates for the treatment of CL. To first validate such an approach and related methods, we used the standard drug **amphotericin B (AmB) in the unilamellar liposomal formulation AmBisome (LAmB)**. The choice for AmBisome as a standard drug was justified by:
 - The availability of earlier reports on its excellent efficacy in the *L. major* – BALB/c mouse model of CL.
 - The large body of scientific literature on its PK and PK/PD properties because of its important role in the treatment of systemic fungal infections.
 - The experience of our industrial partner Pharmidex for the quantification of AmB in biological matrices by LC-MS/MS.
- LAmB is a standard 2nd-line drug in the treatment of (M)CL. However, very little is known about skin distribution and PD to inform clinical use.
- We compared the skin PK of LAmB with those of the deoxycholate form of AmB (DAmB; trade name Fungizone) in a murine model of *L. major* CL. After administration of 5 doses at 1 mg/kg (IV) over 10 days, AmB levels at the target site (the localized lesion) were 3-fold higher for LAmB than for DAmB. For both formulations, drug concentrations in lesions were 20-fold higher than those in the healthy control skin of the same infected mice. Skin PK was based on necropsy and tissue homogenisation.
- We then evaluated how drug levels in the lesion after higher-dosed LAmB treatment (1 mg/kg = acute toxicity limit for DAmB) relate to therapeutic outcomes on day 10. A clear-dose response up to 12.5 mg/kg was found after LAmB administration at day 0, 2, 4, 6, and 8 and there was a clear correlation between dose, intralesional AmB concentration, and relative reduction in parasite load and lesion size ($R^2 > 0.9$).
- Overall, we present the **first PK/PD-based investigation of LAmB in CL**, which can form a basis for the development of optimized clinical dose regimens in patients. Furthermore, the data indicates **encapsulation of antileishmanial drugs in liposomes** could be a suitable strategy for targeted delivery in CL drug development.
- In the frame of the thesis, we confirmed the dose- and skin concentration-dependent *in vivo* activity of intravenous LAmB in murine CL. The PK/PD-based approach to drug evaluation provided a framework to provide a head-to-head comparison of different compounds and (liposomal) formulations, as done in chapter 3.3. Moreover, we hypothesised that it was the local inflammation in the diseased skin tissue that enhanced drug accumulation in lesions, which was investigated in chapter 3.4.

Candidate's contribution:

The candidate generated and analyzed all data described in the paper, except for LC/MS-MS quantification of drug levels in samples and calculation of PK parameters with WinNonLin software (Pharmidex Pharmaceutical Services Ltd.). The candidate prepared the first draft of the manuscript, which was accepted for publication by Antimicrobial Agents and Chemotherapy in December 2017 following academic peer review.

Research paper cover sheet

London School of Hygiene & Tropical Medicine
Keppel Street, London WC1E 7HT
www.lshtm.ac.uk

Registry
T: +44(0)20 7299 4646
F: +44(0)20 7299 4656
E: registry@lshtm.ac.uk

LONDON SCHOOL OF HYGIENE & TROPICAL MEDICINE

RESEARCH PAPER COVER SHEET

PLEASE NOTE THAT A COVER SHEET MUST BE COMPLETED FOR EACH RESEARCH PAPER INCLUDED IN A THESIS.

SECTION A – Student Details

Student	GERT-JAN WIJNANT	
Principal Supervisor	SIMON DROUGHT	
Thesis Title	NEW DRUGS FOR DEVELOPMENT METHODS FOR CLINICAL TRIALS	

If the Research Paper has previously been published please complete Section B. If not please move to Section C

SECTION B – Paper already published

Where was the work published?	AAC	
When was the work published?	DECEMBER 2017	
If the work was published prior to registration for your research degree, give a brief rationale for its inclusion	N/A	
Have you retained the copyright for the work?		Was the work subject to academic peer review? YES

*If yes, please attach evidence of retention. If no, or if the work is being included in its published format, please attach evidence of permission from the copyright holder (publisher or other author) to include this work.

SECTION C – Prepared for publication, but not yet published

Where is the work intended to be published?	/	
Please list the paper's authors in the intended authorship order:	/	
Stage of publication	/	

SECTION D – Multi-authored work

For multi-authored work, give full details of your role in the research included in the paper and in the preparation of the paper. (Attach a further sheet if necessary)	ALL WORK: MANUSCRIPT EXCEPT - LC/MS-MS - WIN-LIN	
--	--	--

Student Signature: [Redacted] Date: 17/11/2018

Supervisor Signature: [Redacted] Date: 18.06.2018

Improving health worldwide www.lshtm.ac.uk

Copyright proof

Re: Copyright for AAC papers: confirmation

DH Drought, Heather <hdrought@asmusa.org>
Today, 16:00
Gert Wijnant

Reply all

Inbox

Label: Staff mailbox default delete after 7 years (7 years) Expires: 25/07/2025 16:00

Greetings,

Thank you for your email. When you choose open access publishing, you/the author retains copyright: <https://creativecommons.org/licenses/by/4.0/>
Regardless of OA status, all ASM authors retain certain rights, including use of their article in their thesis or dissertation: http://journals.asm.org/site/misc/ASM_Author_Statement.xhtml

It is fine to use the manuscript in your thesis/dissertation, but you will need to add to the manuscript once accepted that it was used in the thesis (I see you currently note: "Gert-Jan Wijnant's doctoral project is part of the EuroLeish.Net Training Network (www.euroleish.net).") Please check with production staff after final acceptance/at proof stage to see whether this is sufficient. I will make a note of this on the manuscript for the production staff.

I hope this helps, but please let me know if there are any additional questions.

Very best,
Heather

Heather Drought
Editorial Coordinator
American Society for Microbiology
1752 N Street, N.W., Washington, D.C. 20036-2904
Phone: 202-942-9363 | Fax: 202-942-9355



Relation between Skin Pharmacokinetics and Efficacy in AmBisome Treatment of Murine Cutaneous Leishmaniasis

Gert-Jan Wijnant,^{a,b} Katrien Van Booclaer,^a Vanessa Yardley,^a Andy Harris,^c Sudaxshina Murdan,^b Simon L. Croft^a

^aDepartment of Immunology and Infection, Faculty of Infectious and Tropical Diseases, London School of Hygiene and Tropical Medicine, London, United Kingdom

^bDepartment of Pharmaceutics, UCL School of Pharmacy, London, United Kingdom

^cPharmidex Pharmaceutical Services Ltd., London, United Kingdom

ABSTRACT AmBisome (LAmB), a liposomal formulation of amphotericin B (AmB), is a second-line treatment for the parasitic skin disease cutaneous leishmaniasis (CL). Little is known about its tissue distribution and pharmacodynamics to inform clinical use in CL. Here, we compared the skin pharmacokinetics of LAmB with those of the deoxycholate form of AmB (DAmB; trade name Fungizone) in murine models of *Leishmania major* CL. Drug levels at the target site (the localized lesion) 48 h after single intravenous (i.v.) dosing of the individual AmB formulations (1 mg/kg of body weight) were similar but were 3-fold higher for LAmB than for DAmB on day 10 after multiple administrations (1 mg/kg on days 0, 2, 4, 6, and 8). After single and multiple dosing, intralesional concentrations were 5- and 20-fold, respectively, higher than those in the healthy control skin of the same infected mice. We then evaluated how drug levels in the lesion after LAmB treatment relate to therapeutic outcomes. After five administrations of the drug at 0, 6.25, or 12.5 mg/kg (i.v.), there was a clear correlation between dose level, intralesional AmB concentration, and relative reduction in parasite load and lesion size (R^2 values of >0.9). This study confirms the improved efficacy of the liposomal over the deoxycholate AmB formulation in experimental CL, which is related to higher intralesional drug accumulation.

KEYWORDS pharmacokinetics, pharmacodynamics, amphotericin B, cutaneous leishmaniasis

Cutaneous leishmaniasis (CL) is a neglected vector-borne tropical disease caused by intracellular protozoan *Leishmania* parasites. Current estimates suggest 350 million people at risk, 12 million cases per year, and 1 to 1.5 million new cases annually in more than 98 countries, the majority of which occur in Latin America and the Middle East (1). While mortality is limited for the most common form, localized CL, morbidity is serious due to ulceration, disfigurement, and often permanent scarring after healing of the lesion, which are all associated with social stigmatization. More complex and potentially dangerous forms of CL are diffuse (diffuse cutaneous leishmaniasis, or DCL), chronic (*leishmaniasis recidivans*, or CCL), or destructive to the nasopharyngeal mucosa (mucocutaneous leishmaniasis, or MCL). Current treatments are hampered in their clinical value by toxicity, side effects, variable efficacy, high cost, or invasive administration route. First-line treatment consists of pentavalent antimonials. Second-line chemotherapeutic options include paromomycin, miltefosine, and amphotericin B (AmB). AmB, a macrocyclic polyene antibiotic and important antifungal agent derived from *Streptomyces nodosus*, is active due to complexation with ergosterol in leishmanial cell membranes, leading to the formation of pores and ultimately pathogen death (2). Due to infusion-related and (nephro)toxicity issues of the classic colloidal dispersion with deoxycholate amphotericin B (DAmB; trade name Fungizone), lipid formulations with

Received 28 September 2017 Returned for modification 17 October 2017 Accepted 16 December 2017

Accepted manuscript posted online 20 December 2017

Citation Wijnant G-J, Van Booclaer K, Yardley V, Harris A, Murdan S, Croft SL. 2018. Relation between skin pharmacokinetics and efficacy in AmBisome treatment of murine cutaneous leishmaniasis. *Antimicrob Agents Chemother* 62:e02009-17. <https://doi.org/10.1128/AAC.02009-17>.

Copyright © 2018 Wijnant et al. This is an open-access article distributed under the terms of the Creative Commons Attribution 4.0 International license.

Address correspondence to Simon L. Croft, simon.croft@lshtm.ac.uk.

(Double-click to open attached file)



Relation between Skin Pharmacokinetics and Efficacy in AmBisome Treatment of Murine Cutaneous Leishmaniasis

Gert-Jan Wijnant,^{a,b} Katrien Van Bocxlaer,^a Vanessa Yardley,^a Andy Harris,^c Sudaxshina Murdan,^b Simon L. Croft^a

^aDepartment of Immunology and Infection, Faculty of Infectious and Tropical Diseases, London School of Hygiene and Tropical Medicine, London, United Kingdom

^bDepartment of Pharmaceutics, UCL School of Pharmacy, London, United Kingdom

^cPharmidex Pharmaceutical Services Ltd., London, United Kingdom

ABSTRACT AmBisome (LAmB), a liposomal formulation of amphotericin B (AmB), is a second-line treatment for the parasitic skin disease cutaneous leishmaniasis (CL). Little is known about its tissue distribution and pharmacodynamics to inform clinical use in CL. Here, we compared the skin pharmacokinetics of LAmB with those of the deoxycholate form of AmB (DAmB; trade name Fungizone) in murine models of *Leishmania major* CL. Drug levels at the target site (the localized lesion) 48 h after single intravenous (i.v.) dosing of the individual AmB formulations (1 mg/kg of body weight) were similar but were 3-fold higher for LAmB than for DAmB on day 10 after multiple administrations (1 mg/kg on days 0, 2, 4, 6, and 8). After single and multiple dosing, intralesional concentrations were 5- and 20-fold, respectively, higher than those in the healthy control skin of the same infected mice. We then evaluated how drug levels in the lesion after LAmB treatment relate to therapeutic outcomes. After five administrations of the drug at 0, 6.25, or 12.5 mg/kg (i.v.), there was a clear correlation between dose level, intralesional AmB concentration, and relative reduction in parasite load and lesion size (R^2 values of >0.9). This study confirms the improved efficacy of the liposomal over the deoxycholate AmB formulation in experimental CL, which is related to higher intralesional drug accumulation.

KEYWORDS pharmacokinetics, pharmacodynamics, amphotericin B, cutaneous leishmaniasis

Cutaneous leishmaniasis (CL) is a neglected vector-borne tropical disease caused by intracellular protozoan *Leishmania* parasites. Current estimates suggest 350 million people at risk, 12 million cases per year, and 1 to 1.5 million new cases annually in more than 98 countries, the majority of which occur in Latin America and the Middle East (1). While mortality is limited for the most common form, localized CL, morbidity is serious due to ulceration, disfigurement, and often permanent scarring after healing of the lesion, which are all associated with social stigmatization. More complex and potentially dangerous forms of CL are diffuse (diffuse cutaneous leishmaniasis, or DCL), chronic (*leishmaniasis recidivans*, or CCL), or destructive to the nasopharyngeal mucosa (mucocutaneous leishmaniasis, or MCL). Current treatments are hampered in their clinical value by toxicity, side effects, variable efficacy, high cost, or invasive administration route. First-line treatment consists of pentavalent antimonials. Second-line chemotherapeutic options include paromomycin, miltefosine, and amphotericin B (AmB). AmB, a macrocyclic polyene antibiotic and important antifungal agent derived from *Streptomyces nodosus*, is active due to complexation with ergosterol in leishmanial cell membranes, leading to the formation of pores and ultimately pathogen death (2). Due to infusion-related and (nephro)toxicity issues of the classic colloidal dispersion with deoxycholate amphotericin B (DAmB; trade name Fungizone), lipid formulations with

Received 28 September 2017 Returned for modification 17 October 2017 Accepted 16 December 2017

Accepted manuscript posted online 20 December 2017

Citation Wijnant G-J, Van Bocxlaer K, Yardley V, Harris A, Murdan S, Croft SL. 2018. Relation between skin pharmacokinetics and efficacy in AmBisome treatment of murine cutaneous leishmaniasis. *Antimicrob Agents Chemother* 62:e02009-17. <https://doi.org/10.1128/AAC.02009-17>.

Copyright © 2018 Wijnant et al. This is an open-access article distributed under the terms of the [Creative Commons Attribution 4.0 International license](https://creativecommons.org/licenses/by/4.0/).

Address correspondence to Simon L. Croft, simon.croft@shmt.ac.uk.

an improved tolerability profile and different physicochemical properties were developed, including a phospholipid complex (Abelcet), a dispersion with cholesteryl esters (Amphocil), a multilamellar liposome (Fungisome), and a unilamellar liposome (AmBisome, or LAmB) (3).

No standard dose regimens have been established for LAmB in the treatment of CL, as published data are limited to small case series or individual case reports (4), but clinical success has been achieved with a daily course of 3 mg/kg of body weight for a total dose of 18 to 21 mg/kg. Due to the need for intravenous administration of LAmB and the related risk of systemic adverse effects, it is typically reserved as a 2nd-line treatment for complex CL. This includes patients with (or at risk of) MCL, DCL, or CCL, as well as cases where lesions are large, numerous, potentially disfiguring, unresponsive to earlier therapeutic attempts, and esthetically or practically infeasible to cure locally. General limitations of LAmB include the high price as well as the requirements for cold chain, slow infusion, and hospitalization (5). Despite the relative safety and efficacy of LAmB in CL, fundamental questions about its pharmacology for this disease remain unanswered. Evaluation of pharmacokinetics (PK) and pharmacodynamics (PD) in preclinical models is important to inform optimal clinical use and learn lessons for drug development. A number of studies have looked at the difference in PK and PD properties of AmB formulations in the treatment of invasive fungal pathologies (6–11), but none have done so for CL. Here, we report (i) the single-dose pharmacokinetics of LAmB and DAmB in both healthy and *Leishmania major*-infected BALB/c mice, (ii) skin distribution after multiple dosing of LAmB and DAmB in murine CL, and (iii) the relationship between dose, intralesional AmB concentrations, and response after LAmB treatment at three dose levels.

RESULTS

Single-dose plasma and skin PK in healthy and *L. major*-infected mice. Plasma concentration-versus-time plots after intravenous (i.v.) administration of a single dose of 1 mg/kg LAmB or DAmB to uninfected and *L. major*-infected mice are shown in Fig. 1a and b, respectively. A dose of 1 mg/kg was used as it is the highest tolerated single dose of DAmB which does not cause signs of acute toxicity (data from pilot studies are not shown). Plasma PK were similar between uninfected and infected mice for the two AmB formulations, with comparable maximum concentration of drug in plasma (C_{max}), area under the concentration-time curve (AUC), clearance, half-life ($t_{1/2}$), and volume of distribution (V) (Table 1). However, the plasma profiles for LAmB and DAmB individually were significantly different. Compared to DAmB, LAmB achieved a higher plasma peak and systemic exposure (C_{max} and AUC around 10- and 3-fold greater, respectively) but showed a shorter half-life and lower clearance and volume of distribution. It should be noted that the terminal phase for LAmB was not clearly defined.

Levels of AmB exposure in the rump (lesion site) and back (control site) skin, expressed as the AUC from 0.5 to 48 h ($AUC_{0.5-48}$), are shown in Table 2. In uninfected animals, similar drug distribution profiles in the healthy rump (Fig. 1c) and back (Fig. 1e) tissues were obtained. LAmB gave drug peak levels similar to those of DAmB, around 60 ng/g but at earlier time points (after 30 min versus 2 to 6 h) and only half the total exposure. The rump-to-back $AUC_{0.5-48}$ ratios (1.3 for DAmB and 1.5 for LAmB) indicate that there are limited differences in skin drug exposure based on anatomical location in uninfected mice. In contrast, in *L. major*-infected animals, the presence of the localized cutaneous lesion on the rump (Fig. 1d) strongly enhanced drug accumulation for both formulations compared to that of the CL-uninfected back skin of the same mice (Fig. 1f). Based on the rump-to-back $AUC_{0.5-48}$ ratios, AmB levels are 6-fold higher for LAmB and 8-fold higher for DAmB. Compared to that of DAmB, LAmB had a similar peak concentration in skin (132 ± 28 versus 159 ± 8 $\mu\text{g/g}$) at later time points (24 h versus 6 h), showing a trend of slower drug accumulation into and elimination from the lesion. AmB levels in the rump and back tissue for both formulations in infected mice were around 5-fold higher than those in uninfected mice. Changes in AmB plasma

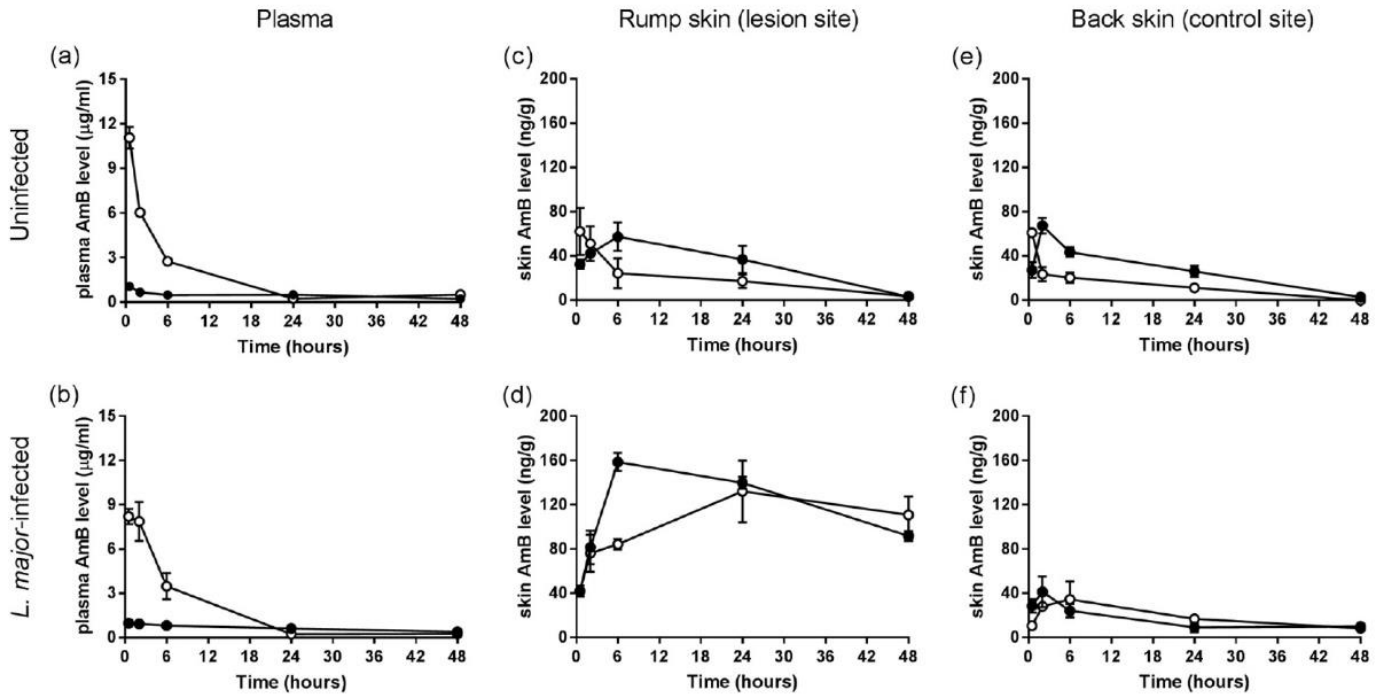


FIG 1 Single-dose pharmacokinetics of the deoxycholate form of AmB (DAmB, ●) and AmBisome (LAmB, ○). Uninfected and *L. major*-infected BALB/c mice received one intravenous dose (1 mg/kg of body weight) of a formulation, after which amphotericin B (AmB) levels in plasma (a and b) and skin at multiple time points were determined. Two skin sites per animal were included: the rump (parasite inoculation site where the localized CL lesion is present in infected [d] but not in uninfected [c] mice) and the back (lesion-free control site in both infected [f] and uninfected [e] animals). Each point represents the means ± SEM (*n* = 4 or 5 per group).

concentrations after 1 mg/kg LAmB or DAmB infusion are not reflective for those in skin tissues. No adverse effects at this dose level were observed for either formulation.

Multiple-dose skin PK and PD in *L. major*-infected mice. Skin distribution after multiple dosing of either LAmB or DAmB (1 mg/kg on days 0, 2, 4, 6, and 8) in CL-infected mice is shown in Fig. 2. On day 10, intralesional levels for LAmB (542 ± 46 ng/g) were 3-fold higher than for those for DAmB (170 ± 18 ng/g; *P* < 0.0001). Comparing these concentrations 48 h after the last dosing to those found during earlier single-dose PK studies at the same time point (LAmB, 110 ± 17 ng/g; DAmB, 92 ± 4 ng/g) (Fig. 1c and d), a gradual and linear drug accumulation in the target tissue during treatment can be assumed for LAmB but not for DAmB. Again, AmB levels in the lesion were significantly higher than those in the healthy back skin for LAmB (20× higher; *P* < 0.0001) and DAmB (12 higher; *P* < 0.0001).

We then compared the resulting efficacy outcomes for LAmB and DAmB after completing five 1-mg/kg treatments. A small reduction in day 10 lesion size compared to that of the untreated (5% dextrose) group (9.9 ± 0.8 mm) was found for LAmB (9.4 ± 0.2 mm) and DAmB (8.7 ± 0.6), but in both cases the difference was not

TABLE 1 Pharmacokinetic profile of the deoxycholate form of AmB and AmBisome in uninfected and *L. major*-infected mice after a single i.v. 1-mg/kg dose^a

PK parameter (unit)	Value(s) for:			
	DAmB		LAmB	
	Uninfected	Infected	Uninfected	Infected
<i>C</i> _{max} (µg/ml)	1.1	1.0	11.1	8.2
AUC (h · µg/ml)	21.5	30.2	62.7	71.0
Clearance (ml/h/kg)	29.6	18.9	14.2	13.5
<i>t</i> _{1/2} (h)	36.1	39.7	10.7	8.5
<i>V</i> (ml/kg)	1458	1075	225	143

^aValues for pharmacokinetic parameters are calculated from the plasma PK profiles seen in Fig. 1a and b.

TABLE 2 Skin distribution of the deoxycholate form of AmB and AmBisome in uninfected and *L. major*-infected mice after a single i.v. 1-mg/kg dose^a

Skin site	AUC _{0.5–48} value for:			
	DAmB		LAmB	
	Uninfected	Infected	Uninfected	Infected
Rump (lesion site)	1,586 ± 495	6,035 ± 273	863 ± 365	5,270 ± 1,003
Back (control site)	1,269 ± 190	710 ± 194	573 ± 142	915 ± 312
Rump-to-back ratio	1.3	8.5	1.5	5.8

^aAUC_{0.5–48} values are calculated from skin PK profiles shown in Fig. 1c, d, e, and f.

significant (*P* value of 0.83 and 0.34, respectively). A lower relative parasite load was also found for LAmB ($2.0 \times 10^7 \pm 0.6 \times 10^7$ parasites/g) and DAmB ($6.1 \times 10^7 \pm 3.4 \times 10^7$ parasites/g), but again without a statistically significant difference compared to the control ($1.6 \times 10^8 \pm 0.5 \times 10^8$ parasites/g; *P* value of 0.12 and 0.23, respectively). As expected, both formulations show some antileishmanial efficacy at five treatments of 1 mg/kg, but the toxicity limit of DAmB (1 mg/kg) does not allow a meaningful comparison at clinically relevant dose levels. Because of this, we further investigated only the dose concentration-response relationship at higher doses for LAmB.

Dose concentration-response of LAmB in *L. major*-infected mice. After *L. major*-infected mice received 5 doses of LAmB at either 0, 6.25, 12.5, or 25 mg/kg LAmB (on days 0, 2, 4, 6 and 8), the dose level was related to the resulting day 10 intralésional AmB concentrations (Fig. 3a) as well as response, indicated by lesion size and parasite load (Fig. 3b and c, respectively). Figure 3d shows the nonlinear-fit sigmoidal dose-response curve plotting the logarithm of these intralésional AmB levels versus relative reductions in parasite load and lesion size compared to the untreated controls (0 mg/kg). The calculated dose required to achieve 50% (ED₅₀) and 90% of maximum effect (ED₉₀) was 9.16 and 16.73 mg/kg for lesion size. For parasite load, ED₅₀ was 7.55 mg/kg and ED₉₀ was 9.16 mg/kg.

We observed a linear dose concentration-response relationship up to 12.5 mg/kg. Between the 0- and 12.5-mg/kg range, correlation was strong between dose concentration (linear regression goodness of fit, $R^2 = 0.99$) and concentration response (R^2 of 0.99 and 0.91 for relative reduction in parasite load and lesion size, respectively). Little additional efficacy was found by doubling the dose from 12.5 to 25 mg/kg, while intralésional AmB levels increased nonlinearly by 5-fold; this resulted in only a small additional reduction in lesion size and parasite load. This indicates that at 25 mg/kg, the near-maximum efficacy of LAmB for this specific treatment regimen had been reached.

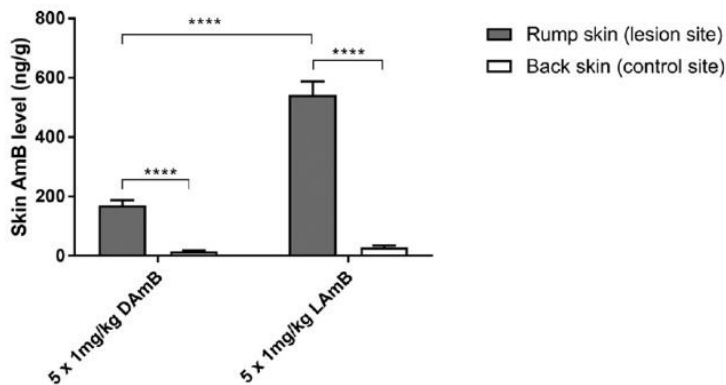


FIG 2 Multiple-dose skin pharmacokinetics of the deoxycholate form of AmB (DAmB) and AmBisome (LAmB). *L. major*-infected BALB/c mice received intravenous doses of 1 mg/kg on days 0, 2, 4, 6, and 8. On day 10 (48 h after the last dosing), skin samples were collected for amphotericin B (AmB) analysis. The CL lesion was localized on the rump, while the back skin served as a lesion-free, healthy control site. Each point represents the means ± SEM (*n* = 4 to 5 per group). Differences were analyzed using 1-way ANOVA followed by Tukey's multiple-comparison tests and considered significant at a *P* value of <0.05 (*) or not significant (ns) if not (****, *P* < 0.0001).

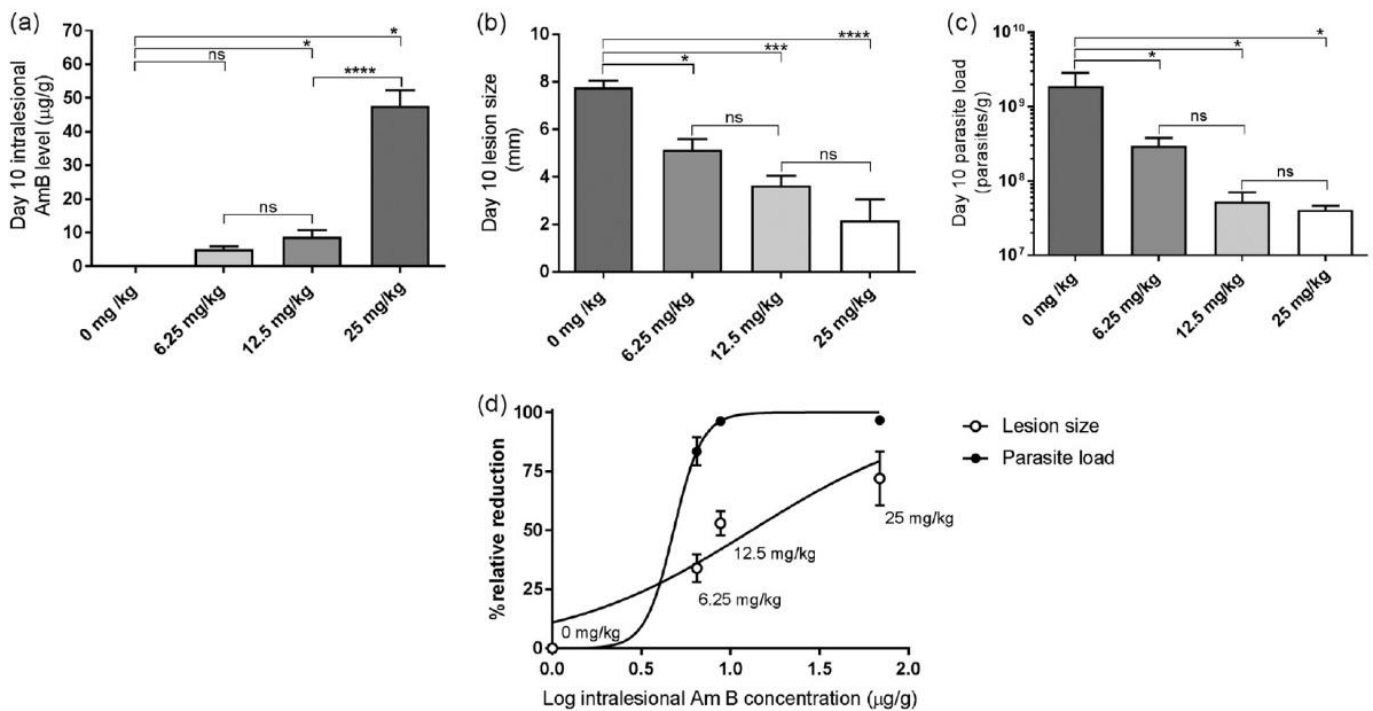


FIG 3 Dose concentration-response relationship of AmBisome (LAmB) in experimental *L. major*-infected mice received five doses of either 5% dextrose (0 mg/kg; untreated control) or 6.25, 12.5, and 25 mg/kg LAmB (i.v.). On day 10, resulting intralesional amphotericin B levels (a), lesion size (b), and parasite load (c) were evaluated. (d) Outcomes are linked in a logarithmic-scale dose-response curve plotting drug concentrations against relative reduction in lesion size and parasite load. Each point represents the means \pm SEM ($n = 4$ to 5 per group). Differences among day 10 outcomes were analyzed using 1-way ANOVA followed by Tukey's multiple-comparison tests and considered significant at P values of <0.05 (*), <0.01 (**), <0.001 (***), and <0.0001 (****). ns, not significant.

Significant reductions in parasite load and lesion size ($P < 0.05$) were found between the control and treated groups at all three dose levels. Doubling of the LAmB dose from 6.25 to 12.5 to 25 mg/kg resulted in a further decrease in parasite load and lesion size, but the differences among the groups were not significant ($P > 0.05$).

DISCUSSION

The pharmacokinetics and pharmacodynamics of many drugs currently used in the treatment of CL, including different formulations of AmB, are poorly understood (12). We have investigated the single- and multiple-dose skin distribution of AmB following dosing with either the unilamellar liposome AmBisome (LAmB) or the micellar deoxycholate salt form of amphotericin B (DAmB). Significant differences in pharmacokinetics were observed between *L. major*-infected and uninfected animals, as well as between the two drug formulations.

We observed an important impact of the CL infection on skin accumulation for both LAmB and DAmB. Drug levels in the localized lesion were over 5- to 20-fold elevated compared to those in healthy skin tissue of the same infected mice, as well as in uninfected animals. The pathological condition of CL-infected skin, mainly caused by the severe localized inflammatory immune response against the *Leishmania* parasites multiplying within dermal macrophages, may explain this phenomenon. After intravenous administration, DAmB dissociates from the colloidal micelles, and over 95% of AmB binds to plasma proteins (13) to form a high-molecular-weight association. LAmB also interacts with proteins, and while 90% of AmB remains stably intercalated in the 60- to 80-nm-sized liposomes (4, 13), coating by opsonins makes the liposomes prone to ingestion by phagocytes in systemic circulation and the reticuloendothelial system in liver and spleen (14). While these complexes have impaired extravasation in healthy skin (continuous endothelium with small vessel pores of 6- to 12-nm diameter [15]), the leaky vasculature at the infection site (increased permeability and disease-inflicted capillary damage) could enhance local drug accumulation (16). Another factor, espe-

cially for LAmB, is the migration of phagocytic monocytes, which can serve as potential drug reservoirs, from the bloodstream to the infection site. This is a characteristic of the early-stage and acute immune response against *Leishmania* (17, 18), causing small, nonulcerated CL nodules (as observed in our *L. major*-infected mice 12 days postinoculation). Little is known about the elimination of AmB from the target site by local metabolism or lymphatic drainage. However, the latter has been hypothesized as a reason behind the much lower activity of liposomal formulations of AmB (19) and sodium stibogluconate (20) when injected intralesionally compared to intravenously. The impact of these individual physiological processes on local drug distribution in skin is difficult to estimate using the current methodology, which is based on total drug levels and is unable to distinguish between intra- or extracellular, as well as free, protein-bound, or liposome-encapsulated AmB. Furthermore, the general limitations of tissue homogenates apply, such as loss of spatial drug disposition within the compartments of the organ of interest. Novel techniques, such as microdialysis and matrix-assisted laser desorption ionization mass spectrometry imaging, have untapped potential in pharmacological CL research to measure unbound concentrations in the dermal interstitial fluid (21) or study drug disposition within the cellular architecture of infected skin (22). These findings about AmB accumulation in diseased tissue also could be relevant in the treatment of deep cutaneous mycoses (such as invasive candidiasis), where the pathogen, like *Leishmania*, is located in the dermis (23) instead of the superficial portions of the epidermis where most fungi typically reside.

Comparing the pharmacokinetics of the individual two AmB formulations, we saw significant differences between LAmB and DAmB, consistent with previous studies (24–27). Plasma concentrations and exposure were much higher for LAmB than DAmB and not reflective of changes in skin tissue levels for either formulation. Drug concentrations at the target site were similar after single intravenous dosing of the individual AmB formulations but were 3-fold higher for LAmB than for DAmB following 5-time administration of the same dose. Recently, Iman and colleagues (27) also investigated the distribution of LAmB and DAmB in *L. major*-infected BALB/c mice, but skin was not evaluated in this study. Increased accumulation of liposomes in inflammatory over healthy sites has also been described for subcutaneous tumors (28), bacterial skin abscesses (29, 30), and fungal infections (31). The so-called enhanced permeation and retention effect, increased drug accumulation at sites of leaky vasculature and defective lymphatic drainage, has been coined as the rationale behind nanoparticle-based drug delivery in cancer and inflammation (16). The data and our understanding of CL histopathology suggest that this effect can also be exploited as a passive targeting strategy in this context by encapsulation of antileishmanial drugs in small (<100 nm), stable (tightly packed phospholipids with cholesterol), unilamellar liposomes (14) similar to AmBisome. Indeed, several promising results have already been achieved with nanoparticles of AmB and other drugs for the treatment of CL (27, 32–37).

Finally, we evaluated how drug concentrations at the infection site after LAmB treatment relate to outcomes. After administration of five consecutive doses, the 1-mg/kg dose of LAmB (as well as DAmB, for which this is the tolerated maximum) proved to be too low to be therapeutic, but a linear dose concentration-response effect was found for 6.25 and 12.5 mg/kg. The clear correlation between intralésional drug levels and treatment outcomes can be explained by the known concentration-dependent manner in which AmB exerts its antimicrobial activity (38). Interestingly, for doubling the LAmB dose from 12.5 to 25 mg/kg, intralésional AmB levels increased by over 5-fold. This could be due to the known phenomenon of saturation of AmB uptake and clearance mechanisms in the organs of the reticuloendothelial system, possibly resulting in higher plasma exposure and increased distribution to other tissues (39). However, little additional efficacy for 25 compared to 12.5 mg/kg was observed. Both of these doses were able to achieve a near-100% reduction in parasite load but not lesion size, indicating the need for longer treatment as the host's response to parasite elimination in the skin is delayed. Results are in line with published data (19, 40) and suggest the clinical superiority of LAmB over DAmB in CL based on enhanced intral-

esional accumulation of the liposome, as well as already known factors, such as better tolerability and potentially shorter treatment courses. Further PK-PD analysis of LAmB is required to inform optimized clinical dose regimens, especially for the different complex forms of CL, as there are known differences in species-specific drug sensitivity (41), histopathology (17), and immunology (18). It is currently unknown to what degree our observations about skin accumulation of LAmB in the *L. major*-BALB/c model are translatable to human CL, but understanding of preclinical PK and PK-PD relationships should improve the use and development of antileishmanial drugs.

In summary, intravenous LAmB has potent and dose-dependent *in vivo* activity against CL due to relatively high drug accumulation within the lesion, which is enhanced by the inflamed state of the infected target tissue and the pharmacokinetic properties of the liposomal formulation.

MATERIALS AND METHODS

Drugs. AmBisome (LAmB; Gilead, United Kingdom) and the deoxycholate form of AmB (DAmB; Bristol-Myers Squibb, United Kingdom) were reconstituted with sterile water per the manufacturer's instructions to yield stock solutions of 4 mg/ml and 5 mg/ml, respectively. These were diluted in 5% aqueous dextrose to a dose of 1 mg/kg (0.02 mg per dose of 200 μ l for mice of a mean weight of 20 g). For LAmB, additional doses of 6.25, 12.5, and 25 mg/kg were similarly prepared. The dilutions were prepared 1 day before starting the experiment and stored at 4°C.

Parasites. *L. major* MHOM/SA85/JISH118 parasites were cultured in Schneider's insect medium (Sigma, United Kingdom) supplemented with 10% heat-inactivated fetal calf serum (HiFCS; Sigma, United Kingdom). These parasites were passaged each week at a 1:10 ratio of the existing culture to fresh medium in 25-ml culture flasks without a filter and incubated at 26°C. For infection of mice, stationary-phase parasites (as confirmed by light microscopy) were centrifuged for 10 min at 2,100 rpm at 4°C. The supernatant was removed and the pellet was resuspended in pure Schneider's insect medium. The number of cells was estimated by microscopic counting with a Neubauer hemocytometer.

***In vivo* L. major models of CL.** Female BALB/c mice around 6 to 8 weeks old were purchased from Charles River Ltd. (Margate, United Kingdom). These mice were kept in humidity- and temperature-controlled rooms (55 to 65% and 25 to 26°C, respectively) and fed water and rodent food *ad libitum*. After acclimatization for 1 week, mice were randomized and subcutaneously (s.c.) injected in the shaven rump above the tail with 200 μ l of a parasite suspension containing 4×10^7 low-passage-number (fewer than 5), stationary-phase *L. major* promastigotes in RPMI medium. Uninfected mice received a similar but parasite-free injection of 200 μ l RPMI medium instead. Twelve days later, when a 4- to 5-mm nonulcerating nodule had formed on the rump of infected animals, mice were allocated to the different experimental groups to ensure comparable lesion sizes.

Ethics statement. All animal experiments were conducted under license X20014A54 according to UK Home Office regulations under the Animals (Scientific Procedures) Act 1986 and EC Directive 2010/63/E.

Single-dose PK study. Uninfected and *L. major*-infected BALB/c mice ($n = 4$ to 5 per group) each received LAmB or DAmB at 1 mg/kg of body weight over a 1- to 2-min period by an intravenous bolus (200 μ l). Plasma, rump (lesion site), and back (control site) skin samples were collected at 0.5, 2, 6, 24, and 48 h postinfection.

Multiple-dose PK and PD study. *L. major*-infected BALB/c mice ($n = 4$ to 5 per group) each received LAmB or DAmB at 1 mg/kg or 5% dextrose over a 1- to 2-min period by an intravenous bolus (200 μ l) on days 0, 2, 4, 6, and 8. Skin samples from rump (lesion site) and back (control site) were collected on day 10 (48 h after the 5th and final drug administration). This day 10 time point of sacrifice allowed direct comparison with the outcomes of the single-dose PK study (last time point, 48 h). The alternate-day dosing regimen was based on earlier data on the efficacy of LAmB in the *L. major*-BALB/c model of CL (19). The PD methodology can be found in the following section.

Dose concentration-response study. *L. major*-infected BALB/c mice ($n = 4$ to 5 per group) each received LAmB (i.v.) at 0, 6.25, 12.5, or 25 mg/kg on days 0, 2, 4, 6, and 8. Lesion size was measured daily in two dimensions (length and width) using digital calipers, and the mean size (average of length and width) was calculated. On day 10, rump (lesion site) and back (control site) skin samples were collected and parasite load was evaluated. The methodology to extract parasite DNA from lesions and quantify parasite load by quantitative PCR has already been described in full detail (42).

Skin sample collection and preparation. After sacrificing mice (using CO₂), skin was harvested by surgical removal from the areas containing the localized CL lesion (at the parasite inoculation site on the rump above the tail, termed the lesion site) and non-CL-infected skin on the back (control site). The skin tissue was cut into fine, long pieces and placed into SureLock microcentrifuge tubes (StarLab, United Kingdom) together with 1 spatula (about 100 mg) of 2-mm zirconium oxide beads (Next Advance, United Kingdom) and 1 ml phosphate-buffered saline (PBS; with 0.9% NaOH, pH 7.4; Sigma, United Kingdom). Samples were ground using a Bullet Blender Storm 24 (NextAdvance, United Kingdom) set at speed 12 for 20 min to obtain a smoothly flowing homogenate and stored at -80°C until further use. The homogenate (50 μ l) was added to 250 μ l of a mixture of 84:16 methanol-dimethyl sulfoxide (DMSO) (high-performance liquid chromatography grade; Fisher Chemical, United Kingdom) containing 200 ng/ml tolbutamide (analytical standard; Sigma, United Kingdom) internal standard for drug extraction and protein precipitation in 96-well plates. Plates were shaken for 10 min at 200 rpm and centrifuged for

15 min at 6,600 rpm at 4°C. One hundred fifty microliters of supernatant was collected and stored at –80°C until analysis. Blanks with and without internal standard as well as calibration samples with known concentrations of AmB (similarly extracted and prepared after spiking 45 μ l blank skin homogenate [derived from untreated BALB/c mice] with 5- μ l working solutions of known AmB concentrations in 1% SDS [Sigma]) were included.

Plasma sample collection and preparation. Blood samples were taken from live animals by needle pricks in the lateral tail veins and collected in Eppendorf tubes preloaded with heparin (2 μ l of a 1,000 U/ml stock in sterile water). After centrifugation at 6,500 rpm at 4°C for 10 min, the supernatant plasma was collected in new tubes. Plasma samples for which concentrations of AmB above the upper limit of quantification were expected were first diluted with drug-free blank plasma derived from untreated BALB/c mice. Twenty microliters of plasma was added to 100 μ l of a 200-ng/ml tolbutamide internal standard in 84:16 methanol-DMSO. Supernatant (60 μ l) was collected and further treated as described for skin samples. Again, blanks with and without internal standard and calibration standards (similarly extracted and prepared after spiking 18 μ l blank plasma [derived from untreated BALB/c mice] with 2- μ l working solutions of known AmB concentrations in 1% SDS [Sigma]) were included.

LC-MS/MS quantification of AmB. The liquid chromatography-tandem mass spectrometry (LC-MS/MS) methodology to quantify AmB levels in experimental leishmaniasis samples was described earlier by Voak et al. (24). Analysis was conducted at Pharmidex Pharmaceutical Services, Ltd. (Stevenage, United Kingdom). The lower limit of quantification was 1 ng/ml.

Pharmacokinetic parameters. Single-dose PK parameters were estimated assuming noncompartmental analysis in WinNonlin. AUC_{0-48} values for skin were calculated using GraphPad Prism, version 7.02.

Statistical analysis. Differences among lesion sizes and parasite loads in the groups were assessed by using one-way analysis of variance (ANOVA) assuming Gaussian distribution followed by Tukey's multiple-comparison test. Data are presented as means and standard errors of the means (SEM). A *P* value of <0.05 was considered statistically significant. All analyses were performed using GraphPad Prism, version 7.02.

ACKNOWLEDGMENTS

The doctoral project of G.-J.W. is part of the EuroLeish.Net Training Network (www.euroleish.net) and has received funding from the European Horizon's 2020 Research and Innovation Programme under Marie Skłodowska-Curie grant agreement number 642609.

We are grateful to Karin Seifert and Andrew Voak for helpful discussions.

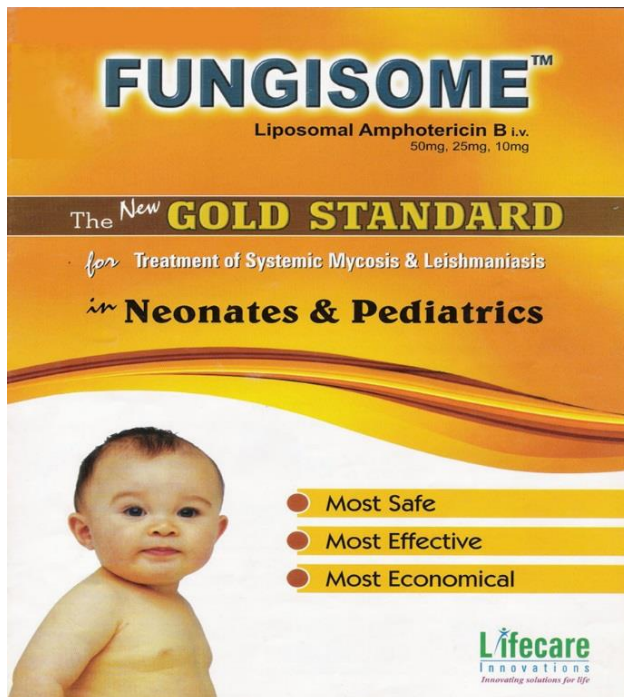
REFERENCES

- Alvar J, Vélez ID, Bern C, Herrero M, Desjeux P, Cano J, Jannin J, den Boer M. 2012. Leishmaniasis worldwide and global estimates of its incidence. *PLoS One* 7:e35671. <https://doi.org/10.1371/journal.pone.0035671>.
- Ramos H, Valdivieso E, Gamargo M, Dagger F, Cohen BE. 1996. Amphotericin B kills unicellular leishmanias by forming aqueous pores permeable to small cations and anions. *J Membr Biol* 152:65–75. <https://doi.org/10.1007/s002329900086>.
- Serrano DR, Ballesteros MP, Schätzlein AG, Torrado JJ, Uchegbu IF. 2013. Amphotericin B formulations—the possibility of generic competition. *Pharm Nanotechnol* 1:250–258. <https://doi.org/10.2174/2211738501999131118125018>.
- Wortmann G, Zapor M, Ressler R, Fraser S, Hartzell J, Pierson J, Weintrob A, Magill A. 2010. Liposomal amphotericin B for treatment of cutaneous leishmaniasis. *Am J Trop Med Hyg* 83:1028–1033. <https://doi.org/10.4269/ajtmh.2010.10-0171>.
- Aronson N, Herwaldt BL, Libman M, Pearson R, Lopez-Velez R, Weina P, Carvalho EM, Ephros M, Jeronimo S, Magill A. 2016. Diagnosis and treatment of leishmaniasis: clinical practice guidelines by the Infectious Diseases Society of America (IDSA) and the American Society of Tropical Medicine and Hygiene (ASTMH). *Clin Infect Dis* 63:e202–e264. <https://doi.org/10.1093/cid/ciw670>.
- van Etten EW, Otte-Lambillion M, van Vianen W, ten Kate MT, Bakker-Woudenberg AJ. 1995. Distribution of liposomal amphotericin B (AmBisome) and amphotericin B-desoxycholate (Fungizone) in uninfected immunocompetent mice and leucopenic mice infected with *Candida albicans*. *J Antimicrob Chemother* 35:509–519. <https://doi.org/10.1093/jac/35.4.509>.
- Groll AH, Giri N, Petraitis V, Petraitiene R, Candelario M, Bacher JS, Piscitelli SC, Walsh TJ. 2000. Comparative efficacy and distribution of lipid formulations of amphotericin B in experimental *Candida albicans* infection of the central nervous system. *J Infect Dis* 182:274–282. <https://doi.org/10.1086/315643>.
- Gondal JA, Swartz RP, Rahman A. 1989. Therapeutic evaluation of free and liposome-encapsulated amphotericin B in the treatment of systemic candidiasis in mice. *Antimicrob Agents Chemother* 33:1544–1548. <https://doi.org/10.1128/AAC.33.9.1544>.
- Clemons KV, Schwartz JA, Stevens DA. 2012. Experimental central nervous system aspergillosis therapy: efficacy, drug levels and localization, immunohistopathology, and toxicity. *Antimicrob Agents Chemother* 56:4439–4449. <https://doi.org/10.1128/AAC.06015-11>.
- Takemoto K, Yamamoto Y, Ueda Y, Sumita Y, Yoshida K, Niki Y. 2006. Comparative study on the efficacy of AmBisome and Fungizone in a mouse model of pulmonary aspergillosis. *J Antimicrob Chemother* 57:724–731. <https://doi.org/10.1093/jac/dkl005>.
- Lestner JM, Howard SJ, Goodwin J, Gregson L, Majithiya J, Walsh TJ, Jensen GM, Hope WW. 2010. Pharmacokinetics and pharmacodynamics of amphotericin B desoxycholate, liposomal amphotericin B, and amphotericin B lipid complex in an in vitro model of invasive pulmonary aspergillosis. *Antimicrob Agents Chemother* 54:3432–3441. <https://doi.org/10.1128/AAC.01586-09>.
- Kip AE, Schellens JHM, Beijnen JH, Dorlo TPC. 19 July 2017. Clinical pharmacokinetics of systemically administered antileishmanial drugs. *Clin Pharmacokinet* <https://doi.org/10.1007/s40262-017-0570-0>.
- Bekersky I, Fielding RM, Dressler DE, Lee JW, Buell DN, Walsh TJ. 2002. Plasma protein binding of amphotericin B and pharmacokinetics of bound versus unbound amphotericin B after administration of intravenous liposomal amphotericin B (AmBisome) and amphotericin B desoxycholate. *Antimicrob Agents Chemother* 46:834–840. <https://doi.org/10.1128/AAC.46.3.834-840.2002>.
- Adler-Moore JP, Gangneux J-P, Pappas PG. 2016. Comparison between liposomal formulations of amphotericin B. *Med Mycol* 54:223–231. <https://doi.org/10.1093/mmy/myv111>.
- Sarin H. 2010. Physiologic upper limits of pore size of different blood capillary types and another perspective on the dual pore theory of

- microvascular permeability. *J Angiogenesis Res* 2:14. <https://doi.org/10.1186/2040-2384-2-14>.
16. Romero EL, Morilla MJ. 2008. Drug delivery systems against leishmaniasis? Still an open question. *Expert Opin Drug Deliv* 5:805–823. <https://doi.org/10.1517/17425247.5.7.805>.
 17. Scott P, Novais FO. 2016. Cutaneous leishmaniasis: immune responses in protection and pathogenesis. *Nat Rev Immunol* 16:581–592. <https://doi.org/10.1038/nri.2016.72>.
 18. Nylén S, Eidsmo L. 2012. Tissue damage and immunity in cutaneous leishmaniasis. *Parasite Immunol* 34:551–561. <https://doi.org/10.1111/pim.12007>.
 19. Yardley V, Croft SL. 1997. Activity of liposomal amphotericin B against experimental cutaneous leishmaniasis. *Antimicrob Agents Chemother* 41:752–756.
 20. New RR, Chance ML. 1980. Treatment of experimental cutaneous leishmaniasis by liposome-entrapped Pentostam. *Acta Trop* 37:253–256.
 21. Azeredo FJ, Dalla Costa T, Derendorf H. 2014. Role of microdialysis in pharmacokinetics and pharmacodynamics: current status and future directions. *Clin Pharmacokinet* 53:205–212. <https://doi.org/10.1007/s40262-014-0131-8>.
 22. Dartois V. 2014. The path of anti-tuberculosis drugs: from blood to lesions to mycobacterial cells. *Nat Rev Microbiol* 12:159–167. <https://doi.org/10.1038/nrmicro3200>.
 23. Chapman SW, Daniel CR. 1994. Cutaneous manifestations of fungal infection. *Infect Dis Clin North Am* 8:879–910.
 24. Voak AA, Harris A, Qaiser Z, Croft SL, Seifert K. 2017. Pharmacodynamics and biodistribution of single-dose liposomal amphotericin B at different stages of experimental visceral leishmaniasis. *Antimicrob Agents Chemother* 61:e00497-17. <https://doi.org/10.1128/AAC.00497-17>.
 25. Proffitt RT, Satorius A, Chiang SM, Sullivan L, Adler-Moore JP. 1991. Pharmacology and toxicology of a liposomal formulation of amphotericin B (AmBisome) in rodents. *J Antimicrob Chemother* 28(Suppl B): 49–61. https://doi.org/10.1093/jac/28.suppl_B.49.
 26. Lee JW, Amantea MA, Francis PA, Navarro EE, Bacher J, Pizzo PA, Walsh TJ. 1994. Pharmacokinetics and safety of a unilamellar liposomal formulation of amphotericin B (AmBisome) in rabbits. *Antimicrob Agents Chemother* 38:713–718. <https://doi.org/10.1128/AAC.38.4.713>.
 27. Iman M, Huang Z, Alavizadeh SH, Szoka FC, Jr, Jaafari MR. 2017. Biodistribution and *in vivo* antileishmanial activity of 1,2-distigmasterylhemisuccinoyl-sn-glycero-3-phosphocholine liposome-intercalated amphotericin B. *Antimicrob Agents Chemother* 61:e02525-16. <https://doi.org/10.1128/AAC.02525-16>.
 28. Charrois GJR, Allen TM. 2003. Rate of distribution of STEALTH liposomes to tumor and skin: influence of liposome diameter and implications for toxicity and therapeutic activity. *Biochim Biophys Acta* 1609:102–108. [https://doi.org/10.1016/S0005-2736\(02\)00661-2](https://doi.org/10.1016/S0005-2736(02)00661-2).
 29. Carmo VAS, de Oliveira MC, das Mota LG, Freire LP, Ferreira RLB, Cardoso VN. 2007. Technetium-99m-labeled stealth pH-sensitive liposomes: a new strategy to identify infection in experimental model. *Braz Arch Biol Technol* 50:199–207. <https://doi.org/10.1590/S1516-89132007000600025>.
 30. Stearne LET, Schifferers RM, Smouter E, Bakker-Woudenberg IAJM, Gysens IC. 2002. Distribution of long-circulating PEG-liposomes in a murine model of established subcutaneous abscesses. *Biochim Biophys Acta* 1561:91–97. [https://doi.org/10.1016/S0005-2736\(01\)00460-6](https://doi.org/10.1016/S0005-2736(01)00460-6).
 31. Takemoto K, Yamamoto Y, Ueda Y. 2006. Influence of the progression of cryptococcal meningitis on brain penetration and efficacy of AmBisome in a murine model. *Chemotherapy* 52:271–278. <https://doi.org/10.1159/000095820>.
 32. Mohamed-Ahmed AHA, Seifert K, Yardley V, Burrell-Saward H, Brocchini S, Croft SL. 2013. Antileishmanial activity, uptake, and distribution of an amphotericin B and poly(α -glutamic acid) complex. *Antimicrob Agents Chemother* 57:4608–4614. <https://doi.org/10.1128/AAC.02343-12>.
 33. Corware K, Harris D, Teo I, Rogers M, Naresh K, Müller I, Shaunak S. 2011. Accelerated healing of cutaneous leishmaniasis in non-healing BALB/c mice using water soluble amphotericin B-polymethacrylic acid. *Biomaterials* 32:8029–8039. <https://doi.org/10.1016/j.biomaterials.2011.07.021>.
 34. de Carvalho RF, Ribeiro IF, Miranda-Vilela AL, de Souza Filho J, Martins OP, de Cintra e Silva DO, Tedesco AC, Lacava ZGM, Bão SN, Sampaio RNR. 2013. Leishmanicidal activity of amphotericin B encapsulated in PLGA-DMSA nanoparticles to treat cutaneous leishmaniasis in C57BL/6 mice. *Exp Parasitol* 135:217–222. <https://doi.org/10.1016/j.exppara.2013.07.008>.
 35. Momeni A, Rasoolian M, Momeni A, Navaei A, Emami S, Shaker Z, Mohebbali M, Khoshdel A. 2013. Development of liposomes loaded with anti-leishmanial drugs for the treatment of cutaneous leishmaniasis. *J Liposome Res* 23:134–144. <https://doi.org/10.3109/08982104.2012.762519>.
 36. Kalat SAM, Khamesipour A, Bavarsad N, Fallah M, Khashayarmanesh Z, Feizi E, Neghabi K, Abbasi A, Jaafari MR. 2014. Use of topical liposomes containing meglumine antimoniate (Glucantime) for the treatment of L. major lesion in BALB/c mice. *Exp Parasitol* 143:5–10. <https://doi.org/10.1016/j.exppara.2014.04.013>.
 37. Ribeiro JBP, Miranda-Vilela AL, Graziani D, de Gomes MRA, Amorim AAS, Garcia RD, de Souza Filho J, Tedesco AC, Primo FL, Moreira JR, Lima AV, Sampaio RNR. 2016. Evaluation of the efficacy of systemic miltefosine associated with photodynamic therapy with liposomal chloroaluminum phthalocyanine in the treatment of cutaneous leishmaniasis caused by *Leishmania (L.) amazonensis* in C57BL/6 mice. *Photodiagn Photodyn Ther* 13:282–290. <https://doi.org/10.1016/j.pdpdt.2015.08.006>.
 38. Ringdén O, Meunier F, Tollemar J, Ricci P, Tura S, Kuse E, Viviani MA, Gorin NC, Klastersky J, Fenaux P. 1991. Efficacy of amphotericin B encapsulated in liposomes (AmBisome) in the treatment of invasive fungal infections in immunocompromised patients. *J Antimicrob Chemother* 28(Suppl B): 73–82.
 39. Al-Saigh R, Siopi M, Siafakas N, Velegraki A, Zerva L, Meletiadiis J. 2013. Single-dose pharmacodynamics of amphotericin B against *Aspergillus* species in an *in vitro* pharmacokinetic/pharmacodynamic model. *Antimicrob Agents Chemother* 57:3713–3718. <https://doi.org/10.1128/AAC.02484-12>.
 40. Yardley V, Croft SL. 2000. A comparison of the activities of three amphotericin B lipid formulations against experimental visceral and cutaneous leishmaniasis. *Int J Antimicrob Agents* 13:243–248. [https://doi.org/10.1016/S0924-8579\(99\)00133-8](https://doi.org/10.1016/S0924-8579(99)00133-8).
 41. Alvar J, Croft S, Olliaro P. 2006. Chemotherapy in the treatment and control of leishmaniasis. *Adv Parasitol* 61:223–274. [https://doi.org/10.1016/S0065-308X\(05\)61006-8](https://doi.org/10.1016/S0065-308X(05)61006-8).
 42. Wijnant G-J, Van Bocxlaer K, Yardley V, Murdan S, Croft SL. 2017. Efficacy of paromomycin-chloroquine combination therapy in experimental cutaneous leishmaniasis. *Antimicrob Agents Chemother* 61:e00358-17. <https://doi.org/10.1128/AAC.00358-17>.

Chapter 3.3:

AmBisome treatment of CL: comparison with Fungisome

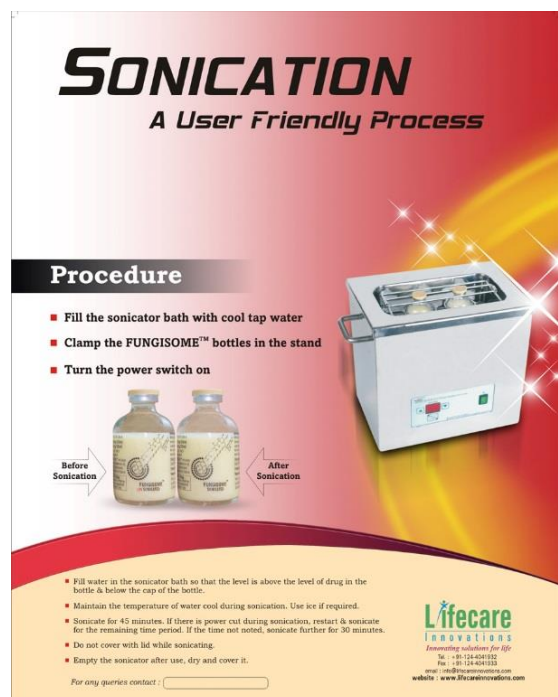


FUNGISOME™
Liposomal Amphotericin B i.v.
50mg, 25mg, 10mg

The *New* **GOLD STANDARD**
for Treatment of Systemic Mycosis & Leishmaniasis
in **Neonates & Pediatrics**

Most Safe
Most Effective
Most Economical

Lifecare
innovations
Innovating solutions for life



SONICATION
A User Friendly Process

Procedure

- Fill the sonicator bath with cool tap water
- Clamp the FUNGISOME™ bottles in the stand
- Turn the power switch on

Before Sonication → After Sonication

- Fill water in the sonicator bath so that the level is above the level of drug in the bottle & below the cap of the bottle.
- Maintain the temperature of water cool during sonication. Use ice if required.
- Sonicate for 45 minutes. If there is power cut during sonication, restart & sonicate for the remaining time period. If the time not sorted, sonicate further for 30 minutes.
- Do not cover with lid while sonicating.
- Empty the sonicator after use, dry and cover it.

For any queries contact :

Lifecare
INNOVATIONS
Innovating solutions for life
Tel : +91-11-4041312
Fax : +91-11-4041313
www.lifecareinnovations.com
www.lifecareinnovations.com

3.3: AmBisome treatment of CL – comparison with Fungisome

ANNEX 3: WIJNANT, G.-J., VAN BOCXLAER, K., YARDLEY, V., HARRIS, A., ALAVIJEH, M., SILVA-PEDROSA, R., ANTUNES, S., MAURICIO, I., MURDAN, S., AND CROFT, S.L. 2018 COMPARATIVE EFFICACY, TOXICITY AND BIODISTRIBUTION OF THE LIPOSOMAL AMPHOTERICIN B FORMULATIONS FUNGISOME® AND AMBISOME® IN MURINE CUTANEOUS LEISHMANIASIS. INTERNATIONAL JOURNAL FOR PARASITOLOGY: DRUGS AND DRUG RESISTANCE.

Key points, novel results and implications

- After investigating skin PK and antileishmanial PD of AmBisome in murine CL (chapter 3.2), we wanted to further study the influence of liposomal drug formulation on biodistribution and efficacy. To do this, we compared AmBisome with Fungisome, an alternative liposomal AmB product called Fungisome which is used in India in VL and PKDL treatment. However, it has not yet been tested against CL.
- Here, we report a **head-to-head comparison of Fungisome with AmBisome** in terms of efficacy, toxicity and skin distribution in the *L. major* BALB/c mouse model of CL.
- Upon intravenous administration at dose levels of 5, 10 and 15 mg/kg of body weight (on days 0, 2, 4, 6 and 8), Fungisome showed clear signs of toxicity (at 15 mg/kg), while AmBisome did not. After complete treatment (day 10), the tolerated doses of 5 and 10 mg/kg Fungisome had significant antileishmanial activity ($ED_{50}=4.0$ and $ED_{90}=12.8$ mg/kg for qPCR-based parasite load and lesion size, respectively), although less than that of AmBisome at identical doses ($ED_{50}=3.0$ and $ED_{90}=8.8$ mg/kg). The efficacy of Fungisome was inferior compared to AmBisome because lower levels of the active agent AmB accumulated within the infected lesion.
- Differences in a number of physicochemical and pharmacokinetic parameters between the two liposomal formulations, which could explain the variable toxicity and efficacy of AmBisome and Fungisome, are discussed in depth in the paper.
- In conclusion, despite possibly being less safe and efficacious than AmBisome at equivalent doses, the moderate *in vivo* activity of Fungisome could indicate a minor role in the systemic pharmacotherapy of CL and PKDL. Moreover, in CL drug development, encapsulation of drugs in AmBisome-like compared to Fungisome-like liposomes could lead to lower toxicity and higher skin accumulation and thus efficacy.
- A new reverse transcriptase qPCR method to measure skin parasite load based on *Leishmania* RNA (rather than DNA) was developed with the help of colleagues at the Institute of Hygiene and Tropical Medicine of Lisbon, Lisbon. For a direct comparison between DNA- and RNA- based parasite load results, please see the supplementary material.
- In the frame of this thesis, we used the **PK/PD-based approach** to demonstrate the **higher efficacy of AmBisome compared to Fungisome** is directly related to **increased drug accumulation at the infection site**. A similar strategy was then applied in chapter 3.5. to compare a new drug candidate, DNDI-0690 with the standard antileishmanial drug paromomycin (chapter 3.1).

Candidate's contribution

The candidate generated and analyzed all data described in the paper, except for LC/MS-MS analysis of drug concentrations in the samples (Pharmidex Pharmaceutical Services Ltd.). As part of the Euroleish Network requirements for mobility of Marie-Curie fellows, the candidate spent time at the Institute of Hygiene and Tropical Medicine in Lisbon, Portugal, to develop a new RT qPCR method for quantification of parasite load. The candidate prepared the first draft of the manuscript, which was accepted for publication by International Journal of Parasitology: Drugs and Drug Resistance in April 2018 following academic peer review.

Research paper cover sheet

London School of Hygiene & Tropical Medicine
Keppel Street, London WC1E 7HT
www.lshtm.ac.uk

REGISTRY
T: +44(0)20 7299 4646
F: +44(0)20 7299 4656
E: registry@lshtm.ac.uk

LONDON SCHOOL OF HYGIENE & TROPICAL MEDICINE

RESEARCH PAPER COVER SHEET

PLEASE NOTE THAT A COVER SHEET MUST BE COMPLETED FOR EACH RESEARCH PAPER INCLUDED IN A THESIS.

SECTION A – Student Details

Student	GERT-JAN WIMANT	
Principal Supervisor	SIMON C ROFF	
Thesis Title	NEW MULTI-DRUG DEVELOPMENT METHODOLOGIES FOR CUTANEOUS LEISHMANIASIS	

If the Research Paper has previously been published please complete Section B. If not please move to Section C

SECTION B – Paper already published

Where was the work published?	ISD: D & DR	
When was the work published?	APRIL 2018	
If the work was published prior to registration for your research degree, give a brief rationale for its inclusion	N/A	
Have you retained the copyright for the work?	Was the work subject to academic peer review?	YES

*If yes, please attach evidence of retention. If no, or if the work is being included in its published format, please attach evidence of permission from the copyright holder (publisher or other author) to include this work.

SECTION C – Prepared for publication, but not yet published

Where is the work intended to be published?	
Please list the paper's authors in the intended authorship order.	
Stage of publication	

SECTION D – Multi-authored work

For multi-authored work, give full details of your role in the research included in the paper and in the preparation of the paper. (Attach a further sheet if necessary)	ALL WORK + MANUSCRIPT EXCEPT: LC/MS-MS
--	--

Student Signature: _____ Date: 17/4/2018

Supervisor Signature: _____ Date: 18.04.2018

Improving health worldwide www.lshtm.ac.uk

Copyright proof



Personal use

Authors can use their articles, in full or in part, for a wide range of scholarly, non-commercial purposes as outlined below:

- Use by an author in the author's classroom teaching (including distribution of copies, paper or electronic)
- Distribution of copies (including through e-mail) to known research colleagues for their personal use (but not for Commercial Use)
- Inclusion in a thesis or dissertation (provided that this is not to be published commercially)
- Use in a subsequent compilation of the author's works
- Extending the Article to book-length form
- Preparation of other derivative works (but not for Commercial Use)
- Otherwise using or re-using portions or excerpts in other works

These rights apply for all Elsevier authors who publish their article as either a subscription article or an open access article. In all cases we require that all Elsevier authors always include a full acknowledgement and, if appropriate, a link to the final published version hosted on Science Direct.

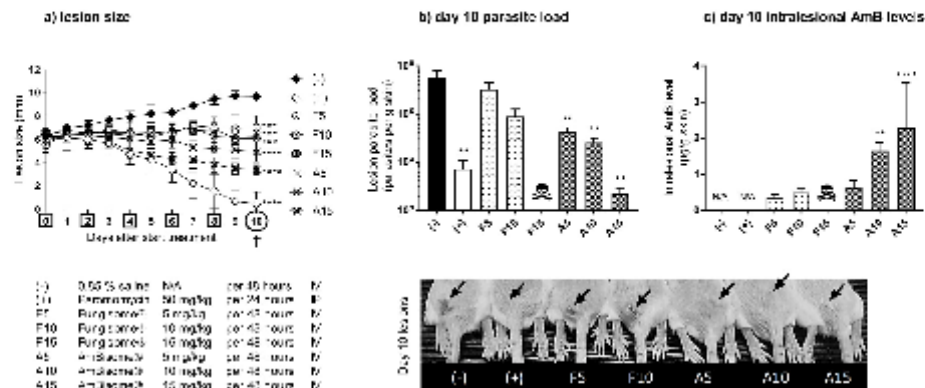


Fig. 1. Comparative efficacy of the liposomal amphotericin B (AmB) formulations AmBisome® (A) and Fungisome® (F) in the *L. major*-BALB/c model of CL. Mice received 10 doses of 50 mg/kg paromomycin (P, +) or five doses of either 0.85% saline (untreated negative control (-) or 5, 10 and 15 mg/kg F and A (IV). During treatment, lesion size was measured daily (a). On day 10, lesion skin samples were collected and parasite load (b) and AmB levels (c) in the tissue were evaluated. The photo on the bottom shows the CL lesions (arrow) on the rump of the mice on day 10. Each point represents the mean ± SD (n = 4–5 per group). ANOVA (1-way for parasite load and intralosomal AmB level, repeated measures for lesion size) followed by Tukey's multiple comparison tests was used to analyse differences between untreated controls and experimental groups. A p-value < 0.05 was considered statistically significant (*: p < 0.05, **: p < 0.001, ***: p < 0.0005, ****: p < 0.0001), p > 0.05 not significant (no marking above bar). †: day of sacrifice. Skull: no data available due to lethal toxicity at this dose level. N/A: not applicable.

Table 1

50% and 90% effective (ED) and lethal (LD) doses (mg/kg) for the liposomal amphotericin B (AmB) formulations AmBisome® (A) and Fungisome® (F) in the *L. major*-BALB/c model of CL, based on toxicity and Fig. 1 data. The number of lethal events per group over the full course of treatment was monitored during treatment for calculation of LD values. At day 10, parasite load (PL) and lesion size (LS) were determined and effect expressed as relative percentage of reduction compared to the untreated control group, which was used to calculate ED values. Therapeutic indices (TI) were calculated as the LD over ED ratio. As no lethal events occurred for A at the tested dose levels, reference LD values from mice (*) were used from the AmBisome® FDA pharmacological review document, application number 050740 (Drug Approval Package).

	AMBSISOME®		FUNGISOME®	
	50%	90%	50%	90%
LD	133.0*	150.0*	123	169
ED ₅₀	3.0	4.5	4.0	11.0
ED ₉₀	8.8	51.3	12.8	102.8
TI ₅₀	44.9	33.0	3.1	1.5
TI ₉₀	15.1	2.9	1.0	0.2

small liposome size (~70 nm) could facilitate extravasation through the leaky capillaries in the inflamed lesion skin (Romero and Morilla, 2008), followed by uptake by the parasitized dermal macrophages. Alternatively, phagocytic monocytes in the blood could carry ingested A while migrating to the infection site (Voak et al., 2017). In contrast to A, the liposomal stability of F in plasma is unknown (possibly releasing 'free' AmB after interaction with (lipo)proteins, Romero and Morilla, 2008) and its systemic exposure is 7-fold lower (1 mg/kg; C_{max} = 1 µg/ml, AUC = 11 µg.h/ml in humans, Gokhale et al., 1993). The 3-fold larger size of F (~220 nm) compared to A enhances its clearance by the reticuloendothelial system following opsonin-coating (80% of the total F dose accumulates in the liver within 30 min, Jadhav et al., 2011; Owens and Peppas, 2006), and could possibly also affect the size-dependent processes of extravasation (Poh et al., 2015), macrophage uptake (Champion et al., 2008) and drug retention in tissues (Tang et al., 2014). The dependency of the final diameter of the small unilamellar F liposomes on the water bath equipment (type, condition,

settings) used for sonication of the multilamellar vesicles could be a concern for safety and quality-assurance. The importance of a strict manufacturing process to control particle size is illustrated by the increased toxicity of other liposomal AmB products Anfrogen and Lambin compared to A, even though their lipid composition is identical. Of the several generic liposomal AmB formulations currently available, F is the only one that has been tested in clinical trials for the treatment of (visceral) leishmaniasis (Adler-Moore et al., 2016).

Our data has implications for both the clinical use of F and drug development for CL. The relatively small scale (n = 4–5), murine model of *L. major* CL (non-cure BALB/c rather than self-curing C57BL/6) and single tested treatment regimen (5 alternate day administrations over 10 days) are limitations of this work. However, the lower tolerated doses, inferior efficacy and much smaller therapeutic window of F compared to A we observed in our murine study might indicate an increased risk of CL treatment failure and/or duration. The proof of flow but significant drug accumulation of F in *L. major* skin lesions and already known activity against *L. donovani* in VL raises the possibility of use in PKDL treatment, be it with similar caveats as for CL. However, the immunological and histopathological nature of the inflammatory skin response in PKDL is different compared to that of localized CL (Mordal et al., 2010; Scott and Novais, 2016; Nylén and Eidsmo, 2012), which could affect the pharmacokinetics of liposomal formulations. Finally, many researchers over the last decades have proposed the encapsulation of antileishmanial drugs into liposomes as a strategy for passive targeting of the CL infection site (Gutiérrez et al., 2016). The data in the present study suggests an advantage for smaller liposomes (70 > 220 nm) with higher stability and exposure in the bloodstream after IV administration.

In conclusion, F could play a minor role in the systemic treatment of (mainly complex) CL, as we observed moderate efficacy in a murine disease model. However, compared to A, the therapeutic index was narrower and the *in vivo* activity was inferior due to lower levels of the active compound AmB delivered to the infected lesion site. Future research should also investigate the effects of the alternative topical formulation Fungisome® Gel (Lifecare Innovations), as it has potential for local treatment for simple, small CL lesions with little risk of complication.



Comparative efficacy, toxicity and biodistribution of the liposomal amphotericin B formulations Fungisome[®] and AmBisome[®] in murine cutaneous leishmaniasis

Gert-Jan Wijnant^{a,b}, Katrien Van Boclaer^a, Vanessa Yardley^a, Andy Harris^c, Mo Alavijeh^c, Rita Silva-Pedrosa^d, Sandra Antunes^{d,e}, Isabel Mauricio^{d,e}, Sudaxshina Murdan^b, Simon L. Croft^{a,*}

^a Department of Immunology and Infection, Faculty of Infectious and Tropical Diseases, London School of Hygiene and Tropical Medicine, London, United Kingdom

^b Department of Pharmaceutics, UCL School of Pharmacy, London, United Kingdom

^c Pharmidex Pharmaceutical Services Ltd, 3rd floor, 14 Hanover Street, London, United Kingdom

^d Unidade de Parasitologia e Microbiologia Médicas, UEI Parasitologia Médica, Instituto de Higiene e Medicina Tropical, Lisbon, Portugal

^e Global Health and Tropical Medicine, Instituto de Higiene e Medicina Tropical, Universidade Nova de Lisboa, Lisbon, Portugal

ARTICLE INFO

Keywords:

Cutaneous leishmaniasis
Amphotericin B
Liposome
Efficacy
Pharmacokinetics

ABSTRACT

Fungisome[®] (F), a liposomal amphotericin B (AmB) product, is marketed in India as a safe and effective therapeutic for the parasitic infection visceral leishmaniasis. Its potential in the treatment of cutaneous leishmaniasis (CL), a disfiguring form of the disease affecting the skin, is currently unknown. Here, we report the evaluation of the efficacy of F in the *Leishmania major* BALB/c murine model of CL, including a head-to-head comparison with the standard liposomal AmB formulation AmBisome[®] (A). Upon intravenous administration at dose levels of 5, 10 and 15 mg/kg of body weight (on days 0, 2, 4, 6 and 8), F showed clear signs of toxicity (at 15 mg/kg), while A did not. After complete treatment (day 10), the tolerated doses of 5 and 10 mg/kg F had significant antileishmanial activity (ED₅₀ = 4.0 and 12.8 mg/kg for qPCR-based parasite load and lesion size, respectively), although less than that of A at identical doses (ED₅₀ = 3.0 and 8.8 mg/kg). The efficacy of F was inferior compared to A because lower levels of the active agent AmB accumulated within the infected lesion. In conclusion, despite possibly being less safe and efficacious than A at equivalent doses, the moderate *in vivo* activity of F could indicate a role in the systemic pharmacotherapy of CL.

1. Introduction

With more than 2 million new cases per year and 350 million people at risk in over 100 countries, leishmaniasis is a major public health problem affecting the poorest of the poor in many parts of the world (Alvar et al., 2012). Leishmaniasis is a disease complex caused by over 20 species of the protozoan parasite *Leishmania* that are transmitted via female sand flies. Different types include visceral leishmaniasis (VL), also known as kala-azar, an often fatal-if-not-treated condition of the reticuloendothelial system predominantly caused by *L. donovani*, and the most common form, cutaneous leishmaniasis (CL). In simple CL, skin lesions caused by species such as *L. major* or *L. mexicana* are localized and self-healing, but leave disfiguring wounds and scars. Infections by other species can lead to rare but severe chronic, diffuse or mucosal CL symptoms (complex CL) (Reithinger et al., 2007). Another form in the clinical spectrum of skin syndromes is post-kala-azar-dermal leishmaniasis (PKDL), a complication of VL where recovered,

otherwise-healthy patients develop pigmentation disorders and a diffuse macular or nodular rash (Zijlstra et al., 2003).

For CL, the pentavalent antimonials sodium stibogluconate (Pentostam[®]) and meglumine antimoniate (Glucantime[®]) remain the standard treatment, despite being associated with a painful and lengthy series of injections, severe side effects and variable treatment outcomes (Aronson et al., 2016). One of the available second-line drugs is the intravenous (IV) polyene antibiotic amphotericin B (AmB), which kills *Leishmania* through pore formation after complexation with ergosterol in its cell membrane (Cohen, 2016). The clinical use of the conventional deoxycholate salt form is limited by infusion-related side effects such as fever and rigor, as well as chronic toxicity (Tonin et al., 2017). AmBisome[®] (A), a liposomal formulation of AmB, is better tolerated and effective against VL in single high dose (7.5–10 mg/kg, Mondal et al., 2014) and in multiple doses against CL (3 mg/kg daily for a total of 21 mg/kg, Wortmann et al., 2010) and PKDL (two cycles of 4 × 5 mg/kg, Basher et al., 2017). Despite A being listed on the World Health

* Corresponding author.

E-mail address: simon.croft@lshtm.ac.uk (S.L. Croft).

Organisation Essential Medicines List, the requirement for cold chain and the high price (at least 18 \$ per vial via donation programmes) often make availability and access in primary health care settings problematic (Bhattacharya and Ali, 2016). Fungisome® (F) is the brand name of an alternative liposomal AmB formulation developed and commercialized since 2003 in India (Sanath et al., 2005). F contains different lipids and has a different formulation, vesicle size, preparation and pharmacokinetic profile compared to A (Kshirsagar, 2014). Assessing pharmaceutical and/or biological equivalence of F to A is complicated because of a lack of clear regulatory guidelines on liposomal generics (Gaspani, 2013). Clinical studies reported effectiveness and safety of F in VL (Bodhe et al., 1999; Mondal et al., 2010) and recent phase II trials have demonstrated > 90% cure rates following short (2 days) or single high dosed (10 mg/kg) therapy (Sundar et al., 2015; Goswami et al., 2016).

A has been used to treat patients with simple (Guery et al., 2017) and mucosal (Rocio et al., 2014) CL. To investigate the pharmacology of A in CL, we have recently applied an approach based on pharmacokinetic pharmacodynamic (PK PD) relationships in mice (Wijnant et al., 2018). For F, in contrast, there is no such information available to describe the link between drug levels in the infected skin and therapeutic outcomes. This is not only a crucial consideration for potential F treatment of CL, but also of PKDL (for which no animal models of disease are available, Desjeux et al., 2013). Our aim was therefore to (i) evaluate the intralesional drug accumulation and efficacy of intravenously administered F at three dose levels in the *L. major* BALB/c murine model of CL and (ii) provide a head-to-head comparison with the standard liposomal AmB formulation A.

2. Materials and methods

2.1. Drugs

Sealed vials of Fungisome® (F, Lifecare Innovations, India) were sonicated in a Camlab TransSonic T460/H water bath for 45 min at $25 \pm 5^\circ\text{C}$ to transform the large multilamellar vesicles (2700–3500 nm, Serrano et al., 2013) into smaller unilamellar liposomes (≈ 220 nm, Jadhav et al., 2011), as per the manufacturer's instructions. For AmBisome® (A, Gilead, UK), 12 ml sterile water was added to the lyophilized powder to reconstitute the unilamellar liposomes (≈ 70 nm, Walsh et al., 1998; Dupont, 2002), also following the manufacturer's protocol. Saline 0.85% and dextrose 5% were used to dilute stocks of F and A respectively to the desired concentrations. Paromomycin sulphate (Sigma, UK) was prepared in phosphate buffered saline (PBS). Dilutions were prepared one day before starting the experiment and stored at 4°C in the dark.

2.2. Murine model of CL

L. major MHOM/SA85/JISH118 parasites were cultured in Schneider's insect medium (Sigma, UK) supplemented with 10% heat-inactivated fetal calf serum (HiFCS, Sigma UK). These were passaged each week at a 1:10 ratio of existing culture to fresh media in 25 ml culture flasks without filter and incubated at 26°C . Stationary phase parasites were centrifuged for 10 min at 2100 rpm and 4°C . The supernatant was removed and the pellet re-suspended in RPMI medium (Sigma, UK). Cell number was estimated by microscopic counting with a Neubauer haemocytometer. Female BALB/c mice around 6–8 weeks old were purchased from Charles River Ltd. (Margate, UK). These mice were kept in humidity- and temperature controlled rooms (55 – 65% and 25 – 26°C , respectively) and fed water and rodent food *ad libitum*. After acclimatization for 1 week, mice were randomized and subcutaneously (s.c.) injected in the shaven rump above the tail with $200\ \mu\text{l}$ of a parasite suspension containing 4×10^7 low-passage-number ($p < 5$), stationary-phase *L. major* promastigotes in RPMI medium. Twelve days later, when a 5- to 6-mm non-ulcerating nodule had formed, mice were

allocated to the different experimental arms to ensure comparable lesion sizes in each group. All animal experiments were conducted under licence X20014A54 according to UK Home Office regulations under the Animals (Scientific Procedures) Act 1986 and EC Directive 2010/63/E.

2.3. Treatment and sample collection

L. major -infected BALB/c mice ($n = 4$ – 5 per group) each received an intravenous bolus ($200\ \mu\text{l}$) of A or F at 5, 10, 15 mg/kg or 0.85% saline (untreated negative control, (–)) over a 1–2 min period on days 0, 2, 4, 6 and 8. The dosing regimen for F and A was based on earlier data on the efficacy of A in the *L. major*-BALB/c model of CL (Wijnant et al., 2018). Due to previous reports of F's toxicity, the dose of 15 mg/kg was not exceeded (Szoka et al., 1987). The positive control group (+) received 10 daily doses of intraperitoneal (IP) 50 mg/kg paromomycin, a regimen with proven efficacy in this CL model (Wijnant et al., 2017; El-On and Hamburger, 1987). On day 10, the experiment was terminated, animals were sacrificed and lesion skin samples were collected.

2.4. Measurement of lesion size and intralesional AmB levels

The methodologies to determine lesion size, homogenize skin samples and measure intralesional AmB levels have been described in full detail in earlier publications (Wijnant et al., 2018). Samples in this study were treated identically. In brief, lesion size (average of width and length) was measured daily during treatment using digital callipers. On day 10, animals were sacrificed and the collected lesions were ground mechanically with zirconium oxide beads in 1 ml of PBS. The drug (AmB) was then extracted from tissue homogenates with 84:16 methanol:DMSO, followed by LC-MS/MS quantification.

2.5. Measurement of parasite load

A 2-step RT qPCR was used to determine parasite load in murine CL lesions. RNA from a $200\ \mu\text{l}$ volume of skin homogenate was extracted using the GRS FullSample Purification kit (Grisp Research Solutions, Portugal). Briefly, samples were lysed, DNA was removed via a genomic DNA mini spin column and the collected flow-through was transferred to an RNA mini spin column and processed following the manufacturer's protocol. After washing, RNA was eluted from the column with $30\ \mu\text{l}$ RNase-free water. Quality and purity of the RNA extract was estimated with a Nanodrop ND1000 (Thermo Fisher Scientific, USA). To avoid contamination or degradation of RNA, all workbench surfaces and materials were cleaned with RNase AWAY® (Thermo Fisher, USA) and samples kept on ice and stored at -80°C until further use. Complementary DNA (cDNA) was then generated from $10\ \mu\text{l}$ of the RNA-extract using the iScript™ cDNA Synthesis Kit (Bio-Rad, USA) on a T100 Thermal Cycler (Bio-Rad, USA) according to the manufacturer's instructions. TaqMan qPCR reactions of $10\ \mu\text{l}$ were performed in duplicate including $2\ \mu\text{l}$ of cDNA, $5\ \mu\text{l}$ GRISP Xpert Fast PROBE master mix (Grisp Research Solutions, Portugal), $0.25\ \mu\text{M}$ probe (StabVida, Portugal) and $0.4\ \mu\text{M}$ of each primer in 96-well PCR plates (VWR, Portugal). Assays were performed in a CFX Connect™ Real-Time PCR Detection System (Bio-Rad, USA). Cycling conditions were as follows: 40 cycles at a denaturation setting of 95°C for 5 min followed by a two-step amplification cycle of 95°C for 10 s and 60°C for 30 s. Each run included triplicates of a negative control, a no template control and the calibration standards (*L. major* DNA from 10^8 to 10^2 parasites). Bio-Rad CFX Manager 3.1 software was used for analysis. The lower limit of detection was 100 parasites. The qPCR methodology (based on amplification of the 18S ribosomal *Leishmania* region), probe and primer sequences (Van Der Meide et al., 2008) and preparation of calibration standards were as described before (Wijnant et al., 2017).

2.6. Dose-response curves

Non-linear fit models (log(agonist) versus normalized response with variable slope) in GraphPad Prism version 7.02 were used to calculate ED₅₀ and LD₅₀ data. Response in treated groups was expressed as relative reduction compared to untreated controls ((signal untreated – signal treated)/signal untreated × 100%).

2.7. Statistical analysis

Analysis of variance (ANOVA) assuming Gaussian distribution (one-way for parasite load and intralesional AmB level, repeated measures for lesion size) followed by Tukey's multiple comparison tests was used to analyse differences between groups. All data is presented as means and standard deviation (SD). A p - value < 0.05 was considered statistically significant. All analyses were performed using GraphPad Prism version 7.02.

3. Results

3.1. Toxic effects of F and A

After *L. major*-infected mice (n = 5) received slow infusions of 5, 10 or 15 mg/kg of either F or A (200 µl over 2 min), no direct adverse effects and signs of acute toxicity were observed during the first 30 min or 24 h after dosing. However, 48 h after drug administration (day 2), one mouse in the 10 mg/kg F and two mice in the 15 mg/kg F group had died. Among the surviving animals, which had been similarly dosed again on day 2, two more mice in the 15 mg/kg F died 24 h later. By day 3, the one surviving mouse in this highest dose F group showed signs of a hunched posture, pilo-erection and weight loss (data not shown) and it was humanely sacrificed by CO₂. No signs of potential CL-related mortality such as severe ulceration, dissemination of the lesion or hepatosplenomegaly (which could confound the cause of death) were observed during autopsies of these F-treated mice. In contrast, in the mice dosed with A (all three dose levels), F (5 and 10 mg/kg) and negative and positive controls, no fatalities were seen during the rest of treatment.

3.2. Efficacy of F and A

3.2.1. Lesion size

The effect of F and A on lesion size over the course of the 10-day IV treatment in the *L. major* –BALB/c model of CL is shown in Fig. 1a. Compared to the untreated controls (–), the lesion size for F was significantly lower in 5 mg/kg and 10 mg/kg groups (p = 0.0007 and 0.0002, respectively). Significant reductions in lesion size were also found for A at all dose levels (p < 0.0005). When the activity of A and F were compared at identical dose levels, differences in lesion size were not significant (5 mg/kg: p = 0.99, 10 mg/kg: p = 0.48). No direct comparison between F and A could be made for 15 mg/kg, due to the lethal effects at this dose level for F. Reductions in lesion size in liposomal AmB-treated groups were lower when compared to those in the positive control (+).

3.2.2. Parasite load

The efficacy of F and A, as evaluated by RT qPCR parasite load on day 10, is shown in Fig. 1b. Compared to the untreated controls, parasite load was lower in the 5 mg/kg and 10 mg/kg F groups, but the differences were not significant (p = 0.51 and 0.06 respectively). In contrast, increasing doses of A resulted in significant reductions in parasite load (all p-values < 0.05). At identical dose levels, the differences between A and F in parasite load were not significant (5 mg/kg: p = 0.39, 10 mg/kg: p = 0.99) and again, no comparison could be made at 15 mg/kg due to toxicity of F at this dose level. All liposomal AmB-treated groups had lower parasite load reductions compared to

the positive control (+), except for the highest dose of A where there was no significant difference (p > 0.999).

3.2.3. Intralesional amphotericin B levels

We determined the drug levels of the active compound AmB within the infected lesion at the end of the experiment (Fig. 1c). At identical dose levels of 5 and 10 mg/kg, intralesional AmB levels were lower for F than for A, but the differences between the groups were not significant (p = 0.96 and 0.18, respectively). Due to fatal toxicity of F at 15 mg/kg, no direct comparison with A could be made at this dose level. As expected, no AmB was detectable in samples from untreated (–) and positive controls (+).

3.3. Therapeutic window of F and A

After the logarithm of the dose level was plotted against percentage response for A and F (data from toxicity section and Fig. 1), 50% and 90% effective (ED) and lethal (LD) doses were calculated (Table 1). Based on the number of lethal events per group over the course of drug administration (A: 0/5 for 5, 10 and 15 mg/kg; F: 0/5 for 5 mg/kg, 1/5 for 10 mg/kg, 4/5 for 15 mg/kg F), LD₅₀ and LD₉₀ could not be calculated for A, but were found to be 12.3 and 16.9 mg/kg for F. Both 50% and 90% effective doses for parasite load and lesion size were higher for F than for A, indicating inferior efficacy. Therapeutic indices (LD/ED) were over 10-fold lower for F compared to A.

4. Discussion

The liposomal multilamellar amphotericin B (AmB) formulation Fungisome® (F) is intravenously administered after sonication for the treatment of VL (Goswami et al., 2016). Little is known about its potential role in CL pharmacotherapy. Here, we evaluated efficacy, toxicity and intralesional drug accumulation of F in direct comparison to the standard liposomal AmB product AmBisome® (A) in the *L. major*-BALB/c model of CL.

Compared to A, F was more toxic and less efficacious; thus, it had a narrower therapeutic index. As the main aim of this work was to evaluate efficacy and not toxicity, we did not perform dose-escalating studies. However, LD₅₀ values were still calculable as multiple unexpected fatal events occurred at the highest dose of F. The observed LD₅₀ for F (12.3 mg/kg) likely underestimates its safety window, as other researchers found a higher murine LD₅₀ (17 mg/kg, Szoka et al., 1987) and doses up to 10–15 mg/kg are tolerated by patients (Sundar et al., 2015). Chronic side effects of the active compound AmB (such as nephrotoxicity, hepatotoxicity and anaemia) were plausible causes of death in the 15 mg/kg F group, because the lipids of the F liposome are non-toxic (Kshirsagar et al., 2005) and we saw no typical signs of acute AmB overdose in mice (convulsions followed by coma). Although F might be more toxic than A (possibly due to higher uptake in the kidney and/or liver, or increased leakage of AmB from the liposome to the blood), its LD₅₀ is still 5-fold higher than that of non-liposomal AmB deoxycholate (LD₅₀ = 2.3 mg/kg, Szoka et al., 1987).

F was mildly efficacious at 5 × 5 mg/kg and 5 × 10 mg/kg, as it caused a significant suppressive effect on lesion development, despite a non-significant reduction in parasite loads. The inferior efficacy of F compared to A could be related to lower intralesional drug concentrations. Levels of AmB in the infected skin have been shown to correlate well to therapeutic outcomes (Wijnant et al., 2018), which can be expected because of the concentration-dependency of its antimicrobial activity (Lestner et al., 2010). The higher accumulation of A over F at the infected skin site could be explained by differences in a number of physicochemical and pharmacokinetic parameters between the two formulations. After intravenous administration of A, 97% of AmB in the bloodstream remains liposome-associated during the first 4 h (Bekersky et al., 2002) and systemic exposure levels are high (1 mg/kg: C_{max} ≈ 10 µg/ml, AUC ≈ 70 µg.h/ml in mice, Wijnant et al., 2018). The

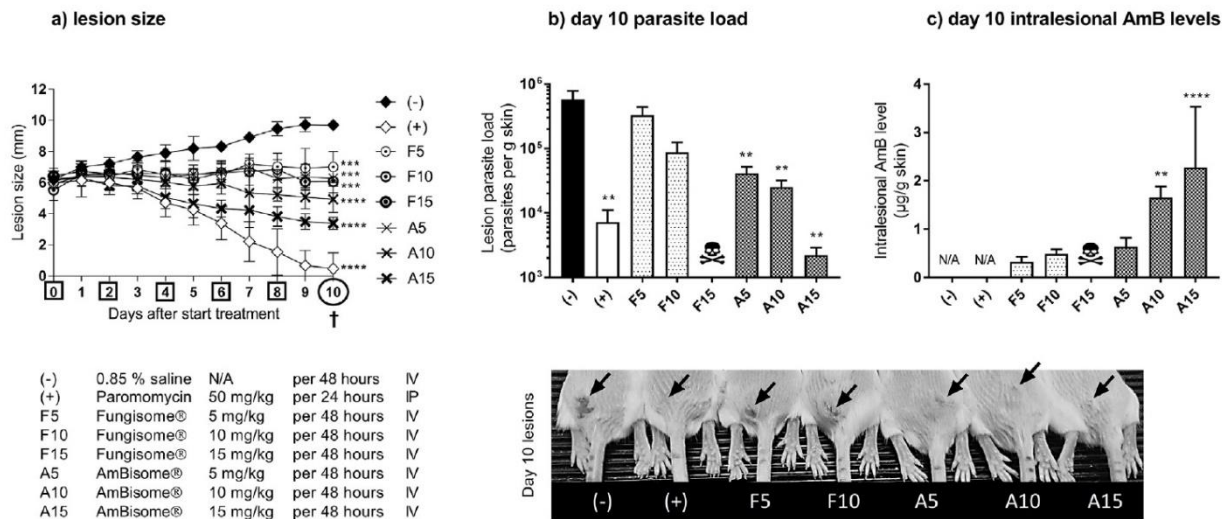


Fig. 1. Comparative efficacy of the liposomal amphotericin B (AmB) formulations AmBisome® (A) and Fungisome® (F) in the *L. major*-BALB/c model of CL. Mice received 10 doses of 50 mg/kg paromomycin (IP, (+)) or five doses of either 0.85% saline (untreated negative control (-)) or 5, 10 and 15 mg/kg F and A (IV). During treatment, lesion size was measured daily (a). On day 10, lesion skin samples were collected and parasite load (b) and AmB levels (c) in the tissue were evaluated. The photo on the bottom shows the CL lesions (arrow) on the rump of the mice on day 10. Each point represents the mean \pm SD (n = 4–5 per group). ANOVA (1-way for parasite load and intralésional AmB level, repeated measures for lesion size) followed by Tukey's multiple comparison tests was used to analyse differences between untreated controls and experimental groups. A p-value < 0.05 was considered statistically significant (*: p < 0.05, **: p < 0.001, ***: p < 0.0005, ****: p < 0.0001), p > 0.05 not significant (no marking above bar). †: day of sacrifice. Skull: no data available due to lethal toxicity at this dose level. N/A: not applicable.

Table 1

50% and 90% effective (ED) and lethal (LD) doses (mg/kg) for the liposomal amphotericin B (AmB) formulations AmBisome® (A) and Fungisome® (F) in the *L. major*-BALB/c model of CL, based on toxicity and Fig. 1 data. The number of lethal events per group over the full course of treatment was monitored during treatment for calculation of LD values. At day 10, parasite load (PL) and lesion size (LS) were determined and effect expressed as relative percentage of reduction compared to the untreated control group, which was used to calculate ED values. Therapeutic indices (TI) were calculated as the LD over ED ratio. As no lethal events occurred for A at the tested dose levels, reference LD values from mice (*) were used from the AmBisome® FDA pharmacological review document, application number 050740 (Drug Approval Package).

	AMBISOME®		FUNGISOME®	
	50%	90%	50%	90%
LD	133.0*	150.0*	12.3	16.9
ED _{PL}	3.0	4.5	4.0	11.0
ED _{LS}	8.8	51.3	12.8	102.8
TI _{PL}	44.9	33.0	3.1	1.5
TI _{LS}	15.1	2.9	1.0	0.2

small liposome size (≈ 70 nm) could facilitate extravasation through the leaky capillaries in the inflamed lesion skin (Romero and Morilla, 2008), followed by uptake by the parasitized dermal macrophages. Alternatively, phagocytic monocytes in the blood could carry ingested A while migrating to the infection site (Voak et al., 2017). In contrast to A, the liposomal stability of F in plasma is unknown (possibly releasing 'free' AmB after interaction with (lipo)proteins, Romero and Morilla, 2008) and its systemic exposure is 7-fold lower (1 mg/kg: $C_{max} \approx 1$ μ g/ml, $AUC \approx 11$ μ g.h/ml in humans, Gokhale et al., 1993). The 3-fold larger size of F (≈ 220 nm) compared to A enhances its clearance by the reticuloendothelial system following opsonin-coating (80% of the total F dose accumulates in the liver within 30 min, Jadhav et al., 2011; Ownes and Peppas, 2006), and could possibly also affect the size-dependent processes of extravasation (Poh et al., 2015), macrophage uptake (Champion et al., 2008) and drug retention in tissues (Tang et al., 2014). The dependency of the final diameter of the small unilamellar F liposomes on the water bath equipment (type, condition,

settings) used for sonication of the multilamellar vesicles could be a concern for safety and quality-assurance. The importance of a strict manufacturing process to control particle size is illustrated by the increased toxicity of other liposomal AmB products Anfrogen and Lambin compared to A, even though their lipid composition is identical. Of the several generic liposomal AmB formulations currently available, F is the only one that has been tested in clinical trials for the treatment of (visceral) leishmaniasis (Adler-Moore et al., 2016).

Our data has implications for both the clinical use of F and drug development for CL. The relatively small scale (n = 4–5), murine model of *L. major* CL (non-cure BALB/c rather than self-curing C57BL/6) and single tested treatment regimen (5 alternate day administrations over 10 days) are limitations of this work. However, the lower tolerated doses, inferior efficacy and much smaller therapeutic window of F compared to A we observed in our murine study might indicate an increased risk of CL treatment failure and/or duration. The proof of low but significant drug accumulation of F in *L. major* skin lesions and already known activity against *L. donovani* in VL raises the possibility of use in PKDL treatment, be it with similar caveats as for CL. However, the immunological and histopathological nature of the inflammatory skin response in PKDL is different compared to that of localized CL (Mondal et al., 2010; Scott and Novais, 2016; Nylén and Eidsmo, 2012), which could affect the pharmacokinetics of liposomal formulations. Finally, many researchers over the last decades have proposed the encapsulation of antileishmanial drugs into liposomes as a strategy for passive targeting of the CL infection site (Gutiérrez et al., 2016). The data in the present study suggests an advantage for smaller liposomes (70 > 220 nm) with higher stability and exposure in the bloodstream after IV administration.

In conclusion, F could play a minor role in the systemic treatment of (mainly complex) CL, as we observed moderate efficacy in a murine disease model. However, compared to A, the therapeutic index was narrower and the *in vivo* activity was inferior due to lower levels of the active compound AmB delivered to the infected lesion site. Future research should also investigate the effects of the alternative topical formulation Fungisome® Gel (Lifecare Innovations), as it has potential for local treatment for simple, small CL lesions with little risk of complication.

Conflicts of interest

None.

Competing interests

No competing interstates to report.

Acknowledgements

Gert-Jan Wijnant's doctoral project is part of the EuroLeish.Net Training Network (www.euroleish.net) and has received funding from the European Horizon's 2020 Research and Innovation Programme under the Marie Skłodowska-Curie grant agreement number 642609. The authors thank Drs. L. and J. Verma, Lifecare Innovations (Lucknow, India) for the generous donation of Fungisome® and Dr. Ana Domingos for laboratory facilities at IHMT.

References

- Adler-Moore, J.P., Gangneux, J.-P., Pappas, P.G., 2016. Comparison between liposomal formulations of amphotericin B. *Med. Mycol.* 54, 223–231.
- Alvar, J., Vélez, I.D., Bern, C., Herrero, M., Desjeux, P., Cano, J., Jannin, J., Boer, M. den, Team, the W.L.C., 2012. Leishmaniasis worldwide and global estimates of its incidence. *PLoS One* 7 e35671. <https://doi.org/10.1371/journal.pone.0035671>.
- Aronson, N., Herwaldt, B.L., Libman, M., Pearson, R., Lopez-Velez, R., Weina, P., Carvalho, E.M., Ephros, M., Jeronimo, S., Magill, A., 2016. Diagnosis and treatment of leishmaniasis: clinical practice guidelines by the infectious diseases society of America (IDSA) and the American society of tropical medicine and hygiene (ASTMH). *Clin. Infect. Dis.* 63, e202–e264. <https://doi.org/10.1093/cid/ciw670>.
- Basher, A., Maruf, S., Nath, P., Hasnain, M.G., Mukit, M.A., Anuwarul, A., Aktar, F., Nath, R., Hossain, A.A., Milton, A.H., Mondal, D., Mohammad Sumsuzzaman, A.K., Rahman, R., Faiz, M.A., 2017. Case report: treatment of widespread nodular post kala-azar dermal leishmaniasis with extended-dose liposomal amphotericin B in Bangladesh: a series of four cases. *Am. J. Trop. Med. Hyg.* 97, 1111–1115. <https://doi.org/10.4269/ajtmh.16-0631>.
- Bekersky, I., Fielding, R.M., Dressler, D.E., Lee, J.W., Buell, D.N., Walsh, T.J., 2002. Plasma protein binding of amphotericin B and pharmacokinetics of bound versus unbound amphotericin B after administration of intravenous liposomal amphotericin B (AmBisome) and amphotericin B deoxycholate. *Antimicrob. Agents Chemother.* 46, 834–840.
- Bhattacharya, P., Ali, N., 2016. Treatment of visceral leishmaniasis: anomalous pricing and distribution of AmBisome and emergence of an indigenous liposomal amphotericin B, FUNGISOME. *J. Parasit. Dis.* 40, 1094–1095. <https://doi.org/10.1007/s12639-014-0607-3>.
- Bodhe, P.V., Kotwani, R.N., Kirodian, B.G., Pathare, A.V., Pandey, A.K., Thakur, C.P., Kshirsagar, N.A., 1999. Dose-ranging studies on liposomal amphotericin B (L-AMP-LRC-1) in the treatment of visceral leishmaniasis. *Trans. R. Soc. Trop. Med. Hyg.* 93, 314–318.
- Champion, J.A., Walker, A., Mitragotri, S., 2008. Role of particle size in phagocytosis of polymeric microspheres. *Pharm Res* 25, 1815–1821. <https://doi.org/10.1007/s11095-008-9562-y>.
- Cohen, B.E., 2016. The role of signaling via aqueous pore formation in resistance responses to amphotericin B. *Antimicrob. Agents Chemother.* 60, 5122–5129. <https://doi.org/10.1128/AAC.00878-16>.
- Desjeux, P., Ghosh, R.S., Dhalaria, P., Strub-Wourgaft, N., Zijlstra, E.E., 2013. Report of the Post Kala-azar Dermal Leishmaniasis (PKDL) Consortium Meeting, New Delhi, India. pp. 27–29. *June 2012. Parasit Vectors* 6, 196. <https://doi.org/10.1186/1756-3305-6-196>.
- Drug Approval Package: AmBisome (Amphotericin B) NDA# 050740 [WWW Document], n.d. URL https://www.accessdata.fda.gov/drugsatfda_docs/nda/97/050740_ambisome_toc.cfm (accessed 11.16.2017).
- Dupont, B., 2002. Overview of the lipid formulations of amphotericin B. *J. Antimicrob. Chemother.* 49 (Suppl 1), 31–36.
- El-On, J., Hamburger, A.D., 1987. Topical treatment of New and Old World cutaneous leishmaniasis in experimental animals. *Trans. R. Soc. Trop. Med. Hyg.* 81, 734–737.
- Gaspari, S., 2013. Access to liposomal generic formulations: beyond AmBisome and Doxil/Caelyx. *Generics and Biosimilars Initiative Journal* 2, 60–62. <https://doi.org/10.5639/gabij.2013.0202.022>.
- Gokhale, P.C., Barapatre, R.J., Advani, S.H., Kshirsagar, N.A., Pandya, S.K., 1993. Pharmacokinetics and tolerance of liposomal amphotericin B in patients. *J. Antimicrob. Chemother.* 32, 133–139.
- Goswami, Rama P., Goswami, Rudra P., Das, S., Satpati, A., Rahman, M., 2016. Short-course treatment regimen of indian visceral leishmaniasis with an indian liposomal amphotericin B preparation (Fungisome™). *Am. J. Trop. Med. Hyg.* 94, 93–98. <https://doi.org/10.4269/ajtmh.14-0657>.
- Guery, R., Henry, B., Martin-Blondel, G., Rouzaud, C., Cordoliani, F., Harms, G., Gangneux, J.-P., Foulet, F., Bourrat, E., Baccard, M., Morizot, G., Consigny, P.-H., Berry, A., Blum, J., Lortholary, O., Buffet, P., Network, the F.C.L.S. group & the L., 2017. Liposomal amphotericin B in travelers with cutaneous and muco-cutaneous leishmaniasis: not a panacea. *PLoS Neglected Trop. Dis.* 11 e0006094. <https://doi.org/10.1371/journal.pntd.0006094>.
- Gutiérrez, V., Seabra, A.B., Reguera, R.M., Khandare, J., Calderón, M., 2016. New approaches from nanomedicine for treating leishmaniasis. *Chem. Soc. Rev.* 45, 152–168. <https://doi.org/10.1039/c5cs00674k>.
- Jadhav, M.P., Nagarsenker, M.S., Gaikwad, R.V., Samad, A., Kshirsagar, N.A., 2011. Formulation and evaluation of long circulating liposomal amphotericin B: a scintigraphic study using ^{99m}Tc in BALB/C mice. *Indian J. Pharmaceut. Sci.* 73, 57–64. <https://doi.org/10.4103/0250-474X.89757>.
- Kshirsagar, N., 2014. Different liposomal amphotericin B formulations for visceral leishmaniasis—Author's reply. *The Lancet Global Health* 2 e450. [https://doi.org/10.1016/S2214-109X\(14\)70270-0](https://doi.org/10.1016/S2214-109X(14)70270-0).
- Kshirsagar, N.A., Pandya, S.K., Kirodian, G.B., Sanath, S., 2005. Liposomal drug delivery system from laboratory to clinic. *J. Postgrad. Med.* 51 (Suppl 1), S5–S15.
- Lestner, J.M., Howard, S.J., Goodwin, J., Gregson, L., Majithiya, J., Walsh, T.J., Jensen, G.M., Hope, W.W., 2010. Pharmacokinetics and pharmacodynamics of amphotericin B deoxycholate, liposomal amphotericin B, and amphotericin B lipid complex in an in vitro model of invasive pulmonary aspergillosis. *Antimicrob. Agents Chemother.* 54, 3432–3441. <https://doi.org/10.1128/AAC.01586-09>.
- Mondal, D., Alvar, J., Hasnain, M.G., Hossain, M.S., Ghosh, D., Huda, M.M., Nabi, S.G., Sundar, S., Matlashewski, G., Arana, B., 2014. Efficacy and safety of single-dose liposomal amphotericin B for visceral leishmaniasis in a rural public hospital in Bangladesh: a feasibility study. *The Lancet Global Health* 2, e51–e57. [https://doi.org/10.1016/S2214-109X\(13\)70118-9](https://doi.org/10.1016/S2214-109X(13)70118-9).
- Mondal, S., Bhattacharya, P., Rahaman, M., Ali, N., Goswami, R.P., 2010. A curative immune profile one week after treatment of Indian kala-azar patients predicts success with a short-course liposomal amphotericin B therapy. *PLoS Neglected Trop. Dis.* 4, e764. <https://doi.org/10.1371/journal.pntd.0000764>.
- Nylén, S., Eidsmo, L., 2012. Tissue damage and immunity in cutaneous leishmaniasis. *Parasite Immunol.* 34, 551–561. <https://doi.org/10.1111/pim.12007>.
- Owens, D.E., Peppas, N.A., 2006. Oponization, biodistribution, and pharmacokinetics of polymeric nanoparticles. *Int. J. Pharm.* 307, 93–102. <https://doi.org/10.1016/j.ijpharm.2005.10.010>.
- Poh, S., Chelvan, V., Low, P.S., 2015. Comparison of nanoparticle penetration into solid tumors and sites of inflammation: studies using targeted and nontargeted liposomes. *Nanomedicine (Lond)* 10, 1439–1449. <https://doi.org/10.2217/nnm.14.237>.
- Reithinger, R., Dujardin, J.-C., Louzir, H., Pirmez, C., Alexander, B., Brooker, S., 2007. Cutaneous leishmaniasis. *Lancet Infect. Dis.* 7, 581–596. [https://doi.org/10.1016/S1473-3099\(07\)70209-8](https://doi.org/10.1016/S1473-3099(07)70209-8).
- Rocio, C., Amato, V.S., Camargo, R.A., Tuon, F.F., Nicodemo, A.C., 2014. Liposomal formulation of amphotericin B for the treatment of mucosal leishmaniasis in HIV-negative patients. *Trans. R. Soc. Trop. Med. Hyg.* 108, 176–178. <https://doi.org/10.1093/trstmh/tru011>.
- Romero, E.L., Morilla, M.J., 2008. Drug delivery systems against leishmaniasis? Still an open question. *Expet Opin. Drug Deliv.* 5, 805–823. <https://doi.org/10.1517/17425247.5.7.805>.
- Sanath, S.S., Gogtay, N.J., Kshirsagar, N.A., 2005. Post-marketing study to assess the safety, tolerability and effectiveness of Fungisome: an Indian liposomal amphotericin B preparation. *J. Postgrad. Med.* 51 (Suppl 1), S58–S63.
- Scott, P., Novais, F.O., 2016. Cutaneous leishmaniasis: immune responses in protection and pathogenesis. *Nat. Rev. Immunol.* 16, 581–592. <https://doi.org/10.1038/nri.2016.72>.
- Serrano, D., Ballesteros, M., Schätzlein, A., Torrado, J., Uchegbu, I., 2013. Amphotericin B formulations – the possibility of generic competition. *Pharm. Nanotechnol.* 1, 250–258. <https://doi.org/10.2174/2211738501999131118125018>.
- Sundar, S., Singh, A., Rai, M., Chakravarty, J., 2015. Single-dose indigenous liposomal amphotericin B in the treatment of Indian visceral leishmaniasis: a phase 2 study. *Am. J. Trop. Med. Hyg.* 92, 513–517. <https://doi.org/10.4269/ajtmh.14-0259>.
- Szoka, F.C., Milholland, D., Barza, M., 1987. Effect of lipid composition and liposome size on toxicity and in vitro fungicidal activity of liposome-intercalated amphotericin B. *Antimicrob. Agents Chemother.* 31, 421–429.
- Tang, L., Yang, X., Yin, Q., Cai, K., Wang, H., Chaudhury, I., Yao, C., Zhou, Q., Kwon, M., Hartman, J.A., Dobrucki, I.T., Dobrucki, L.W., Borst, L.B., Lezmi, S., Helferich, W.G., Ferguson, A.L., Fan, T.M., Cheng, J., 2014. Investigating the optimal size of anticancer nanomedicine. *Proc. Natl. Acad. Sci. U. S. A.* 111, 15344–15349. <https://doi.org/10.1073/pnas.1411499111>.
- Tonin, F.S., Steimbach, L.M., Borba, H.H., Sanches, A.C., Wiens, A., Pontarolo, R., Fernandez-Llimos, F., 2017. Efficacy and safety of amphotericin B formulations: a network meta-analysis and a multicriteria decision analysis. *J. Pharm. Pharmacol.* 69, 1672–1683. <https://doi.org/10.1111/jphp.12802>.
- van der Meide, W., Guerra, J., Schoone, G., Farenhorst, M., Coelho, L., Faber, W., Peekel, I., Schallig, H., 2008. Comparison between quantitative nucleic acid sequence-based amplification, real-time reverse transcriptase PCR, and real-time PCR for quantification of Leishmania parasites. *J. Clin. Microbiol.* 46, 73–78. <https://doi.org/10.1128/JCM.01416-07>.
- Voak, A.A., Harris, A., Qaiser, Z., Croft, S.L., Seifert, K., 2017. Pharmacodynamics and biodistribution of single-dose liposomal amphotericin B at different stages of experimental visceral leishmaniasis. *Antimicrob. Agents Chemother.* 61. <https://doi.org/10.1128/AAC.00497-17>.
- Walsh, T.J., Yeldandi, V., McEvoy, M., Gonzalez, C., Chanock, S., Freifeld, A., Seibel, N.I., Whitcomb, P.O., Jarosinski, P., Boswell, G., Bekersky, I., Alak, A., Buell, D., Barret, J., Wilson, W., 1998. Safety, tolerance, and pharmacokinetics of a small unilamellar liposomal formulation of amphotericin B (AmBisome) in neutropenic patients. *Antimicrob. Agents Chemother.* 42, 2391–2398.
- Wijnant, G.-J., Boexlaer, K.V., Yardley, V., Murdan, S., Croft, S.L., 2017. Efficacy of paromomycin-chloroquine combination therapy in experimental cutaneous

- leishmaniasis. *Antimicrob. Agents Chemother.* 61 e00358-17.
- Wijnant, G.-J., Bocxlaer, K.V., Yardley, V., Harris, A., Murdan, S., Croft, S.L., 2018. Relation between skin pharmacokinetics and efficacy in AmBisome treatment of murine cutaneous leishmaniasis. *Antimicrob. Agents Chemother.* 62 e02009-17.
- Wortmann, G., Zapor, M., Ressner, R., Fraser, S., Hartzell, J., Pierson, J., Weintrob, A., Magill, A., 2010. Liposomal amphotericin B for treatment of cutaneous leishmaniasis. *Am. J. Trop. Med. Hyg.* 83, 1028–1033. <https://doi.org/10.4269/ajtmh.2010.10-0171>.
- Zijlstra, E.E., Musa, A.M., Khalil, E.a.G., el-Hassan, I.M., el-Hassan, A.M., 2003. Post-kala-azar dermal leishmaniasis. *Lancet Infect. Dis.* 3, 87–98.

Chapter 3.4:

Local skin inflammation in cutaneous leishmaniasis as a source of variable pharmacokinetics and therapeutic efficacy of AmBisome[®]



3.4: Local skin inflammation in CL as a source of variable PK and efficacy of AmBisome®

ANNEX 4: WIJNANT, G.-J., VAN BOCXLAER, K., FRANCISCO, A.F., YARDLEY, V., HARRIS, A., ALAVIJEH, M., I., MURDAN, S., AND CROFT, S.L. 2018. LOCAL SKIN INFLAMMATION IN CUTANEOUS LEISHMANIASIS AS A SOURCE OF VARIABLE PHARMACOKINETICS AND THERAPEUTIC EFFICACY OF LIPOSOMAL AMPHOTERICIN B. UNDER REVIEW FOR PUBLICATION BY ANTIMICROBIAL AGENTS AND CHEMOTHERAPY.

Key points, novel results and implications

- In [chapter 3.1](#), we showed that there were differences in *in vivo* drug susceptibilities between *L. major* and *L. mexicana*. In [chapter 3.2](#), we demonstrated that drug accumulation after AmBisome treatment was significantly higher in the *Leishmania*-infected skin than in the healthy, uninfected counterparts. We hypothesized that this was due to local tissue inflammation, which could lead to increased vascular permeability and macrophage recruitment at the infection site. These pathophysiological parameters could cause variable pharmacokinetics of AmBisome. Additionally, the degree of skin inflammation could vary between disease stages and causative parasite species.
- In this chapter, we have **investigated the impact of local skin inflammation on the PK and efficacy of AmBisome** in two murine models of localized CL (*Leishmania major* and *Leishmania mexicana*) at three different stages of disease (papule, initial nodule and established nodule).
- Twenty-four hours after administration of 1 x 25 mg/kg AmBisome (IV) to CL-infected BALB/c mice, drug accumulation in the skin was found to be dependent on the causative parasite species (*L. major* > *L. mexicana*) and the CL disease stage (papule > initial nodule > established nodule > healthy skin). Elevated tissue drug levels were associated with increased vascular permeability (Evans Blue assay) and macrophage infiltration (histomorphometry) in the infected skin, two pathophysiological parameters linked to tissue inflammation. After identical treatment of CL in the two models with 5 x 25 mg/kg AmBisome (IV), intralesional drug concentrations and reductions in lesion size and parasite load (qPCR) were all ≥ 2 -fold higher for *L. major* compared to *L. mexicana*.
- In conclusion, the superior therapeutic efficacy of LAmB against *L. major* compared to *L. mexicana* could be explained in part by improved drug accumulation at the infection site, due to the presence of a more severe local skin inflammation.
- Overall, our data indicate that there might be a need for specific AmBisome treatment guidelines for CL caused by *L. major* in the Middle-East and *L. mexicana* in Latin-America. This is the first time that inflammation and histopathology are linked to PK in CL treatment, which is an important consideration in the development of preclinical drugs and clinical dose regimens.
- We developed a new model of local skin inflammation (the so-called ‘pseudolesion’), and methods to quantify the number of inflammatory cells and macrophages in skin lesions. Moreover, we confirmed the presence of increased blood vessel leakiness, an

important parameter in the tissue distribution of systemic drugs, for the first time in experimental CL using the Evans Blue Assay.

- In the frame of the thesis, this chapter helped to understand the underlying pathophysiological mechanisms that could explain the differences in drug accumulation we have observed in the diseased and the healthy skin in murine CL in chapter 3.2, 3.3 and 3.5.

Candidate's contribution

The candidate generated and analyzed all data described in the paper, except for LC/MS-MS quantification of drug levels (Pharmidex Pharmaceutical Services Ltd.), histological staining (UCL Institute of Neurology) and histomorphometry (Amanda Fortes Francisco, LSHTM). The candidate prepared the first draft of the manuscript, which was accepted for publication in *Antimicrobial Agents and Chemotherapy* in July 2018.

Research paper cover sheet

London School of Hygiene & Tropical Medicine
Keppel Street, London WC1E 7HT
www.lshtm.ac.uk

Registry
T: +44(0)20 7299 4646
F: +44(0)20 7299 4656
E: registry@lshtm.ac.uk

LONDON SCHOOL of HYGIENE & TROPICAL MEDICINE



RESEARCH PAPER COVER SHEET

PLEASE NOTE THAT A COVER SHEET MUST BE COMPLETED FOR EACH RESEARCH PAPER INCLUDED IN A THESIS.

SECTION A – Student Details

Student	GERT-JAN WIJNANT		
Principal Supervisor	SIMON CROFT		
Thesis Title	NEW ORAL & PARENTERAL DEVELOPMENT METHODOLOGIES FOR CUTANEOUS LEISHMANIASIS		

If the Research Paper has previously been published please complete Section B, if not please move to Section C

SECTION B – Paper already published

Where was the work published?	N/A		
When was the work published?	N/A		
If the work was published prior to registration for your research degree, give a brief rationale for its inclusion	N/A		
Have you retained the copyright for the work?*	N/A	Was the work subject to academic peer review?	N/A

**If yes, please attach evidence of retention. If no, or if the work is being included in its published format, please attach evidence of permission from the copyright holder (publisher or other author) to include this work.*

SECTION C – Prepared for publication, but not yet published

Where is the work intended to be published?	AAC		
Please list the paper's authors in the intended authorship order:	SEE ANNEX 4		
Stage of publication	2 ND REVIEW (MINOR CORRECTIONS)		

SECTION D – Multi-authored work

For multi-authored work, give full details of your role in the research included in the paper and in the preparation of the paper. (Attach a further sheet if necessary)	ALL WORK + MANUSCRIPT EXCEPT - LS/MS-MS - HISTOLOGY - HISTOMORPHOMETRY		
--	--	--	--

Student Signature: _____ Date: 17/4/2018

Supervisor Signature: _____ Date: 18.04.2018

Improving health worldwidewww.lshtm.ac.uk

Copyright proof

Re: Copyright for AAC papers: confirmation

 Drought, Heather <hdrought@asmusa.org>
Today, 16:00
Gert Wijnant v

Reply all | v

Inbox

Label: Staff mailbox default delete after 7 years (7 years) Expires: 25/07/2025 16:00

Greetings,

Thank you for your email. When you choose open access publishing, you/the author retains copyright: <https://creativecommons.org/licenses/by/4.0/>
Regardless of OA status, all ASM authors retain certain rights, including use of their article in their thesis or dissertation: http://journals.asm.org/site/misc/ASM_Author_Statement.xhtml

It is fine to use the manuscript in your thesis/dissertation, but you will need to add to the manuscript once accepted that it was used in the thesis (I see you currently note: "Gert-Jan Wijnant's doctoral project is part of the EuroLeish.Net Training Network (www.euroleish.net).") Please check with production staff after final acceptance/at proof stage to see whether this is sufficient). I will make a note of this on the manuscript for the production staff.

I hope this helps, but please let me know if there are any additional questions.

Very best,
Heather

Heather Drought
Editorial Coordinator
American Society for Microbiology
1752 N Street, N.W., Washington, D.C. 20036-2904
Phone: 202-942-9363 | Fax: 202-942-9355



Local Skin Inflammation in Cutaneous Leishmaniasis as a Source of Variable Pharmacokinetics and Therapeutic Efficacy of Liposomal Amphotericin B

Gert-Jan Wijnant,^{a,d} Katrien Van Boclaer,^a Amanda Fortes Francisco,^b Vanessa Yardley,^a Andy Harris,^c Mo Alavijeh,^c Sudaxshina Murdan,^d Simon L. Croft^a

^aDepartment of Immunology and Infection, Faculty of Infectious and Tropical Diseases, London School of Hygiene and Tropical Medicine, London, United Kingdom

^bDepartment of Pathogen Molecular Biology, Faculty of Infectious and Tropical Diseases, London School of Hygiene and Tropical Medicine, London, United Kingdom

^cPharmidex Pharmaceutical Services Ltd., London, United Kingdom

^dDepartment of Pharmaceutics, UCL School of Pharmacy, London, United Kingdom

ABSTRACT Disfiguring skin lesions caused by several species of the *Leishmania* parasite characterize cutaneous leishmaniasis (CL). Successful treatment of CL with intravenous (i.v.) liposomal amphotericin B (LAmB) relies on the presence of adequate antibiotic concentrations at the dermal site of infection within the inflamed skin. Here, we have investigated the impact of the local skin inflammation on the pharmacokinetics (PK) and efficacy of LAmB in two murine models of localized CL (*Leishmania major* and *Leishmania mexicana*) at three different stages of disease (papule, initial nodule, and established nodule). Twenty-four hours after the administration of one 25 mg/kg of body weight LAmB (i.v.) dose to infected BALB/c mice ($n = 5$), drug accumulation in the skin was found to be dependent on the causative parasite species ($L. major > L. mexicana$) and the disease stage (papule $>$ initial nodule $>$ established nodule $>$ healthy skin). Elevated tissue drug levels were associated with increased vascular permeability (Evans blue assay) and macrophage infiltration (histomorphometry) in the infected skin, two pathophysiological parameters linked to tissue inflammation. After identical treatment of CL in the two models with 5×25 mg/kg LAmB (i.v.), intralésional drug concentrations and reductions in lesion size and parasite load (quantitative PCR [qPCR]) were all ≥ 2 -fold higher for *L. major* than for *L. mexicana*. In conclusion, drug penetration of LAmB into CL skin lesions could depend on the disease stage and the causative *Leishmania* species due to the influence of local tissue inflammation.

KEYWORDS cutaneous leishmaniasis, inflammation, pharmacokinetics, liposomal amphotericin B

Leishmaniasis is a vector-borne neglected tropical disease caused by over 20 distinct species of the protozoan *Leishmania* parasite. The two main forms, visceral leishmaniasis (VL) and cutaneous leishmaniasis (CL), continue to pose a major public health problem with significant socioeconomic burden worldwide (1). Current estimates show a global annual incidence of 1 million, 12 million prevalent cases in 98 countries, and over 350 million people at risk of infection (2). CL presents as a wide clinical spectrum of skin syndromes, ranging from severe and rare mucosal leishmaniasis (MCL), diffuse leishmaniasis (DCL) or chronic to the more common, uncomplicated localized leishmaniasis (LCL) lesions. In LCL, a single or limited number of lesions form at the bite site of the parasite-infected female sand fly. A small papule forms, which develops into an initial nodule and then an established nodule with signs of exudation and/or crust

Received 2 April 2018 Returned for modification 29 May 2018 Accepted 3 August 2018

Accepted manuscript posted online 6 August 2018

Citation Wijnant G-J, Van Boclaer K, Fortes Francisco A, Yardley V, Harris A, Alavijeh M, Murdan S, Croft SL. 2018. Local skin inflammation in cutaneous leishmaniasis as a source of variable pharmacokinetics and therapeutic efficacy of liposomal amphotericin B. *Antimicrob Agents Chemother* 62:e00631-18. <https://doi.org/10.1128/AAC.00631-18>.

Copyright © 2018 Wijnant et al. This is an open-access article distributed under the terms of the [Creative Commons Attribution 4.0 International license](https://creativecommons.org/licenses/by/4.0/).

Address correspondence to Simon L. Croft, simon.croft@lshtm.ac.uk.

(double-click to open attached file)



Local Skin Inflammation in Cutaneous Leishmaniasis as a Source of Variable Pharmacokinetics and Therapeutic Efficacy of Liposomal Amphotericin B

Gert-Jan Wijnant,^{a,d} Katrien Van Bocxlaer,^a Amanda Fortes Francisco,^b Vanessa Yardley,^a Andy Harris,^c Mo Alavijeh,^c Sudaxshina Murdan,^d Simon L. Croft^a

^aDepartment of Immunology and Infection, Faculty of Infectious and Tropical Diseases, London School of Hygiene and Tropical Medicine, London, United Kingdom

^bDepartment of Pathogen Molecular Biology, Faculty of Infectious and Tropical Diseases, London School of Hygiene and Tropical Medicine, London, United Kingdom

^cPharmidex Pharmaceutical Services Ltd., London, United Kingdom

^dDepartment of Pharmaceutics, UCL School of Pharmacy, London, United Kingdom

ABSTRACT Disfiguring skin lesions caused by several species of the *Leishmania* parasite characterize cutaneous leishmaniasis (CL). Successful treatment of CL with intravenous (i.v.) liposomal amphotericin B (LAmB) relies on the presence of adequate antibiotic concentrations at the dermal site of infection within the inflamed skin. Here, we have investigated the impact of the local skin inflammation on the pharmacokinetics (PK) and efficacy of LAmB in two murine models of localized CL (*Leishmania major* and *Leishmania mexicana*) at three different stages of disease (papule, initial nodule, and established nodule). Twenty-four hours after the administration of one 25 mg/kg of body weight LAmB (i.v.) dose to infected BALB/c mice ($n = 5$), drug accumulation in the skin was found to be dependent on the causative parasite species ($L. major > L. mexicana$) and the disease stage (papule $>$ initial nodule $>$ established nodule $>$ healthy skin). Elevated tissue drug levels were associated with increased vascular permeability (Evans blue assay) and macrophage infiltration (histomorphometry) in the infected skin, two pathophysiological parameters linked to tissue inflammation. After identical treatment of CL in the two models with 5×25 mg/kg LAmB (i.v.), intralesional drug concentrations and reductions in lesion size and parasite load (quantitative PCR [qPCR]) were all ≥ 2 -fold higher for *L. major* than for *L. mexicana*. In conclusion, drug penetration of LAmB into CL skin lesions could depend on the disease stage and the causative *Leishmania* species due to the influence of local tissue inflammation.

KEYWORDS cutaneous leishmaniasis, inflammation, pharmacokinetics, liposomal amphotericin B

Leishmaniasis is a vector-borne neglected tropical disease caused by over 20 distinct species of the protozoan *Leishmania* parasite. The two main forms, visceral leishmaniasis (VL) and cutaneous leishmaniasis (CL), continue to pose a major public health problem with significant socioeconomic burden worldwide (1). Current estimates show a global annual incidence of 1 million, 12 million prevalent cases in 98 countries, and over 350 million people at risk of infection (2). CL presents as a wide clinical spectrum of skin syndromes, ranging from severe and rare mucosal leishmaniasis (MCL), diffuse leishmaniasis (DCL) or chronic to the more common, uncomplicated localized leishmaniasis (LCL) lesions. In LCL, a single or limited number of lesions form at the bite site of the parasite-infected female sand fly. A small papule forms, which develops into an initial nodule and then an established nodule with signs of exudation and/or crust

Received 2 April 2018 Returned for modification 29 May 2018 Accepted 3 August 2018

Accepted manuscript posted online 6 August 2018

Citation Wijnant G-J, Van Bocxlaer K, Fortes Francisco A, Yardley V, Harris A, Alavijeh M, Murdan S, Croft SL. 2018. Local skin inflammation in cutaneous leishmaniasis as a source of variable pharmacokinetics and therapeutic efficacy of liposomal amphotericin B. *Antimicrob Agents Chemother* 62:e00631-18. <https://doi.org/10.1128/AAC.00631-18>.

Copyright © 2018 Wijnant et al. This is an open-access article distributed under the terms of the [Creative Commons Attribution 4.0 International license](https://creativecommons.org/licenses/by/4.0/).

Address correspondence to Simon L. Croft, simon.croft@lshtm.ac.uk.

formation. The nodule progressively ulcerates and eventually leaves an open wound with raised borders and a crater-like appearance. In most cases, such ulcers slowly self-heal but leave permanent disfiguring scars on the exposed skin areas that are often the cause of serious social stigma (3). Tissue damage and disease in CL are primarily caused by an excessive host immune response against the intracellular infection of dermal macrophages by *Leishmania* spp. (4). As the dermis fills with a dense and diffuse mixed inflammatory cell infiltrate (including macrophages, lymphocytes, neutrophils, mast cells, and plasma cells), the associated edema drives swelling of the tissue. Epidermal changes (hyperkeratosis, acanthosis, and degeneration of the basal layer), connective tissue damage (collagen lysis), and the formation of noncaseating granuloma can occur (5–9). The immunopathology of LCL shows both similarities (chronic, often ulcerative, dermatosis) and differences (clinical presentation, incubation, and resolution time) among different causative *Leishmania* species (10, 11). For example, Old World *L. major* causes so-called “wet” and acute (early ulcerative) CL lesions in the Middle East, seen as large, irregular, and often oozing wounds, which rapidly progress and heal over 2 to 6 months (12, 13). In Central America, New World *L. mexicana* is the responsible agent for “chiclero’s ulcers,” chronic lesions typically found on the ear which spontaneously reepithelize over a period lasting months to even years (14, 15). In a minority of CL cases caused by *L. major* and *L. mexicana*, alternative types of skin lesions with different clinical presentations and immune response can develop (12–15).

Treatment of CL is problematic, as long series of painful injections with the toxic pentavalent antimonials remain the standard therapy (16). A better-tolerated but expensive second-line drug requiring intravenous (i.v.) administration and cold chain is AmBisome (LAmB; Gilead, UK) (17). LAmB is a unilamellar liposomal formulation of the polyene antibiotic amphotericin B (AmB), which forms cidal pores in the leishmanial cell membranes by ergosterol binding (18). Several treatment regimens for a total cumulative dose of 20 to 25 mg/kg of body weight are efficacious against CL and MCL (19). However, therapeutic responses vary for the different causative *Leishmania* species, populations, geographical regions, and clinical settings (20).

We have recently demonstrated that the efficacy of LAmB in murine CL relies on adequate exposure of the active compound AmB at the local site of infection, the skin lesion. Moreover, we also showed higher drug disposition in diseased than in healthy skin (21). Altered pharmacokinetics (PK) at sites of tissue inflammation have been reported previously for antimicrobials (22), anti-inflammatory agents (23), and cancer chemotherapeutics (24). Based on these observations, we formulated three hypotheses, discussed below.

First, the preferential drug distribution of LAmB in CL lesions over uninfected skin can be explained by the presence and the severity of the local skin inflammation. This could vary among different disease stages of CL and among causative parasite species. In the context of LCL skin inflammation, we have focused only on aspects potentially relevant to the pharmacological action of liposomal drugs. The inflammatory response against the *Leishmania* infection at the skin inoculation site involves increased vascular permeability and vasodilatation of dermal blood vessels and the infiltration of several types of immune cells, including macrophages, that play a role in tissue swelling and the formation of skin lesions. Second, the underlying mechanisms for altered drug distribution at the inflammatory site are, at least in part, local capillary leakiness (25–28) and influx of drug-loaded macrophages into the skin (29–34). Third, AmB levels accumulating in lesions following LAmB treatment can be a source of variability in treatment outcomes against different *Leishmania* species. To test the first two hypotheses, we studied the skin PK of LAmB after the administration of a single high dose (1×25 mg/kg i.v.), as well as pathophysiological parameters that could influence the drug distribution process from blood to skin using the Evans blue assay (35–37) and histomorphometry. This was done in infected mice and in control mice with various degrees of skin inflammation, as follows: none (uninfected), high (pseudolesion [PL], a new mouse model of local skin inflammation based on the rat paw edema model [38, 39]), or low (healed lesion [HL], cured of CL by paromomycin sulfate [40]). Figure 1 gives

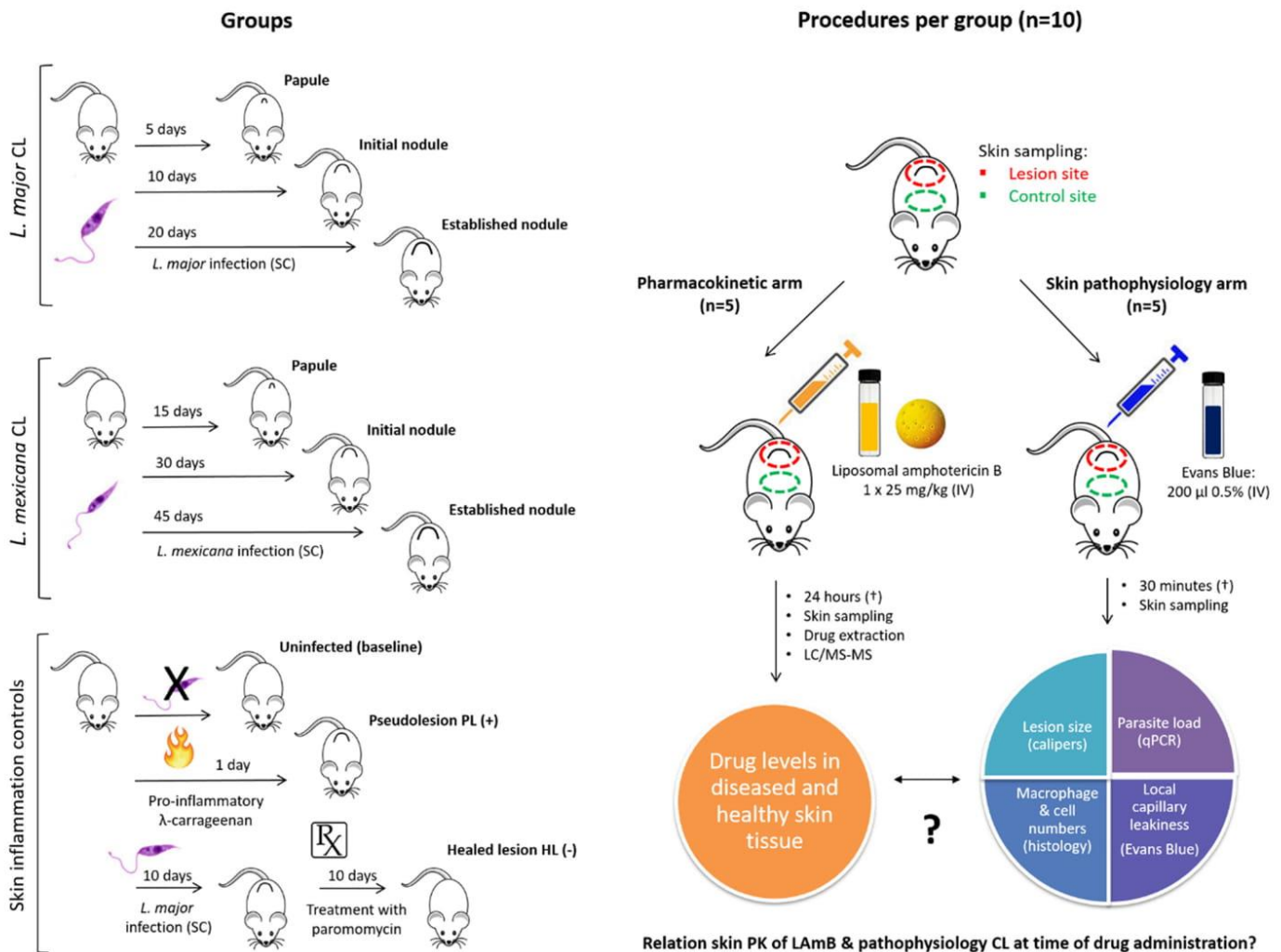


FIG 1 Schematic overview of experimental design to study the influence of skin inflammation in CL on the PK of LAmB.

an overview of the experimental groups and procedures. To investigate the third hypothesis, we compared intralesional drug accumulation and efficacy in *L. major* and *L. mexicana* murine CL following treatment with an identical LAmB dose regimen (5 × 25 mg/kg i.v.).

RESULTS

Pharmacokinetic arm: AmB accumulation in skin after LAmB administration.

Figure 2 shows AmB accumulation (nanograms of AmB per gram of skin tissue; nanograms of AmB per lesion) in infected and healthy control skin at different stages of murine *L. major* or *L. mexicana* CL (papule, initial nodule, and established nodule) 24 h after the administration of a single dose of 25 mg/kg LAmB (i.v.). The morphology of the lesions is shown in Fig. 6a. Table 1 shows AmB lesion-to-healthy-skin ratios, the ratio of the AmB skin level in the lesion over the AmB skin levels in the healthy control skin (calculated from values in Fig. 2, row 1). The ratios indicate that there is a 3-fold decrease in intralesional AmB accumulation when LAmB is administered at late (i.e., established nodule) compared to early (i.e., papule) stages of both *L. major* and *L. mexicana* CL. Drug levels were higher in *L. major* than in *L. mexicana* lesions at all stages of disease. The disposition of AmB in the PL was significantly higher than in healthy skin ($P < 0.0001$). In contrast, AmB accumulation in HL is not significantly different from that in healthy control skin ($P = 0.37$) and is similar to the baseline levels in uninfected mice. Drug distribution patterns are highly comparable when AmB concentrations are ex-

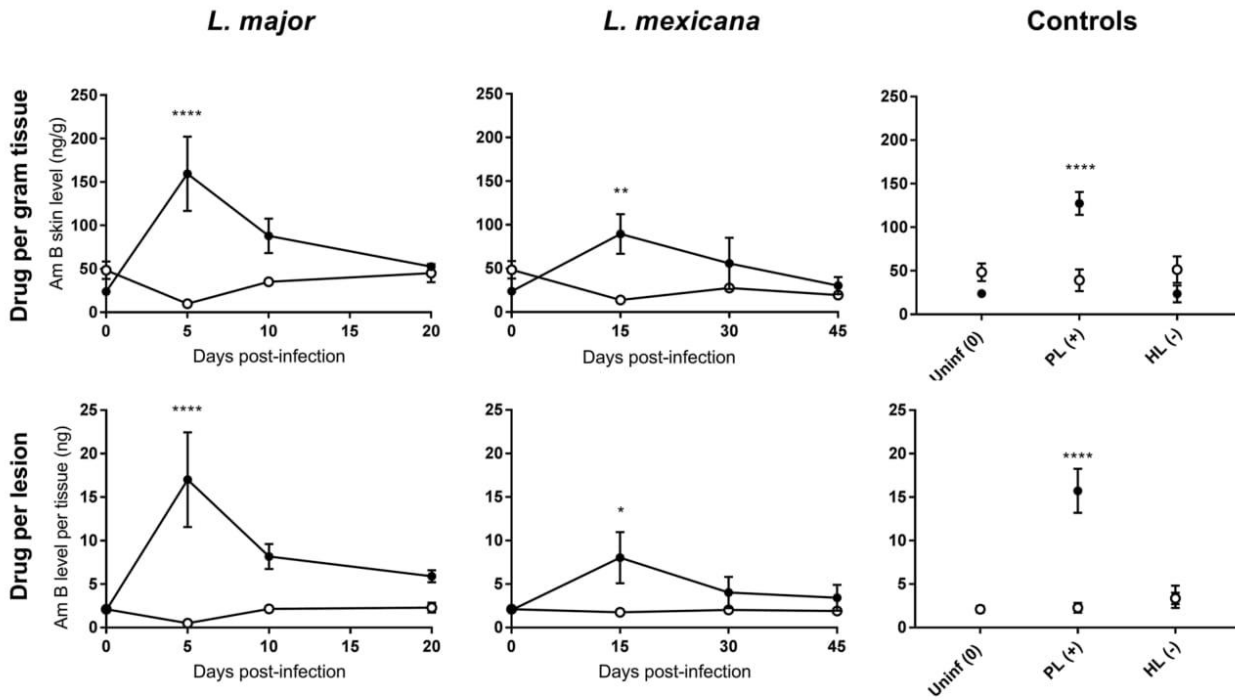


FIG 2 Skin accumulation of amphotericin B (AmB), 24 h after a single intravenous (i.v.) administration of 25 mg/kg AmBisome (LAmB) to CL-infected mice at different time points postinfection and controls. Drug levels were determined in the lesion (●) and healthy control skin (○) site for each animal. CL-infected mice with skin lesions were dosed with LAmB at the time when a papule, an initial nodule, or an established nodule was present on the rump (5, 10, and 20 days after *L. major* infection, respectively, and 15, 30, and 45 days after *L. mexicana* infection, respectively). Controls for skin inflammation were uninfected mice (Uninf), pseudolesion (PL; mice with carrageenan-induced inflammatory skin initial nodule), and healed lesion (HL; mice with paromomycin-cured *L. major* initial nodule). Data are shown as the means ± standard error of the mean (SEM) ($n = 3$ to 5 per group). Statistical analysis was determined with a 2-way ANOVA, followed by Šidák multiple-comparison test. *, $P < 0.05$; **, $P < 0.01$; ***, $P < 0.001$; ****, $P < 0.0001$.

pressed as relative (normalized, in nanograms per gram) or absolute (nanograms per lesion). This indicates that the altered PK of LAmB at different stages of CL is not a consequence of bias introduced by change in tissue volume/weight over the course of infection.

Skin pathophysiology arm: factors affecting the PK of LAmB. (i) Lesion characterization: size and parasite load. Fig. 3 shows the lesion characteristics (top row, lesion size; bottom row, parasite load) at different stages of infection by *L. major* or *L. mexicana* CL (papule, initial nodule, and established nodule). The morphology of the lesions can be seen in Fig. 6 (a images). *L. major* lesions increased in size at a more rapid pace than *L. mexicana*, with different parasite load dynamics over time. During the 20 days following infection with *L. major*, lesion size gradually increased from 0 to around 7 mm, and parasite load remained stable from day 5. Following infection with *L. mexicana*, smaller lesions formed (up to 5 mm), and the parasite load gradually increased. The PL swelling of rump skin had a size comparable to that of CL lesions, but

TABLE 1 Lesion-to-healthy-skin ratios, based on the values found in lesions (rump) and healthy control skin (back) for the variables AmB accumulation, blood vessel permeability, total number of cells, and number of macrophages^a

Variable	Lesion-to-healthy-skin ratio								
	<i>L. major</i> CL			<i>L. mexicana</i> CL			Controls		
	Papule	Initial nodule	Established nodule	Papule	Initial nodule	Established nodule	Uninf	PL (+)	HL (-)
AmB accumulation	16.2	2.5	1.2	3.7	2	1.6	0.5	3.2	0.5
Blood vessel permeability	5.9	9.4	6.8	2.6	12.5	9.5	1.7	11.7	1.2
No. of cells	1.8	2.3	2.4	1.2	1.2	1.4	1	1.6	1.1
No. of macrophages	5.4	7.2	5.1	3	4.8	4.9	0.9	1.5	4.8

^aData are derived from Fig. 2, 4, and 5.

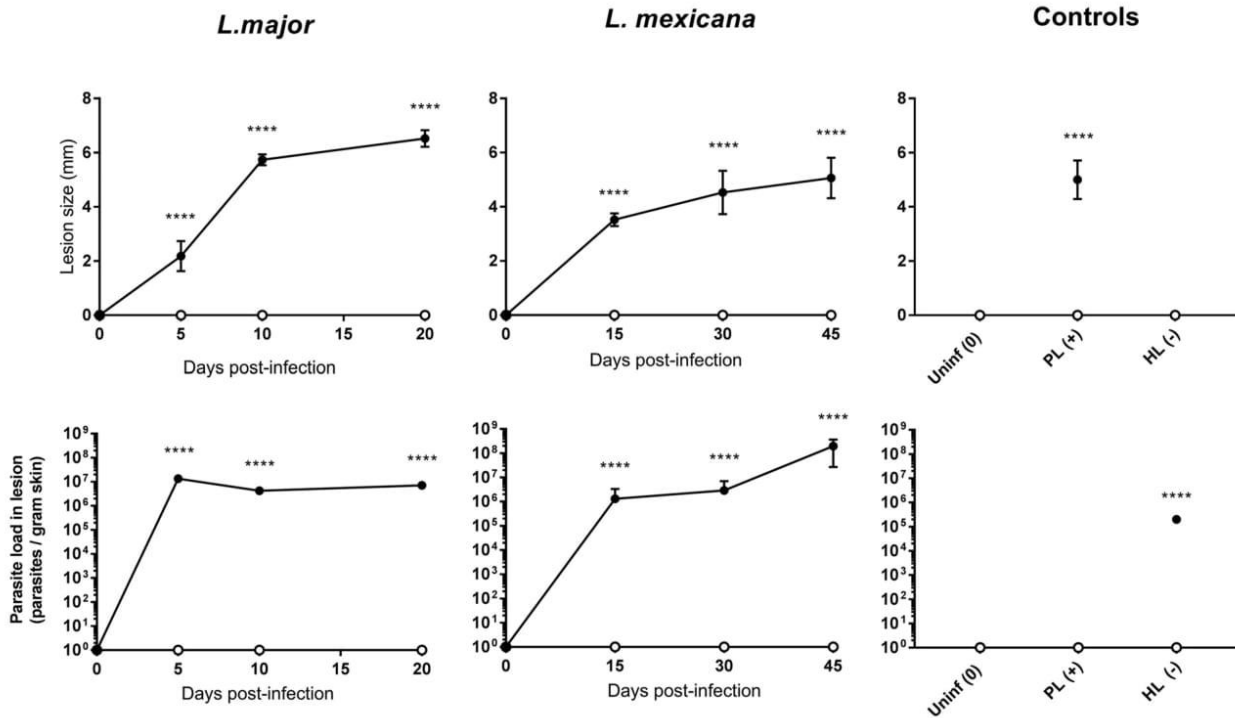
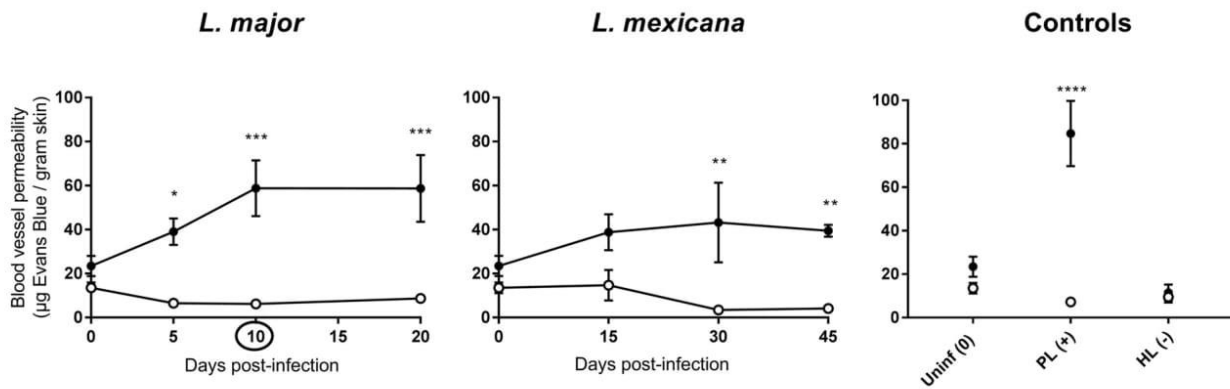


FIG 3 Lesion size (top row) and parasite load (bottom row) into CL-infected mice at different time points postinfection and controls. Lesion size (in millimeters) and parasite load (parasites per gram skin) were determined in the lesion (●) and healthy control skin (○) for each animal. CL-infected mice with skin lesions were measured at the time when a papule, an initial nodule, or an established nodule was present on the rump (5, 10, and 20 days after *L. major* infection, respectively, and 15, 30, and 45 days after *L. mexicana* infection, respectively). Controls for skin inflammation were uninfected mice (Uninf (0)), pseudolesion (PL; mice with carrageenan-induced inflammatory skin initial nodule), and healed lesion (HL; mice with paromomycin-cured *L. major* initial nodule). Data are shown as the means ± SEM ($n = 3$ to 5 per group). Statistical analysis was determined with a 2-way ANOVA, followed by Šidák multiple-comparison test. *, $P < 0.05$; **, $P < 0.01$; ***, $P < 0.001$; ****, $P < 0.0001$.

as expected, no parasites could be detected in this *Leishmania*-free type of skin inflammation. In contrast, the HL (day 20, after 10-day treatment with paromomycin) had a lesion size of 0 ± 0 mm, and the parasite load was around 100-fold lower than in the untreated *L. major* established nodules (day 20). As expected, neither lesion size nor parasite load was measurable in uninfected mice.

(ii) Evans blue and leakiness of dermal capillaries. Fig. 4 shows vascular permeability in infected and healthy control skin at different stages of murine *L. major* or *L. mexicana* CL (papule, initial nodule, and established nodule), as evaluated by the Evans blue assay. The morphology of the lesions can be seen in Fig. 6a. Table 1 shows Evans blue lesion-to-healthy-skin ratios, the ratio of the Evans blue skin level in the lesion over the Evans blue skin levels in the healthy control skin (calculated from the values in Fig. 4). The ratios for *L. major* indicate that compared to healthy control skin, vascular permeability is 6-fold higher in papules and 9-fold higher in initial nodules and established nodules. For *L. mexicana*, there is 3- to 10-fold increase in permeability compared to healthy skin, and the increase is comparable for papules, initial nodules, and established nodules. Blood vessel leakiness was 12-fold higher ($P < 0.0001$) in the PL than in healthy skin. In HL, vascular permeability is not significantly different from that in healthy control skin ($P = 0.99$) and is similar to the baseline levels in uninfected mice. In the photos in Fig. 4, the intense blue coloration of lesions (due to accumulation of the Evans blue dye) provides an additional qualitative confirmation of capillary leakiness at the site of infection. Such a phenomenon is absent in healthy skin tissues.

(iii) Skin histomorphometry: inflammatory cells and macrophages. Fig. 5 shows the number of total cells (top row) and the abundance of macrophages (bottom row) in infected and healthy control skin at different stages of murine *L. major* or *L. mexicana* CL (papule, initial nodule, and established nodule). Figure 6 shows the morphology of the lesions (Fig. 6, a images), the hematoxylin and eosin (H&E) stain (Fig. 6, b images),



Evans Blue treated *L. major*-infected mice (day 10 post-infection):

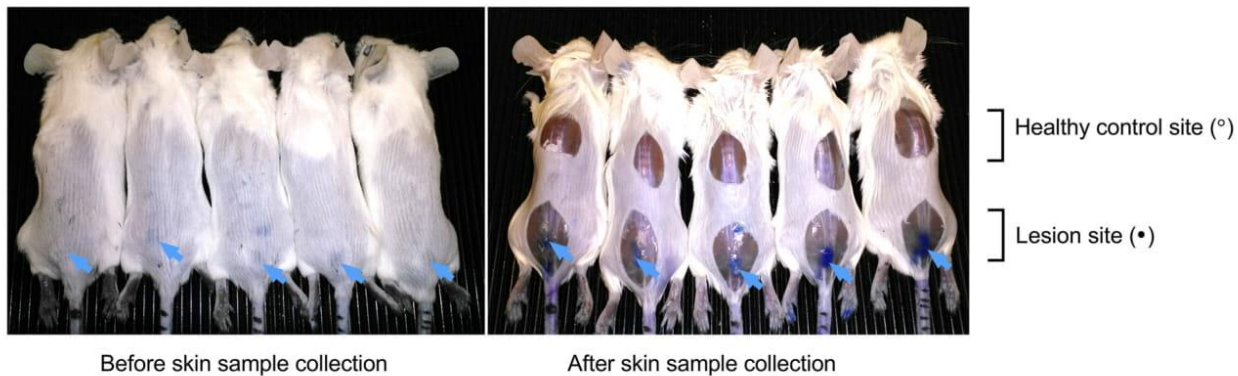


FIG 4 Leakiness of the blood vessels in the skin of CL-infected mice at different time points postinfection and controls. After administration of Evans blue (200 μ l 0.5% i.v.), the amount of the blue dye per gram of tissue was determined in the lesion (●) and healthy control skin (○) for all animals. CL-infected mice with skin lesions were dosed with Evans blue at the time when a papule, an initial nodule, or an established nodule was present on the rump (5, 10, and 20 days after *L. major* infection, respectively, and 15, 30, and 45 days after *L. mexicana* infection, respectively). Controls for skin inflammation were uninfected mice (Uninf), pseudolesion (PL; mice with carrageenan-induced inflammatory skin initial nodule), and healed lesion (HL; mice with paromomycin-cured *L. major* initial nodule). Data are shown as the means \pm SEM ($n = 3$ to 5 per group). Statistical analysis was determined with a 2-way ANOVA, followed by Šidák multiple-comparison test. *, $P < 0.05$; **, $P < 0.01$; ***, $P < 0.001$; ****, $P < 0.0001$. The picture shows *L. major*-infected mice (day 10) after 30 min after administration of Evans blue (i.v.). The arrows point at the blue coloration of the CL lesions (before skin sample collection, left photo) as well as intense blue staining of the underlying thoracolumbar fascia (after skin sample collection, right photo).

and the anti-Iba-1 stain (Fig. 6, c images). Figure 7 examines the H&E and Iba-1 stains of CL lesions in more detail. Table 1 shows total cell and macrophage lesion-to-healthy-skin ratios, the ratio of the total cell and macrophage skin numbers in the lesion over the total cell and macrophage skin numbers in the healthy control skin (calculated from the values in Fig. 5). The ratios indicate that the number of cells in the tissue double in CL lesions as the disease progresses, and a large fraction of the infiltrated inflammatory cells are macrophages. However, the numbers of inflammatory cells and macrophages in *L. major* lesions are higher than those in *L. mexicana* lesions at all stages of disease. In the PL, the number of inflammatory cells was significantly higher than that in healthy skin ($P = 0.0034$), but this was not the case for macrophages specifically ($P > 0.99$). In the HL, the numbers of inflammatory cells and macrophages were not significantly different from those in healthy control skin ($P > 0.05$) and are similar to the baseline levels in uninfected mice.

(iv) Relationship between PK and pathophysiology parameters. Table 1 shows the lesion-to-healthy-skin ratios (parameter value in lesion/parameter value in healthy skin) for AmB accumulation (Fig. 2 data, AmB levels in nanograms per gram), blood vessel permeability (Fig. 4 data), number of cells, and number of macrophages (Fig. 5 data). For uninfected mice, the ratios for AmB, blood vessel permeability, cell numbers, and macrophage numbers were around 1, indicating no difference in the values for these parameters between the lesion site (rump skin) and the healthy site (back skin).

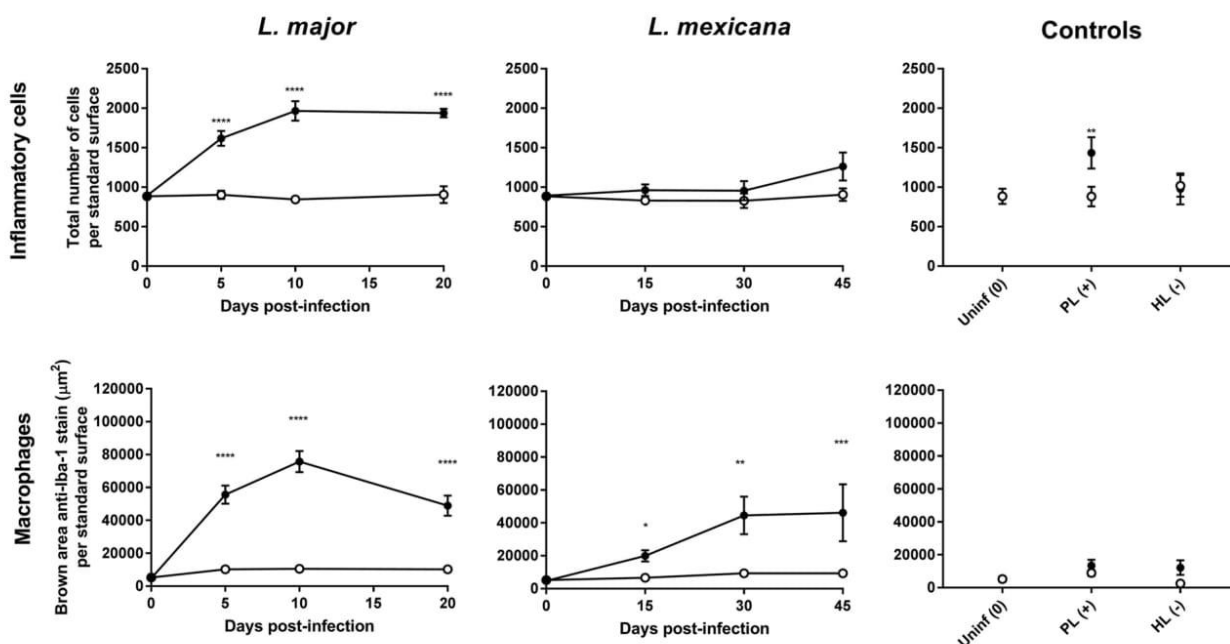


FIG 5 Estimation of the number of cells (top row, H&E stain) and macrophages (bottom row, anti-Iba-1 reaction) at the infected lesion site (rump skin, black bars) and the control site (back skin, white bars) of control mice and CL-infected mice. Measurements in CL-infected mice with skin lesions were performed at the time when a papule, an initial nodule, or an established nodule was present on the rump (5, 10, and 20 days after *L. major* infection, respectively, and 15, 30, and 45 days after *L. mexicana* infection, respectively). Controls for skin inflammation were uninfected mice (Uninf (0)), pseudolesion (PL; mice with carrageenan-induced inflammatory skin initial nodule), and healed lesion (HL; mice with paromomycin-cured *L. major* initial nodule). Standard surface was the picture area showing full skin tissue (epidermis, dermis, and hypodermis) to allow direct comparisons among groups (166,970.7 μm^2). Data are shown as the means \pm SEM ($n = 3$ to 5 per group). Statistical analysis was determined with a 2-way ANOVA, followed by Šidák multiple-comparison test. *, $P < 0.05$; **, $P < 0.01$; ***, $P < 0.001$; ****, $P < 0.0001$.

Comparing *Leishmania*-infected mice to uninfected mice, AmB accumulation, blood vessel permeability, cell numbers, and macrophage numbers were higher at all three stages of disease for both *L. major* and *L. mexicana*. However, these ratios were increased for *L. major* compared to *L. mexicana*. The higher ratios for PL than those for uninfected mice indicate increased drug accumulation, as well as blood vessel leakiness, cell numbers, and macrophages in this alternative type of skin inflammation. For HL, however, all lesion-to-healthy skin ratios were highly similar to the baseline ratios found in healthy mice (except for macrophage number). Similar patterns at different stages of disease were found in *L. major*- and *L. mexicana*-infected mice. A significant increase in ratios for drug accumulation, blood vessel permeability, cell numbers, and macrophage numbers was found in papules (early CL) compared to uninfected mice. In a comparison of the ratios for the papule compared to those for initial nodules and established nodules (later-stage CL), relatively little new additional inflammatory cells and macrophages seemed to infiltrate the skin (for both *L. major* and *L. mexicana*), and blood vessel permeability remained stable (for *L. major* but not *L. mexicana*).

Skin PK and efficacy of LAmB in CL. Finally, we evaluated the efficacy of LAmB against *L. major* and *L. mexicana* in the BALB/c mouse model of CL. Figure 8 shows *in vivo* activity and intralésional AmB accumulation on day 10, after treatment of mice with initial nodules with 5 doses of 25 mg/kg LAmB (i.v.) on alternate days (i.e., on days 0, 2, 4, 6, and 8). LAmB showed *in vivo* activity against both CL-causing parasite species. However, reductions in lesion size and parasite load compared to untreated controls were greater than and significant for *L. major* ($P = 0.011$ and 0.0471) compared to *L. mexicana* ($P = 0.25$ and 0.99). We also observed almost 2-fold higher AmB levels (in nanograms per gram) in *L. major* over *L. mexicana* lesions. In CL-infected skin, drug level concentrations were at least 4-fold higher than those in healthy rump skin of identically uninfected LAmB-treated mice. However, this difference was significant for *L. major* ($P < 0.0001$) but not for *L. mexicana* ($P = 0.15$). The *L. major* data have been reported

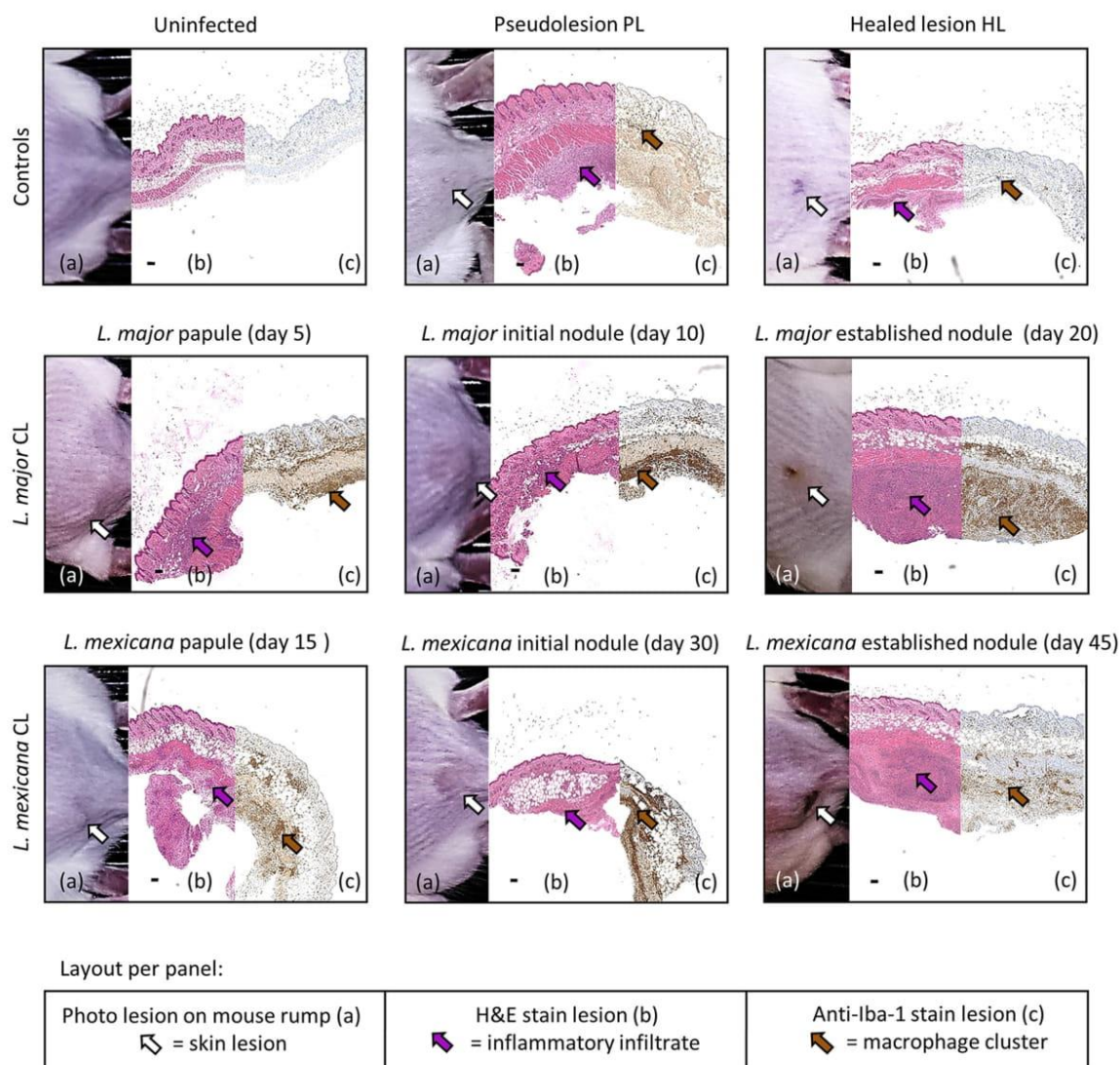


FIG 6 Collage panels of murine skin lesions developed during CL disease progress and controls for skin inflammation. Per panel, photo of the lesion on the rump of the mice (a, white arrow points at lesion), hematoxylin and eosin stain (b, purple arrow points at a cluster of inflammatory cells), and macrophage marker anti-ionized calcium binding adapter molecule 1-antibody stain (c, brown arrow points at a cluster of macrophages). Top row, controls for skin inflammation (uninfected, pseudolesion, and healed lesion). Middle row, *L. major* CL lesions (papule present at 5 days postinfection, initial nodule present at 10 days postinfection, and an established nodule present at 20 days postinfection). Bottom row, *L. mexicana* CL lesions (papule present at 15 days postinfection, initial nodule present at 30 days postinfection, and an established nodule present at 45 days postinfection). (b) Black scale bar = 100 μ m.

earlier (21) but are included to enable a direct comparison with *L. mexicana* (novel data).

DISCUSSION

Local tissue inflammation in infectious disease can alter the pharmacokinetics (PK) and thus therapeutic outcomes of antimicrobials (41–43). In this work, we have confirmed our hypothesis that the inflamed state of skin lesions in CL alters the PK of LAmB following intravenous drug administration in two mouse models of infection. Our results show that AmB accumulation in CL-infected skin is (i) *Leishmania* species specific (greater in *L. major* than in *L. mexicana* lesions) (ii) disease stage specific (papule > initial nodule > established nodule > healthy skin), and (iii) a plausible cause of the superior *in vivo* efficacy of LAmB against *L. major* compared to that against *L. mexicana*.

First, the preferential distribution of LAmB to CL infection sites (*L. major* > *L. mexicana*) compared to uninfected ones could be explained by the presence and the severity of the local inflammatory response against the parasites residing in dermal

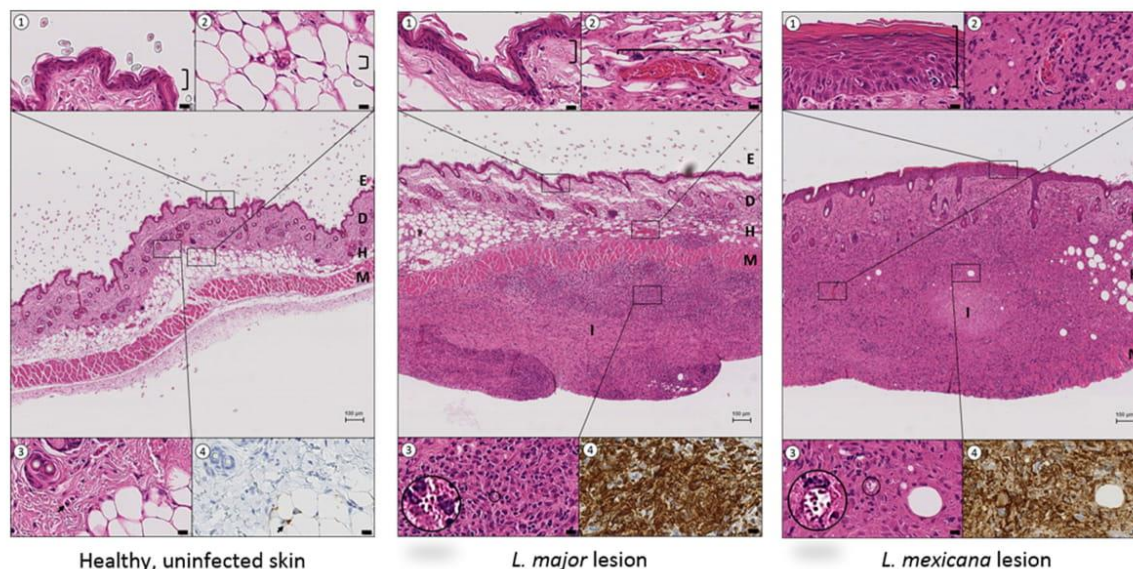


FIG 7 Comparison of mouse skin morphology and macrophage density in healthy, uninfected skin (left), *L. major* CL lesion (20 days postinfection, middle), and *L. mexicana* CL lesion (45 days postinfection, right). The central picture in each panel (H&E stain) shows the structural layers of the skin, epidermis (E), dermis (D) and hypodermis (H), with the underlying muscle (M) at $\times 4$ magnification (bar = 100 μm). The insets (1 to 4) highlight details of the central picture ($\times 80$ magnification, bar = 10 μm). ①, epidermis; ②, dermal capillaries; ③, *Leishmania* amastigotes within parasitophorous vacuoles; ④, anti-Iba-1 stain (macrophage marker) of tissue shown in inset ③. In both the *L. major* and *L. mexicana* CL lesions, intense inflammatory foci (I) are present in the skin, causing severe disruption of the D and H architecture. Compared to healthy uninfected skin, CL lesions also showed (i) epidermal hyperplasia and acanthosis for *L. mexicana* but not for *L. major* (①), (ii) dilated blood vessels, a factor contributing to capillary leakiness (②), and (iii) a large amount of inflammatory cells (③), many of which are macrophages (④).

macrophages. Compared to *L. mexicana*, *L. major* causes more heavily inflamed (exudative) established nodules with a more rapid, aggressive onset in humans (12–15) and mice (3, 44). Several quantitative biomarkers for skin inflammation in our study confirmed this. The leakiness of the dermal capillaries, swelling/edema in the skin tissue (indicated by lesion size), and numbers of infiltrating macrophages or other inflammatory cells were higher in *L. major* than in *L. mexicana* CL at all stages of disease. These findings are consistent with earlier reports (45–47). Moreover, the HL and PL observations support this inflammation-driven theory of enhanced drug accumulation. When the inflammation in *L. major*-infected skin is largely cleared because of parasite elimination by paromomycin treatment (HL), AmB accumulation, blood vessel permeability, and cell numbers return to baseline levels seen in uninfected skin. However, when inflammation is experimentally induced by injection of λ carrageenan (instead of parasites) in rump skin (similar site to that in CL infection), the local drug concentrations after LAmB administration also increase by over 3-fold. Such a phenomenon could be explained by a 10-fold increase in leakiness of the skin capillaries. The new PL model of local skin inflammation, based on subcutaneous injection of λ carrageenan, could be a useful research tool for dermatoses other than CL, such as skin cancers, atopic dermatitis, or psoriasis (48).

Second, the increased intralésional AmB accumulation after intravenous LAmB dosing of mice with CL in earlier stages of disease (papule > initial nodule > established nodule) could be related to changes in infiltration of phagocytes prone to internalize circulating liposomes and, likely to a lesser degree, capillary leakiness in the dermis. When LAmB is administered to mice with early CL, during the initial massive influx of phagocytes and inflammatory cells into the skin as part of the antileishmanial immune response (4, 11), intralésional drug levels could be increased as AmB-loaded cells migrate from the bloodstream to the infection site. Hence, in later stages of disease, when the number of additional macrophages infiltrating the infected tissue is more limited, skin AmB accumulation could be lower. The known role of phagocyte transport in the delivery of various antibiotics (30–32), including liposomal AmB (41), to

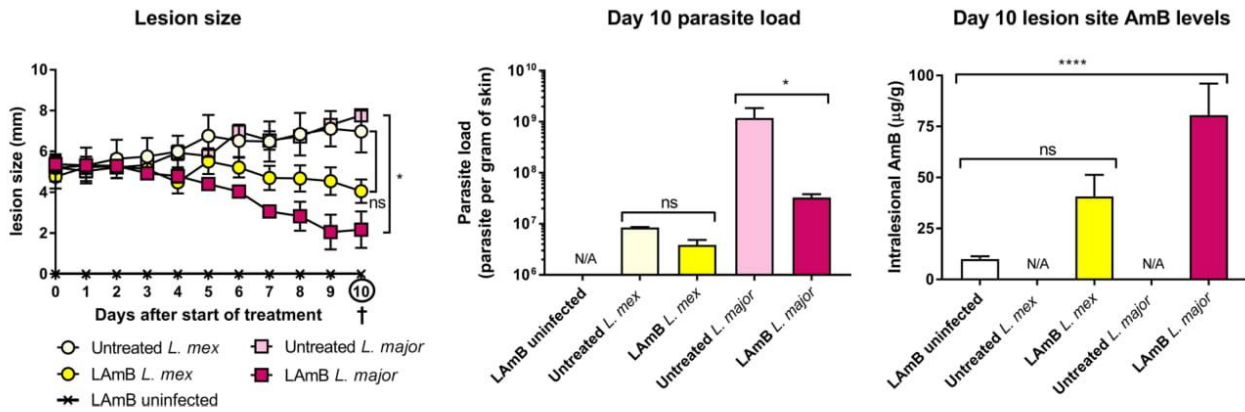


FIG 8 Efficacy and biodistribution of liposomal amphotericin B LAmB in murine models of *L. major* and *L. mexicana* (*L. mex*) CL. Mice were injected (s.c.) with parasite-free medium (uninfected) or infected with *L. major* or *L. mexicana* promastigotes in the rump skin. When a nodular lesion had formed at the inoculation site of CL-infected animals (10 and 30 days postinoculation for *L. major* and *L. mexicana*, respectively), animals received either 5% dextrose (untreated) or 25 mg/kg LAmB (i.v.) on days 0, 2, 4, 6, and 8. During treatment, lesion size (a) was measured daily. On day 10, lesion skin tissues were collected, and parasite load (b) and AmB levels (c) were determined. Each point represents the mean \pm SEM ($n = 3$ to 5 per group). ANOVA (1-way for parasite load and intralesional AmB levels, repeated measures for lesion size), followed by Tukey's multiple-comparison test (*, $P < 0.05$; ****, $P < 0.0001$; ns, not significant) were used. N/A, not applicable.

local infection sites, as well as our PK and histology data, suggests the plausibility of this hypothesis. Confirmative research should distinguish extra- and intracellular levels in circulating and dermal macrophages after LAmB administration. While phagocytes can increase AmB exposure in the lesion, their therapeutic relevance is still unclear. Cellular lysis, resulting in local release of the drug payload, or impaired parasite survival in these "pretreated" macrophages could play a role. Another pathophysiological factor affecting the PK of LAmB is blood vessel leakiness, a result of vasodilatation and enhanced vascular permeability in the inflamed dermis. Here, we confirmed the existence of this phenomenon in experimental CL for the first time. It could facilitate extravasation of the liposomes (~80 nm in size) through the dermal capillaries, which under normal physiological conditions have a pore cutoff size of 6 to 12 nm (21). However, it cannot explain a decrease in AmB disposition in lesions as CL progresses by itself, because we found comparable degrees of capillary leakage in papules, initial nodules, and established nodules. Other factors that could affect cellular and dermal PK, such as plasma and tissue protein binding (49), angiogenesis (50), lymphatic drainage, phagocytic capacity, and activation stage of (parasitized) macrophages (33), skin metabolism, clearance by the reticuloendothelial system (51), or the involvement of (nonmacrophage) immune cells, mediators, or responses, were not evaluated in this study. A similar trend of decreasing drug distribution of LAmB to target organs during later disease stages was also found in murine VL (33). However, interestingly, *Leishmania*-infected livers contain lower rather than higher drug levels than healthy ones.

Third, the *in vivo* activity of LAmB was superior against *L. major* than against *L. mexicana*, likely due to inflammation-enhanced and relatively increased drug levels at the infection site. A clear correlation between drug levels of the leishmanicidal, concentration-dependent antibiotic AmB delivered to the lesion and the efficacy of LAmB in murine CL has already been reported (21, 52). Apart from skin PK, there could also be differences in antileishmanial pharmacodynamics (PD) and the resulting PK/PD relationship. An intrinsic species-specific sensitivity to the active compound AmB is unlikely, as *in vitro* 50% effective concentrations (EC_{50} s) are comparable ($\approx 0.1 \mu\text{M}$) (35). However, the *in vivo* susceptibility could still vary based on the metabolic state of the *L. major* or *L. mexicana* parasites in the skin. In chronic lesions with slow disease onset, a quiescent semidormant phenotype of *L. mexicana* could exist, benefitting its long-term survival and possibly showing reduced drug sensitivity (53–55). Such PK/PD factors could cause variable rate or magnitude of parasite elimination, a combined outcome of drug activity and host immunity. Pharmacogenetic differences between

individual patients and populations (affecting distribution, metabolism, and clearance) might also contribute to additional variation in LAmB efficacy in the clinic (20).

Finally, although BALB/c mice are common in PK studies (56) and *L. major*-BALB/c is a highly reproducible and well-established model for antileishmanial drug evaluation (57), differences between CL in humans (mostly self-curing lesions) and BALB/c mice (nonhealing lesions) (58) should be considered. Our studies used mice with relatively small (<1 cm), local, and uncomplicated CL lesions. Despite variation in the immunological nature of the skin inflammation, the phenomena of capillary leakiness, edema formation, and phagocyte infiltration occur in both mice and humans (59, 60). Thus, our findings could hold treatment implications for CL as well as for other inflammatory (skin) disorders. During preclinical evaluation of novel nanoparticles, a drug delivery strategy used for CL (61), the time of drug administration (relative to disease stage), and causative species are important factors that can affect both PK and PD. In the clinic, LAmB treatment outcomes in CL are already known to be related to the causative *Leishmania* species. A recent observational study in a group of travelers with (M)CL (20) reported differences in the therapeutic success rate of LAmB against *L. infantum* (78%), *L. major* (50%), and *Leishmania Viannia* subgenus species (28%). However, because *L. mexicana* was not included in this work, we cannot directly compare our results in mice to those in humans. In addition, early diagnosis and therapeutic intervention with LAmB could produce enhanced drug exposure in the skin lesion. No present clinical studies have reported on this. In contrast, early treatment of *L. brasiliensis* CL with intramuscular pentavalent antimonials was associated with a 5-fold increased risk of treatment failure (62, 63). Both the impact of parasite species and the age of the lesion in CL on PK and therapeutic efficacy of LAmB (and other antileishmanial drugs) deserve further investigation. Laboratory experiments could investigate outcomes of multidose treatments in alternative models of disease caused by additional *Leishmania* species and strains. The extrapolation of LCL results to the various types of complex CL is complicated by differences in histopathology (blood vessel destruction in advanced MCL [10]) and the nature and severity of the inflammatory response (balance TH1/TH2-type cellular immunity in local versus diffuse CL [3, 4]). Overall, it is clear that the immunohistopathology of CL has a profound impact on drug disposition of antileishmanial agents, both when administered topically (increased permeation through the damaged epidermis [64, 65]) and systemically (enhanced extravasation for liposomal and nonencapsulated drugs [21]).

In conclusion, our data indicate that the severity of inflammatory skin disease in CL could contribute to variable drug penetration in the target tissue and therapeutic efficacy of LAmB. The significant impact of local inflammation on PK and PK/PD is not only an important consideration for the development of new drugs and clinical dose regimens for the treatment of CL but also for other (infectious) diseases with an inflammatory component.

MATERIALS AND METHODS

Parasites, media, and drugs. *L. major* MHOM/SA85/JISH118 and *L. mexicana* MNYC/BZ/62/M379 parasites were cultured in Schneider's insect medium (Sigma, UK) supplemented with 10% heat-inactivated fetal calf serum (HiFCS; Sigma UK). These were passaged each week at a 1:10 ratio of existing culture to fresh media in 25-ml culture flasks without a filter and incubated at 26°C. For infection of mice, stationary-phase parasites were centrifuged for 10 min at 2,100 rpm and 4°C. The supernatant was removed and the pellet resuspended in RPMI medium (Sigma, UK). Cell number was estimated by microscopic counting with a Neubauer hemocytometer. AmBisome (LAmB; Gilead, UK) was reconstituted with 12 ml sterile water (as per the manufacturer's instructions) to yield a stock solution of 4 mg/ml and diluted in 5% aqueous dextrose to achieve a drug dose of 25 mg/kg. Paromomycin sulfate (Sigma) was prepared in phosphate-buffered saline (PBS) to yield 50-mg/kg doses. Lambda carrageenan (Sigma) and Evans blue (Sigma) 0.5% (wt/vol) solutions were made up in phosphate-buffered saline (PBS; Sigma). The drug preparations were stored at 4°C during the experiments.

Experimental groups. Female BALB/c mice around 6 to 8 weeks old and with a mean weight of 18 to 20 g were purchased from Charles River Ltd. (Margate, UK). These were kept in humidity- and temperature-controlled rooms (55 to 65% and 25 to 26°C, respectively) and fed water and rodent food *ad libitum*. Mice were randomized and allowed an acclimatization time of 1 week. All animal experiments were conducted under license 70/8427 according to UK Home Office regulations under the

Animals (Scientific Procedures) Act 1986 and EC Directive 2010/63/E. An overview of the groups is shown in Fig. 1.

Group 1 was the *L. major* CL group. Mice were subcutaneously (s.c.) infected in the shaven rump above the tail with 200 μ l of a parasite suspension containing 4×10^7 of low-passage-number (<5), stationary-phase *L. major* promastigotes in RPMI medium. Lesion size was measured daily with digital calipers (average of length and width) after inoculation as the CL lesions developed into papules, initial nodules, and established nodules. In this animal model of CL, these respective disease stages occurred on days 5, 10, and 20, as shown previously (40). We define a CL lesion as a stationary local skin abnormality at the site of *Leishmania* parasite inoculation (rump). A "papule" is the smallest (2 to 4 mm) CL lesion, a palpable elevation of the skin with no signs of ulceration. An "initial nodule" is a medium-sized (4 to 6 mm) papule that is larger and more defined. An "established nodule" is a larger (5 to 8 mm) CL lesion that is crusted or exudative.

Group 2 was the *L. mexicana* CL group. Mice were infected as described above for *L. major*, but *L. mexicana* promastigotes were used. In this animal model of CL, the disease stages of papule, initial nodule, and established nodule occurred on days 15, 30, and 45 postinoculation (40). The above-described definitions of CL lesion, papule, initial nodule, and established nodule apply.

Group 3 was skin inflammation controls. For the uninfected controls, mice were infected in the shaven rump above the tail with 200 μ l parasite-free RPMI medium (s.c.). For the healed lesion (HL) controls, mice with *L. major* initial nodules (10 days postinoculation, infection as described above) were treated daily for 10 days with 50 mg/kg paromomycin sulfate in PBS (200 μ l via the intraperitoneal [i.p.] route). This regimen has proven efficacy in the *L. major*-BALB/c model of CL (40). A size of 0 mm (complete disappearance of the skin lesion) was considered a near-complete healing and a negative control for skin inflammation. For the "pseudolesion" (PL) control, mice were s.c. injected in the shaven rump above the tail with 25 μ l of 0.5% λ carrageenan in PBS. After 24 h, when a measurable lesion-like but parasite-free swelling of skin had occurred, the pseudolesion was considered a positive control for skin inflammation. These specific concentration and time points were chosen based on similarity to CL lesions and experimental requirements. The resulting diameter of the skin swelling (lesion size) was between 2 and 8 mm (the size of our CL lesions). Moreover, the local inflammation remained for at least 48 h (24 h to reach maximal swelling and another 24 h for the PK experiment). This novel carrageenan-induced model of local rump skin inflammation in mice was based on the well-established model of rat paw inflammation (38, 39), and preparatory studies are shown in the supplemental material.

Procedures per experimental group. Ten mice per group (*L. major* papule, *L. major* initial nodule, *L. major* established nodule, *L. mexicana* papule, *L. mexicana* initial nodule, *L. mexicana* established nodule, uninfected, pseudolesion, and healed lesion) were divided in a pharmacokinetic ($n = 5$) and skin pathophysiology arm ($n = 5$). This allowed simultaneous studying of drug accumulation 24 h after LAmB administration (this time point results in maximal AmB accumulation in skin [21]) and pathophysiology factors affecting pharmacokinetics at the time of drug administration (30 min after administration of Evans blue, standard time for preferential distribution of the dye to inflamed compared to healthy peripheral tissue sites [35–37]). An overview of the procedures performed per group is shown in Fig. 1.

(i) Pharmacokinetic arm. Each animal in this arm ($n = 5$) received an i.v. bolus (200 μ l) of LAmB at a dose level of 25 mg/kg. Twenty-four hours later, animals were sacrificed, and skin samples (from lesion and healthy control site) were collected. The skin samples were homogenized and AmB levels in tissues measured as previously described (21, 33). Briefly, skin tissues were ground mechanically with zirconium oxide beads in 1 ml of PBS. The drug (AmB) was then extracted from tissue homogenates with 84:16 methanol-dimethyl sulfoxide (methanol-DMSO), followed by liquid chromatography-tandem mass spectrometry (LC-MS/MS) quantification. When the expression "AmB levels" or "AmB concentrations" is used in this work without further clarification, it refers to total (liposomal + protein-bound + free) amount of AmB per gram of tissue. Pharmidex Pharmaceutical Services Ltd. performed LC-MS/MS analysis of the samples. The lower limit of quantification was 1 ng/ml.

(ii) Skin pathophysiology arm. Each animal in this arm ($n = 5$) received an intravenous bolus (200 μ l) of 0.5% Evans blue (Sigma, UK). Lesion size (average of width and length in millimeters) was measured with digital calipers. Thirty minutes later, animals were sacrificed, and skin samples (from the lesion and the healthy control site) were collected. These samples were cut into three equal parts, weighed, and used for the evaluations described below.

Capillary leakiness. The first skin fragment was used to evaluate blood vessel leakiness with the Evans blue assay. Evans blue is a blue dye which is, under normal physiological conditions, predominantly restricted to the bloodstream because of high plasma protein binding. However, the protein-dye complex can extravasate at sites of increased vessel leakiness, as is the case in local inflammation. Hence, the amount of Evans blue per gram of tissue is a marker for local vascular permeability (35–37). To extract Evans blue from the skin, tissue sections were placed in 500 μ l formamide in Eppendorf tubes and incubated in a 55°C water bath. After 24 h, tubes were centrifuged for 10 min at 15,000 rpm and 4°C, and supernatants were collected. Absorbance (maximum, 620 nm; minimum, 740 nm) was determined with a SpectraMax M3 plate reader (Molecular Devices, UK). Samples, blanks (formamide), and calibration standards (1:2 serial dilution of 100 μ g/ml Evans blue in formamide) were measured in 96-well plates (200 μ l volumes). After correction against the blank, the amount of Evans blue in samples was expressed per gram of skin tissue.

Parasite load. The second skin tissue fragment was used to evaluate *L. major* and *L. mexicana* parasite loads with DNA-based quantitative PCR, as described previously (40). In brief, skin tissue was homogenized and DNA extracted with a Qiagen DNeasy blood and tissue kit. Two-microliter DNA extract samples (1/100 diluted) were amplified in 10- μ l reaction mixtures in the presence of 5 μ l SensiFAST SYBR

NO-ROX master mix, 0.25 μM probe, and 0.4 μM primers. Triplicates of standards (10^8 to 10^2) and duplicates of unknown samples were included. The tubes were placed in a 72-sample rotor of the Rotor-Gene 3000, set at 40 cycles at a denaturation setting of 95°C for 5 min, followed by a 2-step amplification cycle of 95°C for 10 s and 60°C for 30 s. The lower limit of quantification was 100 parasites per 2 μl .

Skin histomorphometry. The third and final skin fragment was fixed in formalin for 24 h, dehydrated in ethanol, cleared in xylene, and embedded in paraffin. Skin samples were stained with hematoxylin and eosin (H&E) or antibodies against the macrophage/microglia-specific protein iba-1 (anti-Iba-1). All histological procedures were performed at the Institute of Neurology (UCL, London, UK), and blind analysis using the same analyst was conducted at LSHTM. A Leica ST5020 Autostainer was used for H&E staining, according to the standard National Health Service (NHS) diagnostic protocol. Randomly selected images covering skin regions were acquired with a camera (Leica DFC295) attached to a Leica DM3000 light-emitting diode (LED) microscope. Images were digitalized for histomorphometric analysis using the Leica Application Suite V4.5 software. An index of inflammatory cells was assessed by quantifying a standardized test area of 166,970.7 μm^2 per image acquired, with a $\times 20$ objective. The number of cells per image was determined from the average of 6 images/animal, randomly chosen, at $\times 200$ magnification, stained with H&E. An increase in the number of cells compared with uninfected controls was considered indicative of inflammation. Immunohistochemistry reaction for macrophage presence was performed using the Ventana Discovery XT using the Ventana DAB map detection kit. Tissues were pretreated for 40 min with EDTA buffer, incubated for 4 h with the primary antibody (anti-Iba-1, 1/250 dilution; Wako Laboratory Chemicals, Germany), and treated with swine anti-rabbit Dako E0353 antibody for 1 h (manufacturer's protocol). The polyclonal antibodies in the anti-Iba-1 stain label the calcium-binding protein Iba-1, specific to microglia (central nervous system) and macrophages (skin and other tissues). An index of macrophage was assessed by quantifying a standardized test area of 166,970.7 μm^2 per image, acquired with a $\times 20$ objective. The area in brown was determined from an average of 6 randomly chosen images/animal, at $\times 200$ magnification. Increased stained area compared with uninfected controls was considered indicative of macrophage infiltration.

Efficacy of LAmB against *L. major* and *L. mexicana*. Uninfected or *Leishmania*-infected BALB/c mice with nodular CL lesions (10 and 30 days postinoculation for *L. major* and *L. mexicana*, respectively) received five doses (200 μl , i.v.) of either 5% dextrose (untreated control) or LAmB at 25 mg/kg (treated) on alternate days (i.e., on days 0, 2, 4, 6, and 8). During treatment, lesion size was monitored daily. On day 10, animals were sacrificed, lesion samples were collected, and parasite load and AmB drug levels in these tissues were quantified (see above).

Statistical analysis. For the PK and pathophysiology experiments, intralésional AmB accumulation, lesion size, parasite load, capillary leakiness, cell number, and macrophage abundance were compared in infected and uninfected skin of the same mice using a 2-way analysis of variance (ANOVA), followed by a Šidák multiple-comparison test. For the efficacy experiment, ANOVA (1-way for parasite load and intralésional AmB levels, 2-way repeated measures for lesion size) followed by Tukey's multiple-comparison test were used. Data are presented as mean and standard error of the mean (SEM). A *P* value of <0.05 was considered statistically significant. All analyses were performed with GraphPad Prism version 7.02.

SUPPLEMENTAL MATERIAL

Supplemental material for this article may be found at <https://doi.org/10.1128/AAC.00631-18>.

SUPPLEMENTAL FILE 1, PDF file, 0.2 MB.

ACKNOWLEDGMENTS

Gert-Jan Wijnant's doctoral project is part of the EuroLeish.Net Training Network (www.euroleish.net). This work was supported by the European Horizon's 2020 Research and Innovation Programme under the Marie Skłodowska-Curie grant agreement number 642609.

REFERENCES

- Okwor I, Uzonna J. 2016. Social and economic burden of human leishmaniasis. *Am J Trop Med Hyg* 94:489–493. <https://doi.org/10.4269/ajtmh.15-0408>.
- Alvar J, Vélez ID, Bern C, Herrero M, Desjeux P, Cano J, Jannin J, den Boer M, WHO Leishmaniasis Control Team. 2012. Leishmaniasis worldwide and global estimates of its incidence. *PLoS One* 7:e35671. <https://doi.org/10.1371/journal.pone.0035671>.
- Scorza BM, Carvalho EM, Wilson ME. 2017. Cutaneous manifestations of human and murine leishmaniasis. *Int J Mol Sci* 18:E1296. <https://doi.org/10.3390/ijms18061296>.
- Scott P, Novais FO. 2016. Cutaneous leishmaniasis: immune responses in protection and pathogenesis. *Nat Rev Immunol* 16:581–592. <https://doi.org/10.1038/nri.2016.72>.
- Cangussú SD, Souza CC, Campos CF, Vieira LQ, Afonso LCC, Arantes RME. 2009. Histopathology of *Leishmania major* infection: revisiting *L. major* histopathology in the ear dermis infection model. *Mem Inst Oswaldo Cruz* 104:918–922.
- Corware K, Harris D, Teo I, Rogers M, Naresh K, Müller I, Shaunak S. 2011. Accelerated healing of cutaneous leishmaniasis in non-healing BALB/c mice using water soluble amphotericin B-polymethacrylic acid. *Biomaterials* 32:8029–8039. <https://doi.org/10.1016/j.biomaterials.2011.07.021>.
- Gaafar A, el Kadar AY, Theander TG, Permin H, Ismail A, Kharazmi A, el

- Hassan AM. 1995. The pathology of cutaneous leishmaniasis due to *Leishmania major* in Sudan. *Am J Trop Med Hyg* 52:438–442. <https://doi.org/10.4269/ajtmh.1995.52.438>.
8. Andrade ZA, Reed SG, Roters SB, Sadigursky M. 1984. Immunopathology of experimental cutaneous leishmaniasis. *Am J Pathol* 114:137–148.
 9. Kaye PM, Beattie L. 2016. Lessons from other diseases: granulomatous inflammation in leishmaniasis. *Semin Immunopathol* 38:249–260. <https://doi.org/10.1007/s00281-015-0548-7>.
 10. Nylén S, Eidsmo L. 2012. Tissue damage and immunity in cutaneous leishmaniasis. *Parasite Immunol* 34:551–561. <https://doi.org/10.1111/pim.12007>.
 11. Mehregan DR, Mehregan AH, Mehregan DA. 1999. Histologic diagnosis of cutaneous leishmaniasis. *Clin Dermatol* 17:297–304. [https://doi.org/10.1016/S0738-081X\(99\)00048-6](https://doi.org/10.1016/S0738-081X(99)00048-6).
 12. Bari AU. 2012. Clinical spectrum of cutaneous leishmaniasis: an overview from Pakistan. *Dermatol Online J* 18:4.
 13. Abuzaid AA, Abdoon AM, Aldahan MA, Alzahrani AG, Alhakeem RF, Asiri AM, Alzahrani MH, Memish ZA. 2017. Cutaneous leishmaniasis in Saudi Arabia: a comprehensive overview. *Vector Borne Zoonotic Dis* 17:673–684. <https://doi.org/10.1089/vbz.2017.2119>.
 14. Blaylock JM, Wortmann GW. 2012. A case report and literature review of “Chiclero’s ulcer”. *Travel Med Infect Dis* 10:275–278. <https://doi.org/10.1016/j.tmaid.2012.08.005>.
 15. Calvopiña M, Martínez L, Hashiguchi Y. 2013. Cutaneous leishmaniasis “chiclero’s ulcer” in subtropical Ecuador. *Am J Trop Med Hyg* 89:195–196. <https://doi.org/10.4269/ajtmh.12-0690>.
 16. Hodiamont CJ, Kager PA, Bart A, de Vries HJC, van Thiel PPAM, Leenstra T, de Vries PJ, van Vugt M, Grobusch MP, van Gool T. 2014. Species-directed therapy for leishmaniasis in returning travellers: a comprehensive guide. *PLoS Negl Trop Dis* 8:e2832. <https://doi.org/10.1371/journal.pntd.0002832>.
 17. Balasegaram M, Ritmeijer K, Lima MA, Burza S, Ortiz Genovese G, Milani B, Gaspani S, Potet J, Chappuis F. 2012. Liposomal amphotericin B as a treatment for human leishmaniasis. *Expert Opin Emerg Drugs* 17:493–510. <https://doi.org/10.1517/14728214.2012.748036>.
 18. Wortmann G, Zapor M, Ressler R, Fraser S, Hartzell J, Pierson J, Weintrob A, Magill A. 2010. Liposomal amphotericin B for treatment of cutaneous leishmaniasis. *Am J Trop Med Hyg* 83:1028–1033. <https://doi.org/10.4269/ajtmh.2010.10-0171>.
 19. Aronson N, Herwaldt BL, Libman M, Pearson R, Lopez-Velez R, Weina P, Carvalho E, Ephros M, Jeronimo S, Magill A. 2017. Diagnosis and treatment of leishmaniasis: clinical practice guidelines by the Infectious Diseases Society of America (IDSA) and the American Society of Tropical Medicine and Hygiene (ASTMH). *Am J Trop Med Hyg* 96:24–45. <https://doi.org/10.4269/ajtmh.16-84256>.
 20. Guery R, Henry B, Martin-Blondel G, Rouzaud C, Cordoliani F, Harms G, Gangneux J-P, Foulet F, Bourrat E, Baccard M, Morizot G, Consigny P-H, Berry A, Blum J, Lortholary O, Buffet P, French Cutaneous Leishmaniasis Study Group, the LeishMan Network. 2017. Liposomal amphotericin B in travelers with cutaneous and muco-cutaneous leishmaniasis: not a panacea. *PLoS Negl Trop Dis* 11:e0006094. <https://doi.org/10.1371/journal.pntd.0006094>.
 21. Wijnant G-J, Van Bocxlaer K, Yardley V, Harris A, Murdan S, Croft SL. 2018. Relation between skin pharmacokinetics and efficacy in ambisome treatment of murine cutaneous leishmaniasis. *Antimicrob Agents Chemother* 62:e02009-17. <https://doi.org/10.1128/AAC.02009-17>.
 22. Felton T, Troke PF, Hope WW. 2014. Tissue penetration of antifungal agents. *Clin Microbiol Rev* 27:68–88. <https://doi.org/10.1128/CMR.00046-13>.
 23. Ternant D, Ducourau E, Perdriger A, Corondan A, Le Goff B, Devauchelle-Pensec V, Solau-Gervais E, Watier H, Goupille P, Paintaud G, Mulleman D. 2014. Relationship between inflammation and infliximab pharmacokinetics in rheumatoid arthritis. *Br J Clin Pharmacol* 78:118–128. <https://doi.org/10.1111/bcp.12313>.
 24. Slaviero KA, Clarke SJ, Rivory LP. 2003. Inflammatory response: an unrecognized source of variability in the pharmacokinetics and pharmacodynamics of cancer chemotherapy. *Lancet Oncol* 4:224–232. [https://doi.org/10.1016/S1470-2045\(03\)01034-9](https://doi.org/10.1016/S1470-2045(03)01034-9).
 25. Wu NZ, Da D, Rudolf TL, Needham D, Whorton AR, Dewhirst MW. 1993. Increased microvascular permeability contributes to preferential accumulation of stealth liposomes in tumor tissue. *Cancer Res* 53:3765–3770.
 26. Poh S, Chelvam V, Low PS. 2015. Comparison of nanoparticle penetration into solid tumors and sites of inflammation: studies using targeted and nontargeted liposomes. *Nanomedicine (Lond)* 10:1439–1449. <https://doi.org/10.2217/nnm.14.237>.
 27. Blot SI, Pea F, Lipman J. 2014. The effect of pathophysiology on pharmacokinetics in the critically ill patient—concepts appraised by the example of antimicrobial agents. *Adv Drug Deliv Rev* 77:3–11. <https://doi.org/10.1016/j.addr.2014.07.006>.
 28. Sykes EA, Dai Q, Tsoi KM, Hwang DM, Chan WCW. 2014. Nanoparticle exposure in animals can be visualized in the skin and analyzed via skin biopsy. *Nat Commun* 5:3796. <https://doi.org/10.1038/ncomms4796>.
 29. Mehta RT, McQueen TJ, Keyhani A, López-Berestein G. 1994. Phagocyte transport as mechanism for enhanced therapeutic activity of liposomal amphotericin B. *Chemotherapy* 40:256–264. <https://doi.org/10.1159/000239202>.
 30. Girard AE, Cimochowski CR, Faiella JA. 1996. Correlation of increased azithromycin concentrations with phagocyte infiltration into sites of localized infection. *J Antimicrob Chemother* 37(Suppl C):9–19.
 31. Drusano GL. 2005. Infection site concentrations: their therapeutic importance and the macrolide and macrolide-like class of antibiotics. *Pharmacotherapy* 25:150S–158S. <https://doi.org/10.1592/phco.2005.25.12part2.150S>.
 32. Kelly C, Jefferies C, Cryan S-A. 2011. Targeted liposomal drug delivery to monocytes and macrophages. *J Drug Deliv* 2011:727241. <https://doi.org/10.1155/2011/727241>.
 33. Voak AA, Harris A, Kaiser Z, Croft SL, Seifert K. 2017. Pharmacodynamics and biodistribution of single-dose liposomal amphotericin B at different stages of experimental visceral leishmaniasis. *Antimicrob Agents Chemother* 61:e00497-17. <https://doi.org/10.1128/AAC.00497-17>.
 34. Lasic DD, Papahadjopoulos D. 1995. Liposomes revisited. *Science* 267:1275–1276. <https://doi.org/10.1126/science.7871422>.
 35. Radu M, Chernoff J. 2013. An *in vivo* assay to test blood vessel permeability. *J Vis Exp* e50062.
 36. Nidavani RB, Am M, Shalawadi M. 2014. Vascular permeability and Evans blue dye: a physiological and pharmacological approach. *J Appl Pharm Sci* 4:106–113.
 37. Martin Y, Avendaño C, Piedras MJ, Krzyzanowska A. 2010. Evaluation of Evans blue extravasation as a measure of peripheral inflammation. *Protoc Exch* <https://doi.org/10.1038/protex.2010.209>.
 38. Fehrenbacher JC, Vasko MR, Duarte DB. 2012. Models of inflammation: carrageenan- or complete Freund’s adjuvant-induced edema and hypersensitivity in the rat. *Curr Protoc Pharmacol Chapter 5:Unit5.4*. <https://doi.org/10.1002/0471141755.ph0504s56>.
 39. Morris CJ. 2003. Carrageenan-induced paw edema in the rat and mouse. *Methods Mol Biol* 225:115–121.
 40. Wijnant G-J, Van Bocxlaer K, Yardley V, Murdan S, Croft SL. 2017. Efficacy of paromomycin-chloroquine combination therapy in experimental cutaneous leishmaniasis. *Antimicrob Agents Chemother* 61:e00358-17. <https://doi.org/10.1128/AAC.00358-17>.
 41. Brajtburg J, Bolard J. 1996. Carrier effects on biological activity of amphotericin B. *Clin Microbiol Rev* 9:512–531.
 42. Lestner JM, Howard SJ, Goodwin J, Gregson L, Majithiya J, Walsh TJ, Jensen GM, Hope WW. 2010. Pharmacokinetics and pharmacodynamics of amphotericin B deoxycholate, liposomal amphotericin B, and amphotericin B lipid complex in an *in vitro* model of invasive pulmonary aspergillosis. *Antimicrob Agents Chemother* 54:3432–3441. <https://doi.org/10.1128/AAC.01586-09>.
 43. Lopez-Berestein G, Rosenblum MG, Mehta R. 1984. Altered tissue distribution of amphotericin B by liposomal encapsulation: comparison of normal mice to mice infected with *Candida albicans*. *Cancer Drug Deliv* 1:199–205. <https://doi.org/10.1089/cdd.1984.1.199>.
 44. Alexander J, Kaye PM. 1985. Immunoregulatory pathways in murine leishmaniasis: different regulatory control during *Leishmania mexicana* and *Leishmania major* infections. *Clin Exp Immunol* 61:674–682.
 45. El-On J, Lang E, Kuperman O, Avinoach I. 1989. *Leishmania major*: histopathological responses before and after topical treatment in experimental animals. *Exp Parasitol* 68:144–154. [https://doi.org/10.1016/0014-4894\(89\)90091-X](https://doi.org/10.1016/0014-4894(89)90091-X).
 46. Clay GM, Valadares DG, Graff JW, Ulland TK, Davis RE, Scorza BM, Zhanbolat BS, Chen Y, Sutterwala FS, Wilson ME. 2017. An anti-inflammatory role for NLRP10 in murine cutaneous leishmaniasis. *J Immunol* 199:2823–2833. <https://doi.org/10.4049/jimmunol.1500832>.
 47. Andrade-Narvaez FJ, Medina-Peralta S, Vargas-Gonzalez A, Canto-Lara SB, Estrada-Parra S. 2005. The histopathology of cutaneous leishmaniasis due to *Leishmania (Leishmania) mexicana* in the Yucatan peninsula,

- Mexico. *Rev Inst Med Trop Sao Paulo* 47:191–194. <https://doi.org/10.1590/S0036-46652005000400003>.
48. Dainichi T, Hanakawa S, Kabashima K. 2014. Classification of inflammatory skin diseases: a proposal based on the disorders of the three-layered defense systems, barrier, innate immunity and acquired immunity. *J Dermatol Sci* 76:81–89. <https://doi.org/10.1016/j.jdermsci.2014.08.010>.
 49. Oja CD, Semple SC, Chonn A, Cullis PR. 1996. Influence of dose on liposome clearance: critical role of blood proteins. *Biochim Biophys Acta* 1281:31–37. [https://doi.org/10.1016/0005-2736\(96\)00003-X](https://doi.org/10.1016/0005-2736(96)00003-X).
 50. Varricchi G, Granata F, Loffredo S, Genovese A, Marone G. 2015. Angiogenesis and lymphangiogenesis in inflammatory skin disorders. *J Am Acad Dermatol* 73:144–153. <https://doi.org/10.1016/j.jaad.2015.03.041>.
 51. Bekersky I, Fielding RM, Dressler DE, Lee JW, Buell DN, Walsh TJ. 2002. Pharmacokinetics, excretion, and mass balance of liposomal amphotericin B (AmBisome) and amphotericin B deoxycholate in humans. *Antimicrob Agents Chemother* 46:828–833. <https://doi.org/10.1128/AAC.46.3.828-833.2002>.
 52. Wijnant GJ, Van Bocxlaer K, Yardley V, Harris A, Alavijeh M, Silva-Pedrosa R, Antunes S, Mauricio I, Murdan S, Croft SL. 2018. Comparative efficacy, toxicity and biodistribution of the liposomal amphotericin B formulations Fungisome and AmBisome in murine cutaneous leishmaniasis. *Int J Parasitol Drug Drug Resist* 8:223–228. <https://doi.org/10.1016/j.ijpddr.2018.04.001>.
 53. Kloehn J, Saunders EC, O'Callaghan S, Dagley MJ, McConville MJ. 2015. Characterization of metabolically quiescent *Leishmania* parasites in murine lesions using heavy water labeling. *PLoS Pathog* 11:e1004683. <https://doi.org/10.1371/journal.ppat.1004683>.
 54. Mandell MA, Beverley SM. 2017. Continual renewal and replication of persistent *Leishmania major* parasites in concomitantly immune hosts. *Proc Natl Acad Sci U S A* 114:E801–E810. <https://doi.org/10.1073/pnas.1619265114>.
 55. Jara M, Berg M, Caljon G, de Muylder G, Cuypers B, Castillo D, Maes I, Orozco MDC, Vanaerschot CM, Dujardin J-C, Arevalo J. 2017. Macromolecular biosynthetic parameters and metabolic profile in different life stages of *Leishmania braziliensis*: amastigotes as a functionally less active stage. *PLoS One* 12:e0180532. <https://doi.org/10.1371/journal.pone.0180532>.
 56. Zhao M, Lepak AJ, Andes DR. 2016. Animal models in the pharmacokinetic/pharmacodynamic evaluation of antimicrobial agents. *Bioorg Med Chem* 24:6390–6400. <https://doi.org/10.1016/j.bmc.2016.11.008>.
 57. von Stebut E. 2007. Cutaneous Leishmania infection: progress in pathogenesis research and experimental therapy. *Exp Dermatol* 16:340–346. <https://doi.org/10.1111/j.1600-0625.2007.00554.x>.
 58. Mears ER, Modabber F, Don R, Johnson GE. 2015. A review: the current *in vivo* models for the discovery and utility of new anti-leishmanial drugs targeting cutaneous leishmaniasis. *PLoS Negl Trop Dis* 9:e0003889. <https://doi.org/10.1371/journal.pntd.0003889>.
 59. McCormick TS, Stevens SR, Kang K. 2000. Macrophages and cutaneous inflammation. *Nat Biotechnol* 18:25. <https://doi.org/10.1038/71879>.
 60. Pasparkis M, Haase I, Nestle FO. 2014. Mechanisms regulating skin immunity and inflammation. *Nat Rev Immunol* 14:289–301. <https://doi.org/10.1038/nri3646>.
 61. Gutiérrez V, Seabra AB, Reguera RM, Khandare J, Calderón M. 2016. New approaches from nanomedicine for treating leishmaniasis. *Chem Soc Rev* 45:152–168. <https://doi.org/10.1039/C5CS00674K>.
 62. Antonio LDF, Fagundes AT, de Oliveira RDVC, Pinto PG, Bedoya-Pacheco SJ, Vasconcellos EDCFE, Valette-Rosalino MC, Lyra MR, Passos SRL, Pimentel MIF, de Oliveira Schubach A. 2014. Montenegro skin test and age of skin lesion as predictors of treatment failure in cutaneous leishmaniasis. *Rev Inst Med Trop Sao Paulo* 56:375–380. <https://doi.org/10.1590/S0036-46652014000500002>.
 63. Machado P, Araújo C, Da Silva AT, Almeida RP, D'Oliveira A, Jr, Bittencourt A, Carvalho EM. 2002. Failure of early treatment of cutaneous leishmaniasis in preventing the development of an ulcer. *Clin Infect Dis* 34:e69–e73. <https://doi.org/10.1086/340526>.
 64. Van Bocxlaer K, Yardley V, Murdan S, Croft SL. 2016. Drug permeation and barrier damage in *Leishmania*-infected mouse skin. *J Antimicrob Chemother* 71:1578–1585. <https://doi.org/10.1093/jac/dkw012>.
 65. Van Bocxlaer K, Gaukel E, Hauser D, Park SH, Schock S, Yardley V, Randolph R, Plattner JJ, Merchant T, Croft SL, Jacobs RT, Wring SA. 2018. Topical treatment for cutaneous leishmaniasis: dermato-pharmacokinetic lead optimization of benzoxaboroles. *Antimicrob Agents Chemother* 62:e02419-17. <https://doi.org/10.1128/AAC.02419-17>.

Chapter 3.5:

PK and PK/PD-based efficacy evaluation
of the drug candidate DNDI-0690 for
the treatment of CL



3.5: PK and PK/PD-based efficacy evaluation of the drug candidate DNDI-0690 for the treatment of CL

3.5.1. Introduction

DNDI-0690 (figure 21) is a New Chemical Entity (NCE) developed by the non-profit public-private partnership Drugs for Neglected Diseases Initiative (DNDI) for the treatment of VL (132). Chemically, the compound is a 7-substituted nitroimidazooxazine belonging to the nitroimidazole class, a medically important group of nitro-based antimicrobial drugs with a broad spectrum of activity against parasites, mycobacteria, gram-positive and gram-negative bacteria. Examples of important nitro-based antibiotics are metronidazole (amoebiasis, giardiasis, trichomoniasis) nifurtimox (sleeping sickness), benznidazole (Chagas disease) and delamanid (tuberculosis). Nitroimidazoles are prodrugs: the nitro group is crucial to the antimicrobial model of action, as it is reduced to reactive radical species that react with cellular components such as proteins and DNA within the pathogen (186). Indeed, *Leishmania*-specific nitroreductases have already been shown to be responsible for bio-action of nitro-compounds (142). While nitroimidazoles were discovered in the 1950s, there has recently been a renewed interest in this drug class for the treatment of various (neglected) tropical diseases.

Originally identified in a library of potential antitubercular drugs, DNDI-0690 was nominated by DNDI in 2015 as a preclinical candidate after showing excellent *in vitro* activity against a panel of VL and CL *Leishmania* strains. In 2016, activities focussed on pharmaceutical development (synthesis, manufacture, product development). In 2017, a full preclinical toxicology and safety study package was completed. In 2018, the decision was made to conduct Phase I clinical trials in healthy volunteers to assess safety, tolerability and pharmacokinetics in microdosing studies. In terms of PK, the drug candidate has a relatively short plasma half-life (~ 7 hours) and high protein binding (~ 95%). Based on PK and PD mouse and hamster data, the predicted dose range for efficacy against human VL has been calculated between 19 and 52 mg/kg twice daily via the oral route. However, for CL, there is limited PK, PK/PD and efficacy data in animal models available. Such information is required to support further development of the drug candidate into a new oral medication for the treatment of CL (187, 188).

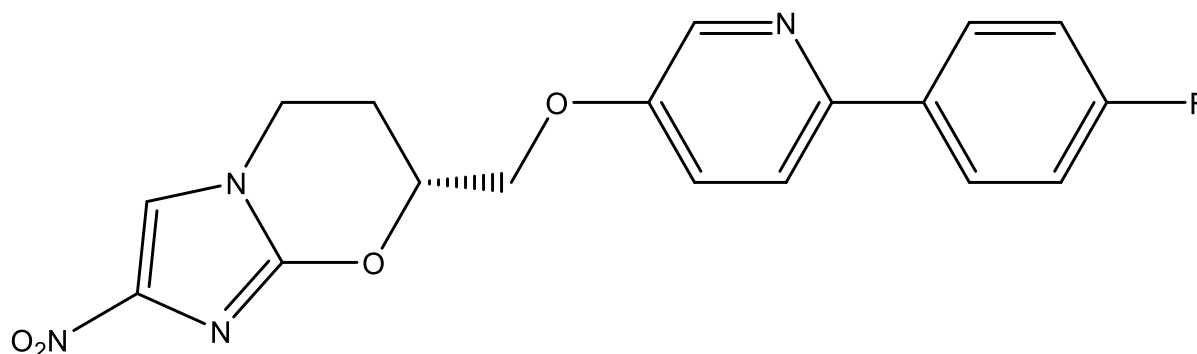


Figure 21: Chemical structure of the nitroimidazole compound DNDI-0690

3.5.2. Physicochemical properties of DNDI-0690

We estimated the physicochemical properties of DNDI-0690 using Chem3D 16.0 software (189). Figure 22 shows the predicted 3D structure of DNDI-0690.

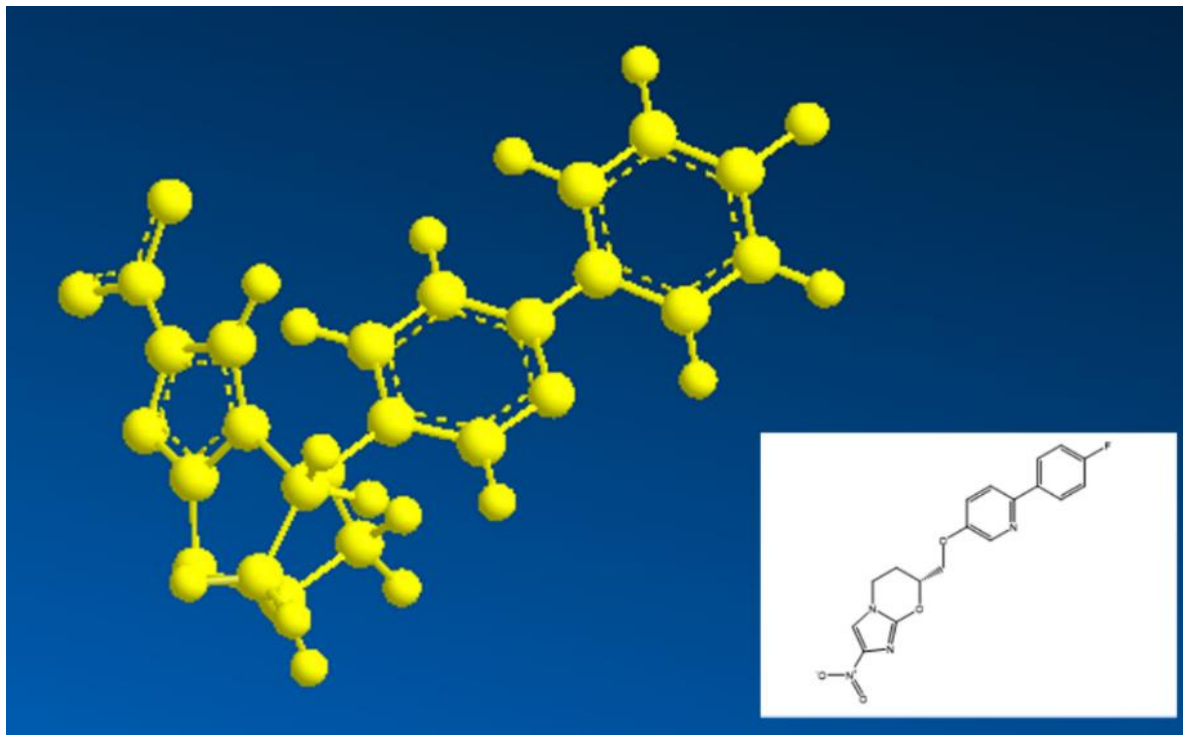


Figure 22: Predicted 3D structure of DNDI-0690 (Chem3D 16.0)

Lipinski's rule of five states that most orally active drugs in humans share particular physicochemical properties, such as low molecular weight (< 500 Da) and moderate lipophilicity while retaining a decent degree of aqueous solubility ($\log P < 5$, maximum 5 hydrogen bond donors and 10 acceptors) (190). Based on a lack of violations of the Lipinski rules (table 3), DNDI-0690 is expected to exert oral bioavailability. DNDI-0690 is a small and moderately lipophilic molecule, indicating that it is likely to pass across biological membranes, but also to have low aqueous solubility.

Table 3: Physicochemical properties of DNDI-0690

Parameter	Value	Violation of Lipinski's rule of 5?
Formula	C ₁₈ H ₁₅ FN ₄ O ₄	N/A
Molecular weight	370.11	< 500: no
LogP	3.27	< 5: no
H-bond donor	0	< 5: no
H-bond acceptor	7	< 10: no

These *in silico* predictions about DNDI-0690 are in line with experimental *in vitro* and *in vivo* results obtained earlier by DNDI: $pK_a=3.95$, $\log D_{pH=7.4}= 2.45$, aqueous solubility = 114 $\mu\text{g/ml}$ (2 $\mu\text{g/ml}$ at pH 7.4) and an oral bioavailability of 20-36 % in male rats (PEG400 suspension, p.o.).

3.5.3. *In vitro* antileishmanial activity of DNDI-0690

Table 4 shows the antileishmanial activity of DNDI-0690 against CL, as determined by microscopy using 72-hour intracellular antileishmanial assays using peritoneal mouse macrophages (data: Dr Katrien Van Bocxlaer, unpublished, reproduced with permission). The results from *in vitro* phenotypic screens show the broad-spectrum activity of DNDI-0690 against a panel of CL-causing *Leishmania* strains and species in low micromolar concentrations. Note that during *in vivo* studies, we used the *L. major* MHOM/SA/85/JISH118 strain, for which the IC₅₀ was 4.58 μ M (= 1.69 μ g/ml).

Table 4: *in vitro* antileishmanial activity of DNDI-0690 (ND: not determined)

<i>Leishmania</i> parasite		IC ₅₀ (μ M)	
Species	Strain	DNDI-0690	AmB (+ control)
<i>L. major</i>	WRAIR	0.32	0.04
<i>L. major</i>	MHOM/SA/85/JISH118	4.58	0.05
<i>L. guyanensis</i>	WRAIR	0.68	0.05
<i>L. mexicana</i>	MNYC/BZ/62/M379	1.91	0.08
<i>L. panamensis</i>	Boynton	0.77	0.07
<i>L. aethiopica</i>	Karthoum	<0.33	0.11
<i>L. tropica</i>	MHOM/AF/2015/HTD7	1.41	ND
<i>L. tropica</i>	WRAIR	1.6	0.03
<i>L. amazonensis</i>	DS Red 2	<1.11	ND

3.5.4. Dose-response of DNDI-0690 in the *L. major*-BALB/c model of CL

3.5.4.1. Aim

DNDI-0690 is a clinical candidate for VL, but much preclinical PK, PD and PK/PD data in animal models of CL to support its development as a potential new medicine for this disease is lacking. The aim of this section was to characterize the dose-response effect of DNDI-0690 in the *L. major*-BALB/c model of CL as well as to link PK and PD parameters at the end of treatment.

3.5.4.2. Materials and methods

Animal model of infection. The experimental procedures to infect female BALB/c mice with *L. major* JISH118 promastigotes were identical to those described in chapters 3.1, 3.2, 3.3 and 3.4. Twelve days after infection, when a 4-6 mm nodule had formed, treatment was started.

Drugs and treatment. DNDI-0690 was administered once daily for 10 days via oral gavage (6.25, 12.5, 25 or 50 mg/kg suspension in polyethyleneglycol 400, PEG400). A head-to-head comparison with systemic paromomycin sulfate (PM, Sigma, UK), a positive control drug for

antileishmanial efficacy in this model (see chapters 3.1., 3.3. and 3.4.), was included at identical doses. However, because of the known poor oral bioavailability of PM (191), the systemic control was administered via the intraperitoneal rather than the oral route (as a solution in PBS). Drug solutions were made up fresh every day due to the unknown chemical stability of DNDI-0690 and PM in their respective vehicles.

Lesion size. Lesion size during treatment was determined daily (average of length and width), as measured with digital callipers.

Parasite load in the lesion. At the end of treatment (24 hours after administering the 10th and final dose), parasite load and DNDI-0690 drug levels were measured in lesion skin. The skin homogenization, *Leishmania* DNA extraction and qPCR method to quantify parasite burden in the lesion was as described in chapter 3.2, with the exception that parasite DNA extracts were not diluted 1/100 but used directly.

DNDI-0690 extraction. Skin tissue was weighed and cut into fine, long pieces and placed into SureLock microcentrifuge tubes (StarLab, UK) together with 1 spatula (about 100 mg) of 2 mm zirconium oxide beads (Next Advance, UK) and 1 ml phosphate buffered saline (PBS, Sigma, UK). Samples were ground using a Bullet Blender Storm 24 (NextAdvance, UK) set at speed 12 for 20 minutes to obtain a smoothly flowing homogenate and stored at -80 °C until further use. Drug extraction and protein precipitation were performed in 96-well plates: homogenate (50 µl) was added to 200 µl acetonitrile (HPLC grade, Fisher Chemical, UK) containing 200 ng/ml tolbutamide as internal standard (analytical standard, Sigma, UK). Plates were shaken for 20 minutes at 900 rpm and centrifuged for 15 minutes at 13000 rpm at 4 °C. Sixty µl supernatant was collected and 60 µl HPLC-grade water was added. The mixture was stored at -80 °C until analysis. Blanks with and without internal standard tolbutamide were included, as were calibration samples with known concentrations of DNDI-0690 (similarly extracted and prepared after spiking 45 µl blank skin homogenate (derived from untreated BALB/c mice) with 5 µl working solutions of known DNDI-0690 concentrations in 1:1 acetonitrile:water (Sigma, UK).

DNDI-0690 LC-MS/MS quantification. All samples were analyzed using a Shimadzu Nexera X2 UHPLC/Shimadzu LCMS 860 at Pharmidex Pharmaceutical Services Ltd. A mobile phase (0.4 ml/min) of water-0.1%formic (channel A) and acetonitrile-0.1%formic acid (channel B) was used to elute sample compound from a Kinetex column packed with 5-µm XB-C₁₈ material column (2.1 mm by 50 mm at 50 °C; Phenomenex, UK). The mobile phase composition was initially 2% B, programmed to increase linearly to 95% B at 1.1 minutes after injection. After 0.7 minutes at 90 % B, the composition was returned to its initial 2% B at 1.8 minutes post-injection. DNDI-0690 was detected by monitoring transition of the parent molecule (m/z 370) to the fragment resulting from electrospray ionization (m/z 198.2). Analyte concentration was quantified against calibration standards prepared in matched control matrix, with aliquots of samples and standards being injected at 5 µl. The limit of quantification was 2 ng/ml.

Statistical analysis. Analysis of variance (ANOVA) assuming Gaussian distribution (one-way for parasite load, repeated measures for lesion size) followed by Tukey's multiple comparison tests was used to analyze differences between groups. All data are presented as means and

standard error of the mean (SEM). A p-value < 0.05 was considered statistically significant. All analyses were performed using GraphPad Prism version 7.02.

Dose-response curves. Non-linear fit models (log(agonist) versus normalized response with variable slope) in GraphPad Prism version 7.02 were used to calculate ED₅₀ and ED₉₀ data. The response in treated groups was expressed as a relative reduction compared to untreated controls ((signal untreated – signal treated)/signal untreated *100 %).

3.5.4.3. Results and discussion

Figure 23 shows the dose-response effect of oral DNDI-0690 in comparison to the positive control drug PM (IP) at equivalent dose levels ranging from 6.25 to 50 mg/kg.

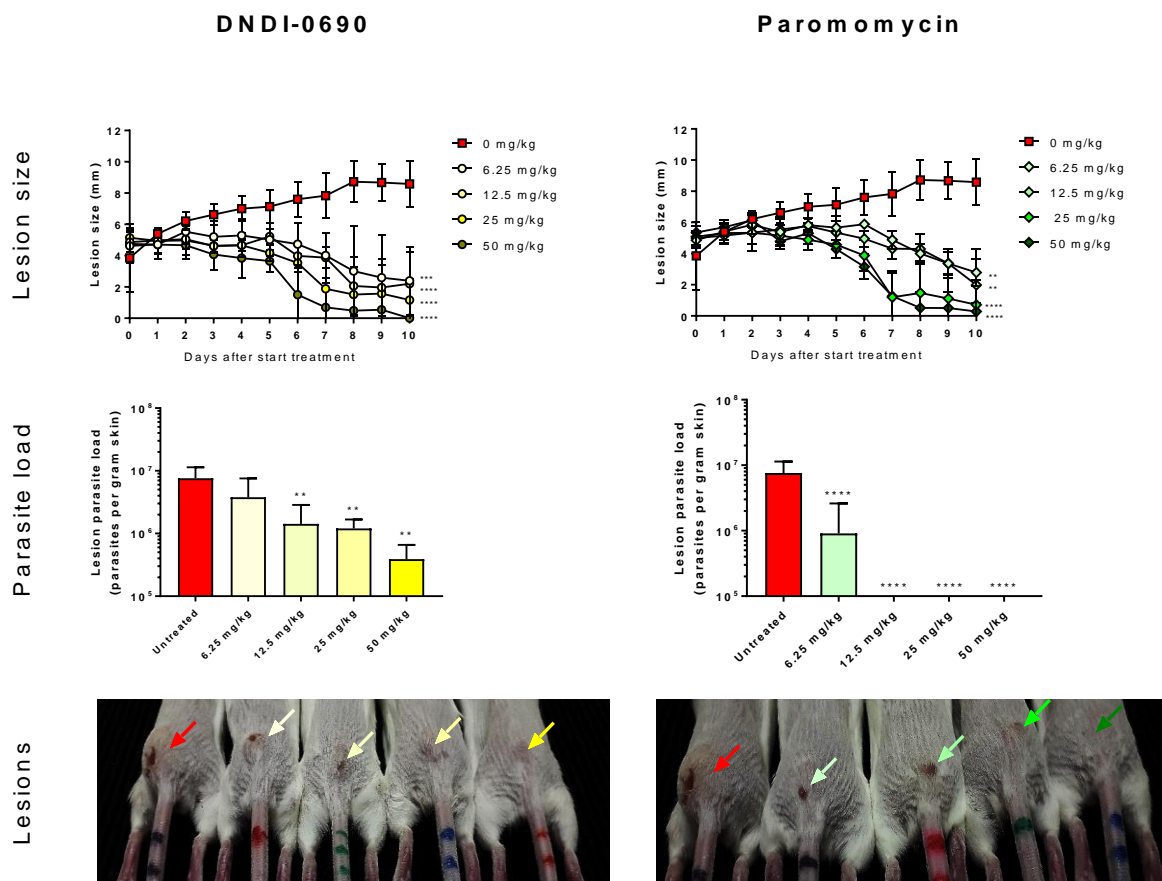


Figure 23: Dose-response effect of oral DNDI-0690 (left) and positive control drug intraperitoneal paromomycin (right) in the *L. major*–BALB/c model of CL. ** = p<0.01, * = p<0.005, **** p <0.001 in comparison to untreated control.**

Over the course of daily treatment for 10 days, both DNDI-0690 and PM caused a significant ($p < 0.01$) reduction in lesion size in comparison to the untreated control (PEG400). By day 10, both the 10 x 50 mg/kg oral DNDI-0690 and 10 x 50 mg/kg intraperitoneal PM dose regimens completely healed the lesion, as the size of the nodules was no longer measurable and only a faint scar remained (figure 19, photos). Significant reductions in parasite burden compared to the oral PEG400 vehicle alone ($p < 0.01$) were observed for DNDI-0690 for doses above and including 12.5 mg/kg. However, the therapeutic efficacy of oral DNDI-0690 was inferior compared to intraperitoneal PM, as parasite load for PM at doses from 12.5 mg/kg were below the limit of quantification of 10^2 parasites per 2 μ l sample.

Table 5 shows the ED₅₀ and ED₉₀ values for lesion size and parasite load that was calculated based on the results of the dose-response study (figure 23) for oral DNDI-0690 and the control drug intraperitoneal PM.

Table 5: Comparative 50 % and 90 % effective doses (lesion size, parasite load) for oral DNDI-0690 and the positive control drug intraperitoneal PM (means).

Drug	Lesion size		Parasite load	
	ED ₅₀	ED ₉₀	ED ₅₀	ED ₉₀
DNDI-0690 (p.o.)	4.5 mg/kg	18.7 mg/kg	4.7 mg/kg	17.9 mg/kg
PM (IP)	6.2 mg/kg	22.8 mg/kg	5.9 mg/kg	6.3 mg/kg

These values indicate that efficacy of DNDI-0690 (p.o.) in comparison to the positive control drug PM (IP) is comparable in terms of reduction in lesion size but inferior in terms of reduction in parasite load. Because no signs of toxicity or fatalities were observed at any tested dose level, no therapeutic index could be calculated.

Finally, drug concentrations within the lesions of DNDI-0690 treated mice at the end of ten-day oral treatment were determined (figure 24).

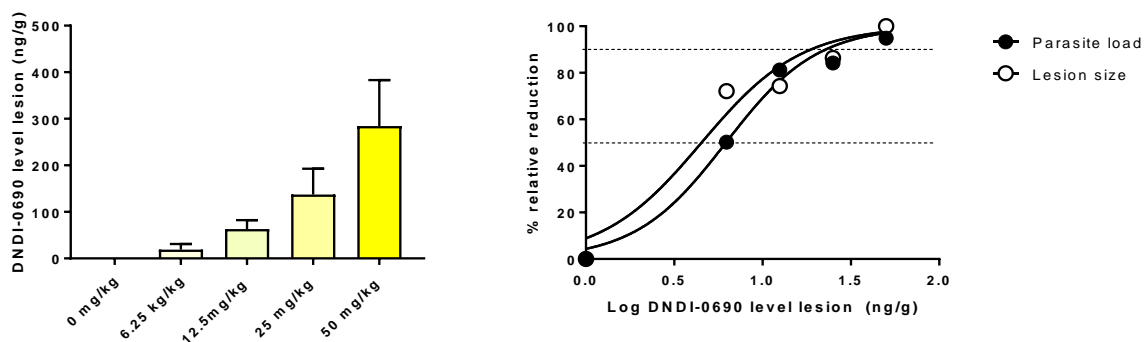


Figure 24: DNDI-0690 levels in the skin lesion (ng/g, 24 hours after 10 doses once daily) in relation to (i) dose level (left) and (ii) relative reduction in parasite load and lesion size compared to the untreated control (right).

A positive correlation ($R^2=0.99$) between dose level and DNDI-0690 levels in the infected skin was found (figure 24, left). Importantly, comparing the effects of different doses of DNDI-0690, elevated drug concentrations in the lesions were associated with superior therapeutic efficacy (figure 24, right).

In conclusion, the nitroimidazole DNDI-0690 is highly efficacious in the rigorous non-cure *L. major* BALB/c model of CL when administered daily for 10 days via the oral route. Doses around 5 mg/kg and 21 mg/kg showed 50% and 90% efficacy, respectively; 50 mg/kg knocks down parasite load by 95% and lesion size by 100% compared to the untreated control. There is a clear relationship between dose, intralésional drug levels (PK) and therapeutic response (PD). These findings justify a further preclinical investigation into DNDI-0690 as a potential oral treatment for CL.

We then aimed to fully characterize the skin PK profile of the compound, to provide a basis for PK/PD modelling and prediction of safe, efficacious doses in humans. In the previous chapters, we used a skin homogenate approach to this end. This requires a high number of animals and measures total drug levels in all layers of the harvested lesion (epidermis, dermis, subcutaneous tissue, muscle) rather than only the pharmacologically active concentrations, i.e. the extracellular, unbound concentration of DNDI-0690 in the dermal interstitial fluid surrounding the parasitized macrophages. To overcome this issue, we optimized another technique to study drug distribution in animal models of CL, called skin microdialysis.

3.5.5. Skin microdialysis of DNDI-0690

3.5.5.1. An introduction to skin microdialysis

Microdialysis (MD) is a technique for sampling substances in the extracellular fluid in living tissue. The principle of MD was originally developed back in the 1960s in the field of neuroscience to study the biochemistry of the rodent brain. However, since the 1990s, it has been successfully applied for the sampling of substances (drugs, inflammatory mediators and endogenous molecules) in virtually any animal or human tissue, including muscle, heart, lung, brain, bone, adipose tissue, neoplastic tissue, blood and skin. Skin microdialysis (SMD) has been used to study topical drug penetration, PK/PD and/or tissue drug distribution for antibiotics, analgesics, antihistamines, non-steroidal anti-inflammatory drugs and local anaesthetics. Inflammatory mediators have been measured with SMD in the skin of healthy volunteers and patients with atopic dermatitis, burn injuries, psoriasis, cold urticarial, complex regional pain syndrome and cutaneous mastocytosis (191).

For CL, the potential of SMD has not yet been explored, in neither animals nor humans. A particular advantage of SMD for CL relates to the fact that it can specifically measure the unbound, pharmacologically active drug concentration, directly in the interstitial space fluid of the dermis, the site that surrounds the *Leishmania*-infected macrophages. Moreover, SMD provides continuous, real-time monitoring of processes in the dermis, circumventing the need for invasive sampling at each desired time point as is the case for traditional methods such as skin blisters, skin stripping or skin biopsies (or necropsies in animals). In addition, these approaches have the disadvantage of measuring total drug tissue levels, which can be misleading because only the free concentration is available to exert antileishmanial activity (168, 169). Table 6 summarizes the differences between the skin homogenate approach used in earlier chapters and this innovative technique (for CL).

Table 6: Comparison between skin homogenate and skin microdialysis to measure drug concentrations in animal models of CL

	Skin homogenate	Skin microdialysis
Procedure	End-point, invasive: <ul style="list-style-type: none"> • 1 animal = 1 time point • Variability between time points (different animals) 	Continuous, minimally invasive: <ul style="list-style-type: none"> • 1 animal = multiple time points • Less variability between time points (same animal)
Measures	<ul style="list-style-type: none"> • Drug and metabolites • Intra- and extracellular • Protein-free and -bound 	<ul style="list-style-type: none"> • Drug and metabolites • Extracellular • Protein-free
Organ	<ul style="list-style-type: none"> • Epidermis • Dermis • Hypodermis 	<ul style="list-style-type: none"> • Dermis
Limitations	<ul style="list-style-type: none"> • High number of animals • Pharmacologically inactive fraction is also measured 	<ul style="list-style-type: none"> • Not suitable for highly lipophilic or highly protein-bound drugs • Need for specialized equipment and technical skills

The basic principle of SMD (figure 25) consists of implanting a small probe in the upper dermis that is perfused with a physiological buffer, mimicking a small blood vessel in the tissue. The probe is essentially a hollow, semi-permeable membrane for dialysis: only molecules with a size smaller than the pores of the membrane (pore cut-off) can permeate into the dialysate. A tubing system connects the skin microdialysis probe to a perfusion inlet (syringe pump with a physiological solution) and a dialysis outlet (collector system). When the probe is perfused at a slow rate (0.5-10 $\mu\text{l}/\text{min}$), substances in the dermal interstitial fluid can passively diffuse across the membrane and compounds of interest can be recovered (192-194).

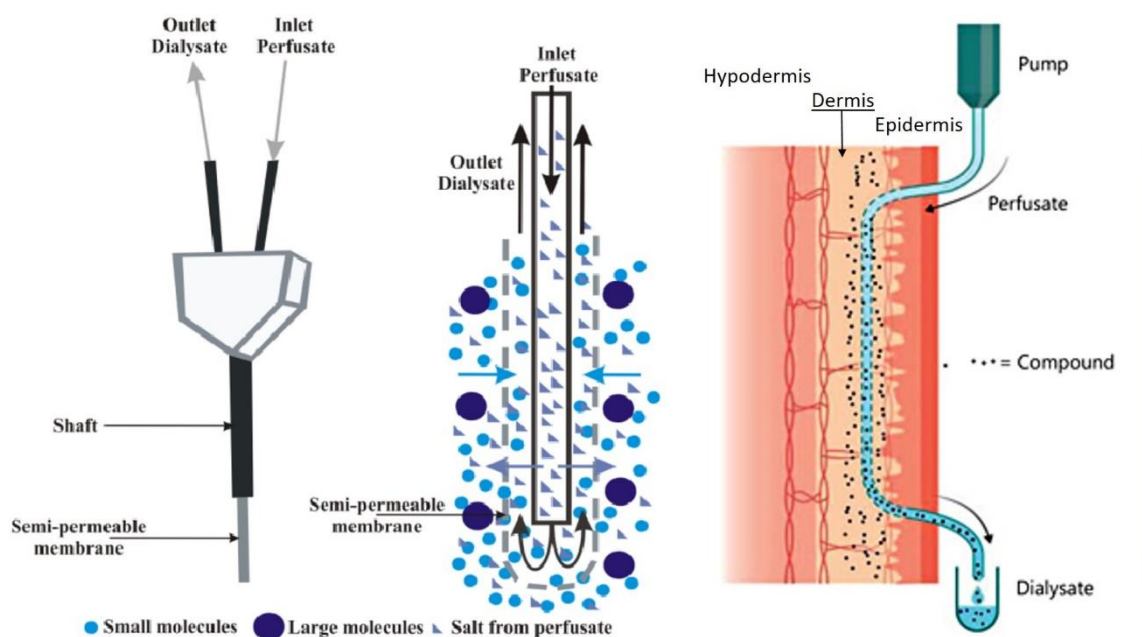


Figure 25: Principles of skin microdialysis

Here, we describe the development of an MD system for pharmacological evaluations in the *L. major* BALB/c mouse model of CL, which allows measurement of protein-free drug concentrations in the infected dermis (target site), as well as healthy control skin (control site) and plasma (systemic exposure).

3.5.5.2. Skin microdialysis: development of the system

The development of the MD for DNDI-0690 was a step-wise process:

- a) Assessing the suitability of DNDI-0690 for microdialysis
- b) Finding a method to restrain mice
- c) Testing of urethane anaesthesia on mice
- d) Inserting the microdialysis probe in skin tissue and tail vein
- e) A test run of the microdialysis system

These steps are detailed in the following pages.

a) Assessing the suitability of DNDI-0690 for microdialysis

During MD sampling, the continuous flow of physiological buffer through the probe causes incomplete equilibration between the drug concentration (C) in the dialysate and that in the medium surrounding the probe. This phenomenon depends on a number of factors related to the drug (protein-binding, molecular weight, lipophilicity), the tissue (temperature, blood flow, metabolism) and the experimental microdialysis set-up (perfusate, flow rate and cut-off size, insertion depth, material, design and length of the probe) (193, 194). Relative recovery (RR) is defined as:

$$RR_{\text{drug}} = C_{\text{drug in dialysate}} / C_{\text{drug in the medium surrounding the probe}}$$

However, not all drugs have a suitable profile for MD. Lipophilic compounds with strong protein-binding properties have not only a low drug fraction that is available to permeate across the probe membrane but also a tendency to stick to the polymeric material of the tubing. This could result in low RR and a final sampled drug concentration below the lower limit of quantification of the analytical technique of choice. DNDI-0690 is a highly protein-bound (95%), small (MW = 370 g/mol) and a relatively lipophilic (logP = 3) molecule. Before engaging in animal studies, the RR of DNDI-0690 first needed to be determined *in vitro*. After consultation with experts at the pharmaceutical company Pharmidex Pharmaceutical Services, a concentric cuprophane microdialysis probe with a 6 kDa cut-off value was purchased (MAB 1.2.4. Cu, Microbiotech, Sweden). The MAB1 series are small, fine and flexible probes designed for sampling of protein-free drugs in peripheral tissues (195).

The aim of the initial *in vitro* recovery study for DNDI-0690 was to ensure (i) reproducible, stable recovery over a nanomolar concentration range and a 4-hour time period and (ii) detectable drug levels in the sampled dialysate based on the sensitivity of the available LC-MS/MS method.

Materials and methods

Figure 26 shows the overview of the *in vitro* microdialysis set-up. A 1 ml syringe was filled with a filtered physiological buffer (artificial cerebrospinal fluid, aCSF) and mounted on the microdialysis pump (Harvard Apparatus 11 plus, UK). aCSF is the standard physiological buffer Pharmidex uses for initial RR studies. The probes were inserted in aCSF-filled vials (20 ml) containing magnetic stirrers in a 37 °C water bath (Sigma, UK), mimicking the *in vivo* environment. The system was connected via tubing (fluorinated ethylene propylene, FEP, Microbiotech Sweden) and tubing adapters (Microbiotech, Sweden) to the filled syringe on the perfusion pump and an automated refrigerated fraction collector (MAB 85, Microbiotech, Sweden) filled with HPLC vials (Thermo Fisher, UK).

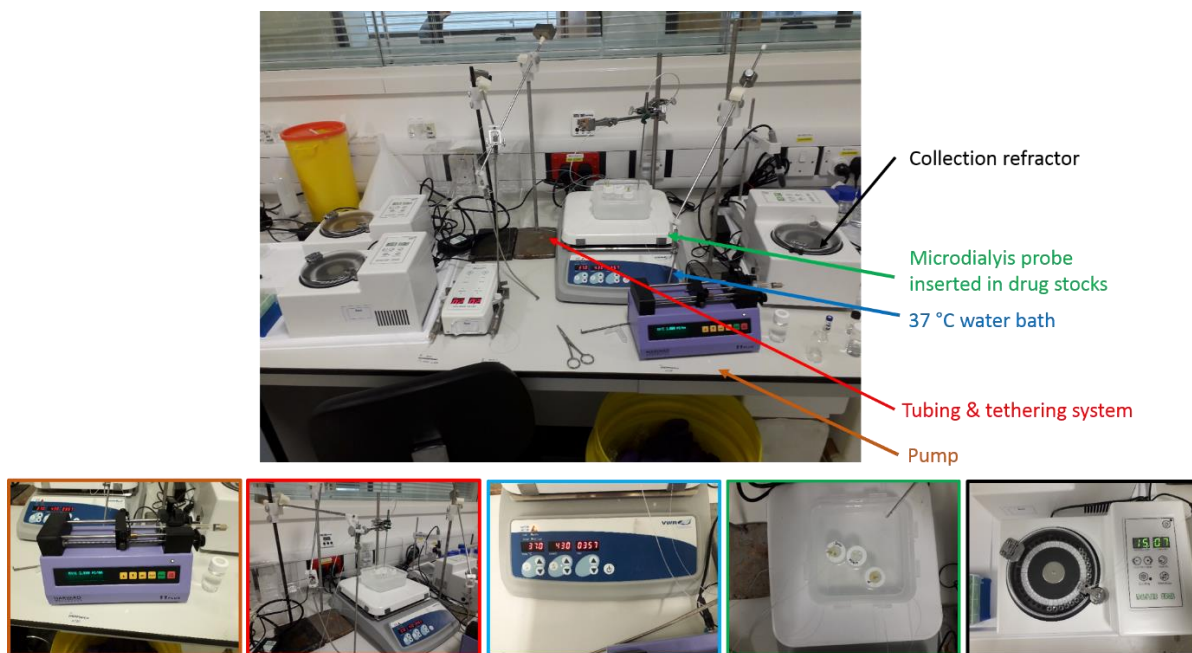


Figure 26: *In vitro* skin microdialysis set-up

Table 7 shows the phases and conditions of the experiment. The experiment was started at a flow rate of 2 $\mu\text{l}/\text{min}$ and a sample collection interval of 15 minutes. After the first 15 minutes (aCSF phase), a 10 μl volume of 100 $\mu\text{g}/\text{ml}$ stock solution of DNDI-0690 in DMSO was added to the vials to yield a final concentration of 50 ng/ml (50 ng/ml phase). After 90 minutes, the DNDI-0690 concentration in the vial was increased to 200 ng/ml by adding 30 μl of the same stock (200 ng/ml phase). Following another 90 minutes of sampling, the probes were transferred to a separate vial containing pure aCSF (wash phase).

Table 7: Overview of the phases of the *in vitro* recovery experiment

Phase	1) Equilibration	2) 50 ng/ml DNDI-0690	3) 200 ng/ml DNDI-0690	4) Wash-out
Microdialysis probe is immersed in a vial containing:	0 ng/ml DNDI-0690 (pure aCSF)	50 ng/ml DNDI-0690 in aCSF	200 ng/ml DNDI-0690 in aCSF	0 ng/ml DNDI-0690 (pure aCSF)
Duration of the phase	15 min	90 min	90 min	45 min
Time from the start of the during experiment:	0 – 15 min	15 – 105 min	105 – 195 min	195 – 240 min

Finally, 10 μl acetonitrile was added to the 30 μl samples in the HPLC vials and analyzed (no further sample preparation) using the same LC-MS/MS method used for quantification of DNDI-609 levels in skin homogenate extracts (see 3.5.4.2).

Results

Figure 27 shows the results of the *in vitro* experiment. No DNDI-0690 is detectable in the dialysate in the first 15 minutes of sampling (equilibration). When the concentration of DNDI-0690 in the vial within which the MD probe is immersed is increased to 50 ng/ml, drug levels in the dialysate rapidly elevate and remain at around 20 ng/ml throughout the 90 minutes of sampling. At a concentration of 200 ng/ml DNDI-0690 in the vial, a similar pattern is observed with dialysate levels rising to 50 ng/ml. Finally, when the probe is transferred to a vial with only pure Ringers physiological solution, DNDI-0690 concentrations in the dialysate return to the baseline levels, i.e. before the addition of drug (washout phase).

Unfortunately, the results for the 50 ng/ml and 200 ng/ml DNDI-0690 samples (taken directly from the vials during the experiment) were unexpected and invalid (50 ng/ml in vial ~ 130 ng/ml; 200 ng/ml ~ 120 ng/ml). This was likely the consequence of an experimental mistake in labelling, sampling or analysis. Hence, the exact RR for DNDI-0690 from this particular MD probe and set-up could not be calculated ($C_{\text{drug in dialysate}}$ known, but $C_{\text{drug in the medium surrounding the probe}}$ unknown). However, it was clear that there was a certainly some recovery of DNDI-0690, because the drug was detectable in dialysate and the drug concentration pattern changed throughout the study as was expected for the different phases (equilibration, 50 ng/ml, 200 ng/ml and wash).

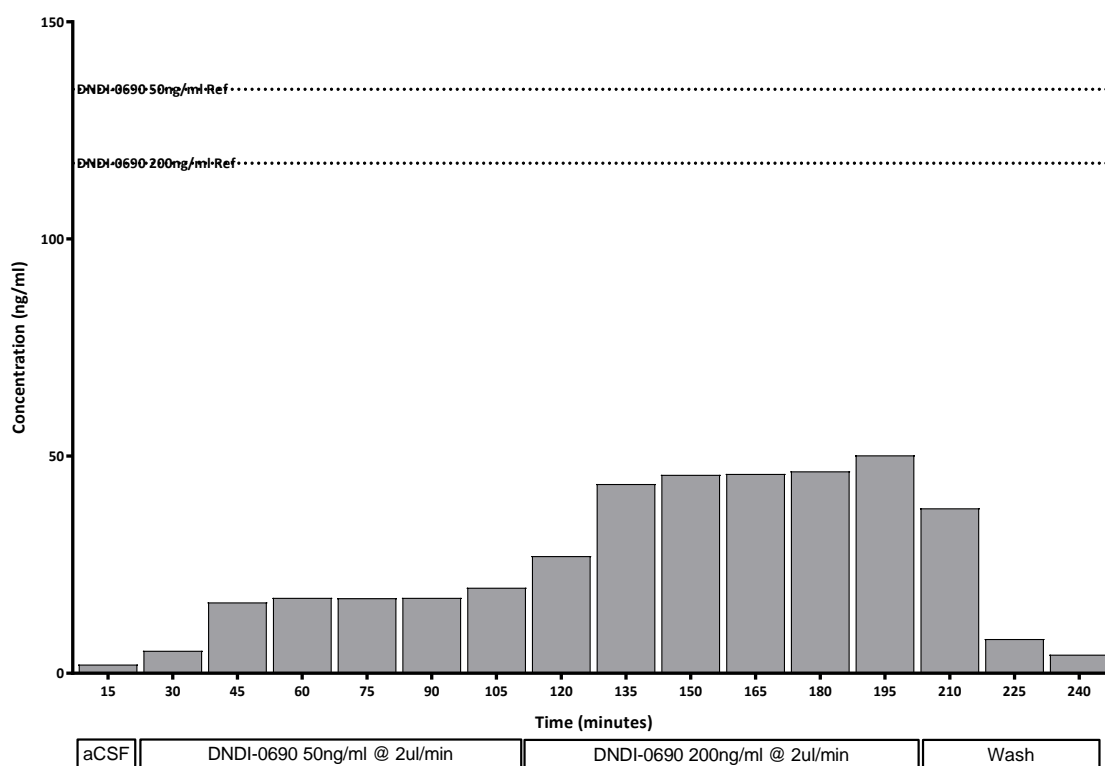


Figure 27: *In vitro* recovery of DNDI-0690.

In conclusion, the exact value of the RR of DNDI-0690 in this MD setting could not be determined. The LC-MS/MS method is sensitive enough to detect DNDI-0690 as the dialysate concentrations were above the lower limit of quantification of 2 ng/ml. A future experiment is required to determine RR, in conditions closely mimicking the *in vivo* set-up (Ringers physiological buffer, the most commonly used perfusate for skin MD studies (193, 194); vial temperature of 32 °C for skin; 37 °C for blood).

b) Finding a method to restrain mice

After confirming that DNDI-0690 is an eligible candidate for MD, the next step was to find a method to use the system in BALB/c mice. All animal experiments described in the following work were conducted under license X20014A54 according to UK Home Office regulations under the Animals (Scientific Procedures) Act 1986 and EC Directive 2010/63/E.

Under ideal conditions, the experiment would be performed in awake animals, as anaesthesia might interfere with physiology and thus PK profile of the drug candidate. At the same time, the small and fragile MD probes needed to remain undamaged and securely in place throughout sampling of drugs in skin and blood. Hence, we needed a method to fully restrain mice and prevent them from interfering with the MD set-up.

Special restraining jackets (Dermal Inserts for Rodents, Lomir Biomedical Inc, Canada) were ordered and tested as a means to immobilize the mice. However, the animals were clearly intimidated and stressed while wearing them. When the jackets were placed within the rodent cage (so the mice could get more familiar with their smell and presence), the animals started nibbling the plastic, posing a potential hazard to their health (see figure 28). Combined with concerns from the ethical and animal welfare committee about the jackets, it was decided to instead anaesthetize the mice during the MD experiments instead of physically restraining them.



Figure 28: Lomir Biomedical rodent jackets on BALB/c mice

c) Testing of urethane anaesthesia on mice

A number of anaesthetics were considered based on ease of use, duration of effect and interference with mouse cardiovascular function (as this can directly affect the PK of oral drugs). Gas isoflurane anaesthesia causes rapid induction, but could interfere with animal physiology (196) and requires regulation of gas and oxygen flow in the midst of an already complex and time-sensitive microdialysis experiment. The most common injectable anaesthetic ketamine (with or without xylazine) increases blood pressure and heart rate and typically causes only short-term hypnosis (30-60 minute), meaning repeated dosing throughout the experiment (197). A better alternative was urethane: an injectable anaesthetic providing long-term narcosis (6-10 hours) at doses of 1-2 g/kg (IP) that produces minimal effects on the cardiovascular system and thus plasma PK (198-200). Due to its carcinogenicity, it is only used for terminal anaesthesia and strict health and safety procedures are required for preparation, storage and waste disposal. While it has been used successfully in rats (198-200) and various mouse strains (201-203), no evidence of use in BALB/c mice could be found in the scientific literature. We, therefore, performed a pilot study to test the anaesthetic effects of urethane on two female BALB/c mice. After discussion with the Named Veterinary Surgeon from the Royal Veterinary College in London, it was concluded that no analgesia was needed to accompany urethane anaesthesia because the dermal probe insertion procedure is minimally invasive and animals would not be allowed to recover. In addition, we gathered advice from colleagues at UCL Ear Institute (who had experience in working with urethane) before starting the pilot study.

The aim of the study was to gather information about the (i) effects of urethane anaesthesia (induction time, narcosis period, complications), (ii) potential issues related to oral gavage under anaesthesia (needed for drug administration of DNDI-0690) and (iii) technical challenges for the placement of the MD probes in skin tissue and/or blood vessels.

Urethane (Sigma, UK) was prepared in sterile water 20 % (w/v) wearing personal protective equipment in a chemical hood and stored in the dark for one week at room temperature before use. Two female BALB/c mice with *L. major* lesions on the rump (infection method: see chapters 3.1, 3.2, 3.3. and 3.4.) administered either 1.6 or 1.9 g/kg urethane (IP) and left in a dark cage in a quiet environment. Induction of anaesthesia was successful at both doses within 10 minutes and animals were placed on a preheated hot plate (37 °C) covered in paper tissue. Rehydration solutions were administered after 1 hour and 4 hours (0.1 ml PBS, SC). Temperature (IR thermometer) and breathing (visual check of the number of breaths per 15 seconds) were measured every 30 minutes. Over the course of the experiment, mice remained anaesthetized for 8 hours, though random movements of head and paws were occasionally observed, especially when exposed to sudden visual or auditory stimulation. As seen in figure 29, the body temperature of the rump skin remained stable (32-33°C) for both urethane doses and breathing patterns were in the expected range (25-40 breaths per 15 seconds, based on advice UCL colleagues).

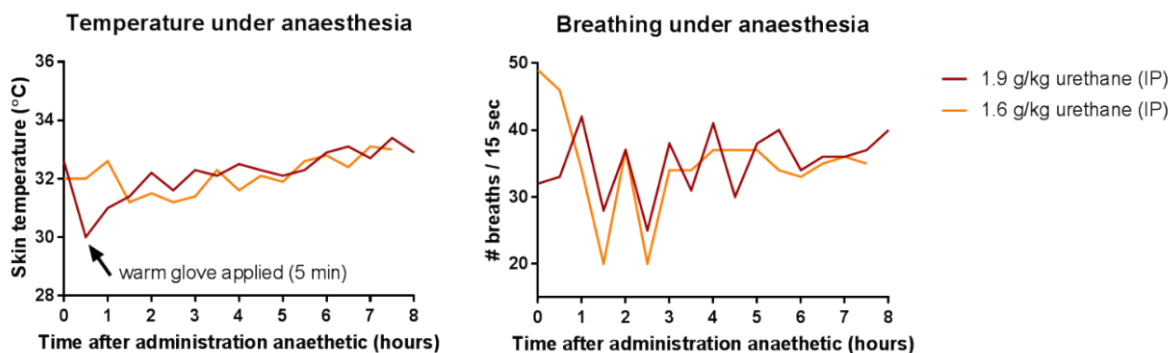


Figure 29: Clinical monitoring of temperature (left graph) and breathing patterns (right graph) of BALB/c mice under the anaesthetic effects of urethane

Finally, we administered 200 μ l of sterile water by oral gavage to the anaesthetized mice. As long as given carefully and the head of the animals was slightly raised, the limited swallowing reflexes of the animals under the effects of urethane did not seem to cause a risk of suffocation or incomplete dosing by vomiting.

In conclusion, 1 x 1.6 g/kg urethane (IP), the lowest effective dose, induces 8 hours anaesthesia in BALB/c mice without hindering oral drug administration. This anaesthetic regimen was used in the following experiments.

d) Inserting the microdialysis probes in skin and tail vein

We then tested insertion of MAB 1.2.4. MD probes (Microbiotech, Sweden) in lesion skin (target site) and in the tail vein (system exposure).

First, the insertion of the probes in the lesion skin was attempted (figure 30, bottom row). The rump skin tissue containing the lesion was held in place with forceps. A 22G needle was placed intradermally and stuck through (in and out) the skin to serve as a guide cannula. The probe was carefully placed inside the needle tip sticking out of the skin. The needle was withdrawn from the skin while holding the probe shaft, leaving the probe inserted into the lesion. The probe shaft was then secured in position by applying tape and contact glue. After the animals were humanely culled (pentobarbital), we surgically removed the lesion skin. It was clear that the probe had been inserted into the lesion as intended: in the middle of the inflammatory mass of the dermis where the *Leishmania* parasite resides. Finally, we recovered the probe from the skin.

We then inserted the probe in the tail vein (figure 30, top row). A glove filled with warm water (~ 37 °C) was placed on the tail for 2 minutes to induce vasodilation. Again, a 22G needle was inserted through the vein (in and out) and the probe was inserted inside the needle. Wrapping tape around the tail appeared sufficient to keep the probe securely in place.

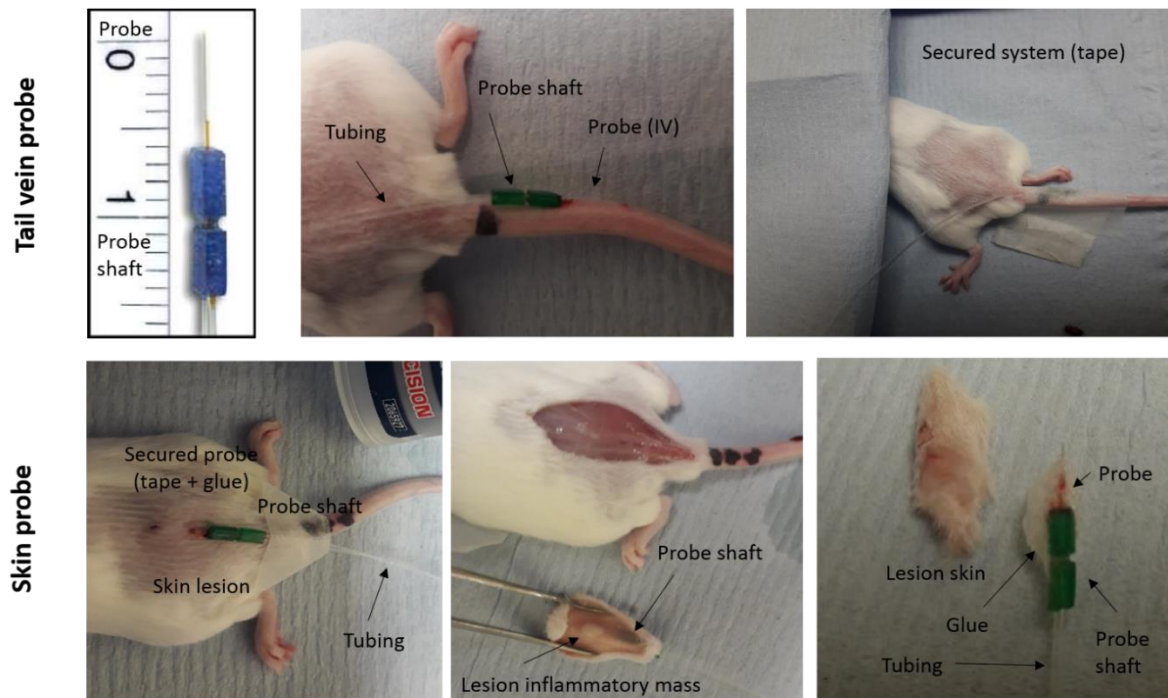


Figure 30: insertion of the microdialysis probe in the tail vein and the lesion skin. Top row (left to right): microdialysis probe, probe inserted in tail vein, probe inserted in tail vein secured by tape. Bottom row (left to right): probe inserted in lesion skin secured by glue, detail confirming intradermal insertion of the probe in the inflammatory mass of the lesion, probe after removal from lesion tissue.

e) A test run of the microdialysis system

After successful placement of probes in lesion skin and tail veins, we set up a very basic microdialysis flow channel to familiarise ourselves with the set-up, practice troubleshooting and control the sample volume (figure 31). A 1 ml syringe filled with the filtered Ringers physiological solution was placed on the perfusate pump and connected via FEP-tubing and adapters to the probe inlet. The probe was inserted intradermally within the lesion on the rump of the mice. The probe outlet tubing was placed in collection vials to check the sampled volumes. Occasional leakage of the system was observed, which could be prevented and resolved by moving the tubing adapters and changing the tubing. Finally, the pump was started at 2 $\mu\text{l}/\text{min}$ and the volumes collected every 15 minutes for 1 hour. The volumes were correct (30 μl) and reproducible.

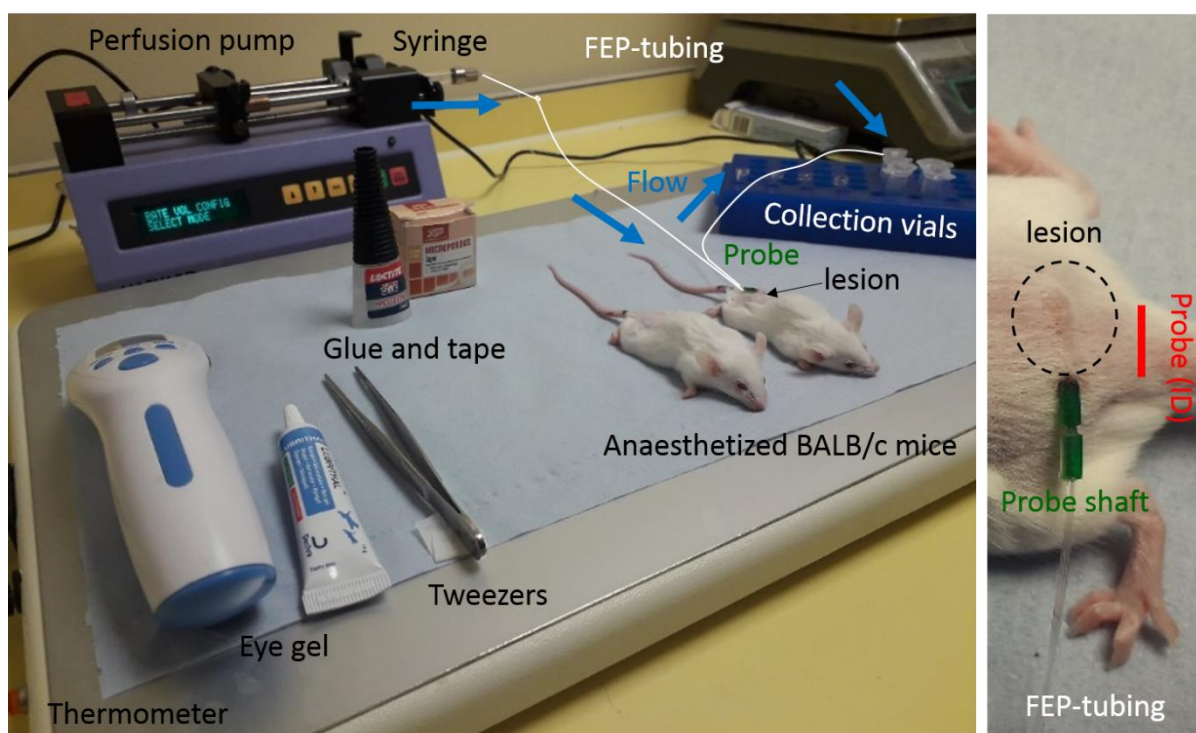


Figure 31: Essential set-up of the *in vivo* skin microdialysis test experiment

3.5.5.3. Lesion, control skin and tail vein microdialysis after oral dosing of DNDI-0690

To study the skin and plasma PK profile of oral DNDI-0690, we performed microdialysis in the lesions, healthy control skin and tail veins of three *L. major*-infected BALB/c mice. Figure 32 gives an overview of the experiment set-up.

Materials and methods

Microdialysis set-up. Nine microdialysis channels were set-up as follows. A syringe with the filtered Ringers physiological solution was mounted on Harvard Apparatus pump set at a flow rate of 2 $\mu\text{l}/\text{minute}$. The syringe was connected via FEP-tubing and adapters (Microbiotech, Sweden) to the inlet of the microdialysis probe (MAB 1.2.4. CU, Microbiotech, Sweden) and the probe outlet was linked via FEP-tubing to the needle of the automated fraction collector (MAB 85, Microbiotech, Sweden) that was filled with empty HPLC vials (0.2 ml crimp top, Thermo Scientific, UK). At a collection interval of 30 minutes, sample volumes were consistently 60 μl , indicating the desired perfusion of the microdialysis probes in the bijoux filled with Ringers.

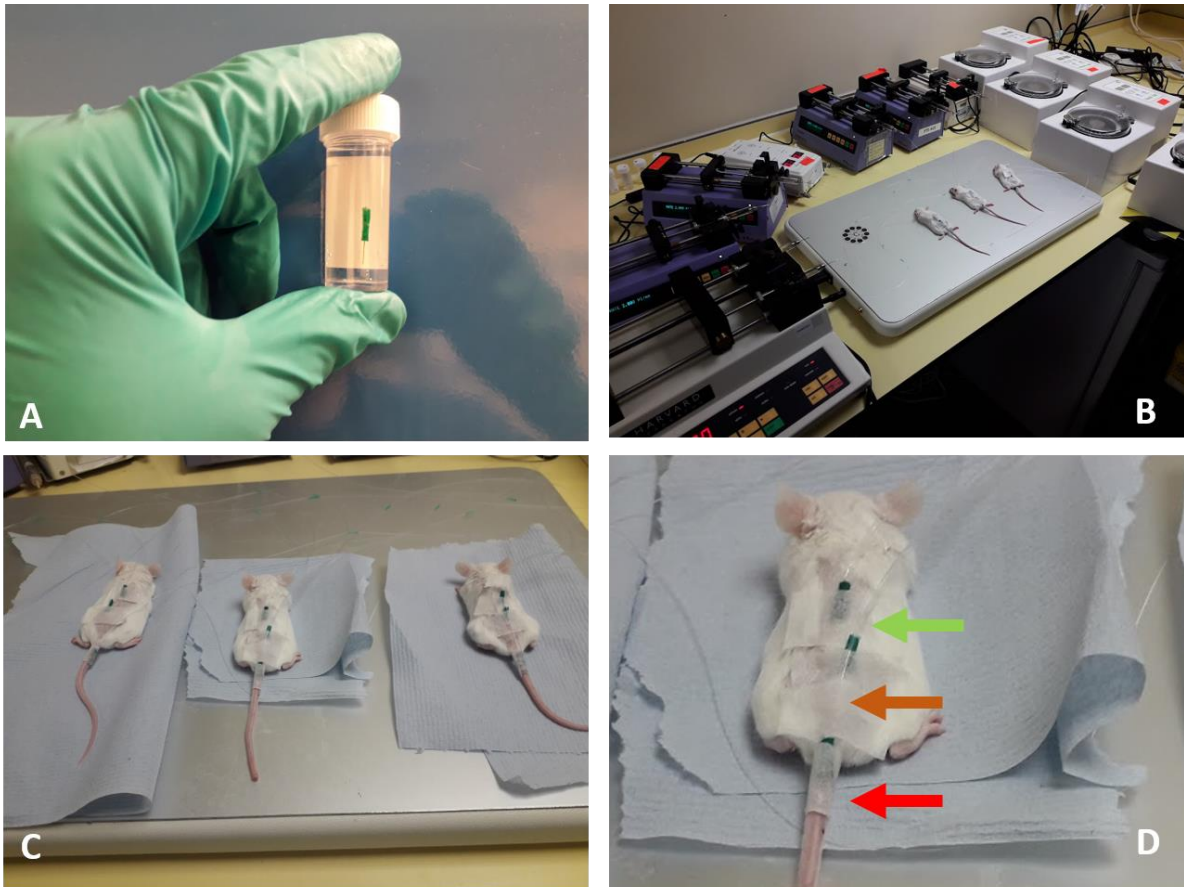


Figure 32: Set-up of lesion, control skin and microdialysis after administration of oral DNDI-0690 in the *L. major*-BALB/c model of CL. A: microdialysis probe (6 kDa cut-off). B: Microdialysis set-up (9 channels) – pumps (left), mice on a hot plate (middle) and automated fraction collectors (right). C: Mice after insertion of probes. D: Detail of one mouse after insertion of microdialysis probes in the lateral tail vein (red arrow), dermal layer of the lesion skin (orange arrow) and dermal layer of healthy control skin (green arrow).

Animals. *L. major*-infected BALB/c mice (n=3) each received 1.6 g/kg urethane (IP): deep anaesthesia (no hind paw reflex) was induced within 10 minutes. After anaesthesia, 200 μ l Ringers physiological solution was administered via neck scruff (SC) to prevent dehydration. Mice were placed on a preheated hot plate to maintain body temperature (37 °C). MD probes were placed in the positions: the dermal skin layer of the CL lesion on the rump, the dermal skin layer of the healthy control skin higher up on the back and the tail vein. Following this order, three probes were installed per mouse. Probes were secured with tape and perfused with a physiological buffer. The animals were allowed to recover from any trauma caused by probe insertion for 30 minutes before drug administration.

Drug administration, animal monitoring and sampling. Then, a single dose of 50 mg/kg DNDI-0690 (200 μ l suspension in PEG400) was administered via oral gavage (t_0 of the PK study). Temperature, breathing pattern and behaviour of the anaesthetized mice were monitored constantly; no abnormalities were observed in the following 5 hours of MD sampling. After 3 hours, another 200 μ l Ringers physiological solution (SC) was administered via the neck scruff

for rehydration. At a collection interval of 30 minutes, sample volumes were consistently 60 μ l, indicating the desired perfusion of the intradermal microdialysis probes. The experiment was terminated after 5 hours of microdialysis sampling and mice were humanely culled by pentobarbital overdose.

Samples. Samples (60 μ l) were collected from the fraction collector every 30 minutes. 20 μ l acetonitrile (ACN) was added immediately and the vials were sealed with a crimp cap (Thermo Scientific, UK). A calibration curve ranging from 100000 to 2 ng/ml was prepared as follows: 6 μ l of known working standard of DNDI-0690 in ACN:H₂O (1:1) was added to 54 μ l of blank Ringers solution and 20 μ l ACN. For blanks, 6 μ l ACN:H₂O (1:1), 54 μ l plain Ringers solution and 20 μ l ACN was used. Samples were stored at – 80 °C until LC-MS/MS analysis (Pharmidex).

Analysis. C_{max} , T_{max} and AUC_{0-48} values for skin were calculated using GraphPad Prism, version 7.02.

Results

Figure 33 shows the PK of DNDI-0690 in the *L. major*-BALB/c model of CL after oral administration of a single dose of 50 mg/kg, as assessed by MD.

In plasma, the C_{max} was 133 ± 32 ng/ml 2 hours after drug administration, indicating the time needed for maximal absorption from the gastrointestinal tract into systemic circulation. Due to the lack of a 24 or 48-time point, the full DNDI-0690 concentration-over-time profile could not be studied during this MD experiment. As a result, no exact $T_{1/2}$ (> 4 h), Cl, Vd and $AUC_{0-\infty}$, could be calculated.

In the peripheral tissues of the healthy skin (control) and the CL lesion, drug accumulation was lower and slower compared to that in plasma. DNDI-0690 exposure (based on AUC_{0-5h} values) in the lesion (115 h.ng/ml) was about 1/3 of that in healthy skin (346 h.ng/ml) and 1/5 of that in plasma (500 h.ng/ml). Maximal drug concentrations in healthy skin ($C_{max} = 93 \pm 42$ ng/ml at 4.5 h) were 3-fold higher compared to those in lesions ($C_{max} = 35 \pm 9$ ng/ml at 5h). DNDI-0690 concentrations in skin tissues increased gradually over time after administration, but were near maximal after 2-3 hours, indicating relatively rapid drug distribution from systemic circulation.

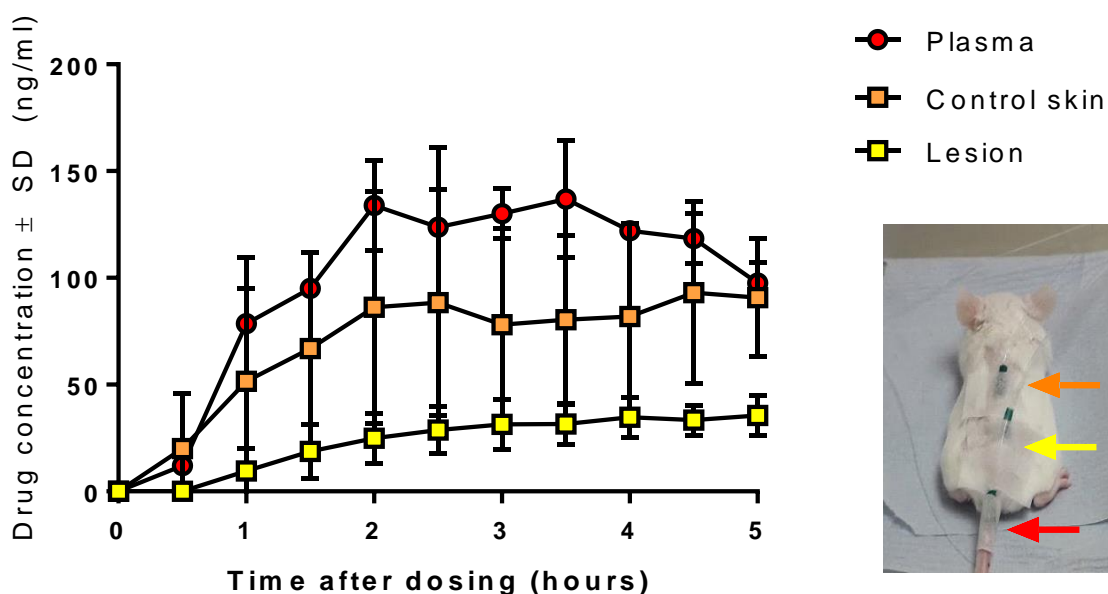


Figure 33: Unbound dermal tissue and plasma concentration-over-time profile of DNDI-0690 after oral administration of a single 50 mg/kg dose to *L. major*-infected BALB/c mice (n=3). Photo: PK sampling sites (microdialysis): plasma (red arrow), healthy control skin (orange arrow) and lesion (yellow arrow).

3.5.6. Discussion

In this chapter, we have evaluated the PK and PD properties of a new oral drug candidate, the nitroimidazole DNDI-0690, in a standard mouse model of CL.

An MD technique was optimized to measure unbound (pharmacologically active) drug concentrations in the dermal layer of the skin lesion (site of action) and other compartments. We have shown that DNDI-0690 accumulates relatively rapidly within skin lesions: near-maximal (for a single dose) nanomolar unbound concentrations are achieved within 2-3 hours of oral dosing. In addition, DNDI-0690 shows different PK profiles in diseased skin, healthy skin and plasma. In the 5 hours following oral dosing, drug exposure in the lesion is about 5-fold lower than in plasma, and, unexpectedly, about 3-fold lower than in control skin. In contrast, we already showed that the inflammation at the infection site in CL enhances local drug accumulation after intravenous administration of different formulations of AmB (chapter 3.2, 3.3. and 3.4). Unbound DNDI-0690 concentrations in the dermal interstitial fluid could be lower in diseased than in healthy skin because higher amounts of drug might reach the skin tissue from the bloodstream (increased vascular permeability, vasodilation), but a large drug fraction could then be bound to inflammatory proteins or ingested by the many immune cells in the dermis (chapter 3.4). As neither protein-bound nor intracellular drug fractions are measured by MD, this could explain the ultimately lower extracellular exposure of DNDI-0690 at the site of infection compared to uninfected counterparts. In any case, this finding illustrates once again the impact of the immunohistopathology of CL on local drug

accumulation in the skin. Differences between AmB and DNDI-0690 PK results could be related to the different sampling methodologies (respectively skin necropsies and MD).

Comparing PK outcomes for DNDI-0690 obtained by MD and skin necropsy sampling (followed by LC-MS/MS), maximal drug concentrations for MD (5 hours after 1 x 50 mg/kg = 35 ng/ml) are about 9-fold lower than for skin necropsies and homogenates (24 hours after 10 x 50 mg/kg = 300 ng/g). Taking into account single *versus* 10-fold dosing, this difference is smaller than expected: homogenates measure total drug levels (protein-bound + protein-free + intracellular + extracellular), while MD measures only the free extracellular fraction of the highly protein-bound (95%) compound DNDI-0690. A homogenate-based repeat of the DNDI-0690 PK study could fully validate MD as a new PK technique as well as discriminate drug fractions in the skin (in relation to their effects) in CL drug research. Important advantages of MD are (i) measuring only protein-free extracellular concentrations (ii) decreasing variability in outcomes (one mouse can yield several PK time points) and (iii) reduction in the numbers of animals required for PK research. In our specific case, where we sampled every 30 minutes for 5 hours, MD on an individual mouse can yield the scientific data equivalent to the use of 10 rodents with the necropsy-based technique, a 90 % reduction in the numbers of animals.

To make pharmacological sense of PK data, it must be interpreted in relation to PD parameters. We showed a fundamental basis for a PK/PD relationship for DNDI-0690, a clear relationship between dose, intralésional drug concentration (PK) and efficacy (PD) in the 6.25 to 50 mg/kg range at the end of 10-day treatment once daily. Using MD, we demonstrated that maximal drug levels in the lesion within 5 hours after 1 x 50 mg/kg drug administration to *L. major*-infected mice (35 ± 9 ng/ml) are around 48-fold lower than the *in vitro* IC₅₀ for *L. major* JISH118 (1690 ng/ml) and 3-fold lower for *L. major* WRAIR (118 ng/ml). However, the actual drug concentrations at the dermal site of infection site should be higher than those observed: the raw experimental MD results have not yet been corrected for incomplete recovery of DNDI-0690. The exact *in vitro* relative recovery is first needed to allow this. In addition, during the *in vivo* dose-response study (figure 24), about 5 to 6 oral doses of 50 mg/kg DNDI-0690 once daily were required to significantly reduce lesion size in comparison to the untreated control. This might indicate that the unbound DNDI-0690 concentrations in the hours following 1 x 50 mg/kg are insufficiently high for immediate parasite elimination. Repeated or more frequent/higher dosing of DNDI-0690 could be required for maximal efficacy in CL. However, because the degree of inflammation (in addition to parasite load) determines lesion size, it is a possible confounder the interpretation of antileishmanial drug activity. Immunological healing of the lesion could be delayed in comparison to the time at which the dermal parasites are killed by DNDI-0690. Rate of kill studies, for example, by daily *in vivo* imaging during treatment with 10 x 50 mg/kg DNDI-0690, can help to clarify this important issue.

Future plans and perspectives for the further preclinical development of DNDI-0690 as a promising drug for the treatment of CL is included in the final thesis discussion (chapter 5).

4. SUMMARY OF KEY FINDINGS

With the aim of supporting the successful discovery and development of much needed new treatments for the parasitic skin infection CL, this thesis provides a strategic approach and a coherent set of R&D methodologies to evaluate PK, PD and PK/PD properties of preclinical drug candidates in animal models of disease. The main findings of the work are:

1. The **poor translational outcomes of the current predictive models** for phenotypic screening of drug activity in CL are illustrated by the lack of *in vitro-in vivo* correlation for a new drug combination of chloroquine and paromomycin. More biologically complex models and associated research methodologies are needed to overcome high compound attrition rates along the R&D pathway.
2. We compared the effects of three different pharmaceutical formulations of the standard drug amphotericin B (the unilamellar liposome AmBisome, the multilamellar liposome Fungisome and the non-liposomal deoxycholate salt Fungizone) in *L. major*-BALB/c mouse models of CL. **The therapeutic efficacy of AmBisome > Fungisome > Fungizone in CL, due to higher tolerated doses and increased drug accumulation at the site of infection.** Moreover, there was a clear relationship between dose, concentration (LC-MS/MS drug levels based on skin homogenates) and response (qPCR parasite load) for AmBisome. This provides a basis for the rational design of better clinical dose regimens, as well as a model for the PK/PD evaluation and comparisons of new drug candidates. Moreover, **encapsulation of antileishmanial compounds in AmBisome-like liposomes** (vesicle size around 80 nm, stable in the blood) could be a strategy to reduce drug toxicity and passive targeting of the dermal site of infection.
3. We then further investigated the role of pathology in CL on PK (and PK/PD) of AmBisome in murine CL. **Local tissue inflammation at the dermal site of infection has a profound effect on the PK** of AmBisome and contributes to a variable *in vivo* efficacy between *L. major* and *L. mexicana*. This is related to pathophysiological alterations in diseased skin, such as increased vascular permeability of the dermal capillaries and tissue infiltration of inflammatory cells.
4. The drug candidate DNDI-0690, a nitroimidazole compound developed by the Drugs for Neglected Diseases *initiative* for VL, also exerts significant efficacy in the *L. major*-BALB/c model of CL when given daily via the oral route for ten days. We observed a dose-concentration-response effect in the 6.25 to 50 mg/kg range; the highest DNDI-0690 dose reduced parasite load by 95% and lesion size by 100% in comparison to untreated controls. Additionally, we confirmed the accumulation of DNDI-0690 at the dermal site of infection within 2-3 hours after oral dosing using microdialysis. **Microdialysis holds much untapped potential for (pre)clinical drug distribution and biomarker studies for CL.** Finally, while more preclinical research on efficacy, safety, PK and PK/PD is required, **our data support further investigation of DNDI-0690 as a promising drug candidate for the oral treatment of CL.**

5. GENERAL DISCUSSION: RECAPITULATION AND FUTURE PERSPECTIVES

There has been significant recent progress in the discovery and development of new drugs for VL, but despite the high unmet medical need, there has been limited advancement for CL. The dermal site of action (rather than spleen, liver and bone marrow for VL) and different drug sensitivities of more than 15 cutaneous *Leishmania* species (rather than *L. donovani* or *L. infantum* for VL) illustrate the need for new methodologies to support and accelerate drug development for CL. In this PhD thesis, we have:

1. Confirmed known scientific challenges and problems in current R&D for CL.
2. Developed new methods to study skin PK and PK/PD in animal models of CL
3. Applied these new research tools to evaluate and select three new candidate treatments
4. Provided rational strategies for future CL drug development

In addition, the lessons and approaches described herein might also be relevant for finding novel treatments for different inflammatory skin disorders (psoriasis, melanoma, dermatitis) or diseases caused by other intra-macrophage pathogens (TB, brucellosis, melioidosis, Q-fever, listeriosis).

5.1. Scientific challenges and problems in current R&D for CL

The variable treatment response in CL based on the different causative species of the *Leishmania* parasite is a well-documented challenge for drug discovery and development for this disease (144, 145). We confirmed this issue in chapters 3.1. and 3.4.: both the standard antileishmanial drugs PM and LAmB exert a superior *in vivo* efficacy against *L. major* compared to *L. mexicana*, at identical dose levels and in the same animal model (BALB/c mouse). In addition, we also demonstrated, for the first time, that such differences in therapeutic efficacy of LAmB could result not only from PD parameters (the variable drug susceptibility of *Leishmania* species) but also from PK factors. We showed how the more severe local inflammation in *L. major* compared to *L. mexicana* CL causes enhanced drug accumulation in the lesions, contributing to the superior efficacy of LAmB against the Old versus the New World parasite (chapter 3.4). These findings indicate the need to test novel compounds against a panel of species and recent clinical isolates of *Leishmania* during early drug development, not only *in vitro* (PD) but also *in vivo* (PK and PD). With more than 15 causative *Leishmania* species and simple, diffuse, mucosal and chronic forms of the CL, it is unlikely that one drug alone will prove to be a panacea, let alone in a single pharmaceutical formulation or standardised clinical dose regimen suitable for disease treatment in the Middle East, Latin America and other endemic settings.

Another issue in R&D for CL is the poor translational outcomes of the current *in vitro* assays used to test for antileishmanial activity, resulting in high compound attrition rates (204). Indeed, the promising activity of a new drug combination of paromomycin and chloroquine in the static, 2D intracellular amastigote model could not be replicated in animal models of neither *L. major* nor *L. mexicana* CL (chapter 3.1.). To predict antileishmanial activity *in vivo*, i.e. parasite survival in response to continually changing drug concentrations in the biologically complex environment of the dermis, the following *in vitro* and *ex vivo* models could be more relevant:

- *In vitro* 3D macrophage and/or skin culture models. Experimental *in vitro* models of wound healing (205), atopic dermatitis (206), psoriasis (207) and melanoma (208) are already available, mostly based on seeding fibroblasts and then keratinocytes on a gel to create a simplified but skin-like tissue structure. However, creating immunocompetent skin models remains fundamentally and technically challenging at present (209). With ongoing advancements in 3D printing and tissue engineering, such models containing macrophages infected with *Leishmania* (transfected with a reporter gene) might soon play a role in the testing of new treatment options for CL.
- *Ex vivo* skin models. Models of bacterial biofilms growing on porcine skin have already been used for the evaluation of antibiotics (210). However, because the pig skin tissue is no longer viable, *Leishmania* would be unlikely to infect the resident macrophages or to survive long-term in this model. While no *ex vivo* skin model is available for CL, antileishmanial drug evaluations for VL have been performed in lymph node tissue (211) and spleen (212) to better simulate pathophysiological infection environments.
- *In vitro* PK/PD models. Recently, our group developed a perfusion system using interstitial fluid flow rates and *L. major*-infected macrophages. Interestingly, for several standard antileishmanial drugs, EC₉₀ values were lower for those derived from flow rather than in static systems (213). While further work is needed to simulate the effect of dynamic drug exposure on parasite survival, such models have great potential to study time-kill behaviour, PK/PD-drivers of efficacy, synergy between drug combinations and susceptibility breakpoints (214).

All of these models are technically challenging, low-to-medium throughput and relatively expensive, and would hence not be suitable for high throughput screening and hit identification. However, they could hold potential for compound evaluation in hit-to-lead, lead selection and preclinical phases, as they are expected to perform better at predicting *in vivo* efficacy than biologically simpler and/or static models. This brings us to another issue in CL drug research: measurement of the predictive value of these preclinical models. Validation of the models, by correlating preclinical predictions with human outcomes, is difficult, because few clinical candidates are being advanced into clinical trials and many CL drugs are repurposed from VL. Overall, such translational gaps between *in vitro* and *in vivo*, as well as between preclinical and clinical phases, highlight the needs for new PK, PD and PK/PD models and methodologies for CL drug development.

5.2. New PK and PK/PD drug development methodologies for CL

In this work, we established and optimized a number of new methods to evaluate *in vivo* skin tissue penetration (PK) and antileishmanial (PD) properties of candidate compounds to assist in early drug development for CL (hit-to-lead, lead optimization, preclinical studies). Such R&D techniques, that could reduce attrition rates related to poor PK, PD and PK/PD characteristics, include:

- A method to study the plasma and skin PK of antileishmanial drugs in animal models of CL, based on combined sampling by **skin necropsies and tail vein bleeding**, followed by drug extraction and LC/MS-MS quantification (chapter 3.2, 3.3 and 3.4.). This approach was used to characterize the plasma and skin PK of a standard antileishmanial drug formulation (LAmB) in the classic *L. major*-BALB/c model of CL (chapter 3.2). In addition, it provided the basis for a simplified but fundamental understanding of PK/PD of LAmB in CL. At the end of treatment, there was a clear correlation between dose, concentration and response. In addition, intralesional levels of the concentration-dependent drug AmB (5-50 µg/g) were above the *in vitro* IC₅₀ value (≈ 2 µg/ml in 72-hour intracellular assays, chapter 3.1). A limitation of this necropsy approach for PK is that it requires a high number of animals and that it might lead to erroneous conclusions about drug levels, as these are a cumulative total (protein-bound/free, intracellular/extracellular) rather than only the pharmacologically active concentrations.
- A method to study the plasma and skin PKs of antileishmanial drugs in animal models of CL, based on combined sampling by **skin and plasma microdialysis**, followed by drug extraction and LC/MS-MS quantification (chapter 3.5.). Compared to the technique described above, skin microdialysis provides continuous real-time monitoring of unbound drug concentrations in the infected dermis and circumvents the need for invasive end-point sampling at each desired time point. Hence, once established and optimized, MD can reduce the cost in early drug development because the number of animals is lower and a wide range of data (PK, possibly PD) can be gathered from a single mouse, reducing variability. In this work, we have used MD to confirm the suitable PK profile of the drug candidate DNDI-0690 for further development for CL. Apart from such applications for preclinical animal models for CL, there is also unexploited potential in humans. MD has already been used extensively to study various skin diseases in the clinic, but not CL, MCL or PKDL. Possible future **applications** of MD in leishmaniasis research could include:
 - **MD: drug distribution in the skin.** Because little is known about the PK and PD properties of the current antileishmanial drugs, treatment regimens are empirical and based on the maximum tolerated doses, rather than rationally designed and optimized. This leaves patients at risk of drug-related adverse and toxic effects, therapeutic failure and relapse of PKDL after initial cure. Monitoring of drug concentrations (and biomarkers, see below) in the infected skin of individual patient could help to provide clinicians with directions for a more effective, shorter or safer treatment of CL. MD can also be a tool to predict intralesional drug

exposure from blood samples, once the plasma-skin drug transfer process has been fully characterized and mathematically described. Such an approach was successfully used to understand skin PK of amoxicillin and cefuroxime for bacterial infections (215).

- **MD/PET: intracellular drug distribution in the skin.** While SMD can be used to measure extracellular drug concentrations in the dermal interstitial fluid, ideally we are interested in intracellular drug levels, the true site of action for *Leishmania*. On the other hand, positron emission tomography (PET) and magnetic resonance spectroscopy (MRS) can track total drug (intracellular, extracellular) levels of radiolabelled drugs. The combined use of MD with such complementary non-invasive drug imaging methods can allow the exploitation of the strengths of the individual techniques. Indeed, the difference of total (PET/MRS) and extracellular (MD) drug levels in tissue gives an estimation of local intracellular drug concentrations (216, 217). In this way, MD/PET has been applied to determine intracellular drug distribution of ¹⁸F-labelled ciprofloxacin in human muscle (218). Dermal MD in the skin lesion during treatment with a radiolabelled drug (candidate) could be a potential tool for translational drug development and clinical research in CL.
- **MD/IVIS: real-time PK/PD.** A powerful combination of methods for CL preclinical drug evaluation would be to match MD directly with *in vivo* imaging (IVIS) of bioluminescent *Leishmania* (219, 220). This way, the drug exposure at the target site can be coupled directly to the magnitude and rate of parasite killing. Apart from continuous PK and PD assessment within the same animal, the outcomes would allow an understanding of PK/PD based on *in vivo* efficacy for PD, rather than relying on *in vitro* IC₉₀ values. Understanding of PK/PD relationships with simulation and modelling can help to predict safe and effective dose regimens during Phase II and III clinical trials, to ultimately saving costs and time to successfully deliver a new medicine.
- **MD: therapeutic biomarkers.** During PK studies for DNDI-0690, we used MD probes with a small cut-off size (5 kDa) to specifically measure only the protein-free drug level in plasma and skin tissue. Pores with larger cut-off sizes (such as 100 kDa) could be used to not only sample drugs from the interstitial fluid of the infected dermis, but also therapeutic biomarkers such as inflammatory cytokines, parasite antigens and macrophage activation markers (221). The search for suitable therapeutic biomarkers that can indicate treatment success or predict failure and relapse in leishmaniasis treatment is an ongoing challenge (222).
- **MD: inflammatory mediators.** Dermal microdialysis is a well-explored research tool to sample cytokines, chemokines and inflammatory mediators and study inflammation, physiology and pathology in atopic psoriasis, contact dermatitis, urticaria, burn injuries, inflammatory pain and wound healing (223). A similar approach could advance our understanding of fundamental immunology and inflammation in CL, MCL and PKDL, possibly contributing to the development of a preventive or therapeutic vaccine.

- **Reverse MD: drug delivery.** Rather than perfusing the probe inserted in the tissue of interest with a physiological buffer, it could also be used as a delivery system to allow drugs in the perfusion fluid to diffuse into the target site. While such a reverse MD approach has already been used for drug delivery to tumours in hospitalized cancer patients (224), it is highly unlikely that it would be feasible, practical or cost-effective for the treatment of CL.
- An **Evans Blue** assay to determine the vascular permeability of the blood vessels at the dermal infection site in animal models of CL. This is an important pathophysiological parameter affecting systemic drug delivery (chapter 3.4.). More sensitive and informative methods from the field of cancer research, such as using fluorescent dextrans of particular sizes to determine pore-cut-off size and other blood vessels properties (225), have not yet been used in CL.
- A **qPCR** assay for the detection of parasite burden in CL lesions, based on amplification of pathogen RNA rather than DNA (chapter 3.3). This reaction involves an additional step where target RNA is first transformed into complementary DNA. Typically, in comparison to DNA-based assays, RNA-based ones for *Leishmania* quantification are more expensive and complex (additional procedure time and handling steps), but also more sensitive (226). In addition, there might be differences in the parasite load outcomes for DNA or RNA-based qPCR, therefore affecting decisions about the most efficacious compound to progress along the R&D pipeline. Indeed, during a comparison of the intralesional parasites after PM, AmBisome and Fungisome treatment, we observed a difference in absolute values for parasite load (DNA>RNA assay). However, the ranking order and dose-dependent trends for these drugs were very similar among DNA and RNA-based assays (see supplementary material). This new qPCR method can be a tool in PD, immunological and diagnostic *Leishmania* studies.
- A **method for quantification of inflammatory cells and macrophages** in CL lesions, based on anti-Iba-1 and H&E stains and computational image analysis (chapter 3.4.). This could be particularly useful in the study of wound healing agents and immunomodulators, alone or in combination with chemotherapeutics, in animal models of CL.
- A murine **model of local inflammation in the skin**, the “pseudolesion”, clearly characterized in terms of histology and vascular permeability of the capillaries (chapter 3.4). This could be applied as a research tool in further PK studies in CL, but also for other skin inflammatory diseases such as atopic dermatitis, psoriasis and cutaneous cancers.

Figure 34 gives a potential screening cascade for drug development for CL focussing on PK and antileishmanial activity and shows where the new methods might be of use to support drug development.

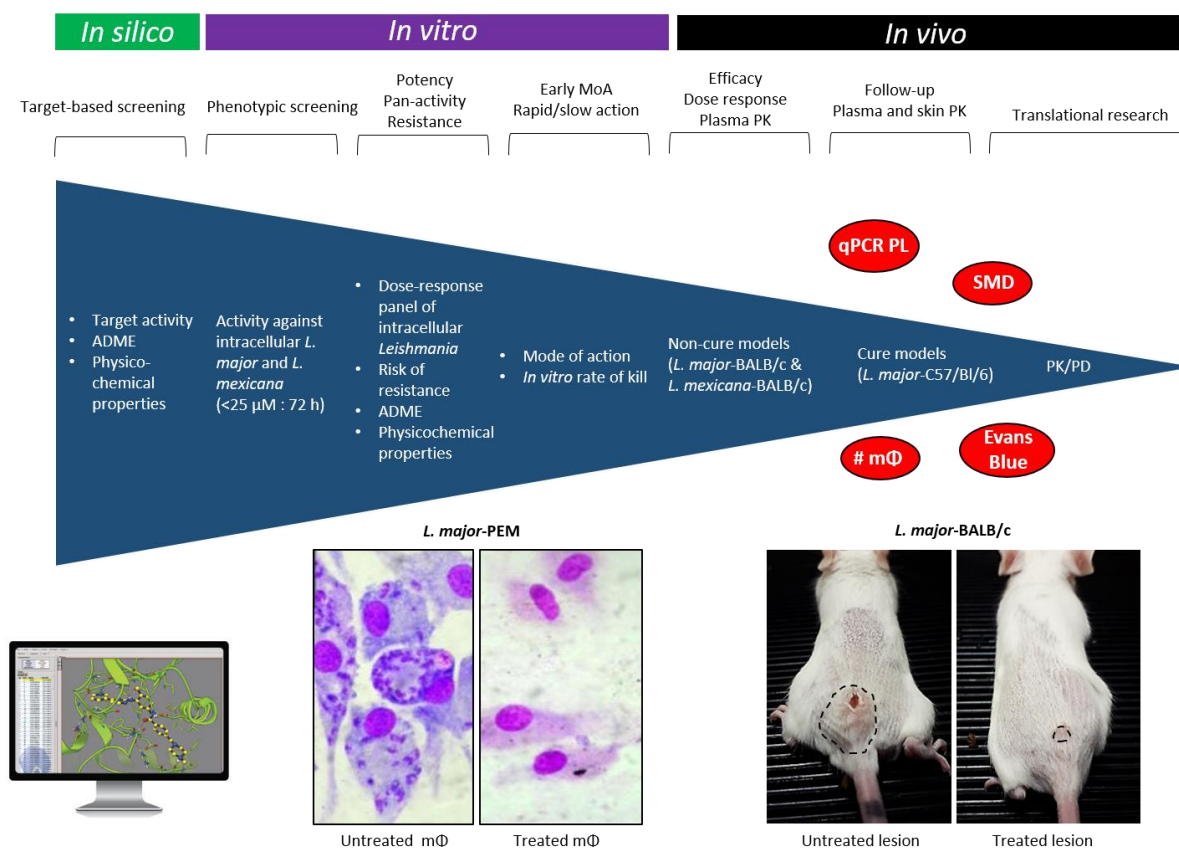


Figure 34: Example of a screening cascade for CL drug development and where the new methodologies (red circles) could be implemented. qPCR PL: quantitate PCR to measure parasite load. #m Φ : image analysis to estimate the number of macrophages in skin tissue. SMD: skin microdialysis.

5.3. New drug candidates tested for the treatment of CL

Using the research methodologies described above, the efficacy and tolerability of the following three drug candidates were evaluated in animal models of CL:

1. **A combination of PM with CQ** (chapter 3.1.). Despite initially promising *in vitro* results, no additional *in vivo* efficacy of the combination therapy could be observed compared to the drugs alone. This combination is therefore unlikely to be worthy of further investigation as a new CL treatment. Lysosomotropic such as CQ remain interesting research tools to investigate how the acid environment the phagolysosome affects cellular drug trafficking towards the parasite target.
2. A multilamellar liposomal formulation of AmB (for IV infusion) called **Fungisome[®]**, already on the market in India from the company Lifecare Innovations (chapter 3.3.). We showed evidence for some - albeit low - *in vivo* efficacy against CL, but its narrow therapeutic index is a cause for concern. Originally targeted at the Indian market to

help overcome the high price and limited access of AmBisome® for the treatment of invasive fungal infections and VL, it remains currently unclear how relevant this liposomal AmB formulation could be in (M)CL therapy in Latin-America and the Middle-East. However, the evidence for drug accumulation in the skin might support a potential role for Fungisome in the pharmacotherapy of PKDL on the Indian Subcontinent. A topical Fungisome cream is also commercially available (227), which might be explored for treatment CL, MCL and PKDL.

3. An oral drug candidate for VL from the non-profit public-private partnership DNDI, the nitroimidazole **DNDI-0690**. We observed excellent oral efficacy (ED₅₀ and ED₉₀ values of ~ 5 and 21 mg/kg, once daily for 10 days.) and no adverse effects for doses as high as 50 mg/kg in the *L. major*-BALB/c mouse model of CL. In addition, we found relatively rapid drug accumulation of DNDI-0690 in skin lesions within around 3 hours of oral dosing. Translational PK modelling and combining PK and PD (*in vitro* IC₉₀, *in vitro* or *vivo* rate of kill) data could provide a basis to predict dose regimens that are efficacious during phase II and III trials. To estimate the actual success rate of DNDI-0690 in CL trials in humans, the following information would assist:
 - Efficacy and dose-response in other animal models of CL caused by different species of *Leishmania*, for example, *L. major*-C57Bl6 mouse, *L. mexicana*-BALB/c mouse, *L. amazonensis*-CBA mouse, *L. braziliensis*-golden hamster. Some researchers argue for performing final preclinical drug evaluations in non-human primate models because they best mimic the pathology and immunology of the disease in humans (158). We believe the choice for monkey models of CL is not justifiable for several ethical and financial reasons, as a combination of different rodent models, with their own strengths and weaknesses, could be used to answer important research questions about drug efficacy, PK and safety.
 - The preclinical toxicology of DNDI-0690 (LD₅₀, LD₉₀, NOAEL, LOEL) has already been characterized by DNDI. During the upcoming phase I trials, a special emphasis should be on testicular side effects: such issues caused a similar nitroimidazole compound with promising activity for VL (DNDI-VL-2098) to be discontinued.
 - Advanced PK/PD. For PK, the unbound concentrations over time of DNDI-0690 in plasma and infected dermis after administration of different single oral dosing (for example, 5, 25 and 50 mg/kg) and repeated dosing (for example, 10 x 50 mg/kg) could be determined (MD). In addition, *in vivo* drug levels surrounding host cells could be simulated using *in vitro* assays, to understand the cellular PK/PD relation between the intracellular DNDI-0690 levels to which the amastigotes are exposed to and antileishmanial activity. For PD, rather than relying solely on *in vitro* IC₉₀ data (based on a single time point) for PK/PD modelling, cidal dynamics should also be investigated: the minimal time required to kill intracellular amastigotes at minimal (IC₅₀), effective (2x IC₅₀) and near-macrophage-toxic drug levels (CC₉₀) (228). Moreover, *in vitro* rate of kill can then be compared to *in vivo* cidal dynamics derived from continuous

parasite load monitoring during treatment with reporter molecules. This could help compare and validate new research methodologies.

- Mode of action studies. The following experiments could provide additional evidence that DNDI-0690 is a prodrug that exerts its antileishmanial effects via formation of reactive radical species: (i) a lack of *in vitro* and *in vivo* activity of synthetic DNDI-0690 analogues without the nitro-function and (ii) variable sensitivity of transgenic *Leishmania* over- or under-expressing specific nitroreductases to DNDI-0690 in comparison to that of the wild-type parasite.
- Assessing the risk of emergence of drug resistance an important part of antimicrobial drug development. However, in CL, there is no evidence of drug resistance for the standard chemotherapeutics, in contrast to VL. In addition, because the nitroimidazole DNDI-0690 is most likely a prodrug (requiring bio-activation in *Leishmania* by nitro-group reduction), the risk of drug resistance could be considered inherently low. Standard procedures to induce experimental resistance *in vitro* and *in vivo* upon repeated sub-therapeutic exposure cycles are available for VL (229, 230). When using similar strategies to assess the risk of drug resistance for DNDI-0690 in CL, the dermal drug concentrations we have measured at the infection site *in vivo* can guide researchers to decide on biologically meaningful drug exposure levels *in vitro*.
- ADME and PK. In terms of metabolism, especially the induction or inhibition of hepatic enzymes and the potential drug-drug interactions. To create efficacious combinations of DNDI-0690 with one or more other drugs, it is important that the components of the combination are all present in the infected dermis in adequate concentrations at the appropriate time to exert a synergetic effect in therapeutic efficacy. Again, understanding PK and PK/PD profiles can assist to here.

Alternatively, the orally bioavailable compound DNDI-0690 might also be produced in a topical pharmaceutical formulation to provide a new local treatment for small, uncomplicated CL skin lesions. Topical delivery is suitable for small (molecular weight < 500 Da) and rather lipophilic drugs: DNDI-0690 does not violate these criteria. Assays to assess *in vitro* permeation, *ex vivo* skin disposition (using Franz diffusion cells/tape stripping) and *in vivo* efficacy (*L. major* / *L. mexicana* - BALB/c / C57Bl6 mouse models) could be used to evaluate drug penetration across the stratum corneum, with or without the presence of chemical permeation enhancers such as DMSO, urea, polyglycoles or ethanol in the topical formulation (159). More advanced cutaneous drug delivery systems, including microneedles and liposomes, or physical methods such as sonophoresis, electrophoresis and iontophoresis have not been explored in CL (231).

In conclusion, based on the previous toxicity and the new *in vivo* efficacy and skin PK data, DNDI-0690 is a promising oral drug candidate for the treatment of CL. However, attrition rates during clinical trials are high. It is therefore important to maintain a strong R&D pipeline with backup drug candidates and provide a direction for future drug development for CL.

5.4. Directions for future R&D for CL

Drug development encompasses a wide range of approaches to find new medicines to treat human disease, including immunotherapy, nanomedicine, small molecules, biologicals, antibodies, gene therapy, recombinant proteins and drug combinations. We will here discuss the potential of liposomes and small molecules in the search of new therapeutics for CL, the two most relevant strategies in the frame of the thesis.

Encapsulation of drugs into liposomes, small spherical vesicles composed of one or more phospholipid bilayers, is a popular and theoretically attractive strategy for the treatment of leishmaniasis. Liposomes are suited for macrophage-targeted therapy, due to improved efficacy, low toxicity, flexibility to modify surface molecules and preferential uptake by the *Leishmania* host cells (232). While the vesicles are rapidly being cleared by the liver and spleen (which is important for VL therapy), the remaining fraction that can penetrate into the skin is prone for uptake by the dermal macrophages (CL) (233). Studies described the successful treatment of experimental CL with various liposomal formulations of PM (234), Sb^V (235), MF (236) and AmB (237), but none have looked into their skin PK. Using the *L. major*-BALB/c model of CL, our work showed that drug levels in the lesion after administration of liposomal AmB (AmBisome) were higher compared to those achieved by non-liposomal deoxycholate AmB and compared to those found in healthy, uninfected skin (chapter 3.2., 3.3, 3.4.). In addition, AmB concentrations at the infection site, therapeutic window and tolerability of the standard LAmB formulation AmBisome (Gilead) were superior compared to alternative Fungisome (Lifecare Innovations) (chapter 3.3). Hence, encapsulation of old and new antileishmanial drugs in AmBisome-like liposomes could be a drug delivery strategy to target the dermal infection site. However, despite a number of rational arguments to support the use of liposomes in CL therapy (see above), there are also major limitations. Intravenous administration of the drug formulations and thus hospitalization is required: liposomes do not address the medical needs of many patients with simple, uncomplicated CL. In the future, the currently still commercially unavailable oral (polymer-coating, microencapsulation (238)) or topical liposomes (ethosomes, transfersomes, ultra-deformable structures (239)) might be more patient-friendly treatment options. In addition, issues related to the high cost, stability in tropical climates, logistics and access to medicines makes one wonder whether liposomes are truly the best way forward to treat a disease affecting populations living in remote areas, poverty and conflict.

Another strategy for CL treatment is based on classic small molecule therapeutics, without the use of nanocarriers. These remain the majority of medicines on the market today, many being instant-release tablets or capsules. Such drug formulations are typically simpler and cheaper to manufacture, but finding small molecule libraries with the right balance of lipophilicity, solubility, metabolism, protein binding and ultimately activity and safety has historically been a major challenge for the pharmaceutical industry (240). Our work has shown that the pathology of CL might present both opportunities and challenges to achieve adequate concentrations of small drugs into the skin, depending on both factors related to the drug and the disease (pathophysiology):

- Drug: For both liposomal and non-liposomal drug formulations of amphotericin B, drug concentrations after intravenous drug administration to infected mice were consistently higher in the diseased skin than in the healthy skin (skin homogenates). Yet for DNDI-0690, a nitroimidazole, the opposite trend was observed after oral dosing (MD). However, the different PK sampling methodologies make interpretation and direct comparison of these results difficult. In any case, both examples show that there are differences in drug distribution in the *Leishmania*-infected and the uninfected skin after systemic drug administration of murine CL. The impact of CL pathology on drug PK should not be ignored during the development of (pre)clinical dose regimens. If less drug reaches the infection site than assumed, parasites might be exposed to subtherapeutic drug levels, possibly leading to treatment failure or the emergence of resistance. On the other hand, if more drug accumulates at the target site than expected, cure of CL might be achievable at lower drug doses or shorter treatment durations, which is especially important for compounds with a narrow therapeutic index.
- Disease: the CL-infection site is characterized by (i) increased vascular permeability and capillary leakiness of the dermal vasculature (chapter 3.4) (ii) a reduced barrier function of the epidermis and (iii) an aqueous environment in the oedema-filled dermis (161). Hence, the histopathology of CL might be exploited for facilitated oral or topical delivery of small molecules to the infected dermis. In contrast, destruction of blood vessels due to tissue necrosis or the formation of thick, impermeable lesion crusts could hinder such drugs to reach the dermal site of action. Differences in pathology between species, as shown for *L. major* and *L. mexicana* contribute to the complexity of the issue. We showed that histopathology and inflammation severely affect the PK of LAmB: AmB levels in the lesion depend on the disease stage when the drug is administered (papule > initial nodule > established nodule). Matrix-assisted laser desorption/ionisation - mass spectrometry (MALDI-MS) is a powerful, yet unexplored technique to help to address such questions about the influence of pathology on PK and PK/PD in CL drug research. Recently, studies on *Mycobacterium tuberculosis*, a pathogen occupying a similar intracellular site as *Leishmania*, used MALDI-MS to evaluate the penetration of TB drugs into lung lesions and visualize therapeutic biomarkers (241, 242). A similar approach could provide a basis to dismiss candidate compounds for CL with impaired or suboptimal drug distribution within skin lesions, granuloma and infected macrophages from the pipeline during the early stages of drug development.

Figure 35 attempts to list the PK path that oral and topical drugs need to take to reach the parasites residing within dermal macrophages.

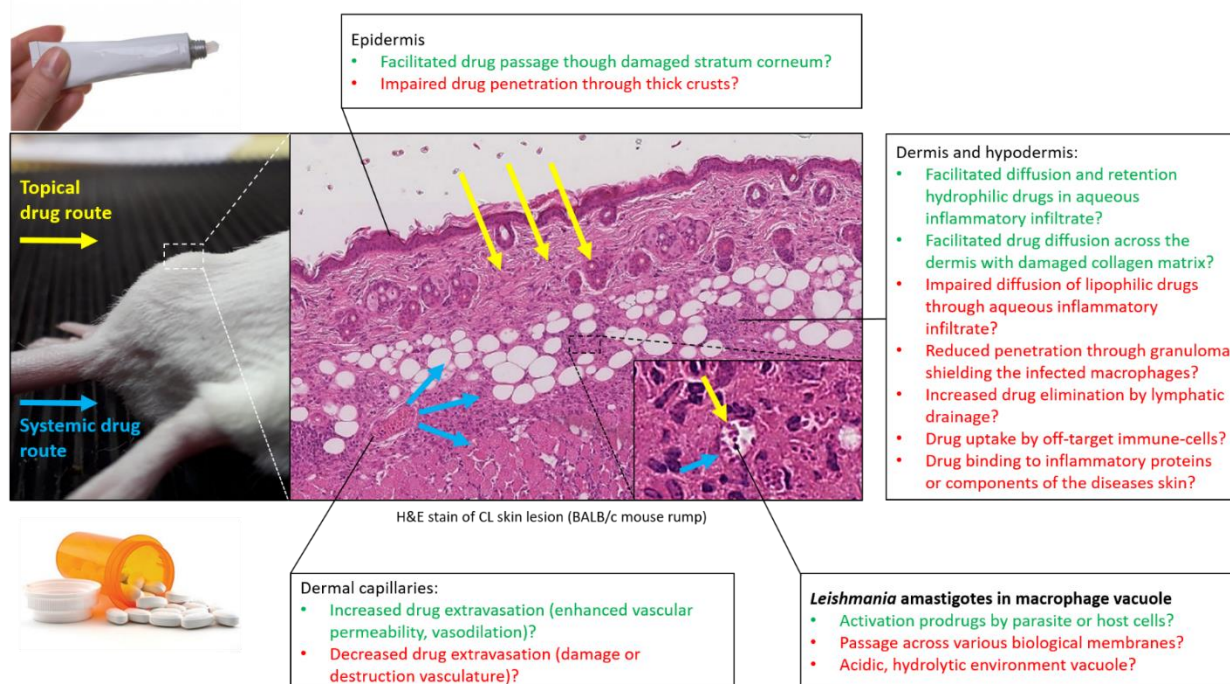


Figure 35: Opportunities (green) and challenges (red) along the pharmacokinetic path of oral (blue) and topical (yellow) drugs against CL.

In overall conclusion, the currently available treatments for CL are not appropriate for the clinical needs of many patients; advances towards the discovery and development of new drugs has been disappointing in comparison to those for VL. To improve this situation, we believe the following challenges across the path from bench to bedside must be addressed:

- Firstly and most fundamentally, to ensure sustainable funding and collaborative drug development efforts from industry, academia, NGOs and governments with a clear scientific strategy and a common target profile. Importantly, in case we manage to eliminate VL in the Indian subcontinent during coming years, before the development of a new medicine for CL, will we be able to maintain R&D interest for the non-fatal yet most common form of leishmaniasis alone?
- Secondly, to continue and expand open access high throughput screening efforts in the public domain to discover new hits and leads with broad-spectrum activity (against different parasites and disease forms), especially those with dermal bioavailability after oral/topical administration and an inherently low risk for the emergence of antimicrobial resistance.
- Thirdly, to establish and validate more powerful predictive models and related research methods to evaluate preclinical drug candidates, so that only those with the highest chance of exerting clinical efficacy against Old and New World CL are moved forward along the R&D pipeline.
- Fourthly, to discover therapeutic biomarkers to indicate cure or the risk of relapse to assess the efficacy of drugs and/or combinations in high quality randomized clinical trials, as well as their effectiveness in routine practice.

- Finally, to overcome barriers to access, for example by drug donations or allowing generic drug manufacturing, so the new medicine is affordable and available to those who need it most, the patients. This is a complex and multifaceted problem in which governments, NGOs, academia, pharmaceutical companies, finance institutions and WHO all have a role to play.

In relation to the third need, this PhD thesis provides a collection of research methodologies and strategies that could support and accelerate successful preclinical R&D for CL. Indeed, these have already proven useful to confirm the promising potential of a new oral drug candidate: DNDI-0690. We hope that it will be the first of many, as attrition rates in the clinic are high. A central message in this work about drug development for CL is that compounds should not be evaluated based on their *in vitro* or *in vivo* antileishmanial activity alone, but also on their combined ability to (i) penetrate into the infected dermal tissue underneath the skin lesions (ii) reach the intracellular pathogen within macrophages and (iii) rapidly exert their antimicrobial effects at these sites. By improving our understanding of the PK and PD properties of old and new CL drugs, to which the novel MD and qPCR methods provide a means, PK/PD can help to bridge translational gaps along the R&D pathway and ultimately bring new medicines to the clinic. We hope that the encouraging trend of collaborative drug discovery and development for NTDs in recent years also creates a momentum to continue our progress towards safe, effective and patient-friendly treatments for CL.

6. REFERENCES IN THE THESIS TEXT

1. Alvar, J. *et al.* Leishmaniasis Worldwide and Global Estimates of Its Incidence. *PLOS ONE* 7, e35671 (2012).
2. Torres-Guerrero, E., Quintanilla-Cedillo, M. R., Ruiz-Esmenjaud, J. & Arenas, R. Leishmaniasis: a review. *F1000Res* 6, (2017).
3. Aronson, N. *et al.* Diagnosis and Treatment of Leishmaniasis: Clinical Practice Guidelines by the Infectious Diseases Society of America (IDSA) and the American Society of Tropical Medicine and Hygiene (ASTMH). *Am J Trop Med Hyg* 96, 24–45 (2017).
4. Dostálová, A. & Volf, P. Leishmania development in sand flies: parasite-vector interactions overview. *Parasit Vectors* 5, 276 (2012).
5. Kaye, P. & Scott, P. Leishmaniasis: complexity at the host-pathogen interface. *Nature Reviews Microbiology* 9, 604–615 (2011).
6. Ramalho-Ortigao, M., Saraiva, E. M. & Traub-Csekö, Y. M. Sand fly-Leishmania interactions: long relationships are not necessarily easy. *Open Parasitol J* 4, 195–204 (2010).
7. Quinnell, R. J. & Courtenay, O. Transmission, reservoir hosts and control of zoonotic visceral leishmaniasis. *Parasitology* 136, 1915–1934 (2009).
8. Singh, N., Mishra, J., Singh, R. & Singh, S. Animal reservoirs of visceral leishmaniasis in India. *J. Parasitol.* 99, 64–67 (2013).
9. Cruz, C. F. R., Cruz, M. F. R. & Galati, E. A. B. Sandflies (Diptera: Psychodidae) in rural and urban environments in an endemic area of cutaneous leishmaniasis in southern Brazil. *Mem. Inst. Oswaldo Cruz* 108, (2013).
10. Alvar, J., Croft, S. & Olliaro, P. Chemotherapy in the Treatment and Control of Leishmaniasis. in *Advances in Parasitology* (ed. Molyneux, D. H.) 61, 223–274 (Academic Press, 2006).
11. Okwor, I. & Uzonna, J. Social and Economic Burden of Human Leishmaniasis. *Am J Trop Med Hyg* 94, 489–493 (2016).
12. Kassi, M., Kassi, M., Afghan, A. K., Rehman, R. & Kasi, P. M. Marring Leishmaniasis: The Stigmatization and the Impact of Cutaneous Leishmaniasis in Pakistan and Afghanistan. *PLoS Negl Trop Dis* 2, (2008).
13. Bennis, I. *et al.* Psychosocial impact of scars due to cutaneous leishmaniasis on high school students in Errachidia province, Morocco. *Infectious Diseases of Poverty* 6, 46 (2017).
14. Reithinger, R. *et al.* Cutaneous leishmaniasis. *Lancet Infect Dis* 7, 581–596 (2007).
15. Olliaro, P. *et al.* Methodology of Clinical Trials Aimed at Assessing Interventions for Cutaneous Leishmaniasis. *PLOS Neglected Tropical Diseases* 7, e2130 (2013).

16. Nylén, S. & Gautam, S. Immunological Perspectives of Leishmaniasis. *J Glob Infect Dis* 2, 135–146 (2010).
17. Manamperi, N. H. *et al.* Histopathological spectrum in acute and chronic Cutaneous Leishmaniasis in Sri Lanka. (2015).
18. Andrade-Narvaez, F. J., Medina-Peralta, S., Vargas-Gonzalez, A., Canto-Lara, S. B. & Estrada-Parra, S. The histopathology of cutaneous leishmaniasis due to *Leishmania (Leishmania) mexicana* in the Yucatan peninsula, Mexico. *Rev. Inst. Med. Trop. Sao Paulo* 47, 191–194 (2005).
19. M, V. Histopathological spectrum in cutaneous leishmaniasis: A study in Oman. *Indian Journal of Dermatology, Venereology, and Leprology* 67, 294 (2001).
20. Handler, M. Z., Patel, P. A., Kapila, R., Al-Qubati, Y. & Schwartz, R. A. Cutaneous and mucocutaneous leishmaniasis: Differential diagnosis, diagnosis, histopathology, and management. *Journal of the American Academy of Dermatology* 73, 911–926 (2015).
21. Scott, P. & Novais, F. O. Cutaneous leishmaniasis: immune responses in protection and pathogenesis. *Nature Reviews Immunology* 16, 581–592 (2016).
22. Tripathi, P., Singh, V. & Naik, S. Immune response to leishmania: paradox rather than paradigm. *FEMS Immunol Med Microbiol* 51, 229–242 (2007).
23. Kaye, P. M. & Beattie, L. Lessons from other diseases: granulomatous inflammation in leishmaniasis. *Semin Immunopathol* 38, 249–260 (2016).
24. Bari, A. U. Clinical spectrum of cutaneous leishmaniasis: an overview from Pakistan. *Dermatol. Online J.* 18, 4 (2012).
25. Kuilder, J. S. *et al.* *Leishmania major* Cutaneous Leishmaniasis in 3 Travelers Returning from Israel to the Netherlands. *Emerg Infect Dis* 22, 2022–2024 (2016).
26. Kumar, R., Ansari, N. A., Avninder, S., Ramesh, V. & Salotra, P. Cutaneous leishmaniasis in Nepal: *Leishmania major* as a cause. *Transactions of the Royal Society of Tropical Medicine and Hygiene* 102, 202–203 (2008).
27. Silveira, F. T., Lainson, R. & Corbett, C. E. Clinical and immunopathological spectrum of American cutaneous leishmaniasis with special reference to the disease in Amazonian Brazil: a review. *Memórias do Instituto Oswaldo Cruz* 99, 239–251 (2004).
28. Handler, M. Z., Patel, P. A., Kapila, R., Al-Qubati, Y. & Schwartz, R. A. Cutaneous and mucocutaneous leishmaniasis: Clinical perspectives. *Journal of the American Academy of Dermatology* 73, 897–908 (2015).
29. Calvopiña, M., Martinez, L. & Hashiguchi, Y. Cutaneous Leishmaniasis “Chiclero’s Ulcer” in Subtropical Ecuador. *Am J Trop Med Hyg* 89, 195–196 (2013).
30. Blaylock, J. M. & Wortmann, G. W. A case report and literature review of “Chiclero’s ulcer”. *Travel Medicine and Infectious Disease* 10, 275–278 (2012).

31. McGwire, B. S. & Satoskar, A. R. Leishmaniasis: clinical syndromes and treatment. *QJM* 107, 7–14 (2014).
32. Control of the leishmaniasis: report of a meeting of the WHO Expert Committee on the Control of Leishmaniasis, Geneva, 22–26 March 2010. (World Health Organization, 2010).
33. Organization, W. H. *Cutaneous leishmaniasis: control in selected countries of the WHO Eastern Mediterranean and African Regions: report of an interregional network meeting, Casablanca, Morocco, 23–24 June 2014*. (World Health Organization, 2015).
34. *Manual for Case Management of Cutaneous Leishmaniasis in the Who Eastern Mediterranean Region*. (World Health Pubns, 2015).
35. WHO | Leishmaniasis in the Americas. Recommendations for the treatment; 2013. WHO Available at: http://www.who.int/neglected_diseases/resources/978-92-75-31752-5/en/. (Accessed: 17th June 2018)
36. Interventions for American cutaneous and mucocutaneous leishmaniasis. | Cochrane. doi:[10.1002/14651858.CD004834.pub2](https://doi.org/10.1002/14651858.CD004834.pub2)
37. Treatments for Old World cutaneous leishmaniasis | Cochrane. doi:[10.1002/14651858.CD005067.pub5](https://doi.org/10.1002/14651858.CD005067.pub5)
38. Markle, W. H. & Makhoul, K. Cutaneous Leishmaniasis Recognition and Treatment. *AFP* 69, 1455–1460 (2004).
39. Alvar, J. & Arana, B. I. Appraisal of Leishmaniasis Chemotherapy, Current Status and Pipeline Strategies Chapter 1: Leishmaniasis, Impact and Therapeutic Needs. in *Drug Discovery for Leishmaniasis* 1–23 (2017). doi:[10.1039/9781788010177-00001](https://doi.org/10.1039/9781788010177-00001)
40. Haldar, A. K., Sen, P. & Roy, S. Use of Antimony in the Treatment of Leishmaniasis: Current Status and Future Directions. *Molecular Biology International* (2011). doi:[10.4061/2011/571242](https://doi.org/10.4061/2011/571242)
41. Goodwin, L. G. Pentostam® (sodium stibogluconate); a 50-year personal reminiscence. *Transactions of the Royal Society of Tropical Medicine and Hygiene* 89, 339–341 (1995).
42. Berman, J. D., Chulay, J. D., Hendricks, L. D. & Oster, C. N. Susceptibility of clinically sensitive and resistant Leishmania to pentavalent antimony in vitro. *Am. J. Trop. Med. Hyg.* 31, 459–465 (1982).
43. Carrió, J. & Portús, M. In vitro susceptibility to pentavalent antimony in Leishmania infantum strains is not modified during in vitro or in vivo passages but is modified after host treatment with meglumine antimoniate. *BMC Pharmacol* 2, 11 (2002).
44. Navin, T. R., Arana, B. A., Arana, F. E., Berman, J. D. & Chajón, J. F. Placebo-controlled clinical trial of sodium stibogluconate (Pentostam) versus ketoconazole for treating cutaneous leishmaniasis in Guatemala. *J. Infect. Dis.* 165, 528–534 (1992).

45. Wyllie, S., Cunningham, M. L. & Fairlamb, A. H. Dual action of antimonial drugs on thiol redox metabolism in the human pathogen *Leishmania donovani*. *J. Biol. Chem.* 279, 39925–39932 (2004).
46. Krauth-Siegel, R. L. & Comini, M. A. Redox control in trypanosomatids, parasitic protozoa with trypanothione-based thiol metabolism. *Biochim. Biophys. Acta* 1780, 1236–1248 (2008).
47. Sereno, D. *et al.* Antimonial-Mediated DNA Fragmentation in *Leishmania infantum* Amastigotes. *Antimicrob Agents Chemother* 45, 2064–2069 (2001).
48. Berman, J. D., Gallalee, J. V. & Best, J. M. Sodium stibogluconate (Pentostam) inhibition of glucose catabolism via the glycolytic pathway, and fatty acid beta-oxidation in *Leishmania mexicana* amastigotes. *Biochem. Pharmacol.* 36, 197–201 (1987).
49. al Jaser, M., el-Yazigi, A., Kojan, M. & Croft, S. L. Skin uptake, distribution, and elimination of antimony following administration of sodium stibogluconate to patients with cutaneous leishmaniasis. *Antimicrob Agents Chemother* 39, 516–519 (1995).
50. Laser, M. A., El-Yazigi, A. & Croft, S. L. Pharmacokinetics of Antimony in Patients Treated with Sodium Stibogluconate for Cutaneous Leishmaniasis. *Pharm Res* 12, 113–116 (1995).
51. Vakil, N. H., Fujinami, N. & Shah, P. J. Pharmacotherapy for leishmaniasis in the United States: focus on miltefosine. *Pharmacotherapy* 35, 536–545 (2015).
52. Croft, S. L. & Engel, J. Miltefosine--discovery of the antileishmanial activity of phospholipid derivatives. *Trans. R. Soc. Trop. Med. Hyg.* 100 Suppl 1, S4-8 (2006).
53. Soto, J. *et al.* Miltefosine for new world cutaneous leishmaniasis. *Clin. Infect. Dis.* 38, 1266–1272 (2004).
54. Mohebali, M. *et al.* Comparison of miltefosine and meglumine antimoniate for the treatment of zoonotic cutaneous leishmaniasis (ZCL) by a randomized clinical trial in Iran. *Acta Trop.* 103, 33–40 (2007).
55. Escobar, P., Matu, S., Marques, C. & Croft, S. L. Sensitivities of *Leishmania* species to hexadecylphosphocholine (miltefosine), ET-18-OCH(3) (edelfosine) and amphotericin B. *Acta Trop.* 81, 151–157 (2002).
56. Moreira, R. A. *et al.* Miltefosine Increases Lipid and Protein Dynamics in *Leishmania amazonensis* Membranes at Concentrations Similar to Those Needed for Cytotoxicity Activity. *Antimicrob. Agents Chemother.* 58, 3021–3028 (2014).
57. Rakotomanga, M., Blanc, S., Gaudin, K., Chaminade, P. & Loiseau, P. M. Miltefosine affects lipid metabolism in *Leishmania donovani* promastigotes. *Antimicrob. Agents Chemother.* 51, 1425–1430 (2007).
58. Uberall, F. *et al.* Hexadecylphosphocholine inhibits inositol phosphate formation and protein kinase C activity. *Cancer Res.* 51, 807–812 (1991).
59. Lucas, A. *et al.* Targeting the PI3K/Akt cell survival pathway to induce cell death of HIV-1 infected macrophages with alkylphospholipid compounds. *PLoS ONE* 5, (2010).

60. Sunyoto, T., Potet, J. & Boelaert, M. Why miltefosine—a life-saving drug for leishmaniasis—is unavailable to people who need it the most. *BMJ Glob Health* 3, e000709 (2018).
61. Castro, M. D. M. *et al.* Pharmacokinetics of Miltefosine in Children and Adults with Cutaneous Leishmaniasis. *Antimicrob. Agents Chemother.* 61, (2017).
62. Kip, A. E., Schellens, J. H. M., Beijnen, J. H. & Dorlo, T. P. C. Clinical Pharmacokinetics of Systemically Administered Antileishmanial Drugs. *Clin Pharmacokinet* 57, 151–176 (2018).
63. Dorlo, T. P. C., Balasegaram, M., Beijnen, J. H. & de Vries, P. J. Miltefosine: a review of its pharmacology and therapeutic efficacy in the treatment of leishmaniasis. *J. Antimicrob. Chemother.* 67, 2576–2597 (2012).
64. Mesa-Arango, A. C., Scorzoni, L. & Zaragoza, O. It only takes one to do many jobs: Amphotericin B as antifungal and immunomodulatory drug. *Front Microbiol* 3, (2012).
65. Dupont, B. Overview of the lipid formulations of amphotericin B. *J. Antimicrob. Chemother.* 49 Suppl 1, 31–36 (2002).
66. Botero Aguirre, J. P. & Restrepo Hamid, A. M. Amphotericin B deoxycholate versus liposomal amphotericin B: effects on kidney function. in *The Cochrane Library* (John Wiley & Sons, Ltd, 2015). doi:[10.1002/14651858.CD010481.pub2](https://doi.org/10.1002/14651858.CD010481.pub2)
67. Gaspani, S. Access to liposomal generic formulations: beyond AmBisome and Doxil/Caelyx. *Generics and Biosimilars Initiative Journal* 2, 60–62 (2013).
68. Gilead Sciences and the World Health Organization Announce Five-Year Visceral Leishmaniasis Collaboration | Gilead. Available at: <http://www.gilead.com/news/press-releases/2016/9/gilead-sciences-and-the-world-health-organization-announce-five-year-visceral-leishmaniasis-collaboration>. (Accessed: 17th June 2018)
69. Ramos, H., Valdivieso, E., Gamargo, M., Dagger, F. & Cohen, B. E. Amphotericin B kills unicellular leishmanias by forming aqueous pores permeable to small cations and anions. *J. Membr. Biol.* 152, 65–75 (1996).
70. Saha, A. K., Mukherjee, T. & Bhaduri, A. Mechanism of action of amphotericin B on *Leishmania donovani* promastigotes. *Mol. Biochem. Parasitol.* 19, 195–200 (1986).
71. Anderson, T. M. *et al.* Amphotericin forms an extramembranous and fungicidal sterol sponge. *Nat Chem Biol* 10, 400–406 (2014).
72. Jahn, B. *et al.* Accumulation of Amphotericin B in Human Macrophages Enhances Activity against *Aspergillus fumigatus* Conidia: Quantification of Conidial Kill at the Single-Cell Level. *Antimicrob Agents Chemother* 42, 2569–2575 (1998).
73. Lin, H.-S., Medoff, G. & Kobayashi, G. S. Effects of Amphotericin B on Macrophages and Their Precursor Cells. *Antimicrobial Agents and Chemotherapy* 11, 154–160 (1977).
74. Yardley, V. & Croft, S. L. Activity of liposomal amphotericin B against experimental cutaneous leishmaniasis. *Antimicrob. Agents Chemother.* 41, 752–756 (1997).

75. Yardley, V. & Croft, S. L. A comparison of the activities of three amphotericin B lipid formulations against experimental visceral and cutaneous leishmaniasis. *International Journal of Antimicrobial Agents* 13, 243–248 (2000).
76. Adler-Moore, J. & Proffitt, R. T. AmBisome: liposomal formulation, structure, mechanism of action and pre-clinical experience. *J. Antimicrob. Chemother.* 49 Suppl 1, 21–30 (2002).
77. Proffitt, R. T., Satorius, A., Chiang, S. M., Sullivan, L. & Adler-Moore, J. P. Pharmacology and toxicology of a liposomal formulation of amphotericin B (AmBisome) in rodents. *J. Antimicrob. Chemother.* 28 Suppl B, 49–61 (1991).
78. Stone, N. R., Bicanic, T., Salim, R. & Hope, W. Liposomal Amphotericin B (AmBisome®): A review of the pharmacokinetics, pharmacodynamics, clinical experience and future directions. *Drugs* 76, 485–500 (2016).
79. Lestner, J. M. *et al.* Pharmacokinetics and Pharmacodynamics of Amphotericin B Deoxycholate, Liposomal Amphotericin B, and Amphotericin B Lipid Complex in an In Vitro Model of Invasive Pulmonary Aspergillosis. *Antimicrob. Agents Chemother.* 54, 3432–3441 (2010).
80. Sundar, S. & Chakravarty, J. Liposomal Amphotericin B and Leishmaniasis: Dose and Response. *J Glob Infect Dis* 2, 159–166 (2010).
81. van der Meide, W. F. *et al.* Evaluation of treatment with pentamidine for cutaneous leishmaniasis in Suriname. *Int. J. Dermatol.* 48, 52–58 (2009).
82. Soto-Mancipe, J., Grogl, M. & Berman, J. D. Evaluation of pentamidine for the treatment of cutaneous leishmaniasis in Colombia. *Clin. Infect. Dis.* 16, 417–425 (1993).
83. Galvão, E. L., Rabello, A. & Cota, G. F. Efficacy of azole therapy for tegumentary leishmaniasis: A systematic review and meta-analysis. *PLoS ONE* 12, e0186117 (2017).
84. Felton, T., Troke, P. F. & Hope, W. W. Tissue Penetration of Antifungal Agents. *Clin. Microbiol. Rev.* 27, 68–88 (2014).
85. Cauwenbergh, G. Skin Kinetics of Azole Antifungal Drugs. in *Current Topics in Medical Mycology* 88–136 (Springer, New York, NY, 1992). doi:[10.1007/978-1-4612-2762-5_4](https://doi.org/10.1007/978-1-4612-2762-5_4)
86. El-On, J., Bazarsky, E. & Sneir, R. Leishmania major: in vitro and in vivo anti-leishmanial activity of paromomycin ointment (Leshcutan) combined with the immunomodulator Imiquimod. *Exp. Parasitol.* 116, 156–162 (2007).
87. Sosa, N. *et al.* Randomized, double-blinded, phase 2 trial of WR 279,396 (paromomycin and gentamicin) for cutaneous leishmaniasis in Panama. *Am. J. Trop. Med. Hyg.* 89, 557–563 (2013).
88. Neal, R. A. The effect of antibiotics of the neomycin group on experimental cutaneous leishmaniasis. *Annals of Tropical Medicine & Parasitology* 62, 54–62 (1968).
89. el-On, J. & Hamburger, A. D. Topical treatment of New and Old World cutaneous leishmaniasis in experimental animals. *Trans. R. Soc. Trop. Med. Hyg.* 81, 734–737 (1987).

90. El-On, J., Livshin, R., Even-Paz, Z. v. i., Hamburger, D. & Weinrauch, L. Topical Treatment of Cutaneous Leishmaniasis. *Journal of Investigative Dermatology* 87, 284–288 (1986).
91. Kim, D. H., Chung, H. J., Bleys, J. & Ghohostani, R. F. Is paromomycin an effective and safe treatment against cutaneous leishmaniasis? A meta-analysis of 14 randomized controlled trials. *PLoS Negl Trop Dis* 3, e381 (2009).
92. Maarouf, M., Lawrence, F., Croft, S. L. & Robert-Gero, M. Ribosomes of Leishmania are a target for the aminoglycosides. *Parasitol. Res.* 81, 421–425 (1995).
93. Maarouf, M., de Kouchkovsky, Y., Brown, S., Petit, P. X. & Robert-Gero, M. In vivo interference of paromomycin with mitochondrial activity of Leishmania. *Exp. Cell Res.* 232, 339–348 (1997).
94. Chawla, B., Jhingran, A., Panigrahi, A., Stuart, K. D. & Madhubala, R. Paromomycin affects translation and vesicle-mediated trafficking as revealed by proteomics of paromomycin - susceptible -resistant Leishmania donovani. *PLoS ONE* 6, e26660 (2011).
95. Ravis, W. R. *et al.* Pharmacokinetics and absorption of paromomycin and gentamicin from topical creams used to treat cutaneous leishmaniasis. *Antimicrob. Agents Chemother.* 57, 4809–4815 (2013).
96. Reithinger, R. *et al.* Efficacy of thermotherapy to treat cutaneous leishmaniasis caused by Leishmania tropica in Kabul, Afghanistan: a randomized, controlled trial. *Clin. Infect. Dis.* 40, 1148–1155 (2005).
97. Sadeghian, G., Nilfroushzadeh, M. A. & Iraj, F. Efficacy of local heat therapy by radiofrequency in the treatment of cutaneous leishmaniasis, compared with intralesional injection of meglumine antimoniate. *Clin. Exp. Dermatol.* 32, 371–374 (2007).
98. Salmanpour, R., Razmavar, M. R. & Abtahi, N. Comparison of intralesional meglumine antimoniate, cryotherapy and their combination in the treatment of cutaneous leishmaniasis. *Int. J. Dermatol.* 45, 1115–1116 (2006).
99. Cardona-Arias, J. A., Vélez, I. D. & López-Carvajal, L. Efficacy of thermotherapy to treat cutaneous leishmaniasis: a meta-analysis of controlled clinical trials. *PLoS ONE* 10, e0122569 (2015).
100. Dalton, J. E. & Kaye, P. M. Immunomodulators: use in combined therapy against leishmaniasis. *Expert Rev Anti Infect Ther* 8, 739–742 (2010).
101. Miranda-Verastegui, C. *et al.* First-line therapy for human cutaneous leishmaniasis in Peru using the TLR7 agonist imiquimod in combination with pentavalent antimony. *PLoS Negl Trop Dis* 3, e491 (2009).
102. Santos, J. B. *et al.* Antimony plus recombinant human granulocyte-macrophage colony-stimulating factor applied topically in low doses enhances healing of cutaneous Leishmaniasis ulcers: a randomized, double-blind, placebo-controlled study. *J. Infect. Dis.* 190, 1793–1796 (2004).

103. Hotez, P. J. *et al.* Eliminating the Neglected Tropical Diseases: Translational Science and New Technologies. *PLoS Neglected Tropical Diseases* 10, e0003895 (2016).
104. Liese, B. H., Houghton, N. & Teplitskaya, L. Development assistance for neglected tropical diseases: progress since 2009. *Int Health* 6, 162–171 (2014).
105. Paul, S. M. *et al.* How to improve R&D productivity: the pharmaceutical industry's grand challenge. *Nat Rev Drug Discov* 9, 203–214 (2010).
106. DiMasi, J. A., Feldman, L., Seckler, A. & Wilson, A. Trends in risks associated with new drug development: success rates for investigational drugs. *Clin. Pharmacol. Ther.* 87, 272–277 (2010).
107. Morgan, S., Grootendorst, P., Lexchin, J., Cunningham, C. & Greyson, D. The cost of drug development: A systematic review. *Health Policy* 100, 4–17 (2011).
108. Klug, D. M., Gelb, M. H. & Pollastri, M. P. REPURPOSING STRATEGIES FOR TROPICAL DISEASE DRUG DISCOVERY. *Bioorg Med Chem Lett* 26, 2569–2576 (2016).
109. Alvar, J., Yactayo, S. & Bern, C. Leishmaniasis and poverty. *Trends Parasitol.* 22, 552–557 (2006).
110. de Melo, E. C. & Fortaleza, C. M. C. B. Challenges in the Therapy of Visceral Leishmaniasis in Brazil: A Public Health Perspective. *J Trop Med* 2013, (2013).
111. Olliaro, P. *et al.* Methodology of Clinical Trials Aimed at Assessing Interventions for Cutaneous Leishmaniasis. *PLoS Negl Trop Dis* 7, (2013).
112. González, U. *et al.* Designing and Reporting Clinical Trials on Treatments for Cutaneous Leishmaniasis. *Clin Infect Dis* 51, 409–419 (2010).
113. Avorn, J. The \$2.6 billion pill--methodologic and policy considerations. *N. Engl. J. Med.* 372, 1877–1879 (2015).
114. Ator, M. A., Mallamo, J. P. & Williams, M. Overview of drug discovery and development. *Curr Protoc Pharmacol* Chapter 9, Unit9.9 (2006).
115. Arrowsmith, J. & Miller, P. Trial watch: phase II and phase III attrition rates 2011-2012. *Nat Rev Drug Discov* 12, 569 (2013).
116. Adams, D. J. The Valley of Death in anticancer drug development: a re-assessment. *Trends Pharmacol Sci* 33, 173–180 (2012).
117. Denayer, T., Stöhr, T. & Van Roy, M. Animal models in translational medicine: Validation and prediction. *New Horizons in Translational Medicine* 2, 5–11 (2014).
118. Langhans, S. A. Three-Dimensional in Vitro Cell Culture Models in Drug Discovery and Drug Repositioning. *Front Pharmacol* 9, (2018).
119. Potter, W. Z. Optimizing Early “Go/No Go” Decisions in CNS Drug Development. *Expert Rev Clin Pharmacol* 8, 155–157 (2015).

120. Simpkin, V. L., Renwick, M. J., Kelly, R. & Mossialos, E. Incentivising innovation in antibiotic drug discovery and development: progress, challenges and next steps. *The Journal of Antibiotics* 70, 1087–1096 (2017).
121. Dealmakers, B. June 2018. *BioPharma Dealmakers* Available at: <https://biopharmadealmakers.nature.com/rooms/319-june-2018>. (Accessed: 23rd June 2018)
122. AstraZeneca to sell small molecule antibiotics business to Pfizer. Available at: <https://www.astrazeneca.com/investor-relations/Stock-exchange-announcements/AstraZeneca-to-sell-small-molecule-antibiotics-business-to-Pfizer-24082016.html>. (Accessed: 23rd June 2018)
123. Nwaka, S. *et al.* Advancing Drug Innovation for Neglected Diseases—Criteria for Lead Progression. *PLoS Negl Trop Dis* 3, (2009).
124. Croft, S. L. Public-private partnership: from there to here. *Trans. R. Soc. Trop. Med. Hyg.* 99 Suppl 1, S9-14 (2005).
125. Yildirim, O., Gottwald, M., Schüler, P. & Michel, M. C. Opportunities and Challenges for Drug Development: Public–Private Partnerships, Adaptive Designs and Big Data. *Front Pharmacol* 7, (2016).
126. DNDi Achievements – DNDi. Available at: <https://www.DNDi.org/achievements/>. (Accessed: 23rd June 2018)
127. Aerts, C., Sunyoto, T., Tediosi, F. & Sicuri, E. Are public-private partnerships the solution to tackle neglected tropical diseases? A systematic review of the literature. *Health Policy* 121, 745–754 (2017).
128. WHO | Contribution of pharmaceutical companies to the control of neglected tropical diseases. *WHO* Available at: http://www.who.int/neglected_diseases/pharma_contribution/en/. (Accessed: 26th June 2018)
129. London Declaration on Neglected Tropical Diseases. *Uniting to Combat NTDs* Available at: </london-declaration-neglected-tropical-diseases/>. (Accessed: 23rd June 2018)
130. NTD Drug Discovery Booster – DNDi. Available at: <https://www.DNDi.org/diseases-projects/open-innovation/drug-discovery-booster/>. (Accessed: 23rd June 2018)
131. Nagle, A. S. *et al.* Recent Developments in Drug Discovery for Leishmaniasis and Human African Trypanosomiasis. *Chem Rev* 114, 11305–11347 (2014).
132. Update of DNDi’s leishmaniasis R&D pipeline - 2017. 12
133. Khare, S. *et al.* Proteasome inhibition for treatment of leishmaniasis, Chagas disease and sleeping sickness. *Nature* 537, 229–233 (2016).

134. Mowbray, C. E. Chapter 2: Anti-leishmanial Drug Discovery: Past, Present and Future Perspectives. in *Drug Discovery for Leishmaniasis* 24–36 (2017). doi:[10.1039/9781788010177-00024](https://doi.org/10.1039/9781788010177-00024)
135. Target Product Profile – Cutaneous Leishmaniasis – DNDi. Available at: <https://www.DNDi.org/diseases-projects/leishmaniasis/tpp-cl/>. (Accessed: 23rd June 2018)
136. Kenakin, T. P. Chapter 9 - Pharmacokinetics. in *A Pharmacology Primer (Third Edition)* 179–214 (Academic Press, 2009). doi:[10.1016/B978-0-12-374585-9.00009-8](https://doi.org/10.1016/B978-0-12-374585-9.00009-8)
137. Müller, M., dela Peña, A. & Derendorf, H. Issues in Pharmacokinetics and Pharmacodynamics of Anti-Infective Agents: Distribution in Tissue. *Antimicrob Agents Chemother* 48, 1441–1453 (2004).
138. Croft, S. L. Leishmania and other intracellular pathogens: selectivity, drug distribution and PK-PD. *Parasitology* 145, 237–247 (2018).
139. Garnier, T. & Croft, S. L. Topical treatment for cutaneous leishmaniasis. *Curr Opin Investig Drugs* 3, 538–544 (2002).
140. Dartois, V. The path of anti-tuberculosis drugs: from blood to lesions to mycobacterial cells. *Nat Rev Microbiol* 12, 159–167 (2014).
141. Smith, D. A., Di, L. & Kerns, E. H. The effect of plasma protein binding on in vivo efficacy: misconceptions in drug discovery. *Nat Rev Drug Discov* 9, 929–939 (2010).
142. Voak, A. A. *et al.* An essential type I nitroreductase from *Leishmania major* can be used to activate leishmanicidal prodrugs. *J. Biol. Chem.* 288, 28466–28476 (2013).
143. Strebhardt, K. & Ullrich, A. Paul Ehrlich’s magic bullet concept: 100 years of progress. *Nat. Rev. Cancer* 8, 473–480 (2008).
144. Onufrak, N. J., Forrest, A. & Gonzalez, D. Pharmacokinetic and Pharmacodynamic Principles of Anti-infective Dosing. *Clin Ther* 38, 1930–1947 (2016).
145. Croft, S. L., Yardley, V. & Kendrick, H. Drug sensitivity of *Leishmania* species: some unresolved problems. *Trans. R. Soc. Trop. Med. Hyg.* 96 Suppl 1, S127-129 (2002).
146. Croft, S. L., Sundar, S. & Fairlamb, A. H. Drug Resistance in Leishmaniasis. *Clin Microbiol Rev* 19, 111–126 (2006).
147. Kloehn, J., Saunders, E. C., O’Callaghan, S., Dagley, M. J. & McConville, M. J. Characterization of metabolically quiescent *Leishmania* parasites in murine lesions using heavy water labeling. *PLoS Pathog.* 11, e1004683 (2015).
148. Jara, M. *et al.* Macromolecular biosynthetic parameters and metabolic profile in different life stages of *Leishmania braziliensis*: Amastigotes as a functionally less active stage. *PLOS ONE* 12, e0180532 (2017).
149. Mandell, M. A. & Beverley, S. M. Continual renewal and replication of persistent *Leishmania major* parasites in concomitantly immune hosts. *PNAS* 114, E801–E810 (2017).

150. Seifert, K., Escobar, P. & Croft, S. L. In vitro activity of anti-leishmanial drugs against *Leishmania donovani* is host cell dependent. *J. Antimicrob. Chemother.* 65, 508–511 (2010).
151. Yardley, V. & Koniordou, M. II. Methodologies and Medicinal Chemistry Strategies to Discover and Develop New Treatments Chapter 4: Drug Assay Methodology in Leishmaniasis: From the Microplate to Image Analysis. in *Drug Discovery for Leishmaniasis* 55–76 (2017). doi:[10.1039/9781788010177-00055](https://doi.org/10.1039/9781788010177-00055)
152. Martin, J., Cantizani, J. & Peña, I. Chapter 5: The Pursuit of Novel Anti-leishmanial Agents by High-throughput Screening (HTS) of Chemical Libraries. in *Drug Discovery for Leishmaniasis* 77–100 (2017). doi:[10.1039/9781788010177-00077](https://doi.org/10.1039/9781788010177-00077)
153. Pampaloni, F., Reynaud, E. G. & Stelzer, E. H. K. The third dimension bridges the gap between cell culture and live tissue. *Nat. Rev. Mol. Cell Biol.* 8, 839–845 (2007).
154. Young, E. W. K. & Simmons, C. A. Macro- and microscale fluid flow systems for endothelial cell biology. *Lab Chip* 10, 143–160 (2010).
155. Pelkonen, O., Turpeinen, M. & Raunio, H. In vivo-in vitro-in silico pharmacokinetic modelling in drug development: current status and future directions. *Clin Pharmacokinet* 50, 483–491 (2011).
156. Chung, T. D. Y., Terry, D. B. & Smith, L. H. In Vitro and In Vivo Assessment of ADME and PK Properties During Lead Selection and Lead Optimization – Guidelines, Benchmarks and Rules of Thumb. in *Assay Guidance Manual* (eds. Sittampalam, G. S. et al.) (Eli Lilly & Company and the National Center for Advancing Translational Sciences, 2004).
157. Yardley, V. & Croft, S. L. Chapter 93 - Animal Models of Cutaneous Leishmaniasis. in *Handbook of Animal Models of Infection* (eds. Zak, O. & Sande, M. A.) 775–781 (Academic Press, 1999). doi:[10.1016/B978-012775390-4/50232-3](https://doi.org/10.1016/B978-012775390-4/50232-3)
158. Mears, E. R., Modabber, F., Don, R. & Johnson, G. E. A Review: The Current In Vivo Models for the Discovery and Utility of New Anti-leishmanial Drugs Targeting Cutaneous Leishmaniasis. *PLOS Neglected Tropical Diseases* 9, e0003889 (2015).
159. Van Bocxlaer, K. *et al.* Topical Treatment for Cutaneous Leishmaniasis: Dermato-Pharmacokinetic Lead Optimization of Benzoxaboroles. *Antimicrob. Agents Chemother.* 62, (2018).
160. Van Bocxlaer, K., Yardley, V., Murdan, S. & Croft, S. L. Topical formulations of miltefosine for cutaneous leishmaniasis in a BALB/c mouse model. *J. Pharm. Pharmacol.* 68, 862–872
161. Van Bocxlaer, K., Yardley, V., Murdan, S. & Croft, S. L. Drug permeation and barrier damage in *Leishmania*-infected mouse skin. *J. Antimicrob. Chemother.* 71, 1578–1585 (2016).
162. Nettey, H. *et al.* Assessment of formulated amodiaquine microparticles in *Leishmania donovani* infected rats. *J Microencapsul* 34, 21–28 (2017).

163. Balaraman, K. *et al.* In vitro and in vivo antileishmanial properties of a 2-n-propylquinoline hydroxypropyl β -cyclodextrin formulation and pharmacokinetics via intravenous route. *Biomed. Pharmacother.* 76, 127–133 (2015).
164. Joice, A. C. *et al.* Antileishmanial Efficacy and Pharmacokinetics of DB766-Azole Combinations. *Antimicrob. Agents Chemother.* 62, (2018).
165. Jiménez-Antón, M. D. *et al.* Pharmacokinetics and disposition of miltefosine in healthy mice and hamsters experimentally infected with *Leishmania infantum*. *Eur J Pharm Sci* 121, 281–286 (2018).
166. Voak, A. A., Harris, A., Qaiser, Z., Croft, S. L. & Seifert, K. Pharmacodynamics and Biodistribution of Single-Dose Liposomal Amphotericin B at Different Stages of Experimental Visceral Leishmaniasis. *Antimicrob. Agents Chemother.* 61, (2017).
167. Mouton, J. W. *et al.* Tissue concentrations: do we ever learn? *J Antimicrob Chemother* 61, 235–237 (2008).
168. Gonzalez, D., Schmidt, S. & Derendorf, H. Importance of Relating Efficacy Measures to Unbound Drug Concentrations for Anti-Infective Agents. *Clin Microbiol Rev* 26, 274–288 (2013).
169. Deitchman, A. N., Heinrichs, M. T., Khaowroongrueng, V., Jadhav, S. B. & Derendorf, H. Utility of Microdialysis in Infectious Disease Drug Development and Dose Optimization. *AAPS J* 19, 334–342 (2017).
170. Grogl, M. *et al.* Drug Discovery Algorithm for Cutaneous Leishmaniasis. *Am J Trop Med Hyg* 88, 216–221 (2013).
171. Meibohm, B. & Derendorf, H. Basic concepts of pharmacokinetic/pharmacodynamic (PK/PD) modelling. *Int J Clin Pharmacol Ther* 35, 401–413 (1997).
172. Ambrose, P. G. *et al.* Pharmacokinetics-Pharmacodynamics of Antimicrobial Therapy: It's Not Just for Mice Anymore. *Clin Infect Dis* 44, 79–86 (2007).
173. Tan, Y.-M., Clewell, H., Campbell, J. & Andersen, M. Evaluating Pharmacokinetic and Pharmacodynamic Interactions with Computational Models in Supporting Cumulative Risk Assessment. *Int J Environ Res Public Health* 8, 1613–1630 (2011).
174. Sager, J. E., Yu, J., Ragueneau-Majlessi, I. & Isoherranen, N. Physiologically Based Pharmacokinetic (PBPK) Modeling and Simulation Approaches: A Systematic Review of Published Models, Applications, and Model Verification. *Drug Metab Dispos* 43, 1823–1837 (2015).
175. Brill, M. J. E., Kristoffersson, A. N., Zhao, C., Nielsen, E. I. & Friberg, L. E. Semi-mechanistic pharmacokinetic–pharmacodynamic modelling of antibiotic drug combinations. *Clinical Microbiology and Infection* 24, 697–706 (2018).

176. Morgan, P. *et al.* Can the flow of medicines be improved? Fundamental pharmacokinetic and pharmacological principles toward improving Phase II survival. *Drug Discov. Today* 17, 419–424 (2012).
177. Rajman, I. PK/PD modelling and simulations: utility in drug development. *Drug Discovery Today* 13, 341–346 (2008).
178. Guideline on the qualification and reporting of physiologically based pharmacokinetic (PBPK) modelling and simulation. http://www.ema.europa.eu/docs/en_GB/document_library/Scientific_guideline/2016/07/WC500211315.pdf (accessed 30-6-18)
179. De-Risking Antibiotic Drug Development with PK-PD. Available at: <https://pharmaceutical.report/view-resource.aspx?id=2328>. (Accessed: 30th June 2018)
180. Tängdén, T. *et al.* The role of infection models and PK/PD modelling for optimising care of critically ill patients with severe infections. *Intensive Care Med* 43, 1021–1032 (2017).
181. Asín-Prieto, E., Rodríguez-Gascón, A. & Isla, A. Applications of the pharmacokinetic/pharmacodynamic (PK/PD) analysis of antimicrobial agents. *J. Infect. Chemother.* 21, 319–329 (2015).
182. Guideline on the use of pharmacokinetics and pharmacodynamics in the development of antimicrobial medicinal products. 17
183. White, N. J. Pharmacokinetic and Pharmacodynamic Considerations in Antimalarial Dose Optimization. *Antimicrob Agents Chemother* 57, 5792–5807 (2013).
184. Lyons, M. A. & Lenaerts, A. J. Computational pharmacokinetics/pharmacodynamics of rifampin in a mouse tuberculosis infection model. *J Pharmacokinet Pharmacodyn* 42, 375–389 (2015).
185. Voak, A. A. *et al.* Pharmacodynamics and cellular accumulation of amphotericin B and miltefosine in *Leishmania donovani*-infected primary macrophages. *J. Antimicrob. Chemother.* 73, 1314–1323 (2018).
186. Ang, C. W., Jarrad, A. M., Cooper, M. A. & Blaskovich, M. A. T. Nitroimidazoles: Molecular Fireworks That Combat a Broad Spectrum of Infectious Diseases. *J. Med. Chem.* 60, 7636–7657 (2017).
187. DNDI-0690 – DNDi. Available at: <https://www.DNDi.org/diseases-projects/portfolio/nitroimidazole/>. (Accessed: 28th June 2018)
188. RFP_DNDi_0690_pre-IND_package.pdf. https://www.DNDi.org/wp-content/uploads/2016/01/RFP_DNDi_0690_pre-IND_package.pdf (accessed: 30th June 2018)
189. PerkinElmer Informatics Support Home – Technical Support. Available at: <http://www.cambridgesoft.com/support/ProductHomePage.aspx?KBCatID=112>. (Accessed: 28th June 2018)

190. Lipinski, C. A. Drug-like properties and the causes of poor solubility and poor permeability. *Journal of Pharmacological and Toxicological Methods* 44, 235–249 (2000).
191. K. Pinjari, M. J. S., Somani, R. & Gilhotra, R. M. Investigation of in vitro absorption, distribution, metabolism, and excretion and in vivo pharmacokinetics of paromomycin: Influence on oral bioavailability. *Indian J Pharmacol* 49, 297–303 (2017).
192. Benfeldt, E., Hansen, S. H., Vølund, A., Menné, T. & Shah, V. P. Bioequivalence of Topical Formulations in Humans: Evaluation by Dermal Microdialysis Sampling and the Dermatopharmacokinetic Method. *Journal of Investigative Dermatology* 127, 170–178 (2007).
193. Serup, J., Jemec, G. B. E. & Grove, G. L. *Handbook of Non-Invasive Methods and the Skin, Second Edition*. (CRC Press, 2006).
194. Groth, L. Cutaneous microdialysis. Methodology and validation. *Acta Derm Venereol Suppl (Stockh)* 197, 1–61 (1996).
195. Product Detail. Available at: <http://www.microbiotech.se/index-filer/Page1376.htm>. (Accessed: 28th June 2018)
196. Constantinides, C., Mean, R. & Janssen, B. J. Effects of Isoflurane Anesthesia on the Cardiovascular Function of the C57BL/6 Mouse. *ILAR J* 52, e21–e31 (2011).
197. Kurdi, M. S., Theerth, K. A. & Deva, R. S. Ketamine: Current applications in anesthesia, pain, and critical care. *Anesth Essays Res* 8, 283–290 (2014).
198. Maggi, C. A. & Meli, A. Suitability of urethane anesthesia for physiopharmacological investigations in various systems. Part 2: Cardiovascular system. *Experientia* 42, 292–297 (1986).
199. Loch, J. M., Potter, J. & Bachmann, K. A. The influence of anesthetic agents on rat hepatic cytochromes P450 in vivo. *Pharmacology* 50, 146–153 (1995).
200. Azeredo, F. J. *et al.* Does the Anesthetic Urethane Influence the Pharmacokinetics of Antifungal Drugs? A Population Pharmacokinetic Investigation in Rats. *J Pharm Sci* 104, 3314–3318 (2015).
201. Huh, Y. & Cho, J. Urethane anesthesia depresses activities of thalamocortical neurons and alters its response to nociception in terms of dual firing modes. *Front Behav Neurosci* 7, (2013).
202. Ewald, A. J., Werb, Z. & Egeblad, M. Preparation of Mice for Long-Term Intravital Imaging of the Mammary Gland. *Cold Spring Harb Protoc* 2011, pdb.prot5562 (2011).
203. Smith, P. P. & Kuchel, G. A. Continuous Uroflow Cystometry in the Urethane-Anesthetized Mouse. *Neurourol Urodyn* 29, 1344–1349 (2010).
204. Zulfiqar, B., Shelper, T. B. & Avery, V. M. Leishmaniasis drug discovery: recent progress and challenges in assay development. *Drug Discov. Today* 22, 1516–1531 (2017).

205. Carlson, M. W., Alt-Holland, A., Egles, C. & Garlick, J. A. Three-Dimensional Tissue Models of Normal and Diseased Skin. *Curr Protoc Cell Biol* CHAPTER, Unit-19.9 (2008).
206. Sriram, G., Bigliardi, P. L. & Bigliardi-Qi, M. Full-Thickness Human Skin Equivalent Models of Atopic Dermatitis. *Methods Mol. Biol.* (2018). doi:[10.1007/7651_2018_163](https://doi.org/10.1007/7651_2018_163)
207. Niehues, H. & van den Bogaard, E. H. Past, present and future of in vitro 3D reconstructed inflammatory skin models to study psoriasis. *Exp. Dermatol.* 27, 512–519 (2018).
208. Müller, I. & Kulms, D. A 3D Organotypic Melanoma Spheroid Skin Model. *J Vis Exp* (2018). doi:[10.3791/57500](https://doi.org/10.3791/57500)
209. Pupovac, A. *et al.* Toward Immunocompetent 3D Skin Models. *Adv Healthc Mater* 7, e1701405 (2018).
210. Kim, B. S. *et al.* 3D cell printing of in vitro stabilized skin model and in vivo pre-vascularized skin patch using tissue-specific extracellular matrix bioink: A step towards advanced skin tissue engineering. *Biomaterials* 168, 38–53 (2018).
211. Peniche, A. G. *et al.* Development of an Ex Vivo Lymph Node Explant Model for Identification of Novel Molecules Active against *Leishmania major*. *Antimicrob. Agents Chemother.* 58, 78–87 (2014).
212. Osorio, Y., Travi, B. L., Renslo, A. R., Peniche, A. G. & Melby, P. C. Identification of Small Molecule Lead Compounds for Visceral Leishmaniasis Using a Novel Ex Vivo Splenic Explant Model System. *PLOS Neglected Tropical Diseases* 5, e962 (2011).
213. O’Keeffe, A. Development of Novel Predictive 2D and 3D in Vitro Models For Anti-Leishmanial Drug Testing. (London School of Hygiene & Tropical Medicine, 2018).
214. Budha, N. R., Lee, R. B., Hurdle, J. G., Lee, R. E. & Meibohm, B. A Simple in vitro PK/PD Model System to Determine Time-Kill Curves of Drugs against Mycobacteria. *Tuberculosis (Edinb)* 89, 378–385 (2009).
215. Shukla, C., Patel, V., Juluru, R. & Stagni, G. Quantification and prediction of skin pharmacokinetics of amoxicillin and cefuroxime. *Biopharm Drug Dispos* 30, 281–293 (2009).
216. Müller, M. Microdialysis in clinical drug delivery studies. *Adv. Drug Deliv. Rev.* 45, 255–269 (2000).
217. Erdo, F. Microdialysis Techniques In Pharmacokinetic and Biomarker Studies Past, Present and Future Directions A Review. *Journal of Clinical & Experimental Pharmacology* 5, (2015).
218. Langer, O. *et al.* Combined PET and microdialysis for in vivo assessment of intracellular drug pharmacokinetics in humans. *J. Nucl. Med.* 46, 1835–1841 (2005).
219. Dube, A., Gupta, R. & Singh, N. Reporter genes facilitating discovery of drugs targeting protozoan parasites. *Trends in Parasitology* 25, 432–439 (2009).

220. Thalhofer, C. J. *et al.* In vivo imaging of transgenic Leishmania parasites in a live host. *J Vis Exp* (2010). doi:[10.3791/1980](https://doi.org/10.3791/1980)
221. Kip, A. E. *et al.* Systematic Review of Biomarkers To Monitor Therapeutic Response in Leishmaniasis. *Antimicrob. Agents Chemother.* 59, 1–14 (2015).
222. Kip, A. E. *et al.* Macrophage Activation Marker Neopterin: A Candidate Biomarker for Treatment Response and Relapse in Visceral Leishmaniasis. *Front Cell Infect Microbiol* 8, 181 (2018).
223. Hersini, K. J., Melgaard, L., Gazerani, P. & Petersen, L. J. Microdialysis of inflammatory mediators in the skin: a review. *Acta Derm. Venereol.* 94, 501–511 (2014).
224. Sauermann, R. & Zeitlinger, M. Microdialysis in Internal Organs and Tumors. in *Microdialysis in Drug Development* 303–333 (Springer, New York, NY, 2013). doi:[10.1007/978-1-4614-4815-0_16](https://doi.org/10.1007/978-1-4614-4815-0_16)
225. Pink, D. B. S., Schulte, W., Parseghian, M. H., Zijlstra, A. & Lewis, J. D. Real-Time Visualization and Quantitation of Vascular Permeability In Vivo: Implications for Drug Delivery. *PLOS ONE* 7, e33760 (2012).
226. van der Meide, W. *et al.* Comparison between Quantitative Nucleic Acid Sequence-Based Amplification, Real-Time Reverse Transcriptase PCR, and Real-Time PCR for Quantification of Leishmania Parasites. *J Clin Microbiol* 46, 73–78 (2008).
227. Fungisome Gel, Fungisome Gel Manufacturers, Fungisome Gel Suppliers, Fungisome Gel Manufacturers India. Available at: <http://www.lifecareinnovations.com/fungisomegel.html>. (Accessed: 9th July 2018)
228. Maes, L. *et al.* In vitro ‘time-to-kill’ assay to assess the cidal activity dynamics of current reference drugs against Leishmania donovani and Leishmania infantum. *J Antimicrob Chemother* 72, 428–430 (2017).
229. Hefnawy, A., Berg, M., Dujardin, J.-C. & De Muylder, G. Exploiting Knowledge on Leishmania Drug Resistance to Support the Quest for New Drugs. *Trends in Parasitology* 33, 162–174 (2017).
230. Hendrickx, S. *et al.* In Vivo Selection of Paromomycin and Miltefosine Resistance in Leishmania donovani and L. infantum in a Syrian Hamster Model. *Antimicrob. Agents Chemother.* 59, 4714–4718 (2015).
231. Zaid Alkilani, A., McCrudden, M. T. C. & Donnelly, R. F. Transdermal Drug Delivery: Innovative Pharmaceutical Developments Based on Disruption of the Barrier Properties of the stratum corneum. *Pharmaceutics* 7, 438–470 (2015).
232. Gutiérrez, V., Seabra, A. B., Reguera, R. M., Khandare, J. & Calderón, M. New approaches from nanomedicine for treating leishmaniasis. *Chem Soc Rev* 45, 152–168 (2016).
233. Shaw, C. & Carter, K. Drug delivery: lessons to be learnt from Leishmania studies. *Nanomedicine* 9, 1531–1544 (2014).

234. Ferreira, L. S., Ramaldes, G. A., Nunan, E. A. & Ferreira, D. L. A. M. In Vitro Skin Permeation and Retention of Paromomycin from Liposomes for Topical Treatment of the Cutaneous Leishmaniasis. *Drug Development and Industrial Pharmacy* 30, 289–296 (2004).
235. New, R. R. C., Chance, M. L. & Heath, S. The treatment of experimental cutaneous leishmaniasis with liposome-entrapped Pentostam. *Parasitology* 83, 519–527 (1981).
236. Momeni, A. *et al.* Development of liposomes loaded with anti-leishmanial drugs for the treatment of cutaneous leishmaniasis. *J Liposome Res* 23, 134–144 (2013).
237. Varikuti, S. *et al.* Topical treatment with nanoliposomal Amphotericin B reduces early lesion growth but fails to induce cure in an experimental model of cutaneous leishmaniasis caused by *Leishmania mexicana*. *Acta Trop.* 173, 102–108 (2017).
238. Sohail, M. F. *et al.* Advancements in the oral delivery of Docetaxel: challenges, current state-of-the-art and future trends. *Int J Nanomedicine* 13, 3145–3161 (2018).
239. Thakur, K., Sharma, G., Singh, B., Chhibber, S. & Katare, O. P. Current State of Nanomedicines in the Treatment of Topical Infectious Disorders. *Recent Pat Antiinfect Drug Discov* (2018). doi:[10.2174/1574891X13666180529103804](https://doi.org/10.2174/1574891X13666180529103804)
240. Stocks, M. Chapter 3 - The small molecule drug discovery process – from target selection to candidate selection. in *Introduction to Biological and Small Molecule Drug Research and Development* (eds. Ganellin, R., Roberts, S. & Jefferis, R.) 81–126 (Elsevier, 2013). doi:[10.1016/B978-0-12-397176-0.00003-0](https://doi.org/10.1016/B978-0-12-397176-0.00003-0)
241. Prideaux, B. *et al.* The association between sterilizing activity and drug distribution into tuberculosis lesions. *Nat. Med.* 21, 1223–1227 (2015).
242. Blanc, L., Lenaerts, A., Dartois, V. & Prideaux, B. Visualization of Mycobacterial Biomarkers and Tuberculosis Drugs in Infected Tissue by MALDI-MS Imaging. *Anal. Chem.* 90, 6275–6282 (2018).

7. APPENDIX

7.1. Networks, partners and institutes

7.1.1. Euroleish



The aim of the EUROLEISH-NET programme is to provide the selected candidates the **tools to start and consolidate their careers** in the field of infectious disease control and leishmaniasis in particular. The training programme will promote **scientific excellence, multidisciplinary, and autonomy** to increase the employability of the researchers.

The core of the training programme is the PhD research projects conducted by the 15 selected candidates and each supervised by two specialized senior scientists from two institutions. Additionally, the researchers will benefit from group coaching at regular intervals in a number of retreats

- **Scientific excellence:** the 15 PhD students will engage each in a **three-year PhD** research project linked to non-academic institutions (e.g. private sector and/or **public-private alliances**). All trainees will be hosted by **centres of excellence** for leishmaniasis research located in **Europe**. Researchers will **develop their skills** (i.e. laboratory, analytical, epidemiology, etc) under the supervision of two senior scientists from different institutions. The research projects aim to lead to a **PhD award** and a series of **high impact scientific publications**.
- **Multi-disciplinarity:** The PhD projects offered include **basic, translational and implementation research projects, and this combination will allow for challenging interactions within the network. Individual research projects draw from different scientific disciplines** (i.e. molecular biology and epidemiology, drug discovery, vector control and immunology). Researchers will be inducted into a large, diverse and global research community with a strong European basis and focused on a common goal, leishmaniasis control. During their training, **all researchers will spend (1) at least 6 months in a non-academic (e.g. SME, NGO) institution and (2) a minimum of 2-3 months abroad to conduct part of their project.**
- **Autonomy:** Researchers will be encouraged to **take responsibility on the design, development and management of their research projects** in coordination with the supervisors.

This project has received funding from the **European Union's Horizon 2020 research and innovation programme** under the Marie Skłodowska-Curie International Training Network *grant agreement No 642609*.

Extracted from: <http://www.euroleish.net/about>

7.1.2. Pharmidex Pharmaceutical Services Ltd.



Pharmidex provides translational solutions using its world-renowned expertise in CNS/oncology, drug discovery and ADMET/pharmacokinetics. Founded in the UK in 2002, Pharmidex operates in state-of-the-art facilities in London and Stevenage to provide high-quality bespoke experimental data to support drug discovery and development.

Extracted from: <https://www.pharmidex.com/>

7.1.3. Institute of Hygiene and Tropical Medicine, Lisbon



DESDE 1902

INSTITUTO DE HIGIENE E
MEDICINA TROPICAL

UNIVERSIDADE NOVA DE LISBOA

IHMT's mission is the development of scientific research in Biomedical Sciences, Tropical Medicine and Public Health, and the development of cooperation and dissemination of information in the Portuguese speaking countries. Thus, IHMT (www.ihmt.unl.pt) is an important player in specific health issues and the only Portuguese institution dedicated to the study of health in those countries. Furthermore, IHMT offers clinical services to travelers and has reference laboratories for diagnosis of the so-called tropical diseases.

Extracted from: <http://www.ihmt.unl.pt/en/>

7.1.4. Drugs for Neglected Diseases *initiative*



Drugs for Neglected Diseases *initiative*

Founded in 2003 to address the needs of patients with the most neglected diseases, DNDi is a collaborative, patients' needs-driven, not-for-profit drug R&D organization.

The vision: to improve the quality of life and the health of people suffering from neglected diseases by using an alternative model to develop drugs for these diseases, and by ensuring equitable access to new and field-relevant health tools. In this not-for-profit model, driven by the public sector, a variety of players collaborate to raise awareness of the need to research and develop drugs for those neglected diseases that fall outside the scope of market-driven research and development (R&D). They also build public responsibility and leadership in addressing the needs of these patients.

The mission:

- To develop new drugs or new formulations of existing drugs for **people living with neglected diseases**. Acting in the public interest, DNDi bridges existing R&D gaps in essential drugs for these diseases by initiating and coordinating drug R&D projects in collaboration with the international research community, the public sector, the pharmaceutical industry, and other relevant partners.
- DNDi's **primary focus** has been the development of drugs for the **most neglected diseases**, such as human African trypanosomiasis (HAT, or sleeping sickness), leishmaniasis, and Chagas disease, while considering engagement in **R&D projects for other neglected patients** (e.g. malaria, paediatric HIV, filarial infections) and development of diagnostics and/or vaccines to address unmet needs that others are unable or unwilling to address.
- In pursuing these goals, DNDi enables R&D networks built on global collaborations. While harnessing existing support capacities in countries where the diseases are endemic, DNDi contributes to **strengthening capacities in a sustainable manner**, including through know-how and technology transfers in the field of drug R&D for neglected diseases.
- In order to address the evolving needs of public health importance and maintain DNDi's commitment to delivering on the objectives of the current portfolio of diseases, a **dynamic portfolio approach** has been adopted. This enables DNDi to take on new disease areas with various operating models while completing objectives in current diseases.

Extracted from: <https://www.DNDi.org/about-DNDi/vision-mission/>

7.2. Supplementary material

7.2.1. DNA- and RNA- based qPCR results

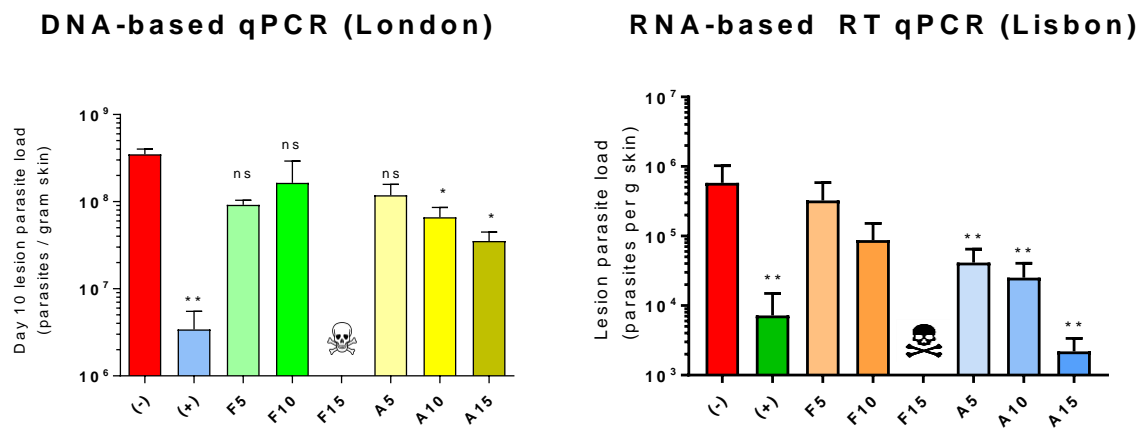


Figure 36: Outcomes of the DNA- and RNA-based qPCR methods to quantify parasite load (see chapter 5.3)

- The general trend in parasite burden is very similar for both qPCR methods among the groups: untreated negative control (-) > Fungisome (F) > AmBisome (A) > paromomycin positive control (+).
- The absolute values in terms of parasite load are about a 100-fold higher for all groups for the DNA-based compared to the RNA-based qPCR. This is likely a consequence of the 1/100 dilution step of DNA extracts that was needed for the DNA method to give robust, accurate and reproducible results.